RESEARCH REPORT

VTT-R-02755-11

††

Duct venting of gas explosions

Authors: Risto Lautkaski

Confidentiality: Public

Report's title	
Duct venting of gas explosions	
Customer, contact person, address	Order reference
Project name Duct venting	Project number/Short name 42982
Author(s) Risto Lautkaski	Pages 179
Keywords gas explosion, dust explosion, vent duct, empirical methods	Report identification code VTT-R-02755-11

Summary

A part of the comparison of methods for vent dimensioning of gas explosions by Razus and Krause (2001) has been revised. The semi-empirical methods by Bradley and Mitcheson (1978) and Molkov et al. (1999) were equally accurate for tests with covered vent.

Empirical correlations for duct vented gas and dust explosions were combined with the Molkov method to predict explosion overpressures measured in tests of duct vented gas explosions. Since 29 of the 65 tests were made with town gas-air mixtures, the values of burning velocity and expansion factor of such mixtures have been estimated.

The correlations by Bartknecht (1993) and Siwek (1998) had comparable accuracies. The methods for duct vented dust explosions by Tamanini and Fischer (2003) and Ural (2005) were less accurate.

Two new engineering correlations by Di Benedetto et al. (2007, 2008) were found flawed. The parameters of the earlier correlation were fitted to test data. The later correlation was complemented with a term containing vent opening pressure. The revised correlations provided predictions comparable to those made with the methods by Bartknecht (1993) and Siwek (1998).

Confidentiality	Public

Espoo 6.6.2011

Written by

Risto Lautkaski
Senior Research Scientist

Accepted by

Timo Vanttola
Technology Manager

VTT's contact address
P. O. Box 1000, FI-02044 VTT

Distribution

The use of the name of the VTT Technical Research Centre of Finland (VTT) in advertising or publication in part of this report is only permissible with written authorisation from the VTT Technical Research Centre of Finland.

Contents

1 Introduction

The basic problem of explosion venting of an enclosure of volume V filled with a flammable gas-air mixture is to select the vent area A_v so that the explosion overpressure does not exceed a maximum permissible value. The first systematic tests were performed by Cubbage and co-workers in the 1950s. The test data was used to derive experimental correlations that could be used to select A_v. Alternatively, the correlations could be used to predict P_{red} for given values of V and A_v.

NFPA 68 divides the vent area dimensioning methods into those for low-strength and those for high-strength enclosures. Low-strength enclosures are defined as those capable of withstanding overpressures no larger than 0.1 bar. Those capable of withstanding higher overpressures are called high-strength enclosures.

The correlations for calculating the vent area A_v for gas and dust explosions in high-strength enclosures included in NFPA 68, EN 14994 and EN 14991 have been derived by Bartknecht (1993). They are based on an extensive program of explosion tests of flammable gas or dust mixtures in tanks and silos. The test data itself, however, is confidential.

The problem with empirical venting formulas is that their validity outside the range of parameters used in the tests is not known. To overcome this limitation, semi-empirical formulas have been derived based on models of vented gas explosion.

Bradley and Mitcheson (1978a) developed a model of vented gas explosion for the purpose of processing the available test data into simple formulas for vent area dimensioning. The model was applied to a large amount of mainly small-scale test data in the open literature. The aim was to derive a "safe recommendation" for the vent size A_v so that it should provide an upper limit to all test results. This lead into two curves, one for initially uncovered vents and the other for initially covered vents (Bradley and Mitcheson 1978b).

The most recent semi-empirical method is by Molkov and coworkers. Molkov (1999) has used data of tests in enclosures of volumes from 0.02 to 4000 m^3 and of different shapes with mixtures ignited at different points and by different ignition sources to derive a semi-empirical correlation for the ratio χ/μ, where χ describes flame front stretch due to flow and turbulence near an open vent and μ is a generalised discharge coefficient.

Often the unburned and burned material released from a vent can create a serious threat to personnel or to vulnerable equipment located near the vent. In situations where such a threat exists, installing a vent duct to redirect the discharge to a safe location is a common solution. The disadvantage of a vent duct is the back pressure generated rendering venting through a duct less effective.

Bartknecht (1993) and Siwek (1998) have derived correlations to estimate the peak overpressure of a duct vented enclosure $P_{red, vd}$. These correlations are based on the same confidential test data as the vent design correlations by Bartknecht

(1993) and are intended to be applied with the latter ones. They have been incorporated into NFPA 68 (2007), EN 14994 and EN 14991. For dust explosions, NFPA 68 (2007) presents the equations by Ural (2005), based on both confidential and open test data.

Since explosions in duct vented enclosures are still poorly understood, no models have been developed for them. Thus, there is no basis for semi-empirical correlations.

Ferrara et al. (2006) have performed computational fluid dynamics (CFD) simulations on laboratory-scale vessels. The simulations showed that the main mechanism affecting the pressure during gas explosion in a ducted vessel is the violent combustion, which occurs in the initial section of the vent duct. This phenomenon is referred as "burn-up". Because of the burn-up, the pressure impulse in the duct induces temporarily a flow reversal across the vent thus enhancing the burning rate by means of turbulisation of the main vessel.

Russo and Di Benedetto (2007) have reviewed existing design methods for ducted venting of gas and dust explosions. Comparison of the methods to predict P_{red} was done with data from mainly laboratory scale gas explosion tests in the same way as Razus and Krause (2001) did with data from medium scale gas explosion tests. The Molkov method was found to give better predictions for the values of P_{red} than the Bradley and Mitcheson correlations.

Although the methods in NFPA 68 (2002) and VDI 3673 are extensions of semi-empirical formulas for simply vented high-strength enclosures, Russo and Di Benedetto (2007) used them in connection with experimental values of P_{red} and values predicted with the Molkov method to predict $P_{red, vd}$ for the same mainly laboratory scale gas explosion tests.

Di Benedetto et al. (2007, 2008) have used this test data also to derive two engineering correlations for ducted venting. The first one is an extension of the correlation by Yao. The second one is an extension of the Molkov method. They, however, have not validated the new correlations in the way they did for existing ones.

In this study, the comparison by Razus and Krause (2001) of simply vented gas explosions is revised. In addition, the evaluation of correlations for ducted venting methods by Russo and Di Benedetto (2007) is revised and the two engineering correlations are validated. A number of trivial errors have been detected and corrected. Finally, a new correlation for ducted venting is proposed.

2 Basics of vented gas explosions

2.1 Burning velocity

A basic quantity of premixed gas flames is the laminar burning velocity S_0 [m/s]. This is the velocity at which a planar flame front (thin reaction zone) travels in a laminar flow with respect to the unburned mixture immediately ahead of it. The burning velocity is usually measured in a test apparatus in which the flow velocity

of the mixture is adjusted so that the flame front is stationary. The Bunsen burner burning premixed gas has been used to measure burning velocities (Figure 1).

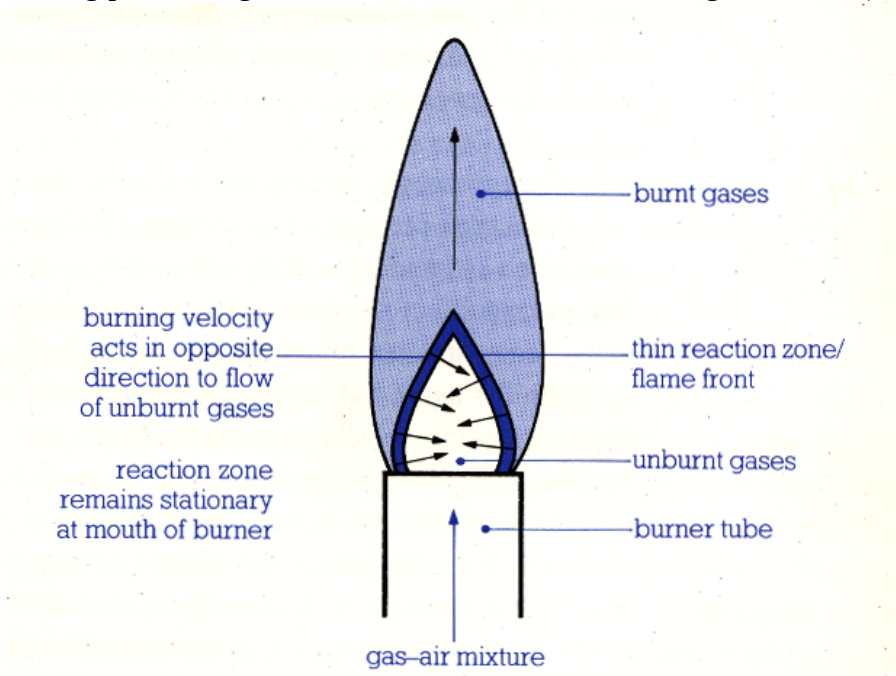

Figure 1. Stationary premixed flame of a Bunsen burner (Harris 1983).

The value of the laminar burning velocity is determined by molecular transport processes, such a heat and mass transfer within the flame front. The burning velocity is a function of gas concentration, reaching a maximum just on the fuel rich side of the stoichiometric concentration. This maximum value, sometimes called the fundamental burning velocity, is tabulated for several gases e.g. in NFPA 68.

The laminar burning velocity of a given fuel-air mixture is a key parameter governing a lot of the properties of combustion. Therefore, much effort has been undertaken to measure this parameter accurately for several fuel-air mixtures. A problem with measuring S_0 is that the shape of the flow and the flame appear to influence the result. This is the reason why early experimental data showed significant scattering when plotted together.

Flame cooling, curvature, strain and stretch appeared to be very complicated phenomena, which are now investigated separately. To determine S_0, the flame should be as flat as possible, in ideal case one-dimensional. However, flat flames traditionally stabilise on a burner, which implies heat loss and therefore do not represent an adiabatic state. It is thus necessary to circumvent these problems using either a non-adiabatic flat flame or an adiabatic stretched flame:

— In case of a burner-stabilised flat flame, the flame can be tuned until it stabilises e.g. because the inlet velocity becomes higher than S_0. The heat loss is determined as a function of the inlet velocity. The results are then extrapolated to zero heat loss, corresponding to an adiabatic state.

— In case of a stretched flame, experiments are performed at various stretch rates. These stretch rates are plotted and extrapolated to zero stretch.

As generally known, extrapolations are always surrounded with uncertainties. This holds especially for the case of burning velocities of stretched flames, where the modelling is necessarily simplified and relies heavily on experiments. In 1993, a method was developed that does not need any extrapolation due to either stretch or heat loss effects.

The flame is stabilised on a brass plate of 2 mm thickness, perforated with small holes. With an appropriate chosen perforation pattern, the flame remains flat. Because the burner plate is rather thin, the temperature distribution in the plate approaches a one-dimensional distribution, only dependent on the radius. The temperature distribution is measured with small thermocouples and it actually corresponds to the heat loss from the flame to the burner plate. The burner plate is heated to keep its temperature at about 85 °C, which will cause the unburned gas mixture to heat up. By doing so, the heat loss necessary for stabilising the flame can be compensated by the heat gain of the unburned mixture. With this burner, it is possible to create flat, stretchless, adiabatic flames in the laboratory (Bosschaart 2002).

The standard NFPA 68 contains a compilation of fundamental burning velocities of selected gases and vapours. Table D.1(a) in NFPA 68 is based on data in (NACA 1957) where the ratios of fundamental burning velocities of the gases and vapours to that of propane are given. The value of for propane used to calculate the ratio was 0.390, 0.430 or 0.465 m/s depending on the experimental method. NFPA 68 uses the reference value of 0.46 m/s for propane.

The values of fundamental burning velocity of gases and vapours used in the experiments discussed in this report are given in Table 1. The values of S_0 of stoichiometric mixtures are *italicised.* In addition to NFPA 68, the values by Bradley and Mitcheson (1978b) and Molkov et al. (1993) as well as those measured with the new method by Bosschaart (2002) are given, if available. The accuracy of the new method is ± 0.005 m/s.

Table 1. Fundamental burning velocities

fuel	NACA, ratio	NFPA 68, m/s	Bosschaart, m/s	B & M, m/s	Molkov, m/s
methane	0.87	0.40	0.372 *0.357*	*0.43*	0.38
ethane	1.03	0.47	0.423 *0.407*	—	—
propane	1	0.46	0.407 *0.395*	0.46	0.37 *0.335*
n-butane	0.97	0.45	0.384 *0.371*	—	—
acetylene	3.62	1.66	—	1.54	—
acetone	1.17	0.54	—	—	*0.335*
CS_2	1.27	0.58	—	—	—

It is seen that the value of fundamental burning velocity of propane 0.46 m/s used as the reference by NFPA 68 and also by Bradley and Mitcheson (1978b) is 13±1 % larger than the value 0.407± 0.005 m/s by Bosschaart (2002). On the other hand, the value used by Molkov is 9±1 % smaller than the value by Bosschaart (2002).

The value of fundamental burning velocity of methane 0.40 m/s in NFPA 68 is 7.5±1.5 % larger than the value 0.372± 0.005 m/s by Bosschaart (2002). The

value for stoichiometric methane-air 0.43 m/s used by Bradley and Mitcheson (1978b) is 20±2 % larger than the value 0.357± 0.005 m/s by Bosschaart (2002).

The value of burning velocity of stoichiometric acetone 0.335 m/s by Molkov is consistent with the recent experimental and calculated value 0.345 m/s by Pichon et al. (2009). The value in NFPA 68 0.54 m/s based on (NACA 1957) is seen to be erroneous.

The recent and most accurate values of S_0 should be used when interpreting experimental results and developing new correlations. In this report, however, only existing correlations are used to predict explosion pressures for tests where P_{red} was not measured. Those values of S_0 will be used that were used to develop the correlations even if the deviate from the recent ones.

For a given fuel concentration, the burning velocity S_0 is dependent on both temperature and pressure. For the purpose of engineering studies, the dependence is usually taken to be (Metghalci & Keck 1982)

$$S_0 = S_r \left(\frac{T_0}{T_r} \right)^{\alpha} \left(\frac{p}{p_0} \right)^{\beta} \quad (1)$$

where p_0 [bar] and T_0 [K] are the initial pressure and temperature, p [bar] is the pressure and T_r [K] is the temperature at which the reference value of burning velocity S_r [m/s] has been measured. The exponent α is usually set equal to 2. The exponent β is substance specific. Actually, the pressure dependence of S_0 is quite weak since the value of β is about 0.25 for hydrocarbons (Shepherd et al. 1997) and about 0.2 for lean hydrogen-air mixtures (Gelfand 2000).

Eq. (1) can be simplified when gas explosions in an enclosure are modelled. The temperature of unburned gas mixture T_u [K] can be predicted using the isentropic relationship

$$T_u = T_0 \left(\frac{p}{p_0} \right)^{1-1/\gamma_u} \quad (2)$$

where γ_u is the ratio of specific heat capacities C_p/C_v of the unburned mixture. Insertion of Eq. (2) into Eq. (1) gives

$$S_0 = S_r \left(\frac{p}{p_0} \right)^{\alpha-\alpha/\gamma_u-\beta} = S_r \left(\frac{p}{p_0} \right)^{\varepsilon} \quad (3)$$

Molkov et al. (2000) use the values $\varepsilon = 0.30$, $\varepsilon = 0.31$ and $\varepsilon = 0.32$ for methane and natural gas, propane, and acetone, respectively.

2.2 Flame speed

In a gas explosion, the flame front is travelling away from the ignition point in a moving gas-air mixture. The expansion of combustion products acts as a piston pushing the unburned mixture away from the point of ignition. It is helpful to think the piston as a porous one, permitting the unburned mixture to flow through. The velocity of the flame front with respect to some fixed position is the sum of the flow and burning velocities. This velocity is called the flame speed v_f [m/s].

Assuming that the gas mixture is initially at rest, the flow is laminar, the flame surface is smooth and the burned gases are at all times trapped behind the

expanding flame front, the relationship between the flame speed and burning velocity can be expressed as (Harris 1983)

$$v_f = ES_0 \quad (4)$$

The expansion factor E is the ratio of final and initial volume of the mixture at constant pressure

$$E = \frac{N_f}{N_0}\frac{T_f}{T_0} \quad (5)$$

where N_f and N_0 are the final and initial number of moles and T_f and T_0 are the final and initial temperature [K] of the mixture. When adiabatic combustion can be assumed the final temperature is equal to the adiabatic flame temperature T_{ad} [K].

The assumption of burned gases trapping is valid for several geometries e.g.:

— in a pipe closed at one end and ignited at that end
— in a tank ignited at centre.

Figure 2 presents the effect of flame geometry on the flame speed in two idealised cases. A smooth flame with a constant area propagates in a tube with a circular cross-section towards the open end. The flame front is assumed to be either planar (Fig. 2A) or hemispherical (Fig. 2B). In the former case, $v_f = ES_0$ and in the latter case, $v_f = 2ES_0$.

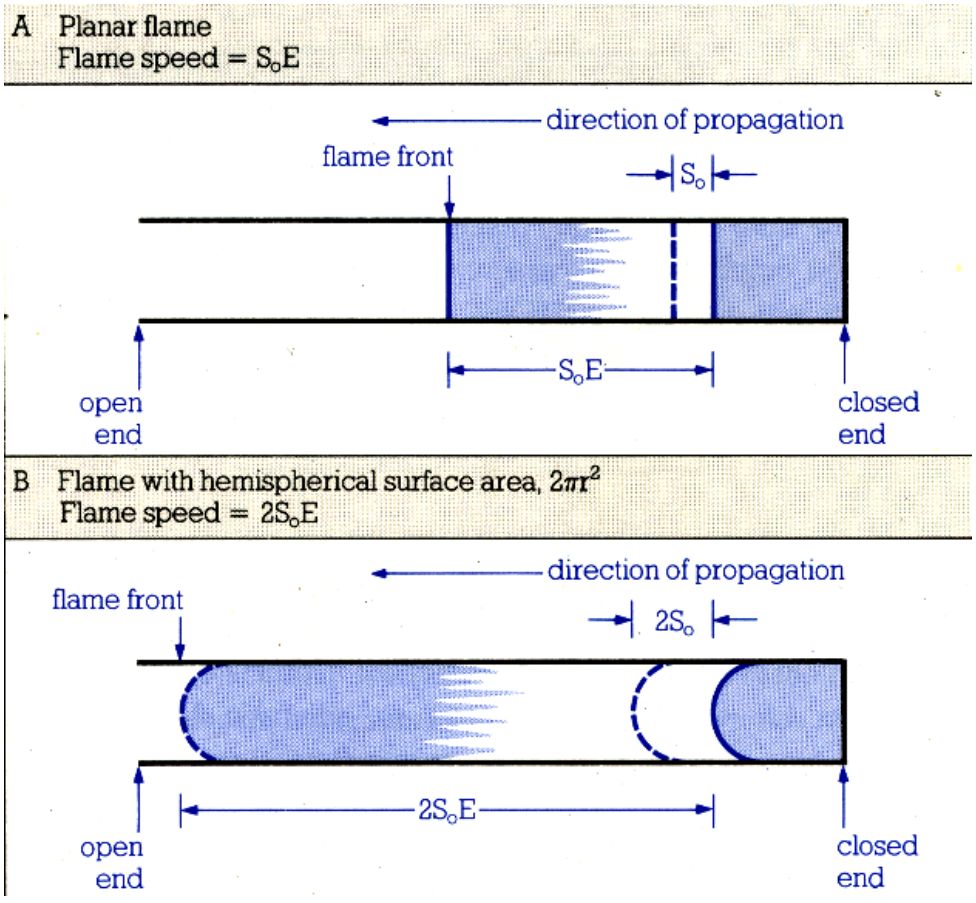

Figure 2. Effect of flame area on flame speed. A. Planar flame. B. Flame with a hemispherical surface area (Harris 1983).

In reality, when a flame front propagates in any geometry, it can develop a cellular structure showing peaks and troughs, often collectively called wrinkles. The volume production of burned gases, which expand to drive the flame front forward, is proportional to the actual surface area of the flame. This effect can be considered by adding an area correction to Eq. (4) (Harris 1983)

$$v_f = E\frac{A_f}{A_n}S_0 \qquad (6)$$

where A_f and A_n are the actual and idealised (laminar) flame areas [m^2].

Unfortunately, there is no simple method to predict the actual flame area A_f. It is to be stressed that the burning velocity is a fundamental property of any gas-air mixture, the flame speed is not. The flame speed is a useful concept and the laminar flame speed is a lower limit to the real (turbulent) flame speed.

In gas explosions, there are other effects which may increase the flame speed even considerably. The most important one is turbulence which can be generated by factors such as

— wall friction (especially effective in pipe explosions)
— high flow velocities e.g. near an explosion vent
— obstacles throttling the flow and generating vortices in their wakes.

The flame speed of a front propagating in a turbulent flow is affected by the turbulence in two ways:

— the large turbulent eddies increase the flame area
— the small turbulent eddies increase the diffusion of heat and mass.

Both effects increase the flame speed v_f; the large eddies by increasing the area ratio A_f/A_n and the small ones by increasing the burning velocity from the laminar one to the turbulent burning velocity S_f.

When a flammable mixture fills a cubical enclosure and is ignited at the centre, flame front remains spherical until it touches the walls. Consequently, the flame speed is only moderately accelerated and reaches a final value less than about 10 m/s.

In an elongated enclosure with the length to diameter ratio L/D less than 5, spherical propagation of the flame takes place only in the initial stage of the explosion. Subsequently, the flame front will proceed swiftly in an axial direction where it will contact a precompressed flammable mixture. This will cause the violence of the explosion to increase and oscillations are superimposed on the course of explosion. For elongated vessels with L/D > 5, even transition of deflagration to detonation can occur (Bartknecht 1981).

3 Venting guidelines

3.1 Origin of pressure peaks

The basic problem of explosion venting of an enclosure of volume V [m^3] filled with a flammable gas-air mixture is to select the vent area A_v [m^2] so that the

explosion overpressure does not exceed a maximum permissible value of P_{red} [kPa]. The first systematic tests were performed by Cubbage and co-workers in the 1950s. The test data was used to derive experimental correlations that could be used to select A_v. Alternatively, the correlations could be used to predict P_{red} for given values of V and A_v.

In these tests, two successive pressure peaks were recorded. The creation of the first peak P_1 can be described as follows: Before the vent opens, the pressure increase is caused by the production of hot combustion products generated by the flame front travelling at the flame speed v_f. The rate of volume generation dV/dt (here V is the volume of gas mixture at initial pressure [m^3]) is the difference of hot combustion products appearing and unburned mixture disappearing (Bradley & Mitcheson 1978a)

$$\frac{dV}{dt} = 4\pi r_f^2 v_f E - 4\pi r_f^2 v_f = 4\pi r_f^2 v_f (E-1) \qquad (7)$$

where r_f [m] is the flame radius.

Pressure in the room is equalised by compression waves travelling at sound velocity and reflecting from the walls of the room. Thus, at any moment the internal overpressure P [Pa] will be the same throughout the room.

When the vent is fully open, the flow of gases can be calculated from the formula of incompressible flow (Harris 1983)

$$\frac{dV}{dt} = C_d A_v \sqrt{\frac{2P}{\rho}} \qquad (8)$$

where C_d is the discharge coefficient and ρ [kg/m^3] is the gas density.

If the vent opening pressure P_{stat} is low, the flame radius r_f and, consequently, the rate of volume generation Eq. (7) are small. If A_v is large enough, the outflow rate Eq. (8) will be larger than the rate of volume generation Eq. (7). The gas volume in the room will decrease as will the pressure. In this way, the first pressure peak P_1 is generated.

If the vent opens early, the flame radius r_f keeps increasing and the rate of volume generation in Eq. (7) becomes soon larger than the outflow rate Eq. (8). Then the internal pressure P rises until hot combustion products start to flow out of the vent. Their density is the density of the unburned mixture divided by the expansion factor E. Consequently, the outflow rate Eq. (8) is suddenly increased by the factor $E^{1/2}$. The outflow rate Eq. (8) becomes again larger than the rate of volume generation Eq. (7), resulting in the second pressure peak P_2.

3.2 Experiments by Cubbage and Simmonds

The purpose of the study by Cubbage and Simmonds (1955) was to derive a formula for the dimensioning of explosion relief vents in industrial drying ovens. The main series of explosion tests using town gas-air mixtures were carried out in sealed ovens. The first sealed oven consisted of a steel case with a brick lining and had a volume of 1.47 m^3. By removing a part of the brick lining, the volume was increased to 2.78 m^3. Considerable difficulties were experienced with this oven and no permanently satisfactory form of sealing was found.

Further experimental ovens were constructed entirely of steel and designed to withstand a 34 kPa overpressure. Two cubical ovens of this type were used with volumes of 0.23 and 2.83 m^3, respectively. Tests were also performed in a standard type oven with a volume of 4.08 m^3, that had been used in a factory.

Since it was necessary to base the design of explosion reliefs on data obtained under the most severe conditions, experiments were first carried out to determine what concentration of the gas and also which position of ignition gave rise to the highest explosion pressure. The variation of explosion pressure with the concentration of town gas was found from experiments carried out in the 1.47 m^3 oven with a square vent of 0.84 m^2 area closed by a relief weighing 16.3 kg/m^2. The concentration of town gas was varied from approximately 5 to 50 %. The results are shown in Figure 3. Cubbage and Simmonds (1955) have fitted a curve to the 17 experimental points.

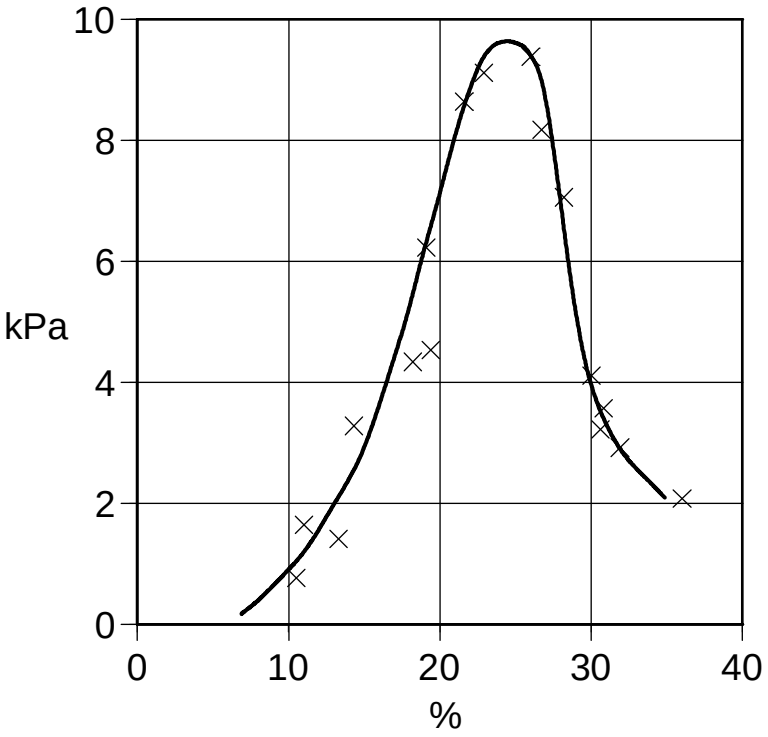

Figure 3. Variation of explosion pressure developed in a vented oven with composition of town gas-air mixture. The original figure of Cubbage & Simmonds (1955) has been redrawn in SI units.

It is clear from Fig. 3 that the maximum pressure was developed using a mixture containing 24 to 25 % of town gas. Subsequently, many more results were obtained and it was decided that the most violent mixture contained 25 % of town gas. This was about the concentration for which flame speed is a maximum, as would be expected.

The variation of explosion pressure with the ignition position was investigated in the 2.83 m^3 oven with a vent of 1.49 m^2 area closed by a relief weighing 4.88 kg/m^2. It was found that the pressure was greatest for central ignition and decreased slightly as the ignition position was moved away from the centre.

The pressures developed by explosions of town gas-air mixtures containing 25 % of gas and centrally ignited were measured over a range of weights for the 1.47 m^3 oven with a vent of 0.84 m^2, the 2.78 m^3 oven with vent areas from 0.47 to 1.24 m^2, and the 0.23 m^3 oven with vent areas from 0.09 to 0.37 m^2. It was found that the value of the first pressure peak P_1 was linearly proportional to the mass per unit area of the vent cover w [kg/m^2] for constant values of V and A_v. It was also found that P_1 was linearly proportional to the vent coefficient K defined as

$$K = \frac{A_c}{A_v} \tag{9}$$

where A_c [m^2] is the area of the cross-section of the enclosure where the vent is inserted. The slope of the line P_1 against K depended on the value of w. It was also found that P_1 was inversely proportional to the cube root of V.

Since the appearance of second pressure peak P_2 coincides with the arrival of the flame front at the vent opening, the average flame speed v_f could be deduced from the time of the second pressure peak P_2. Because all tests were performed with central ignition, v_f was calculated as the ratio of the distance of the centre from the nearest wall to the time of occurrence of the second pressure peak.

The average flame speed was also estimated from the initial value of time derivative dP/dt. For early stages of the explosion before the vent has opened, explosion overpressure P can be estimated with the so-called cubic law (Harris 1983)

$$P = p_0 \frac{4\pi}{3V} E^2 (E-1)(S_0 t)^3 = p_0 \frac{4\pi}{3V} \frac{E-1}{E} (v_f t)^3 \tag{10}$$

where p_0 [Pa] is the initial absolute pressure, in these tests the atmospheric pressure.

Cubbage and Simmonds (1955) found that a straight line could be fitted over the early part of $P^{1/3}$ against t curves. The two methods to estimate v_f were applied to the results of about 90 tests with a 25 % town gas-air mixture in the 0.23, 1.47 and 2.78 m^3 ovens for a range of w and A_v. In Figure 4 the curve fitted to the values of v_f calculated using Eq. (10) has been drawn with a solid line. Cubbage and Simmonds (1955) do not give the values of the expansion factor E used in the calculation. The curve fitted to the values of v_f calculated from the time of P_2 is drawn with a dashed line.

It is seen from Fig. 4 that the two methods give almost the same values for v_f. Except for rich mixtures above 30 %, they differ less than 3 %. Cubbage and Simmonds (1955) conclude that the agreement between the results obtained by the two methods confirmed the explanation given by them for the origin of the second pressure peak. It also justified the assumption that the flame speed was constant since the value derived using Eq. (10) applied to the first few inches of the flame travel, while the value obtained from the second pressure peak applied to the full oven width.

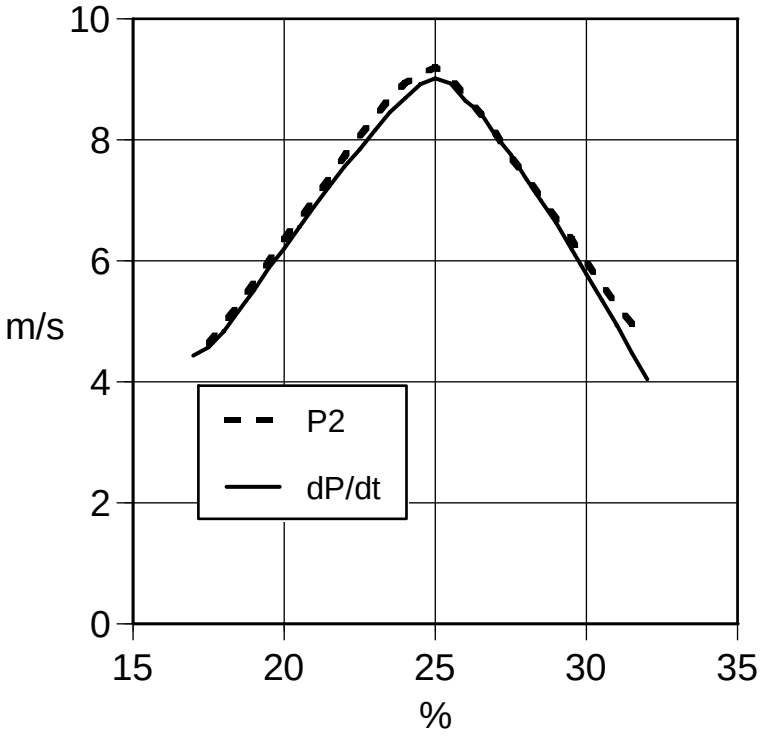

Figure 4. Variation of average flame speed in a vented oven with composition of town gas-air mixture. The original figure of Cubbage & Simmonds (1955) has been redrawn in SI units.

Tests were performed using methane as a fuel over a range of w in the 2.78 m^3 oven with a 1.14 m^2 vent and in the 0.23 m^3 oven with a 0.30 m^2 vent. The concentration of methane was chosen so that it produced the greatest pressures. It was found that the ratio of the pressure developed using methane to that for town gas for the same value of w was independent of w. As this ratio was also the same for both sets of experiments, for which V and A_v were different, it depends only on the fuel used.

Tests were also performed with acetylene, acetone, diethyl ether and carbon disulphide in the 0.23 m^3 oven with a 0.30 m^2 vent. Two values of w were used, namely 21.4 kg/m^2 and 7.8 kg/m^2. For each fuel, a plot was made and the concentration giving maximum pressure was determined from this graph. The results of the tests with the respective concentrations giving maximum pressure are given in Table 2.

According to Cubbage and Simmonds (1955), the overpressure of the first pressure peak P_1 in kPa can be predicted by the correlation

$$P_1 = \frac{S_0\left(0.43Kw + 2.8\right)}{V^{1/3}} \qquad (11)$$

The second pressure peak P_2 in kPa can be predicted by

$$P_2 = 5.8 S_0 K \qquad (12)$$

The values of P_1 and P_2 predicted with Eqs. (11) and (12), respectively, are given in Table 2. Except for acetylene, the experimental values are well predicted.

Table 2. Measured and predicted peak pressures

w	S_0	v_f	P_1	P_2	Eq. (11)	Eq. (12)
fuel	m/s	m/s	kPa	kPa	kPa	kPa
21.4 kg/m^2						
town gas	1.19	9.45	26.9	8.95	27.8	8.6
methane	0.37	3.50	8.25	2.75	8.65	2.7
CS_2	0.43	4.55	11.0	2.75	10.1	3.1
acetone	0.30	3.35	6.9	—	7.0	—
ether	0.37	3.95	8.95	—	8.65	—
7.8 kg/m^2						
town gas	1.19	9.45	14.5	8.95	12.5	8.6
acetylene	1.31	14.0	26.2	11.7	13.7	9.5
methane	0.37	3.50	4.8	2.75	3.05	2.7

When the values of the actual burning velocity were calculated by dividing the experimental value of the flame speed by the expansion factor E, they were found to be 30 % higher than S_0. Cubbage and Simmonds (1955) attribute this finding to the greater mixing occurring in the flames in ovens than in laminar burner flames. This conclusion is examined more closely in Table 3.

Table 3. Measured flame speeds

fuel	v_f, m/s	E	v_f/E, m/s	S_0, m/s	ratio
town gas	9.0	6.64	1.36	1.07–1.22	1.27–1.11
methane	3.50	7.48	0.47	0.37	1.27
CS_2	4.55			0.52	
acetone	3.35	7.9	0.42	0.32	1.31
ether	3.95				
acetylene	14	8.8	1.59	1.48	1.07

One explanation is the deformation of the flame front near the vent due to the flow of unburned mixture towards the latter. The deformed pear-shaped flame front enters the vent earlier than a spherical one. On the other hand, the deformation of the flame front does not affect the flame speed calculated from the initial slope of the pressure curve.

3.3 Bradley and Mitcheson correlations

Bradley and Mitcheson (1978b) presented a simple model for the estimation of overpressure in a vented gas explosion. The model defines two dimensionless parameters S and A. The parameter S is the ratio of gas flow velocity ahead the flame front to sound velocity c [m/s] in the unburned gas

$$S = \frac{S_0(E-1)}{c} \qquad (13)$$

and the parameter A is the ratio of the effective vent area C_dA_v (where C_d = 0.6) to the internal surface area of the enclosure A_s [m^2]

$$A = \frac{C_d A_v}{A_s} \qquad (14)$$

The model was applied to a large amount of mainly small-scale test data obtained under zero or low initial turbulence of the mixture. The length to diameter ratio L/D of the test enclosures ranged from 1 to 5. The aim was to derive a "safe

recommendation" for the vent size A_v so that it should provide an upper limit to all test results.

This lead into two curves, one for initially uncovered vents and the other for initially covered vents opening at P_{stat} (Figure 4).

The part of the curve for initially uncovered vents with P_{red} lower than 1.01 bar (A/S > 0.84) is defined as

$$\frac{A}{S} \geq \left(\frac{0.71\,bar}{P_{red}} \right)^{1/2} \quad or \quad P_{red}/bar \geq 0.71 \left(\frac{A}{S} \right)^{-2} \tag{15}$$

and the part with P_{red} greater than 1.01 bar (0.02 < A/S < 0.84) as

$$\frac{A}{S} \geq \exp\left(\frac{0.66\,bar - P_{red}}{2.03\,bar} \right) \quad or \quad P_{red}/bar = 0.66 - 2.03 \ln\left(\frac{A}{S} \right) \tag{16}$$

The curve for covered vents was based on the criterion that the maximum explosion overpressure P_{red} should not exceed P_{stat}. The part of the curve with P_{red} lower than 1.01 bar (A/S > 3.5) is defined as

$$\frac{A}{S} \geq \left(\frac{12.48\,bar}{P_{stat}} \right)^{1/2} \quad or \quad P_{stat}/bar \geq 12.48 \left(\frac{A}{S} \right)^{-2} \tag{17}$$

and the part with P_{red} greater than 1.01 bar (0.13 < A/S < 3.5) as

$$\frac{A}{S} \geq \left(\frac{2.43\,bar}{P_{stat}} \right)^{1.43} \quad or \quad P_{stat}/bar \geq 2.43 \left(\frac{A}{S} \right)^{-0.70} \tag{18}$$

Eqs. (17) and (18) have been derived assuming $P_{red} = P_{stat}$. When $P_{red} > P_{stat}$, the correlation by Bradley and Mitcheson (1978b) can be written as

$$\frac{A}{S} \leq 3.53 \frac{(P_{stat}/bar)^{0.3}}{(P_{red}/bar)^{0.8}} \quad or \quad P_{red}/bar = 4.84\,(P_{stat}/bar)^{0.375} \left(\frac{A}{S} \right)^{-1.25} \tag{19}$$

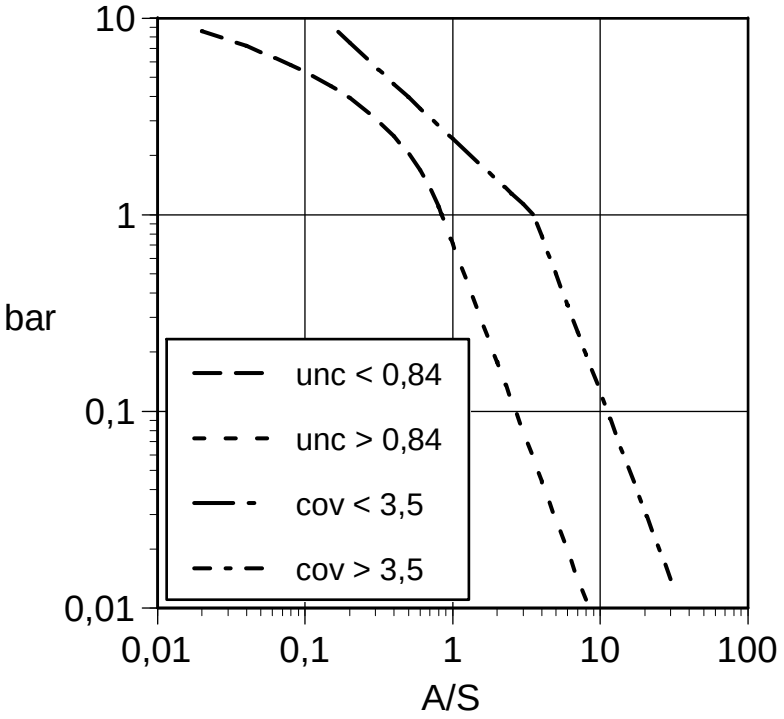

Figure 5. Correlations giving P_{red} for initially uncovered and covered vents, respectively, as functions of A/S (Bradley and Mitcheson 1978b).

3.4 Four peaks model

Later tests revealed that the time dependence of overpressure resulting from vented gas explosion in a room can be described in terms of four distinct peaks which can (but do not have to) occur. The four peaks are (British Gas 1990, Gardner & Hulme 1995):

P_1 which is associated with the pressure drop following the removal of the explosion relief vent and subsequent venting of unburned gas.

P_2 which is associated either with the pressure pulse following the venting of burned gas, or caused by a possible external explosion due to ignition of previously vented unburned gas by the flame emerging from the vent.

P_3 a long duration but generally small amplitude peak associated with the maximum rate of combustion within the room (this typically occurs when the flame front reaches the walls).

P_4 which is an oscillatory pressure peak attributed to excitation of acoustic resonances in the gaseous combustion products. The resulting high combustion rate may cause a significant net overpressure to be developed in the room.

Catlin et al. (1993) have split the second peak into two successive, partly overlapping peaks. The first or P_v follows the venting of burned gas and the second or P_2 results from the external explosion.

Normally, P_3 will not be the dominant peak in a vented explosion, and will be considerable smaller than P_1. Obstacles in the room prevent the formation of the standing acoustic wave necessary for the generation of P_4. The latter can also be prevented by covering the walls with a sound absorbing lining (British Gas 1990).

3.5 Molkov correlations

Molkov (1999) has used data from explosion tests performed during the last 30 years to improve the Bradley and Mitcheson method. Tests were performed in enclosures of volumes from 0.02 to 4000 m^3 and of different shapes with hydrocarbon-air and hydrogen-air mixtures ignited at different points and by different ignition sources. Initially open as well as initially closed vents with vent opening pressures P_{stat} up to 2 bar were used. Molkov (1999) defines the so-called Bradley number Br as

$$Br = \frac{A_v}{V^{2/3}} \frac{c}{S_0\left(E - \dfrac{1-1/\gamma_b}{1-1/\gamma_u}\right)} \tag{20}$$

where γ_u and γ_b are the ratios of specific heat capacities in the unburned mixture and burned gases, respectively, and the so-called turbulent Bradley number Br_t as

$$Br_t = \frac{\sqrt{\dfrac{E}{\gamma_u}}}{\sqrt[3]{36\pi}} \frac{Br}{\dfrac{\chi}{\mu}} \tag{21}$$

where χ describes flame front stretch due to flow and turbulence near an open vent and μ is a generalised discharge coefficient. Note that the internal surface

area of a sphere is in the denominator of Eq. (21) since $(36\pi)^{1/3}\ V^{2/3}$ is equal to A_s. Molkov (1999) has used test data to derive the following semi-empirical correlation for the ratio χ/μ

$$\frac{\chi}{\mu} = \alpha \left[\frac{\left(1+10\,V^{1/3}\right)\left(1+0.5Br^{\beta}\right)}{1+\frac{p_{stat}}{p_0}} \right]^{\gamma} \qquad (22)$$

where V is the enclosure volume [m^3], p_{stat} is vent opening absolute pressure [bar] and p_0 the initial pressure [bar]. The empirical parameters for hydrocarbon-air mixtures are $\alpha = 1.75$, $\beta = 0.5$ and $\gamma = 0.4$ (Molkov 1999). Earlier values were $\alpha = 0.9$, $\beta = 1$ and $\gamma = 0.37$ (Molkov et al. 1999). Russo and Di Benedetto (2007), however, use the value $\gamma = 0.4$ for both parameter sets. This usage is followed in the present report.

Molkov (1999) proposes the following "universal correlation" for the explosion overpressure P_{red}

$$P_M = Br_t^{-2.4} \qquad (23)$$

where the dimensionless reduced pressure P_M is defined as P_{red}/p_0. Eq. (23) is valid for $P_M \leq 1$ and $Br_t \geq 1$. For the opposite case i.e. $P_M > 1$ and $Br_t < 1$ the correlation is

$$P_M = 7 - 6Br_t^{0.5} \qquad (24)$$

According to the Eqs. (20) to (24), P_{red} decreases with increasing P_{stat} which is unphysical. To amend this shortcoming and to match experimental data on vented propane-air explosions at initial atmospheric and elevated pressures (Pegg et al. 1992), Molkov (2001) multiplied the correlation (22) for χ/μ by $p_0^{0.6}$ and redefined the quantity P_M as

$$P_M = \frac{\frac{p_{red}}{p_0} - 1}{\left(\frac{p_{stat}}{p_0}\right)^{3/2}} \qquad (25)$$

where p_{red} is explosion absolute pressure [bar].

For enclosures with initial pressure p_0 equal to atmospheric pressure p_a, Eqs. (22) and (25) can be expressed in terms of the overpressures P_{stat} and P_{red} as

$$\frac{\chi}{\mu} = \alpha \left[\frac{\left(1+10\,V^{1/3}\right)\left(1+0.5Br^{\beta}\right)}{2+\frac{P_{stat}}{p_a}} \right]^{\gamma} \qquad (26)$$

and

$$P_M = \frac{P_{red}/p_a}{\left(P_{stat}/p_a + 1\right)^{3/2}} \qquad (27)$$

Note that $P_M = P_{red}/p_a$ for initially open vents with $P_{stat} = 0$.

3.6 NFPA 68

The U.S. standard NFPA 68 divides the vent area dimensioning methods into those for low-strength and those for high-strength enclosures. Low-strength enclosures are defined as those capable of withstanding overpressures no larger than 0.1 bar. All buildings are low-strength enclosures. High-strength enclosures are defined as those capable of withstanding overpressures larger than 0.1 bar.

For low-strength enclosures, NFPA 68 uses a modified version of the Runes' formula. The original Runes' formula was based on the assumption that the maximum pressure developed in a vented explosion occurs when the rate of volume generation Eq. (7) and the outflow rate Eq. (8) are equal. The volume generation rate Eq. (7) is taken to have its maximum value which is assumed to occur at maximum flame area i.e. just before the flame is quenched by contact with the walls. On this basis, Runes (1972) presents an equation relating A_v and P_{red}

$$A_v = \frac{C_R L_1 L_2}{P_{red}^{1/2}} \tag{28}$$

where L_1 and L_2 [m] are the two largest dimensions of the room. In effect, the ratio L_1L_2/A_v is the vent coefficient K. Thus, Eq. (28) can also be expressed as

$$P_{red} = C_R^2 K^2 \tag{29}$$

The derivation of Eq. (29) actually leads to an equation for the prediction of P_3. The method predicts significantly larger vent sizes A_v than are necessary in non-turbulent explosions, even for large volumes V and/or elongated enclosures. In turbulent explosions, Eq. (29) would provide reasonable estimates for P_{red}, if an appropriate value for the parameter C_R could be defined. However, there is no acceptable way to determine C_R for turbulent explosions, other than full-scale experiment. For this reason, British Gas (1990) does not recommend the Runes' method.

However, NFPA 68 recommends the use of a modified version of Eq. (28)

$$A_v = \frac{C_S A_s}{P_{red}^{1/2}} \tag{30}$$

where A_s [m^2] is the internal surface area of the enclosure, P_{red} is the reduced pressure [bar] and C_S [$bar^{1/2}$] is an experimental constant depending on the value of the laminar burning velocity S_0. The 2002 edition of NFPA 68 recommends fixed values for the constant C_S, namely 0.013 $bar^{1/2}$ for anhydrous ammonia, 0.037 $bar^{1/2}$ for methane and 0.045 $bar^{1/2}$ for gases with S_0 less than 1.3 times that of propane.

The 2007 edition of NFPA 68 gives an expression relating C_S and S_0 that has been derived from tests and investigations of industrial explosions

$$C_S = 1.57 \cdot 10^{-1} S_0^2 + 1.57 \cdot 10^{-2} S_0 + 0.0109 \tag{31}$$

Eq. (31) is stated to be valid for $0.08 \le S_0 \le 0.6$ m/s and $P_{red} \le 0.1$ bar.

The method for calculating the vent area A_v for gas explosions in a high-strength enclosure included in NFPA 68 and EN 14994 has been derived by Bartknecht (1993). The method is based on an extensive program of explosion tests of flammable gas mixtures in tanks and silos.

Explosion characteristics of a gas-air mixture are described by the maximum rate of pressure rise in a closed vessel multiplied by the cube root of vessel volume.

$$\left(\frac{dP}{dt}\right)_{\max} V^{1/3} = K_G \qquad (32)$$

This quantity is called deflagration index of gas (NFPA 68) or gas explosion constant (EN 14994). The value of K_G varies depending on test conditions, such as type and amount of ignition energy and volume of test vessel. Bartknecht (1993) measured the value of K_G and the maximum overpressure P_m [bar] in a 5 dm^3 closed test vessel at room temperature using a 10 J spark as ignition source.

The area A_v of a vent opening at static overpressure P_{stat} required to limit the overpressure in a near-cubic enclosure with volume V to the value P_{red} can be calculated with the correlation by Bartknecht (1993)

$$A_v = \left[\frac{0.1265\log K_G - 0.0567}{P_{red}^{0.5817}} + \frac{0.1754\left(P_{stat} - 0.1\right)}{P_{red}^{0.5722}}\right] V^{2/3} \qquad (33)$$

The limitations of validity of Eq. (33) are:

— the length to diameter ratio L/D of the enclosure must not exceed 2
— $P_m \leq 8$ bar
— 50 bar·m/s $\leq K_G \leq$ 550 bar·m/s
— 0.1 bar $\leq P_{stat} \leq$ 0.5 bar
— $P_{red} \leq 2$ bar
— $P_{red} - P_{stat} > 0.05$ bar
— $V \leq 1000$ m^3.

According to Siwek (1996), the use of Eq. (33) can be extended to low-strength enclosures with $P_{red} < 0.1$ bar by simply inserting $P_{stat} = 0.1$ bar i.e. by omitting the second term.

For L/D values from 2 to 5, the vent area calculated from Eq. (33) is increased by

$$\Delta A = \frac{A_v K_G}{750}\left(\frac{L}{D} - 2\right)^2 \qquad (34)$$

Bartknecht (1993) also derived similar equations for vented explosions of dusts described by values of the maximum pressure in a closed vessel P_m and dust deflagration index K_{St}.

$$A_v = \left[\frac{3.264\cdot 10^{-5} P_m K_{St}}{P_{red}^{0.569}} + \frac{0.27\left(P_{stat} - 0.1\right)}{P_{red}^{0.5}}\right] V^{0.753} \qquad (35)$$

The limitations of validity of Eq. (35) are:

— L/D ≤ 2
— 5 bar $\leq P_m \leq$ 12 bar
— 10 bar·m/s $\leq K_{St} \leq$ 300 bar·m/s
— 0.1 $\leq P_{stat} \leq$ 1 bar
— 0.1 $\leq P_{red} \leq$ 2 bar
— 0.1 $\leq V \leq$ 10 000 m^3.

For elongated enclosures, the vent area calculated from Eq. (35) is increased by

$$\Delta A = A_v\left(-4.305\log P_{red} + 0.758\right)\log\frac{L}{D} \qquad (36)$$

However, if 1.5 bar ≤ P_{red} ≤ 2 bar, ΔA = 0. Here L is the length of the enclosure when vents are placed at one end.

The standard NFPA 68 (2007 edition) uses the equations by Ural (2005)

$$A_v = 10^{-4}\left(1+1.54P_{stat}^{4/3}\right)K_{St}V^{3/4}\sqrt{\frac{P_m}{P_{red}}-1} \qquad (37)$$

The limitations of validity of Eq. (37) are the same as those of Eq. (35) except for P_{stat} ≤ 0.75 bar.

For L/D values from 2 to 6, the vent area is calculated as follows

$$A_{v1} = A_v\left[1+0.6\left(\frac{L}{D}-2\right)^{0.75}\exp\left(-0.95P_{red}^2\right)\right] \qquad (38)$$

3.7 Comparison of venting guidelines

Razus and Krause (2001) compared several empirical and semi-empirical venting guidelines that were available in 2000. The comparison included the Bradley and Mitcheson correlations for initially covered vents Eqs. (17) to (19), Molkov correlations Eqs. (20) to (24) with the parameters α = 0.9, β = 1 and γ = 0.37, modified Runes equation Eq. (30), and some earlier formulae. The methods were used to predict the experimental values of P_{red} in four data sets, namely 15 tests with stoichiometric methane-air, 10 tests with stoichiometric natural gas-air, 16 tests with 4.0 to 5.25 % propane-air, and 2 tests with stoichiometric hydrogen-air mixtures.

Except for the two tests by Runes in a 204 m^3 enclosure, the enclosure volume ranged from 0.65 to 49 m^3. There were 11 tests with initially open vents. In the remaining 32 tests, P_{stat} ranged from 0.012 to 0.50 bar. To test the methods, the relative error e [%] was calculated for each method and each of the four data sets as the sum of the deviations between the predicted and the experimental values of p_{red} as follows

$$e = \frac{100}{N}\sum_{1}^{N}\frac{p_{red,pred}-p_{red,\exp}}{p_{red,\exp}} \qquad (39)$$

Absolute pressures p_{red} were used probably because the relative changes in low overpressures can be large and yet insignificant. Razus and Krause (2001) present results of the comparison in the form of bar charts. The best predictions were made with Eqs. (20) to (24), Eq. (19), and Eqs. (17) to (18). Eq. (30) gave the poorest predictions. However, all the data used to plot the bar charts are given in tabular form. Repeating the calculations, the values of relative error are found and presented in Table 4. (The error in the experimental values of propane tests 10 to 12 has been rectified as explained below.)

Russo and Di Benedetto (2007) prefer the sum of absolute values of the deviations e_{abs} [%] to Eq. (39) and this method will be used also in this report

$$e_{abs} = \frac{100}{N}\sum_{1}^{N}\frac{\left|p_{red,pred}-p_{red,\exp}\right|}{p_{red,\exp}} \qquad (40)$$

Values of e_{abs} calculated from the data of Razus and Krause (2001) are presented in Table 4.

Table 4. Relative errors of the predictions

fuel	tests	error	Eq. (17/18)	Eq. (19)	α= 0.9, β= 1
natural gas	10/4	Eq. (39)	+156 %	+43 %	+14 %
methane	15/13	Eq. (39)	+30 %	+14 %	–31 %
propane	16/11	Eq. (39)	+37 %	+36 %	–22 %
natural gas	10/4	Eq. (40)	156 %	43 %	14 %
methane	15/13	Eq. (40)	31 %	22 %	36 %
propane	16/11	Eq. (40)	47 %	69 %	45 %

Although 11 of the tests were made with initially open vents, the corresponding Bradley and Mitcheson correlations Eqs. (15) and (16) were not tested. These correlations are now compared to those for initially covered vents Eqs. (17) to (19). Of the 11 tests with initially open vents, 2 were made with stoichiometric methane-air, 6 with stoichiometric natural gas-air, and 3 with 5.0 to 5.25 % propane-air mixture.

The experimental data in Table 5 is taken from (Catlin et al. 1997). Tests 2, 3 and 4, denoted by Catlin et al. (1997) as M3, M6 and M8, were performed in a 2.3 m^3 test vessel. Tests 5, 6 and 7, denoted as M32, M30 and M34, were performed in a 0.675 m^3 test vessel. Length to diameter ratio L/D of both vessels was 3. The vent cover was weakly mounted with nominal zero failure pressure. All tests were performed with 10 % natural gas-air mixture. The natural gas used contained at least 93 % methane.

The experimental data in Table 6 is taken from (Moen et al. 1982), Zalosh (1970), (Yao 1974) and (Solberg et al. 1980).

Methane test 14 was performed in a 10 m long, 2.5 m diameter tube with stoichiometric (9.5 %) methane-air mixture. One end of the tube was fully open and the other end was attached to an ignition tube. The pressure inside the tube was monitored by 7 pressure transducers mounted in the tube wall at various positions along the tube. The average of P_{red} measured near the ignition end, in the middle and near the end of the tube was less than 0.1 bar. The maximum value was 0.12 bar (Moen et al. 1982).

Methane test 15 was performed in an explosion bunker 3.1 m high, 2.0 m wide and 5.4 m long, vented through hinged vent panels which were kept closed by gravity. Upon deployment, steel cables held the vents in a horizontal configuration so that they did not obstruct the flow of vented gas. Five successful tests named I-6 to I-10 were performed with 10±0.5 % methane-air with vent area A_v ranging from 1.5 to 3.0 m^2. The highest value of the second pressure peak P_2 = 0.15 bar was reached in test I-7. In this test, the first pressure peak P_1 was 0.04 bar. In addition to one vent with area of 1.5 m^2, a second similar vent opened midway into the test (Zalosh 1970). Razus and Krause (2001) use an equivalent vent area of 2.57 m^2.

Propane test 14 was performed in a 0.76 m^3 cubical chamber with 5 % propane-air mixture. There was an initially open circular vent of area 0.29 m^2 (Yao 1974). Molkov (1999) has extracted the value P_{red} = 0.05 bar from Figure 5 of (Yao 1974).

Propane tests 15 and 16 were performed in a 35 m^3 prismatic steel module (2.5 m × 3.5 m × 4.0 m) with 5.25 % propane-air mixture. There was an initially open circular vent of area 1.0 m^2. In test 15 the mixture was ignited near the vent and in test 16 at centre (Solberg et al. 1980). Molkov (1999) has extracted the values P_{red} = 0.76 bar (test 15) and P_{red} = 1.39 bar (test 16) from Figure 5 of (Solberg et al. 1980). The effect of ignition location on P_{red} cannot be estimated with any of the methods. It has to be included within the random variations.

The parameters S_0 and E used in the present calculation are those by Bradley and Mitcheson (1978b). For methane-air and natural gas-air mixtures: S_0 = 0.43 m/s, E = 7.52 and c = 353 m/s. Consequently, S = $7.94 \cdot 10^{-3}$. The parameters used for 5 % propane-air mixtures are S_0 = 0.38 m/s, E = 7.97 and c = 336 m/s. Consequently, S = $7.88 \cdot 10^{-3}$. Razus and Krause (2001) use the values for 4 % propane-air mixture: S_0 = 0.46 m/s, E = 7.90 and c = 339 m/s also for these tests with 5.0 to 5.25 % propane-air mixture. The results of the calculation are given in Tables 5 and 6 and the values of A/S with the experimental P_{red} are plotted in Figure 6.

Table 5. Prediction of P_{red} for tests with natural gas-air (uncovered vent)

test	2	3	4	5	6	7
V, m^3	2.3	2.3	2.3	0.675	0.675	0.675
A_s, m^2	11.72	11.72	11.72	5.18	5.18	5.18
A_v, m^2	0.365	0.159	0.09	0.185	0.076	0.041
$A \times 10^3$	18.7	8.14	4.61	21.4	8.81	4.75
A/S	2.31	1.01	0.57	2.65	1.09	0.588
Eq. (15), bar	0.13	0.70	1.79	0.10	0.60	1.73
Eq. (18), bar	1.35	2.41	3.60	1.23	2.29	3.52
exp., bar	0.055	0.205	0.435	0.025	0.15	0.35

Table 6. Prediction of P_{red} for tests with methane-air and propane-air (unc. vent)

test	meth. 14	meth. 15	prop. 14	prop. 15	prop. 16
V, m^3	49.1	33.5	0.76	35	35
A_s, m^2	88.3	67.5	5.0	65.5	65.5
A_v, m^2	3.46	2.57	0.29	1.0	1.0
$A \times 10^3$	23.5	22.8	34.8	91.6	91.6
A/S	2.96	2.87	4.45	1.17	1.17
Eq. (15), bar	0.081	0.086	0.036	0.52	0.52
Eq. (18), bar	1.14	1.16	0.63	1.77	1.77
exp., bar	0.12	0.15	0.05	0.76	1.39

Except for test 16, the experimental points for methane and propane follow closely the curve for initially uncovered vents. The values of P_{red} measured for natural gas-air are quite low.

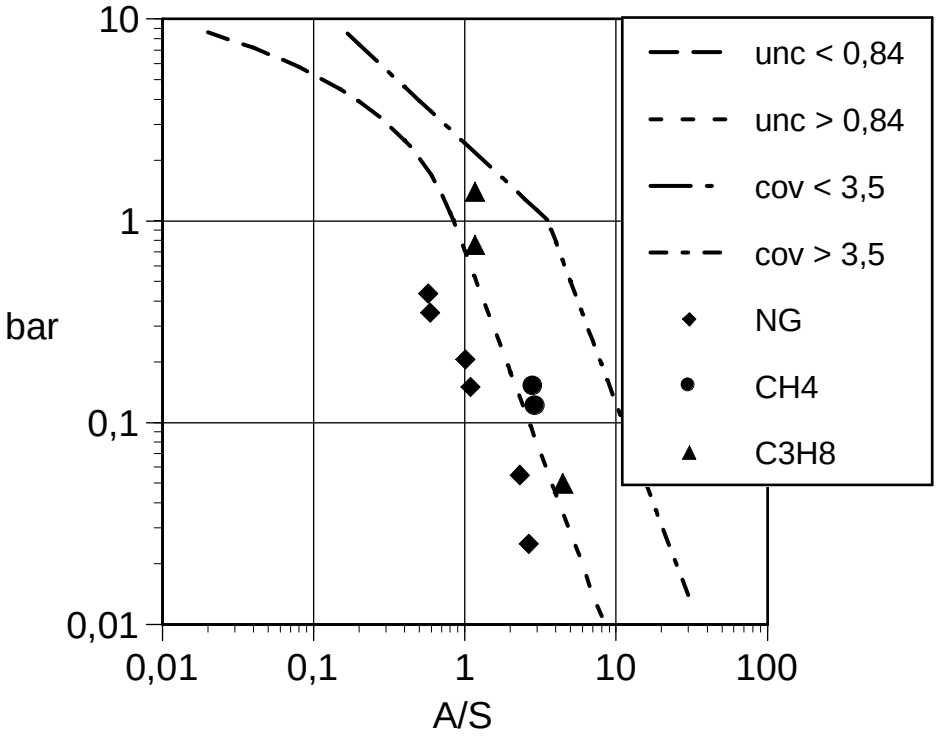

Figure 6. Values of the ratio A/S with the experimental values of P_{red} in tests with an initially uncovered vent.

To validate Molkov correlations Eqs. (20) to (24) (for initially uncovered vent, Eq. (25) reduces to $P_M = P_{red}/p_0$), the values of S_0, E, c and γ_u by Molkov (1999) are used. For methane-air and natural gas-air mixtures: S_0 = 0.38 m/s, E = 7.40, c = 343 m/s and γ_u =1.39. The parameters used for 5 % propane-air mixtures are S_0 = 0.29 m/s, E = 7.90, c = 338 m/s and γ_u =1.365.

Table 7. Prediction of P_{red} for tests with natural gas-air (uncovered vent)

test	2	3	4	5	6	7
V, m^3	2.3	2.3	2.3	0.675	0.675	0.675
A_v, m^2	0.365	0.159	0.09	0.185	0.076	0.041
Br	28.3	12.3	6.97	32.5	13.3	7.19
α, β= 0.9, 1						
χ/μ	5.85	4.33	3.59	5.30	3.84	3.13
Br_t	2.31	1.36	0.92	2.92	1.66	1.10
P_{red}, bar	0.14	0.49	1.25	0.08	0.30	0.81
α, β= 1.75, 0.5						
χ/μ	6.44	5.75	5.37	5.66	5.00	4.64
Br_t	2.09	1.02	0.619	2.74	1.27	0.739
P_{red}, bar	0.17	0.96	2.31	0.09	0.57	1.87
exp., bar	0.055	0.205	0.435	0.025	0.15	0.35

Table 8. Prediction of P_{red} for tests with methane-air and propane-air (unc. vent)

test	meth. 14*	meth. 15*	prop. 14*	prop. 15*	prop. 16*
V, m^3	49.1	33.5	0.76	35	35
A_v, m^2	3.46	2.57	0.29	1.0	1.0
Br	34.8	33.4	56.8	15.2	15.2
α, β= 0.9, 1					
χ/μ	9.33	8.74	6.38	6.59	6.59
Br_t	1.78	1.82	4.42	1.15	1.15
P_{red}, bar	0.25	0.24	0.03	0.73	0.73
α, β= 1.75, 0.5					
χ/μ	9.81	9.27	6.00	8.35	8.35
Br_t	1.69	1.72	4.70	0.91	0.91
P_{red}, bar	0.29	0.28	0.025	1.30	1.30
exp., bar	0.12	0.15	0.05	0.76	1.39

The experimental values of P_{red} with the calculated values of Br_t are plotted in Figure 7. The values of Br_t calculated with the old parameter set α = 0.9 and β = 1 are plotted with open symbols and those calculated with the new one α = 1.75 and β = 0.5 with closed symbols.

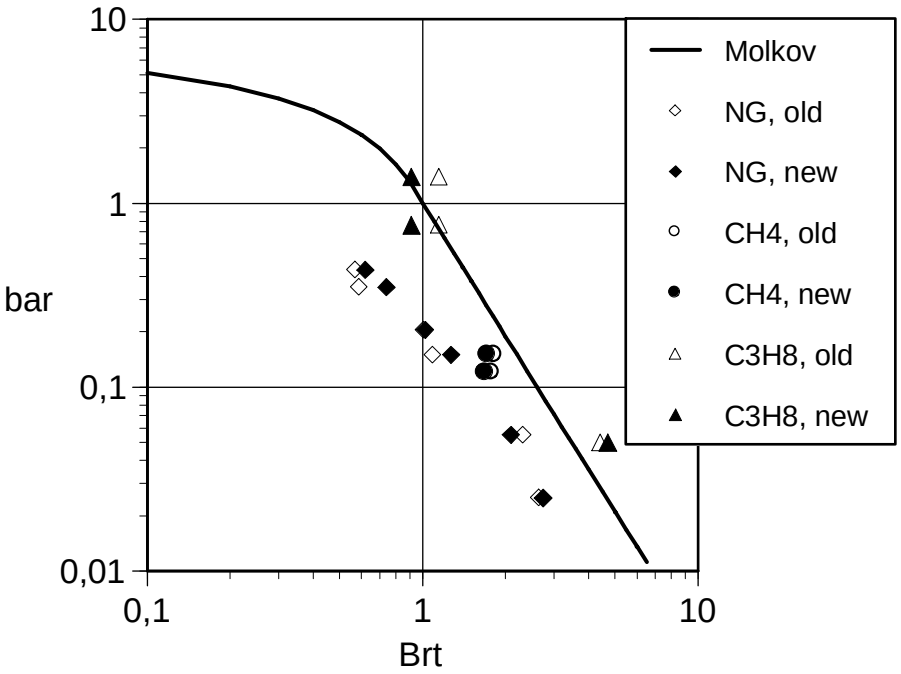

Figure 7. Values of Br_t with the experimental values of P_{red} in tests with an initially uncovered vent.

To calculate the relative error, the gauge pressures in Tables 5 to 8 are converted into absolute ones and inserted in Eq. (40). The results are presented in Table 9.

Table 9. Relative errors of the predictions (uncovered vent)

fuel	tests	Eq. (15)	Eq. (17/18)	α = 0.9, β = 1	α = 1.75, β = 0.5
natural gas	6	48 %	176 %	23 %	59 %
methane, propane	5	12 %	61 %	10 %	13 %
all fuels	11	32 %	124 %	17 %	38 %

It is seen from Table 9 that Eqs. (17/18) overestimate the results of the tests with initially uncovered vents, whereas Eq. (15) gives significantly better results. The earlier version of Molkov correlations with $\alpha = 0.9$ and $\beta = 1$ gives the best predictions and the later version with $\alpha = 1.75$ and $\beta = 0.5$ has an accuracy comparable to that of Eq. (15) by Bradley and Mitcheson (1978b).

Next, the Bradley and Mitcheson correlations Eqs. (18) and (19) are applied to tests with covered vents. There were 4 tests with natural gas-air and 13 tests both with methane-air and propane-air.

The experimental data in Table 10 is taken from (Cooper et al. 1986) and (Harrison & Eyre 1987). The parameters and result of test 1 is taken from Figure 4b of (Cooper et al. 1986). The test was performed with 10 % natural gas-air mixture.

The tests 8, 9 and 10 were performed by Harrison and Eyre (1987) in a 30.4 m^3 explosion chamber, 5.92 m long, 2.38 m wide and 2.16 m high. The tests were denoted as B6, B5 and B7, respectively. The vent was covered by thin polythene sheeting. The values of P_{stat} in these tests were assumed equal to the P_1 values extracted by Molkov (1999) from Figure 2 of (Harrison & Eyre 1987). All tests were performed with 10 % natural gas-air mixture. The natural gas used by Harrison and Eyre (1987) was a mixture of 96 % methane and 4 % ethane.

The experimental data in Table 11 is taken from Bartknecht (1993). Data for tests 1 and 2 have been extracted from (upper) Figure 2.223, which presents test data and fitted curves for P_{red} in a 1 m^3 cylindrical vessel as a function of the vent opening pressure P_{stat} for three values of vent area A_v. In tests 1 and 2, P_{stat} was 0.5 bar and A_v was 0.16 and 0.36 m^2, respectively. The data for tests 3 to 6 has been produced by reading the values of P_{red} corresponding to the vent areas A_v = 0.1, 0.2 and 0.3 m^3 and the values of P_{stat} = 0.1, 0.2 and 0.5 bar from the curves of (lower) Figure 2.223.

The experimental data in Table 12 is taken from Bartknecht (1993) and Pasman et al. (1974). The data for tests 7 to 11 has been read from the curves of (lower) Figure 2.223 of Bartknecht (1993). The tests 12 and 13 were performed by Pasman et al. (1974) in a cylindrical vessel of 0.97 m internal diameter and 0.95 m^3 volume with stoichiometric (9.5 %) methane-air. Molkov (1999) has extracted the values P_{red} = 2.0 bar (test 12) and P_{red} = 1.0 bar (test 13) from Figure 3 of (Pasman et al. 1974).

The experimental data in Table 13 is taken from Bartknecht (1993), Runes (1972) and Molkov (1999). The data for tests 1 to 3 has been read from the curve of Figure 2.219 of Bartknecht (1993). Tests 4 and 5 were performed in Sweden in 1957 with a 204 m^3 enclosure (Runes 1972). Since the value of P_{stat} is not given, these tests cannot be used to validate Eq. (19) or Eqs. (20) to (25). Test 6 was performed by Molkov (1999) in a cylinder with a diameter of 2.0 m, a length of 2.5 m using a 4.05 % propane-air mixture.

The experimental data in Table 14 is taken from (Harrison & Eyre 1987) and (Pegg et al. 1992). Test 7 was performed in the same 30.4 m^3 explosion chamber

as methane tests 8, 9 and 10. It is denoted by Harrison and Eyre (1987) as B17 and the measured value of P_{red} is 0.425 bar. Razus and Krause (2001) give a value of 0.70 bar for this test, which is erroneous.

Tests 8 to 12 were performed by Pegg et al. (1992) in a cylindrical vessel of 0.91 m internal diameter and 0.65 m^3 volume. The tests 8, 9, 10, 11 and 12 are denoted by Pegg et al. (1992) as 131Q, 132Q, 133Q, 130T and 138T, respectively. Razus and Krause (2001) give values of P_{red} that are 1 bar higher than original ones for the tests 10, 11 and 12. Probably, they have thought that the values by Pegg et al. (1992) are gauge pressures although they are absolute pressures.

The test 13 was performed by DeGood and Chatrathi (1991) in a cylindrical vessel with V = 2.6 m^3, L/D = 2.3, A_v = 0.56 m^2. Razus and Krause (2001) give the following, erroneous values V = 0.029 m^3 and A_v = 0.034 m^2. On the other hand the ratio L/D has the correct value. The values of P_{stat} = 0.103 bar and P_{red} = 0.19 bar are correct. The latter is the mean value from tests 507, 508 and 509 where a vent cover with w = 3.3 kg/m^2 was used.

The calculation results are presented in Tables 10 to 14 and Figure 8.

Table 10. Prediction of P_{red} for tests with natural gas-air (covered vent)

test	1	8	9	10
V, m^3	2.41	30.4	30.4	30.4
A_s, m^2	11.6	64.0	64.0	64.0
A_v, m^2	0.264	1.33	2.74	1.33
P_{stat}, bar	0.14	0.012	0.023	0.04
$A \times 10^3$	13.7	12.5	25.7	12.5
A/S	1.70	1.54	3.18	1.54
Eq. (18), bar	1.68	1.79	1.08	1.79
Eq. (19), bar	1.19	0.53	0.27	0.84
exp., bar	0.06	0.21	0.22	0.54

Table 11. Prediction of P_{red} for tests with methane-air (covered vent)

test	1	2	3	4	5	6
V, m^3	1	1	1	1	1	1
A_s, m^2	6	6	6	6	6	6
A_v, m^2	0.16	0.36	0.1	0.1	0.1	0.2
P_{stat}, bar	0.5	0.5	0.1	0.2	0.5	0.1
$A \times 10^3$	16	36	10	10	10	20
A/S	2.01	4.53	1.26	1.26	1.26	2.52
Eq. (18), bar	1.49	0.61	2.07	2.07	2.07	1.27
Eq. (19), bar	1.55	0.56	1.52	2.23	2.66	0.64
exp., bar	1.40	0.64	1.40	2.19	1.95	0.84

Table 12. Prediction of P_{red} for tests with methane-air (covered vent)

test	7	8	9	10	11	12	13
V, m^3	1	1	1	1	1	0.95	0.95
A_s, m^2	6	6	6	6	6	5.5	5.5
A_v, m^2	0.2	0.2	0.3	0.3	0.3	0.05	0.1
P_{stat}, bar	0.2	0.5	0.1	0.2	0.5	0.32	0.16
$A\times10^3$	20	20	30	30	30	5.45	10.9
A/S	2.52	2.52	3.78	3.78	3.78	0.687	1.37
Eq. (18), bar	1.27	1.27	0.87	0.87	0.87	3.16	1.95
Eq. (19), bar	0.83	1.17	0.38	0.50	0.70	5.0	1.63
exp., bar	1.48	1.11	0.43	0.77	0.59	2.0	1.0

Table 13. Prediction of P_{red} for tests with propane-air (covered vent)

test	1	2	3	4	5	6
V, m^3	1	1	1	204	204	11
A_s, m^2	6	6	6	219	219	28.3
A_v, m^2	0.2	0.4	0.6	21.6	17.3	1.36
P_{stat}, bar	0.1	0.1	0.1	?	?	0.05
$A\times10^3$	20	40	60	63.5	50.9	28.8
C, %	4.0	4.0	4.0	4.0	4.0	4.05
S_0, m/s	0.45	0.45	0.45	0.45	0.45	0.45
E	7.98	7.98	7.98	7.98	7.98	7.98
$S\times10^3$	9.40	9.40	9.40	9.40	9.40	9.40
A/S	2.13	4.26	6.38	6.76	5.42	3.07
Eq. (18), bar	1.43	0.69	0.31	0.27	0.42	0.49
Eq. (19), bar	0.79	0.33	0.20	—	—	0.38
exp., bar	1.00	0.32	0.14	0.03	0.06	0.09

Table 14. Prediction of P_{red} for tests with propane-air (covered vent)

test	7	8	9	10	11	12	13
V, m^3	30.4	0.65	0.65	0.65	0.65	0.65	2.6
A_s, m^2	64	2.86	2.86	2.86	2.86	2.86	11.2
A_v, m^2	0.58	0.0182	0.0182	0.0324	0.073	0.099	0.56
P_{stat}, bar	0.4	0.65	0.65	0.72	0.86	0.86	0.103
$A\times10^3$	5.44	3.82	3.82	6.80	15.3	20.8	29.8
C, %	4.45	4.8	4.8	4.8	4.8	4.8	5.0
S_0, m/s	0.44	0.40	0.40	0.40	0.40	0.40	0.38
E	8.06	8.00	8.00	8.00	8.00	8.00	7.97
$S\times10^3$	9.27	8.33	8.33	8.33	8.33	8.33	7.88
A/S	0.587	0.458	0.458	0.816	1.84	2.50	3.78
Eq. (18), bar	3.53	4.19	4.19	2.80	1.59	1.28	0.87
Eq. (19), bar	6.6	10.8	10.8	4.9	2.12	1.44	0.81
exp., bar	0.42	5.21	5.30	4.58	2.13	1.74	0.19

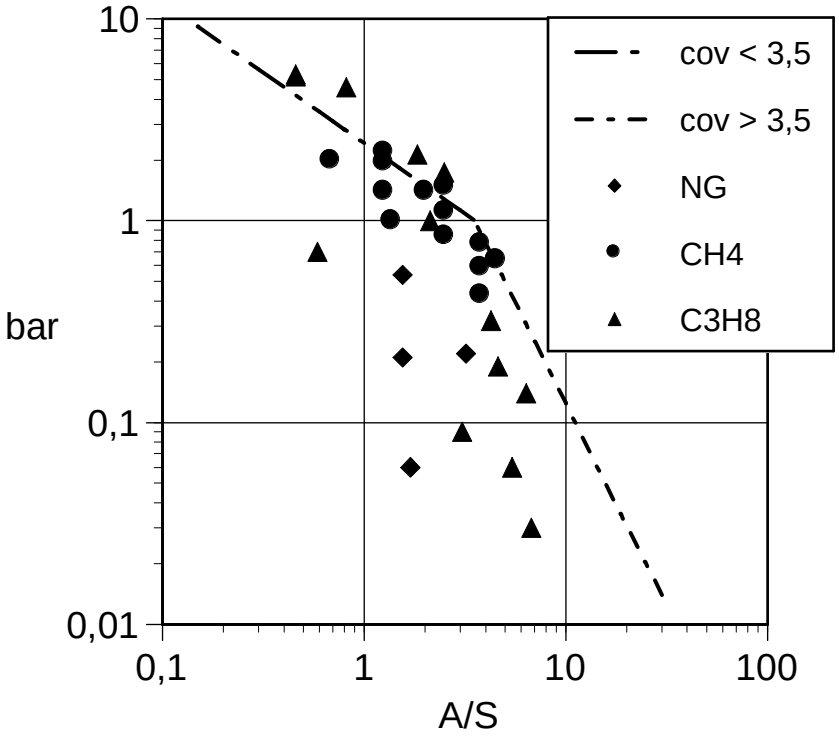

Figure 8. Values of the ratio A/S with the experimental values of P_{red} in tests with a covered vent.

The predictions with the earlier (α = 0.9 and β = 1) and later (α = 1.75 and β = 0.5) Molkov correlations are presented in Tables 15 to 19. The tests that Molkov (1999) has used to demonstrate the superiority of his method over Eq. (30) have been marked with an asterisk (*).

Table 15. Prediction of P_{red} for tests with natural gas-air (covered vent)

test	1	8*	9*	10*
V, m^3	2.41	30.4	30.4	30.4
A_v, m^2	0.264	1.33	2.74	1.33
P_{stat}, bar	0.14	0.012	0.023	0.04
Br	19.8	18.4	38.0	18.4
α, β = 0.9, 1				
χ/μ	5.02	6.91	9.02	6.88
Br_t	1.88	1.27	2.01	1.28
P_M	0.22	0.56	0.19	0.55
P_{red}, bar	0.27	0.57	0.19	0.59
α, β = 1.75, 0.5				
χ/μ	6.00	8.39	9.29	8.35
Br_t	1.58	1.05	1.95	1.05
P_M	0.34	0.89	0.20	0.88
P_{red}, bar	0.41	0.91	0.20	0.94
exp., bar	0.06	0.21	0.22	0.54

Table 16. Prediction of P_{red} for tests with methane-air (covered vent)

test	1	2	3	4	5	6*
V, m^3	1	1	1	1	1	1
A_v, m^2	0.16	0.36	0.1	0.1	0.1	0.2
P_{stat}, bar	0.5	0.5	0.1	0.2	0.5	0.1
Br	21.6	48.6	13.5	13.5	13.5	27.0
α, β = 0.9, 1						
χ/μ	4.37	5.93	3.96	3.89	3.70	5.09
Br_t	2.36	3.91	1.63	1.66	1.74	2.53
P_M	0.128	0.038	0.311	0.298	0.264	0.108
P_{red}, bar	0.23	0.07	0.36	0.39	0.48	0.12
α, β = 1.75, 0.5						
χ/μ	5.12	5.78	5.15	5.06	4.81	5.66
Br_t	2.01	4.01	1.25	1.27	1.34	2.27
P_M	0.187	0.036	0.585	0.560	0.496	0.139
P_{red}, bar	0.34	0.07	0.67	0.73	0.91	0.16
exp., bar	1.40	0.64	1.40	2.19	1.95	0.84

Table 17. Prediction of P_{red} for tests with methane-air (covered vent)

test	7	8	9	10	11	12*	13*
V, m^3	1	1	1	1	1	0.95	0.95
A_v, m^2	0.2	0.2	0.3	0.3	0.3	0.05	0.1
P_{stat}, bar	0.2	0.5	0.1	0.2	0.5	0.32	0.16
Br	27.0	27.0	40.5	40.5	40.5	6.98	13.97
α, β= 0.9, 1							
χ/μ	5.00	4.75	5.93	5.82	5.53	3.04	3.94
Br_t	2.58	2.72	3.26	3.32	3.49	1.10	1.69
P_M	0.10	0.09	0.06	0.055	0.05	0.80	0.28
P_{red}, bar	0.14	0.17	0.07	0.075	0.09	1.21	0.35
α, β= 1.75, 0.5							
χ/μ	5.56	5.29	6.02	5.91	5.62	4.54	5.09
Br_t	2.32	2.44	3.21	3.27	3.44	0.73	1.31
P_M	0.13	0.12	0.06	0.06	0.05	1.86	0.52
P_{red}, bar	0.18	0.22	0.07	0.075	0.095	2.81	0.65
exp., bar	1.48	1.11	0.43	0.77	0.59	2.0	1.0

Table 18. Prediction of P_{red} for tests with propane-air (covered vent)

test	1	2	3	6	7
V, m^3	1	1	1	11	30.4
A_v, m^2	0.2	0.4	0.6	1.36	0.58
P_{stat}, bar	0.1	0.1	0.1	0.05	0.4
C, %	4.0	4.0	4.0	4.05	4.8
S_0, m/s	0.335	0.335	0.335	0.335	0.32
Br	28.3	56.6	84.9	38.9	8.82
α, β= 0.9, 1					
χ/μ	5.18	6.74	7.89	7.95	5.00
Br_t	2.72	4.18	5.35	2.43	0.878
P_M	0.091	0.032	0.018	0.118	1.38
P_{red}, bar	0.10	0.037	0.021	0.13	2.27
α, β= 1.75, 0.5					
χ/μ	5.70	6.34	6.76	8.14	7.12
Br_t	2.47	4.44	6.24	2.38	0.616
P_M	0.014	0.028	0.012	0.125	2.29
P_{red}, bar	0.13	0.032	0.014	0.135	3.77
exp., bar	1.00	0.32	0.14	0.09	0.42

Table 19. Prediction of P_{red} for tests with propane-air (covered vent)

test	8	9	10	11	12	13
V, m^3	0.65	0.65	0.65	0.65	0.65	2.6
A_v, m^2	0.018	0.018	0.032	0.073	0.099	0.56
P_{stat}, bar	0.65	0.65	0.72	0.86	0.86	0.103
C, %	4.8	4.8	4.8	4.8	4.8	5.0
S_0, m/s	0.32	0.32	0.32	0.32	0.32	0.29
Br	3.59	3.59	6.40	14.4	19.5	48.2
α, β= 0.9, 1						
χ/μ	2.28	2.28	2.66	3.40	3.80	7.12
Br_t	0.783	0.783	1.20	2.10	2.56	3.37
P_M	1.69	1.69	0.647	0.168	0.105	0.054
P_{red}, bar	3.56	3.56	1.45	0.42	0.26	0.063
α, β= 1.75, 0.5						
χ/μ	3.84	3.84	4.03	4.36	4.55	6.95
Br_t	0.465	0.465	0.789	1.64	2.14	3.45
P_M	2.91	2.91	1.67	0.304	0.161	0.051
P_{red}, bar	6.12	6.12	3.73	0.77	0.41	0.059
exp., bar	5.21	5.30	4.58	2.13	1.74	0.19

The experimental values of P_M were found by inserting the experimental P_{red} and P_{stat} into Eq. (25). They are plotted in Figure 9 with the calculated values of Br_t. The values of Br_t calculated with the old parameter set $\alpha = 0.9$ and $\beta = 1$ are plotted with open symbols and those calculated with the new one $\alpha = 1.75$ and $\beta = 0.5$ with closed symbols.

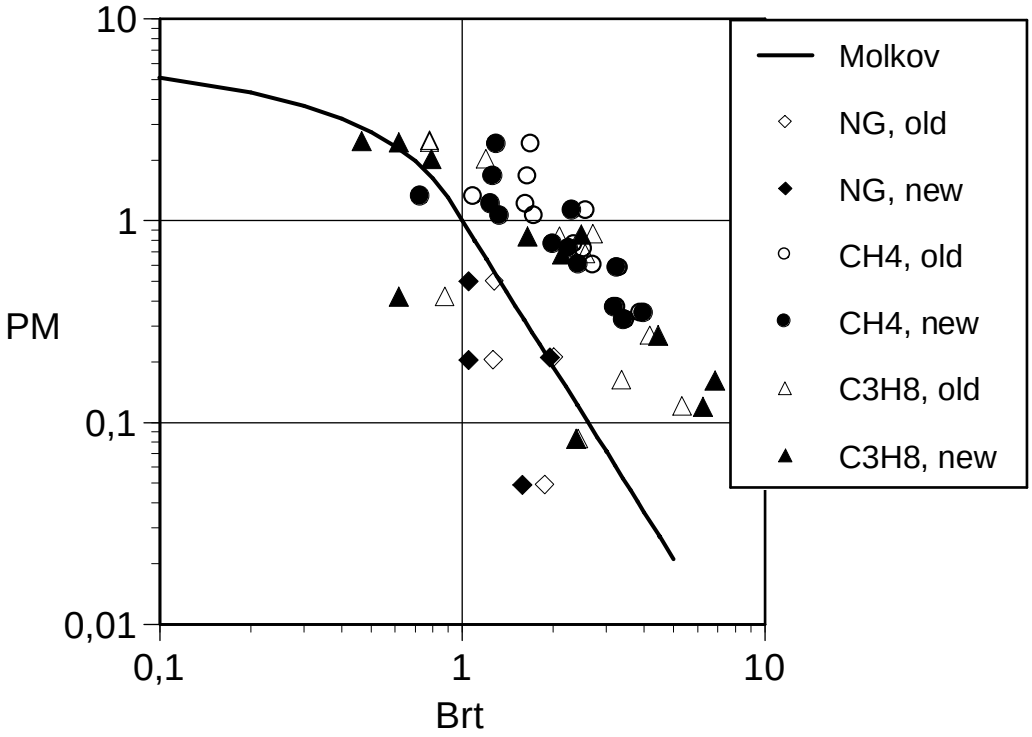

Figure 9. Values of Br_t with the experimental values of P_M in tests with a covered vent.

To calculate the relative error, the gauge pressures in Tables 14 to 19 are converted into absolute pressures and inserted in Eq. (40). The results are presented in Table 20.

Table 20. Relative errors of the predictions (covered vent)

fuel	tests	Eq. (17/18)	Eq. (19)	$\alpha = 0.9$, $\beta = 1$	$\alpha = 1.75$, $\beta = 0.5$
natural gas methane propane	4 13 13/11	108 % 17 % 40 %	39 % 18 % 65 %	13 % 40 % 40 %	28 % 35 % 42 %
meth., prop.	26/24	28 %	40 %	40 %	38 %
all fuels	30/28	39 %	39 %	36 %	37 %

3.8 Initially elevated pressures

Molkov (2001) extended his method to enclosures with initially elevated pressures ($p_0 > p_a$) on the basis of results from the tests by Pegg et al. (1992). These authors performed tests with 4.8 % propane-air mixture in a cylindrical vessel of volume 0.65 m^3 and length to diameter ratio L/D of 1.2. Tests were performed at atmospheric pressure (p_0 = 1.01 bar) and three elevated pressures (p_0 = 3.04, 5.07 and 7.10 bar) with different values of p_{stat} and A_v. In some tests, the flammable mixture was made turbulent with two horizontally opposed fans. In the remaining tests, the mixture was initially quiescent.

Molkov (2001) analysed the experimental pressure traces by Pegg et al. (1992) and found that

— the ratio χ/μ was practically independent of the presence of initial turbulence

— the turbulence generated by the two fans enhanced the flame surface area by 1.53–1.65 times compared to initially quiescent mixture for deflagration in a closed vessel

— the turbulence factor χ for both quiescent and turbulent mixtures in a closed vessel increased slightly with p_0

— the ratio χ/μ increased slightly with p_0

— the decrease of the ratio χ/μ with the increase of p_{stat} agreed with Eq. (22)

— the increase of A_v resulted in growth of the ratio χ/μ at least in the range of p_0 from 1 bar to 3 bar.

From the pressure traces by Pegg et al. (1992), Molkov (2001) derived experimental values of χ and μ. The values of the ratio χ/μ thus found were used to calculate the corresponding turbulent Bradley number Br_t. The values of the parameters S_0 and E used to calculate Br and Br_t are given in Table 21. In Table 21, the values of P_M are calculated by inserting the experimental values of p_0, p_{stat} and p_{red} into Eq. (25). The letters Q and T stand for initially quiescent and turbulent mixtures. The values of P_M and Br_t are plotted in Figure 10.

Table 21. Evaluation of the tests by Pegg et al. (1992)

test	p_0, bar	p_{stat}, bar	p_{red}, bar	P_M	S_0, m/s	E	Br	χ/μ	Br_t
131Q	1.01	1.65	6.22	2.47	0.31	7.95	3.67	4.10	0.447
132Q	1.01	1.65	6.31	2.51	0.31	7.95	3.67	4.04	0.454
133Q	1.01	1.72	5.59	2.04	0.31	7.95	6.55	5.58	0.585
130T	1.01	1.86	3.14	0.84	0.31	7.95	14.79	7.13	1.036
138T	1.01	1.86	2.75	0.69	0.31	7.95	20.14	9.00	1.117
134Q	3.04	4.00	20.26	3.75	0.33	7.90	7.30	9.68	0.375
135Q	3.04	4.14	17.24	2.94	0.33	7.90	11.43	11.08	0.513
136Q	3.04	4.83	16.71	2.25	0.33	7.90	11.43	9.71	0.586
139T	3.04	4.34	10.90	1.52	0.33	7.90	22.46	13.07	0.855
140T	3.04	5.10	12.44	1.42	0.33	7.90	22.46	13.33	0.838
144T	3.04	5.24	8.20	0.75	0.33	7.90	26.54	11.76	1.122
131Q	5.07	7.44	28.92	2.65	0.35	7.96	12.96	11.69	0.554
129Q	5.07	6.96	19.37	1.75	0.35	7.96	18.68	11.48	0.813
141T	5.07	8.27	13.10	0.76	0.35	7.96	25.45	11.25	1.130
142Q	5.07	9.03	15.66	0.88	0.35	7.96	25.45	11.83	1.074
143Q	5.07	9.03	12.48	0.61	0.35	7.96	25.45	10.53	1.208
145Q	5.07	8.82	14.54	0.81	0.35	7.96	30.08	13.64	1.102
159Q	7.10	9.72	34.10	2.37	0.32	8.01	26.35	20.33	0.649
148T	7.10	9.99	22.86	1.33	0.32	8.01	31.14	17.11	0.912
149Q	7.10	9.72	20.31	1.16	0.32	8.01	31.14	16.04	0.973
160Q	7.10	11.99	22.48	0.99	0.32	8.01	31.14	15.52	1.005
161T	7.10	12.41	18.63	0.70	0.32	8.01	31.14	13.68	1.140
162T	7.10	12.68	15.43	0.49	0.32	8.01	31.14	12.50	1.248

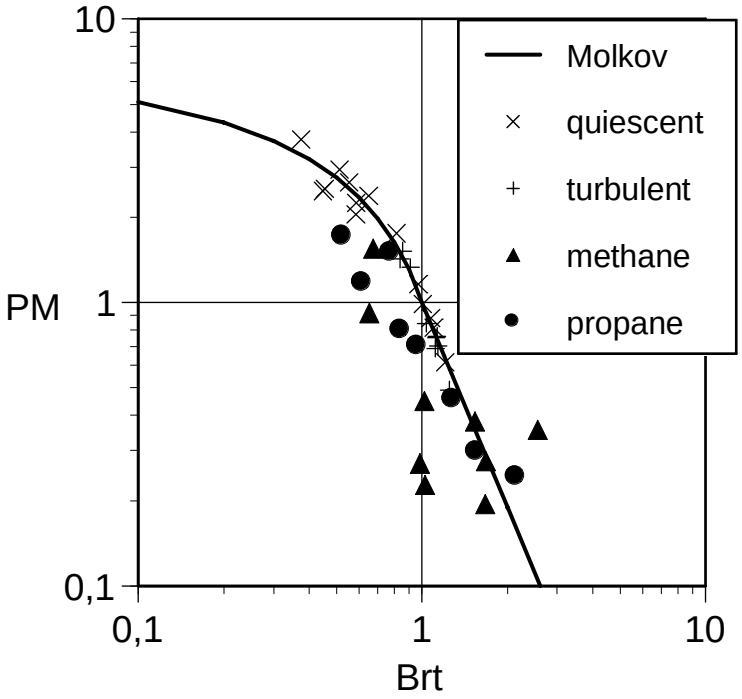

Figure 10. The experimental values of P_M and Br_t (Molkov 2001) redrawn. The test data by Pegg et al. (1992) is shown with crosses and those by Chaineaux and Dannin (1992) with closed symbols.

The correlations Eqs. (23) to (25) are seen to give very good predictions of the test data by Pegg et al. (1992).

Molkov (2001) proceeds to apply the revised correlations to the tests by Chaineaux and Dannin (1992). These authors performed tests with 10.4 % methane-air and 4.8 % propane-air mixtures in a cylindrical vessel of volume 1 m^3 and length to diameter ratio L/D of 4. Tests were performed at four elevated pressures (p_0 = 1.5, 3.0, 4.5 and 5.0 bar) with different values of p_{stat} and A_v.

They also calculated the burning velocity from the propagation times of the flame front between two ionisation gauges mounted at distances of 90 and 140 mm from the ignition source in a spherical vessel of volume 2 m^3. Molkov (2001) uses these values of S_0 and the values of E equal to 7.4 and 7.95 for methane-air and propane-air, respectively. The value of specific heat ratio γ_u is 1.39 and 1.365 for methane-air and propane-air, respectively. The calculation of Br_t by Molkov (2001) is presented in Table 21. In the test with propane-air and p_0 =4.5 bar, the value of the peak pressure p_{red} was lower than the vent opening pressure p_{stat}. This test was excluded of the analysis.

Molkov (2001) comments that the data by Chaineaux and Dannin (1992*)* in Fig. 10 is more scattered than that by Pegg et al. (1992). This may be due to different methods of reducing experimental data. Pegg et al. (1992) used a running average method to filter out the violent pressure oscillations superimposed on the pressure-time trace in the tests with initially quiescent mixtures. Chaineaux and Dannin (1992) do not provide details whether pressure oscillations are included in the values of p_{red} in Table 22.

Table 22. Evaluation of the tests by Chaineaux and Dannin (1992)

fuel	p_0, bar	p_{stat}, bar	p_{red}, bar	P_M	S_0, m/s	E	Br	χ/μ	Br_t
CH_4	1.5	1.8	2.2	0.36	0.38	7.4	40.37	7.53	2.559
CH_4	1.5	1.8	2.25	0.38	0.38	7.4	22.27	6.90	1.541
CH_4	1.5	1.75	2.35	0.45	0.38	7.4	13.92	6.51	1.020
CH_4	3.0	3.85	4.2	0.28	0.39	7.4	39.34	11.20	1.677
CH_4	3.0	3.45	4.0	0.27	0.39	7.4	21.70	10.52	0.985
CH_4	3.0	3.35	6.25	0.92	0.39	7.4	13.56	9.93	0.652
CH_4	4.5	4.75	5.45	0.19	0.28	7.4	54.79	15.68	1.668
CH_4	4.5	5.15	5.75	0.23	0.28	7.4	30.23	14.08	1.025
CH_4	5.0	6.1	15.45	1.55	0.27	7.4	19.59	13.91	0.672
C_3H_8	1.5	1.85	2.0	0.24	0.44	7.95	30.95	7.19	2.149
C_3H_8	1.5	1.8	2.4	0.46	0.44	7.95	17.08	6.65	1.282
C_3H_8	1.5	1.7	2.95	0.8	0.44	7.95	10.67	6.34	0.841
C_3H_8	3.0	3.55	4.15	0.3	0.39	7.95	34.92	11.20	1.557
C_3H_8	3.0	4.05	6.3	0.7	0.39	7.95	19.27	9.98	0.963
C_3H_8	3.0	3.4	7.25	1.17	0.39	7.95	12.04	9.75	0.616
C_3H_8	4.5	4.85	4.1	—	—	—	—	—	—
C_3H_8	5.0	5.2	12.95	1.5	0.33	7.95	22.77	14.69	0.774
C_3H_8	5.0	5.45	14.75	1.71	0.33	7.95	14.34	13.66	0.524

Di Benedetto et al. (2005) discuss the problem of two vessels linked with a duct such as used in the tests by Singh (1994). In the latter tests, the primary vessel volume was varied 0.022–0.077 m^3. The duct length was 0.26 m and its diameter was varied in the range 0.016–0.051 m. The volume of the secondary vessel was varied 0.0015–0.0068 m^3. Tests were performed with methane-air and propane-air mixtures. Initially, the gas mixture in the system was at atmospheric pressure.

After ignition in the primary vessel, flame propagation pushes the mixture through the duct into the secondary vessel. As a consequence, pressure in the latter vessel rises. When the flame enters the secondary vessel, the initial pressure p_i is higher than atmospheric. Furthermore, the flame injection from the duct into the secondary vessel generates intense turbulence, thus leading to an increase in the flame speed.

Eventually, the pressure peak in the secondary vessel after the flame has entered can be much higher than the adiabatic value evaluated from initial atmospheric conditions. This is the result of the balance in the secondary vessel between the rate of production of burned gases and the mass flow through the duct towards the primary vessel. The prediction of the peak pressure in the secondary vessel p_k is needed for any mitigation purpose. However, the value of p_i is also necessary as it represents the pressure at which ignition occurs in the secondary vessel, having influence on the value of p_k.

Di Benedetto et al. (2005) propose to use the Molkov method Eqs. (20) to (25) for the evaluation of p_k because it takes explicitly into account the effects of the initial pressure which in the case of linked vessels is p_i. They calculate the values of Br_t and P_M from the test data by Singh (1977) and add the corresponding data points to Fig. 10. The resulting plot is reproduced as Figure 11.

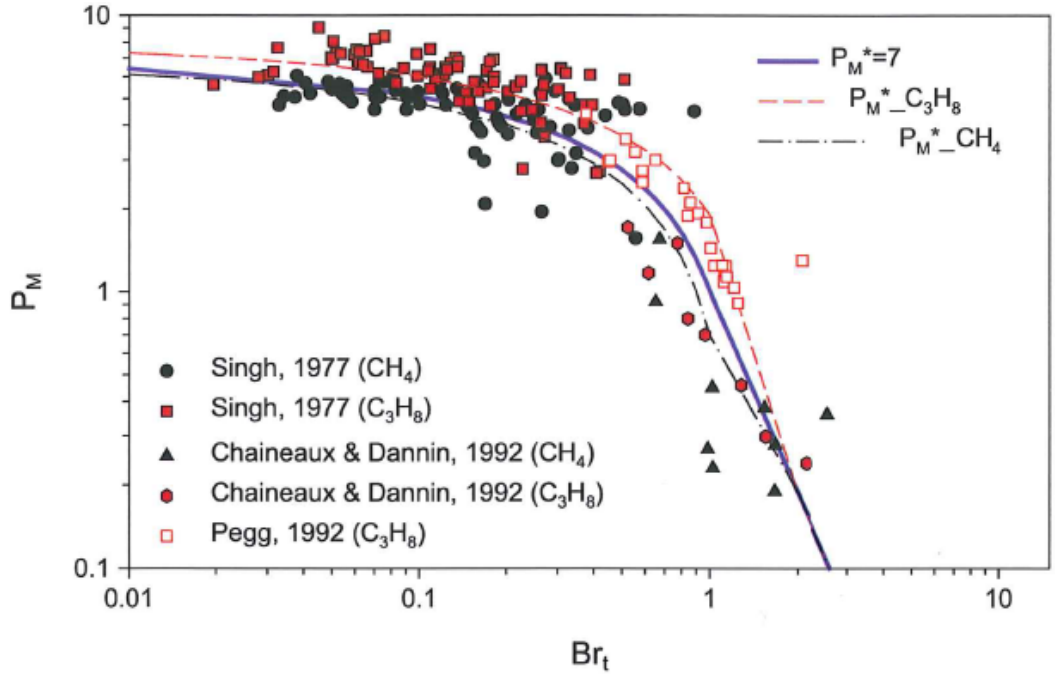

Figure 11. The experimental values of P_M and Br_t (Di Benedetto et al. 2005).

Di Benedetto et al. (2005) conclude on the basis of Fig. 11 that data of simply vented vessels by Pegg et al. (1992) and Chaineaux and Dannin (1992) are better fitted if the number 7 in Eq. (24) is replaced by the ratio P_m/p_0 which would vary if different fuels are used. They use the values 6.7 and 8.2 for methane and propane, respectively.

$$P_M = \frac{P_m}{p_0} - 6Br_t^{0.5} \qquad (41)$$

The range of application of Eq. (41) depends on the value of P_m. In the Molkov method, the curves of Eqs. (23) and (24) intersect at $Br_t = 1$. When a value of P_m/p_0 larger than 7 is used, the intersection shifts to larger values of Br_t. In the opposite case with $P_m/p_0 < 7$, the curves do not intersect. Fig. 11 shows that Di Benedetto et al. (2005) use Eq. (41) for $Br_t \leq 1$ and Eq. (23) for $Br_t \geq 2$. In the range of $1 < Br_t < 2$, the values of P_M are interpolated with a power law: $P_M = 6.7Br_t^{-5.8}$ for methane and $P_M = 2.2Br_t^{-3.54}$ for propane. This is of course an arbitrary choice.

Comparison of Figs. 10 and 11 with each other shows that experimental points corresponding to the tests by Pegg et al. (1992) in Fig. 11 have larger P_M values than those in Fig. 10. Besides, Di Benedetto et al. (2005) present two conflicting definitions for P_M, namely scaled overpressure in Nomenclature and scaled absolute pressure in Section 3.1.4. A scrutiny of Fig. 11 shows that the data points corresponding to the tests by Pegg et al. (1992) have been calculated with the latter, erroneous definition for P_M whereas the correct definition Eq. (24) has been used to plot those corresponding to the tests by Chaineaux and Dannin (1992).

This casts doubt on the validity of Eq. (41), based only on Fig. 11. With the correct values of P_M (Fig. 10), the data points corresponding to the tests by Pegg et al. (1992) are much better predicted by Eq. (24) than by Eq. (41). Those corresponding to the tests by Chaineaux and Dannin (1992) are more scattered and roughly equally well predicted by Eq. (24) and by Eq. (41).

4 Effect of vent ducts

Often the unburned and burned material released from a vent can create a serious threat to personnel or to vulnerable equipment located near the vent. In situations where such a threat exists, installing a vent duct to redirect the discharge to a safe location is a common solution. The disadvantage of a vent duct is the back pressure generated rendering venting through a duct less effective. Factors expected to affect P_{red} are (Ural 2005)

— inertia of the fuel-air mixture occupying the duct
— flame speed and flame acceleration in the enclosure as well as in the duct
— the fact that fuel-air mixture in the duct is limited to that originally in the enclosure
— flow resistance
— wave propagation and interactions in the duct
— choking of the duct due to flow resistance or combustion heat release.

4.1 Bartknecht correlations

Bartknecht (1993) attributes the back pressure to turbulent combustion of the gas mixture in the duct. According to him, the effect of a duct is particularly strong when the flame speed in the duct attains sound velocity, which is to be expected when the duct length L_d [m] exceeds about 3 m. For vent ducts with lengths less than 3 m, vent area A_v must be chosen so that the corresponding overpressure without the duct P'_{red} would be

$$P'_{red} = 0.779 P_{red,vd}^{1.161} \quad (42)$$

For vent ducts with 3 m < L_d ≤ 6 m, a similar equation is given

$$P'_{red} = 0.1723 P_{red,vd}^{1.936} \quad (43)$$

Eqs. (42) and (43) are included in NFPA 68 (2002). In NFPA 68 (2007), the selection of correlation is based both on duct length L_d and length to diameter ratio L_d/D_d. Eq. (42) is to be applied for L_d < 3 m and L_d/D_d < 4. Eq. (43) is to be applied for 3 m < L_d ≤ 6 m or L_d/D_d > 4. However, Eq. (43) is not valid for L_d> 6 m.

Bartknecht (1993) presents equations similar to Eqs. (42) and (43) for the estimation of the effect of a vent duct on overpressures in a vented dust explosion. For vent ducts with lengths L_d less than 3 m, vent area A_v must be chosen so that the corresponding overpressure without the duct P'_{red} would be

$$P'_{red} = 0.3936 P_{red,vd}^{1.529} \quad (44)$$

For vent ducts with 3 m < L_d ≤ 6 m, a similar equation is given

$$P'_{red} = 0.1002 P_{red,vd}^{2.0938} \quad (45)$$

Eqs. (44) and (45) are included in NFPA 68 (1998).

Since Eqs. (42) to (45) have been derived from the same (confidential) test data as Eqs. (33) to (36), they have the same limits of validity as the latter equations.

The withdrawn German guideline for venting of dust explosions VDI 3673 uses a method to account the effect of vent duct on A_v by Siwek (1998). According to Siwek (1998), no further increase of $P_{red, vd}$ occurs when a particular vent duct length L_s [m] is exceeded. Simultaneous measurements of flame speed in the duct

have shown that v_f reaches the order magnitude of sound velocity in the compressed medium. Mainly based on experiments with 1 m^3 and 2.4 m^3 vessels, Siwek (1998) derives an empirical numeric value equation for L_s

$$L_s = 3.764 P_{red}^{-0.3724} \quad (46)$$

which is valid for 0.1 bar ≤ P_{red} ≤ 2 bar. With longer ducts, only the duct resistance has an additional influence on the overpressure in the vessel. Therefore, L_s will be the maximum length that has to be considered.

In the guideline VDI 3673, the coefficient in Eq. (46) has been increased by about 20 % (Moore & Siwek 2002)

$$L_s = 4.564 P_{red}^{-0.37} \quad (47)$$

Experiments have shown that the effect of a vent duct on explosion overpressures decreases markedly with increased L/D ratio of the enclosure. The overpressure for an enclosure with L/D = 1 with a vent duct $P_{red, vd}$ can be calculated from the equation

$$\frac{P_{red,vd}}{P_{red}} = 1 + 17.3 \left(\frac{A_v}{V^{0.753}} \right)^{1.6} L_d \quad (48)$$

For L/D = 6, the overpressure with vent duct $P_{red, vd}$ can be calculated from the equation

$$P_{red,vd} = (0.0586\, L_d + 1.023) P_{red}^{0.981 - 0.01907\, L_d} \quad (49)$$

Determination of the influence of a vent duct for cases where P_m ≤ 2 bar and 1 < L/D < 6 is by linear interpolation from Eqs. (48) and (49). Of course, the values of P_{red} must be calculated for the cases L/D = 1 and L/D = 6 from Eqs. (35) and (36).

The European standard for dust explosion venting EN 14491 contains Eqs. (47) and (48) modified so that the duct lengths L_s and L_d are divided by duct diameter D_d. Thus, sound velocity is attained at

$$L_s / D_d = 4.564 P_{red}^{-0.37} \quad (50)$$

and the overpressure for an enclosure with a vent duct $P_{red, vd}$ is calculated from the equation

$$\frac{P_{red,vd}}{P_{red}} = 1 + 17.3 \left(\frac{A_v}{V^{0.753}} \right)^{1.6} \frac{L_d}{D_d} \quad (51)$$

Eq. (49) is not included in EN 14491.

Eqs. (50) and (51) are mainly based on tests with a 18.5 m^3 vessel. The two sets of equations, Eqs. (47) and (48) and Eqs. (50) and (51), give similar predictions for vessel volumes about 30 m^3. The VDI 3673 equations, Eqs. (47) and (48), give more realistic predictions for volumes up to 30 m^3 whereas the EN 14491 equations, Eqs. (50) and (51), give more realistic predictions for volumes larger than 30 m^3 (Siwek & van Wingerden 2006).

NFPA 68 (2002) recommends the use of Eqs. (46) and (51). NFPA 68 (2007) contains the equations derived by Ural (2005). He criticizes the statement by Siwek (1998) justifying Eq. (46) as contradicting the science of gas dynamics. Consequently, he has eliminated this concept. The vent area required when a duct is attached to the vent opening $A_{v,vd}$ is calculated iteratively from the following equations.

$$A_{v,vd} = A_{v1}(1+1.18E_1^{0.8}E_2^{0.4})\sqrt{\frac{\sum_i \zeta_i}{1.5}} \quad (52)$$

where A_{v1} is the vent area of the enclosure without a vent duct calculated with Eqs. (37) and (38), and $\sum\zeta_i$ is the sum of flow resistance coefficients of the vent duct. The value of the corresponding sum for venting tests without duct has been set at 1.5. The dimensionless quantity E_1 is defined as

$$E_1 = \frac{A_v L_d}{V} \quad (53)$$

and the quantity E_2 as

$$E_2 = \frac{10^4 A_v}{K_{St}\left(1+1.54P_{stat}^{4/3}\right)V^{3/4}} \quad (54)$$

The sum of flow resistance coefficients $\sum\zeta_i$ is calculated assuming fully rough flow regime where the friction factor is only a function of the internal duct surface effective roughness ε

$$\sum_i \varsigma_i = 1.5 + \frac{L_d / D_d}{\left[1.14 + 2\log\left(\frac{D_d}{\varepsilon}\right)\right]^2} + 0.35n_{45} + 1.12n_{90} \quad (55)$$

where n_{45} and n_{90} are the number of 45° and 90° bends, respectively.

The recommended way of iterating Eq. (52) is to replace A_v in Eqs. (53) and (54) by the actual vent area. Then, different values of $P_{red} = P_{red,\,vd}$ are inserted into Eqs. (37) and (38) until the value of $A_{v,vd}$ calculated with Eq. (52) becomes approximately equal to the actual vent area. If the L/D of the enclosure is lower than 2, Eq. (38) is not used, $A_{vl} = A_v$, and the value of $P_{red,\,vd}$ can be solved from Eq. (37).

Under certain circumstances, there can be two solutions for the vent area $A_{v,vd}$. In these cases, the smaller value shall be used. When the equations do not provide a solution for vent area, the design shall be modified by decreasing the vent duct length L_d or strengthening the vessel to contain a higher P_{red} or both.

4.2 Tamanini model

Tamanini and Fischer (2003) assume that the effect of the presence of a duct in vented dust explosions results mainly in reducing the effective vent area. They develop an empirical correlation that replaces, in the correlation valid for simply vented vessels, the actual ducted vent area and duct cross section A_v with an effective open vent of appropriate reduced area A_{eff} [m^2]. The expression for this correlation is

$$\frac{A_v}{A_{eff}} = 1 + 5\Gamma^{3/2}\Phi_d\Psi_d^{1/4} \quad (56)$$

where Γ is the vent parameter, calculated as

$$\Gamma = C_d\sqrt{\gamma_a\frac{\gamma_a+1}{2}\frac{RT_i}{M_a}\frac{A_v}{V^{2/3}}\frac{P_m}{K_{St}}} \quad (57)$$

where γ_a is the specific heat ratio of air, R is the universal gas constant 8.314 J mol^{-1} K^{-1} and M_a is the average molecular mass of air, Φ_d is the duct inertia parameter

$$\Phi_d = \frac{L_d V^{1/3}}{A_v} \frac{M_a}{RT_i} \left(\frac{K_{St}}{P_m} \right)^2 \quad (58)$$

and Ψ_d is the friction loss parameter

$$\Psi_d = \left(0.005 \frac{A_d}{A_v} + 0.35 n_{45} + 1.2 n_{90} \right) \frac{V}{L_d A_v} \quad (59)$$

where A_d [m^2] is the is the internal surface area of the duct.

For a straight duct with circular cross section Eq. (60) can be written as

$$\Psi_d = 0.005 \pi \frac{D_d V}{A_v^2} \quad (60)$$

4.3 Duct venting experiments

Cubbage and Marshall (1972) performed explosion tests with stoichiometric gas-air mixtures in a 0.136 m^3 vessel. The vessel was vented by an orifice whose size was varied so that the vent coefficient K ranged from 4 to 77. In some tests, a duct with a diameter of 76 mm and length to diameter ratio L_d/D_d of 4, 28 or 160 was fitted to the orifice. The gas-air mixture was contained by a polythene bag with a volume of 0.5 dm^3 located at vessel centre.

Most experiments were performed with natural gas with 78.2 % methane, 13.5 % ethane, 4.6 % propane and 1.8 % butane, 0.2 % higher hydrocarbons, 0.3 % nitrogen and 1.4 % oxygen + argon. Stoichiometric natural gas is said to have a burning velocity of 0.36 m/s. To study the effect of S_0 on pressure rise, some tests were performed with stoichiometric town gas with a composition given in Table 25 and S_0 about 0.74 m/s.

Russo and Di Benedetto (2007) have extracted some explosion pressures measured by Cubbage and Marshall (1972) with stoichiometric natural gas. The test results are given in Table 23.

Table 23. Results of the tests by Cubbage and Marshall (1972)

P_{red}, no duct, bar	L_d, m	$P_{red, vd}$, bar
0.07	0.3	0.07
0.07	2.13	0.11
0.07	12.2	0.13

McCann et al. (1985) have performed explosion tests with stoichiometric (9.5 %) methane in two cubical vessels with internal side of 0.18 and 0.38 m, respectively. Circular vents, with diameters ranging from 25 to 160 mm were used. The vents were covered with papers of various quality and thickness or with aluminium foil. These materials along with the different vent areas gave an adequate range of vent opening pressures.

The purpose of the study was to investigate various pressure oscillations and instabilities occurring during a vented explosion. They could be either standing acoustic modes of the vessel or Helmholtz oscillations caused by the coupling of volume generation rate Eq. (7) to the burning velocity by Eq. (3). For values of the vent coefficient K up to 4.2, such oscillations occurred. To show that the

pressure oscillations were of the latter type, several duct lengths were used with the smaller vessel, ranging from 0.1 to 0.5 m, while the vent area was kept constant. No duct was used with the larger vessel.

Russo and Di Benedetto (2007) have extracted the explosion pressures measured in the smaller vessel with a duct from Figure 2 of (McCann et al. 1985). They assume that the vent was initially open, which contradicts the description of the test apparatus. The origin of the value of P_{red} = 0.079 bar is unclear. The vent area A_v used in the tests (0.01 m^2 which corresponds to K = 3.25) has been retrieved using the data for oscillation period and sound velocity for the three duct lengths. The test results are given in Table 24.

Table 24. Results of the tests by McCann et al. (1985)

side 0.18 m	K = 3.25		side 0.38 m	K = 18.4
P_{red}, no duct, bar	L_d, m	$P_{red, vd}$, bar	P_{stat}, bar	P_{red}, bar
0.079	0.105	0.10	0.30	0.28
0.079	0.30	0.19	0.40	0.40
0.079	0.50	0.17	0.503	0.50

Kordylewski and Wach (1986) have performed explosion tests with town gas in a 20 dm^3 spherical vessel. The vessel had at one end a 25 mm opening connected to a steel tube with equal diameter and the other end fully open. The tube length was varied between 0 m (i.e. no tube) and 2.5 m. While the vessel was being filled, the open end was covered with a rubber plug. The composition of town gas is given in Table 25. Using the molar masses M_i and molar specific heat capacities C_p and C_v of the components, the average molar mass M and the molar specific heat capacities C_p and C_v of town gas at 20 °C are calculated. The heavier hydrocarbons C_mH_n are replaced by ethane C_2H_6.

Table 25. Composition of town gas, volume per cent

comp.	M_i, g/mol	C_p/R	C_v/R	KW86	KW88	CM72	MW07
CH_4	16	4.28	3.27	30.2	24.4	31.6	25.3
C_2H_6	30	6.29	5.25	2.0	1.8	0.7	2.3
CO	28	3.51	2.51	6.6	8.4	1.6	5.5
H_2	2	3.46	2.46	45.6	46.8	51.6	54.5
CO_2	44	4.48	3.45	3.0	3.6	1.5	2.3
O_2	32	3.54	2.53	0.4	0.2	0.3	0.5
N_2	28	3.51	2.50	12.2	14.8	12.7	9.6
M, g/mol				13.1	13.5	11.1	11.2
C_p/R				3.81	3.76	3.76	3.76
C_v/R				2.80	2.76	2.76	2.76
LFL, %				5.3	5.7	5.0	4.9
C_{st}, %				17.9	19.8	18.6	20.3
UFL, %				31	34	31.5	33.7

In addition to the Polish town gases used by Kordylewski and Wach (1986, 1988), compositions of British town gas (Cubbage & Marshall 1972) and German town gas (Milani & Wünnig 2007) are given in Table 25. It seems that in Table 1 of (Cubbage & Marshall 1972) the percentages of CO_2 and N_2 have been interchanged. This probable misprint has been corrected to make the CO_2 and N_2

concentrations of the British town gas comparable to those of the Polish and German town gases.

The influence of the town gas concentration on P_{red}, $P_{red,\ vd}$, and $(dP/dt)_{max}$ without and with a 2.5 m long tube is depicted in Figure 12. The influence of tube length L_d on $P_{red,\ vd}$ and $(dP/dt)_{max}$ for 20 % town gas concentration is shown in Figure 13.

Fig. 12 shows that P_{red}, $P_{red,\ vd}$ and $(dP/dt)_{max}$ have a maximum value at 25 % concentration irrespective of whether the venting takes place through the duct or not. This was expectable because these curves are qualitative similar to the laminar burning velocity S_0 as a function of town gas concentration. Fig. 13 shows an unexpected result: both $P_{red,\ vd}$ and $(dP/dt)_{max}$ have a strong maximum at L_d = 0.3 m or L_d/D_d = 12.

Note that the curve fits of P_{red} and $P_{red,\ vd}$ in Fig. 12 intersect near 30 % town gas concentration. At this concentration, the value of $P_{red,\ vd}$ is only about half the value of P_{red}. Such a decrease of explosion pressure when a duct is added to the explosion vessel has not been observed in the other tests of the data set used by Russo and Di Benedetto (2007).

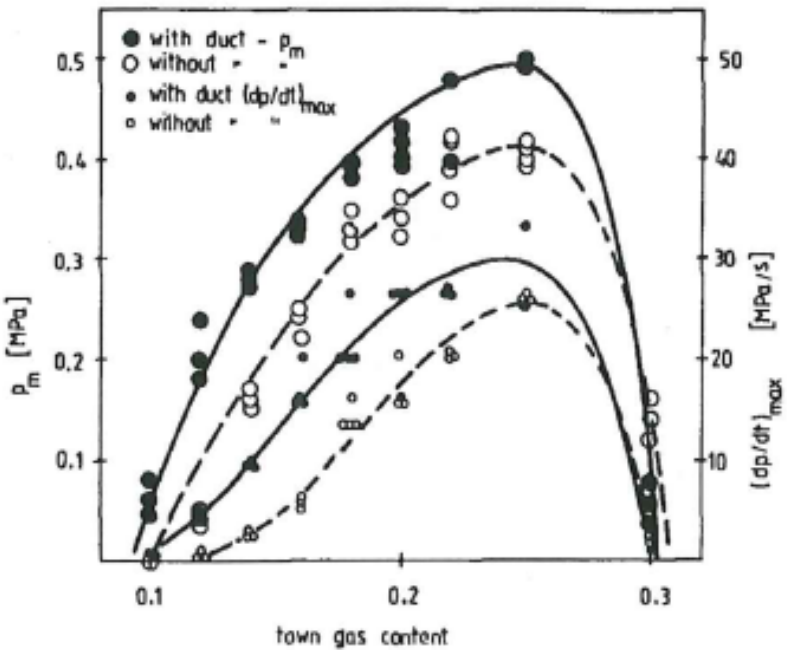

Figure 12. The influence of the town gas concentration on P_{red}, $P_{red,\ vd}$, and $(dP/dt)_{max}$ without and with a 2.5 m long tube (Kordylewski and Wach 1986).

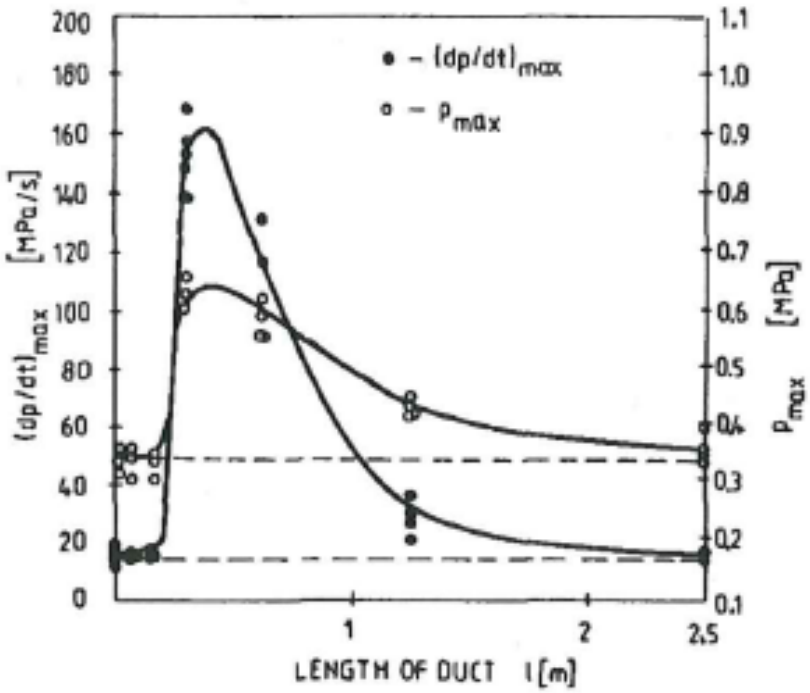

Figure 13. The influence of tube length on $P_{red, vd}$ and $(dP/dt)_{max}$ for 20 % town gas concentration (Kordylewski and Wach 1986).

Figs. 12 and 13 show that Kordylewski and Wach (1986) made three or four tests with each concentration or duct length value. Russo and Di Benedetto (2007) have extracted the highest explosion pressures P_{red} and $P_{red, vd}$ from Figs. 12 and 13. These values are presented in Table 26.

Table 26. Results of the tests by Kordylewski and Wach (1986)

C, %	P_{red}, bar	L_d, m	$P_{red, vd}$, bar
10	0	2.5	0.82
12	0.5	2.5	2.38
14	1.7	2.5	2.91
16	2.5	2.5	3.47
18	3.4	2.5	4.0
20	3.6	2.5	4.3
22	4.2	2.5	4.82
25	4.2	2.5	5.0
30	1.6	2.5	0.82
20	3.7	0.04	3.68
20	3.7	0.17	3.68
20	3.7	0.3	6.71
20	3.7	0.61	6.36
20	3.7	1.26	4.57
20	3.7	2.5	4.0

In the test with 30 % town gas-air mixture, the value of $P_{red, vd}$ 0.82 bar is only about about half the value of P_{red} 1.6 bar.

Kordylewski and Wach (1988) report the results of additional tests in a 22 dm^3 vessel. All the tests were performed with 18 % concentration of town gas whose composition is given in Table 25. To study the effect of pipe diameter, 21 mm and

35 mm tubes were used along with the 25 mm tube. Tube lengths up to L_d/D_d = 200 were used. Using a duct with L_d/D_d = 100, $P_{red, vd}$ was found to be almost independent of duct diameter D_d, while P_{red} decreased steeply with increasing D_d (Figure 14).

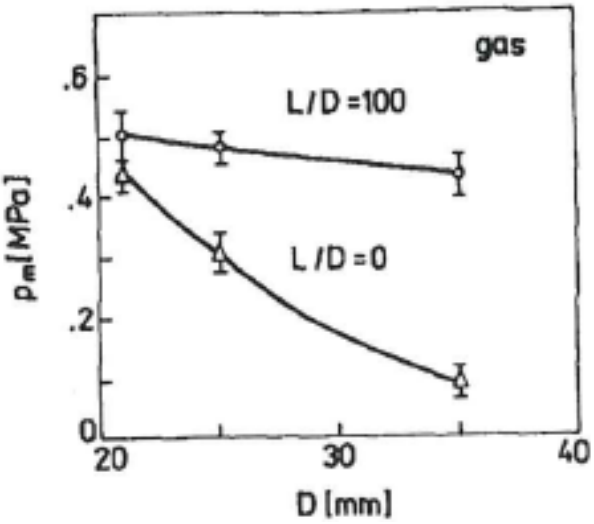

Figure 14. The influence of tube diameter D_d on explosion overpressure for two tube lengths (Kordylewski and Wach 1988).

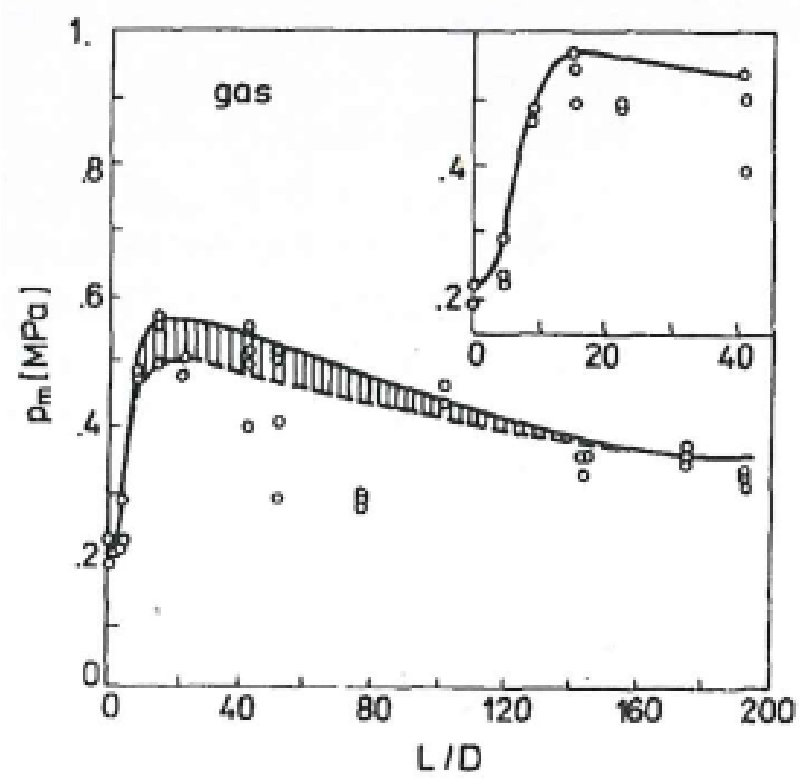

Figure 15. The influence of tube length to diameter ratio L_d/D_d on $P_{red, vd}$ for 18 % town gas concentration and D_d = 35 mm (Kordylewski and Wach 1988).

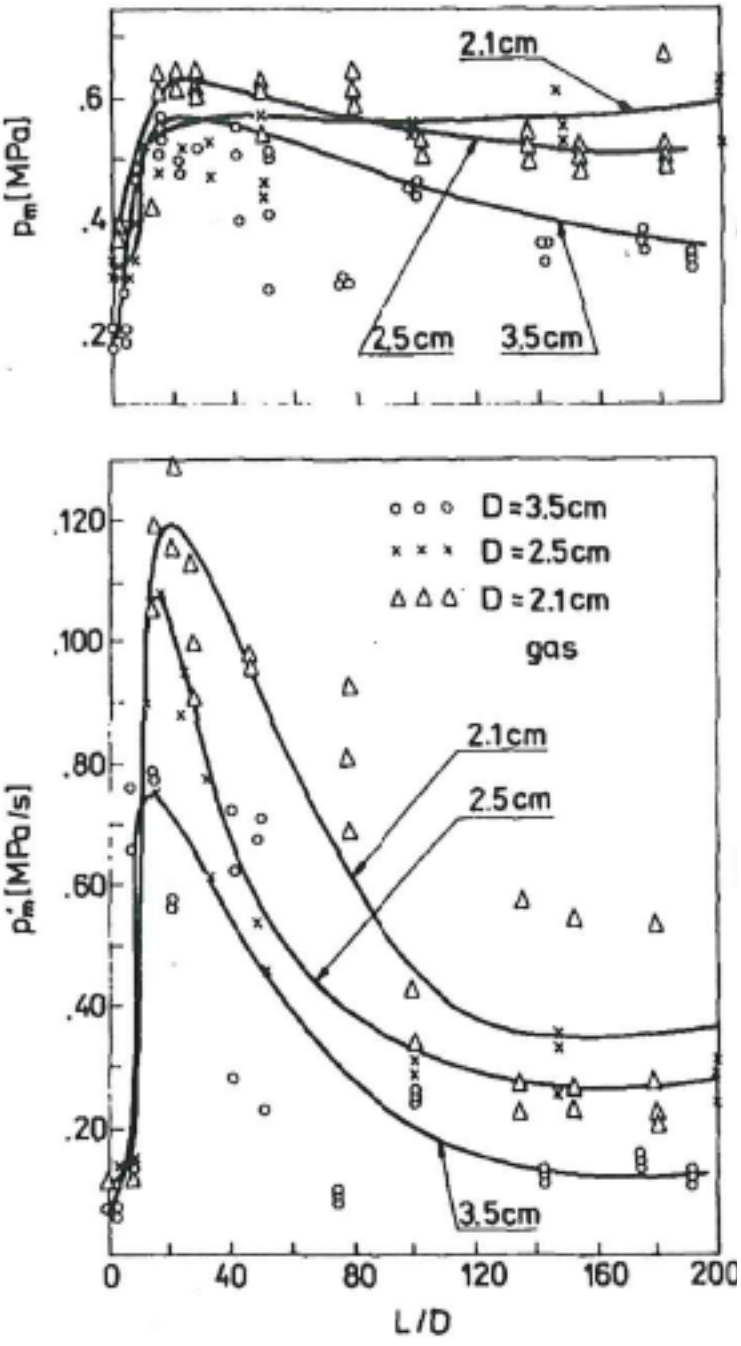

Figure 16. The influence of L_d/D_d on $P_{red,\,vd}$ for 18 % town gas concentration (upper plot). The tube diameter is 21, 25 or 35 mm. Note that the labels for 21 mm and 25 mm tubes have been interchanged (Kordylewski and Wach 1988).

Figs. 15 and 16 show that Kordylewski and Wach (1988) have made three or four tests with each duct length value. Russo and Di Benedetto (2007) have extracted the highest measured explosion pressures P_{red} and $P_{red,\,vd}$. The correct value of $P_{red,\,vd}$ for L_d = 2.8 m, however, is 3.0 bar and not 2.14 bar as used by Russo and Di Benedetto (2007). These values are presented in Table 27.

Table 27. Results of the tests by Kordylewski and Wach (1988)

D_d, mm	P_{red}, bar	L_d, m	$P_{red, vd}$, bar
35	2.0	0.16	3.0
35	2.0	0.32	4.82
35	2.0	0.54	5.65
35	2.0	0.8	4.82
35	2.0	1.4	5.13
35	2.0	1.75	5.18
35	2.0	2.8	3.0
35	2.0	3.5	4.64
35	2.0	4.91	3.57
35	2.0	6.14	3.75
35	2.0	6.75	3.39
21	4.2	2.5	5.0
25	3.0	2.5	4.73
35	1.0	2.5	4.2

DeGood and Chatrathi (1991) have performed explosion tests with 5 % propane in a 2.6 m^3 cylindrical vessel with a length to diameter ratio L/D of 2.3. The vessel was vertical with a 0.61 m × 0.91 m vent located on the top. Nominal vent opening pressure P_{stat} was 0.1 bar and vent surface mass 4.9 kg/m^2. Tests were performed without and with a vent duct having a cross section equal to that of the vent. Three values were used for length of the vent duct L_d: 1, 2 and 3 m. The mixture was ignited at the centre, and for L_d = 3 m, also at the bottom of the vessel. Test results are given in Table 28. The values of P_{red} and $P_{red, vd}$ are mean values of the number of tests given in brackets.

Table 28. Results of the tests by DeGood and Chatrathi (1991)

ignition	P_{red}, bar	L_d, m	$P_{red, vd}$, bar
centre	0.20 (7)	1	0.185 (5)
centre	0.20 (7)	2	0.300 (5)
centre	0.20 (7)	3	0.385 (5)
bottom	0.15 (4)	3	1.01 (1)

Note that the addition of a 1 m long duct to the vessel gave slightly lower value of $P_{red, vd}$ than P_{red}. This was not due to random deviations since the tests were repeated as shown in Table 28.

Molkov et al. (1993) have performed explosion tests with stoichiometric (4.9 %) acetone vapour-air mixture at different initial temperatures T_0 in 0.027, 2 and 10 m^3 cylindrical vessels with L/D equal to 1, 2.6 and 3.4, respectively. The ducts vented to receiver vessels of volume 0.05, 3.2 and 12 m^3, respectively, with an initial pressure of 0.2 bara. Different values of duct diameter D_d, duct length L_d and vent opening pressure P_{stat} were used. The values of S_0 corresponding to T_0 have been calculated with Eq. (1).

The mixture was ignited at vessel centre. Test results are given in Table 29. In two tests marked with a dagger (†), the membrane that closed the vent did not open fully. In the test denoted with an asterisk (*), the mixture was ignited near the vent.

Table 29. Results of the tests by Molkov et al. (1993)

V, m^3	D_d, mm	L_d, m	P_{stat}, bar	S_0, m/s	$P_{red, vd}$, bar
0.027	50	—	0.22	0.29	0.6
0.027	50	1.83	0.19	0.26	5.0†
0.027	50	2.35	0.24	0.28	4.4
0.027	50	2.35	0.24	0.28	3.5
0.027	50	2.35	1.64	0.29	1.9
0.027	50	1.83	1.41	0.29	4.4†
2	200	—	0.14	0.315	3.0*
2	200	4	0.14	0.325	4.3
2	200	10	0.14	0.335	5.2
2	380	10	0.14	0.295	2.15
10	500	25	0.1	0.32	4.1
10	500	25	0.05	0.27	2.8

Ponizy and Leyer (1999a) have performed explosion tests with stoichiometric propane in a 3.66 dm^3 cylindrical vessel with a length to diameter ratio L/D of 3.7. The tube diameters D_d used were 16, 21, 36 and 53 mm. Tube length L_d ranged from 0.6 to 2.6 m. The tube was open at both ends. The mixture was ignited at the rear end of the vessel. No tests were performed without a duct. Russo and Di Benedetto (2007) have extracted the measured explosion pressures $P_{red,vd}$ from Fig. 9 of Ponizy and Leyer (1999a). These are presented in Table 30.

Table 30. Results of the tests by Ponizy and Leyer (1999a)

D_d, mm	L_d, m	$P_{red, vd}$, bar
16	0.6	1.45
21	0.6	1.17
36	0.6	1.27
16	1.1	1.80
21	1.1	1.45
36	1.1	1.92
16	2.6	1.92
21	2.6	1.55
36	2.6	1.92
53	2.6	2.11

Ponizy and Leyer (1999b) performed additional tests with stoichiometric propane in the 3.66 dm^3 cylindrical vessel. Pipe diameter D_d was 36 mm and pipe length L_d 1.7 m. The mixture was ignited either at rear, in centre or near the vent. In addition to an open vent (P_{stat} = 0), several values of the vent opening pressure were used. Test results from Tables 1 to 3 in Ponizy and Leyer (1999b) are presented in Table 31. The values of $P_{red, vd}$ in Table 31 are mean values of the number of tests in brackets.

Table 31. Results of the tests by Ponizy and Leyer (1999b)

ignition	P_{stat}, bar	$P_{red, vd}$, bar
centre	0	2.01 (10)
centre	0.3	2.16 (2)
centre	0.91	2.66 (5)
centre	2.3	3.37 (5)
rear	0	1.76 (7)
rear	0.32	1.88 (2)
rear	0.83	1.81 (5)
near vent	1.11	1.27 (2)
near vent	2.24	2.24 (2)

4.4 Effects of a vent duct on venting

Russo and Di Benedetto (2007) perform a critical review on existing methods to estimate the effects of a vent duct on venting of gas explosions. They note that different phenomena have been studied as possible causes of the increased severity of the explosion in an enclosure vented through the duct:

1. Frictional losses in the duct.
2. Duct gas column inertia.
3. Burn-up in the duct.
4. Acoustic oscillations.

In order to reduce the peak pressure P_{red} in enclosures without a vent duct, the vent area A_v has to be increased. In the presence of a duct, however, an increase of A_v and the duct diameter D_d does not always lead to a decrease in P_{red}. The effect of D_d on gas explosion behaviour was studied by Kordylewski & Wach (1988), Molkov et al. (1993), and Ponizy and Leyer (1999a) in different configurations and for different fuels.

In all the experiments by Kordylewski & Wach (1986, 1988) and Molkov et al. (1993), an increase in D_d decreased P_{red}. Kordylewski & Wach (1988) reported only a weak dependence of P_{red} on D_d (Fig. 14). Later, Ponizy and Leyer (1999a) found that P_{red} exhibited a minimum on increasing D_d. In Figure 17, the data of P_{red} as a function of D_d in Table 30 are shown.

In enclosures without a vent duct, the ignition position strongly affects P_{red}. When the ignition location is close to the vent area, burned gases are vented at an early stage of the combustion, and this allows a reduction of P_{red}. In the case of a central ignition, venting is less effective and the flame propagation in both directions causes flame instabilities which increase the flame area A_f and P_{red}. At the same time central ignition favours a reduction of P_{red} due to heat losses to enclosure walls.

In the presence of a duct, similar behaviour is observed. Ponizy and Leyer (1999b) carried out experiments at different vent opening pressures P_{stat} with ignition in the centre, at the rear wall or near the vent. Table 31 shows that P_{red} increases when ignition occurs at centre with respect to both rear wall and near vent ignition. Ignition near vent had the smallest value of P_{red} since in this case no intensification of combustion in the vessel was observed. In the case of rear

ignition, the flow rate of unburned gas through the vent is higher. This decreases the amount of unburned mixture remaining in the vessel at the moment of burn-up in the vent duct and the resulting backflow.

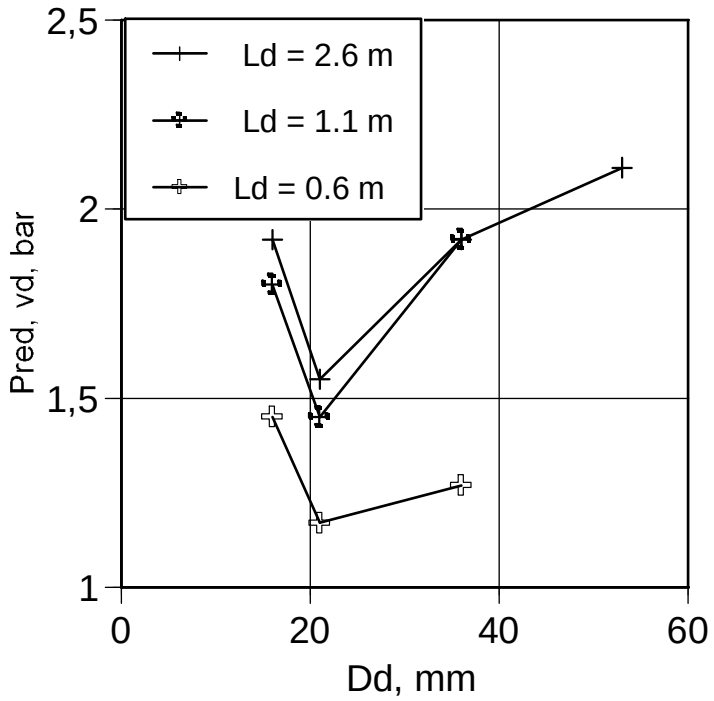

Figure 17. Effect of vent duct diameter D_d on P_{red} (Ponizy and Leyer 1999a).

The duct length L_d is one of the most important parameters affecting the explosion behaviour. The data by Kordylewski & Wach (1988) (Fig. 15) shows that P_{red} exhibited a maximum at $L_d/D_d = 15$. The most extensive study on the effect of L_d was performed by Ponizy and Leyer (1999a). They observed that by increasing L_d the pressure in the vessel when the flame reaches the duct entrance increases. They attributed this behaviour to both frictional drag and the inertia of the gas column in the duct. An increase in L_d and, hence, of frictional drag and the inertia of the gas column results in reduced outflow and a higher fraction of unburned mixture present in the vessel. Consequently, the intensification process is much more effective, causing a higher combustion rate and P_{red} in the vessel.

Moreover, Ponizy and Leyer (1999a) showed that L_d also affected the turbulent mixing in the duct, which increased as L_d increased. Consequently, quenching phenomena in the duct are more pronounced at lower values of L_d. Quenching is strongly affected by both L_d and D_d. Indeed, it is more pronounced for smaller values of L_d and D_d. In this case, an increase in L_d or D_d should decrease P_{red}. The competition between frictional drag and gas column inertia and quenching phenomena could result in non-monotonic trend of peak pressure as a function of L_d. If frictional drag and gas column inertia are not present, L_d only affects the quenching and is compensated by D_d. This could explain the peak in Fig. 13. However, these observations require justification (Russo and Di Benedetto 2007).

The effect of vent opening pressure P_{stat} was studied by Ponizy and Leyer (1999b), Molkov et al. (1993) and Molkov (1994). These results were obtained for different vessel volumes, duct diameters and lengths, ignition positions and fuels. Ponizy and Leyer (1999b) observed that in the case of central and rear ignition the

combustion intensification process is the same as that induced for freely vented explosions initiated near the rear wall.

Molkov (1994) found that at low P_{stat} values (P_{stat} < 1 bar) $P_{red, vd}$ increased with increasing P_{stat}, while the opposite behaviour was observed at higher values (P_{stat} > 1 bar). He explained this result as follows. At high values of P_{stat}, the gas mixture in the vessel is almost completely burned. As a consequence, when the vent opens, the turbulent explosion in the duct does not have any effect on the turbulence inside the vessel due to lack of "power". At low values of P_{stat}, when the vent opens, the mixture in the vessel is still not completely burned. Then, after significant and fast energy release during the explosion in the duct, the turbulence in the vessel and combustion intensity increase due to backflow.

On the contrary, the data of Ponizy and Leyer (1999b) in Table 31 show an increase in $P_{red, vd}$ with increasing P_{stat} for both central and near vent position of the ignition. Moreover, most of the experimental data refer to tests carried out with an initially open vent.

Most of the experiments reported in the literature have been performed with small (< 1 m^3) vessels. Molkov (1994) performed experiments in both small and large vessels and showed that by increasing the vessel volume, P_{red} can increase. This result was explained by taking into account the effect of turbulence induced by the backflow of the gas from the duct to the vessel. He commented that when larger vessels are considered, the turbulence in the vessel can be higher due to the increase in Reynolds number.

5 Validation of correlations

5.1 Bartknecht method

Russo and Di Benedetto (2007) use all the published data from gas explosion tests with a vent duct to validate the correlations presented in the literature. First, they test the validity of the assumption of Bartknecht (1993) that $P_{red, vd}$ is a function of P_{red} and the duct length L_d, which can be taken into account stepwise. The corresponding correlations Eqs. (39) and (40) assume that the effect of duct diameter D_d, vessel volume V and vent opening pressure P_{stat} is included in the correlation for P_{red}.

They plot the experimental data points of $P_{red, vd}$ as a function of P_{red} given in Tables 26 to 29. The correlations Eqs. (42) and (43), however, have been misinterpreted so that the quantity P'_{red} is understood to be the value of $P_{red, vd}$. The relevant correlations are (Bartknecht 1993)

$$P_{red,vd} = 1.24 P_{red}^{0.8614} \quad (61)$$

and

$$P_{red,vd} = 2.48 P_{red}^{0.5165} \quad (62)$$

The plots by Russo and Di Benedetto (2007) are redrawn as Figures 18 and 19 where Eqs. (61) and (62) are drawn as curves. Note that Eq. (61) has been extrapolated beyond its limit of validity $P_{red} \leq 2$ bar.

Russo and Di Benedetto (2007) conclude that P_{red} cannot be viewed as the unique parameter affecting $P_{red, vd}$. It is clear that for a fixed value of P_{red} different values of $P_{red, vd}$ are possible. It is also seen from Figs. 18 and 19 that Eqs. (61) and (62) are non-conservative i.e. they underestimate the value of $P_{red, vd}$.

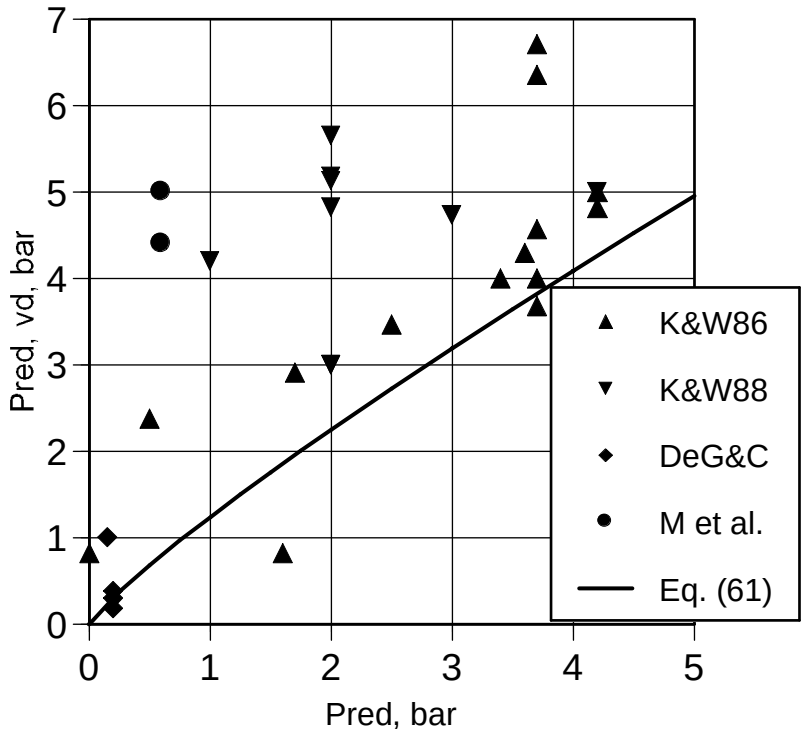

Figure 18. Effect of vent duct (L_d < 3 m) on P_{red}. Experimental points and Eq. (61).

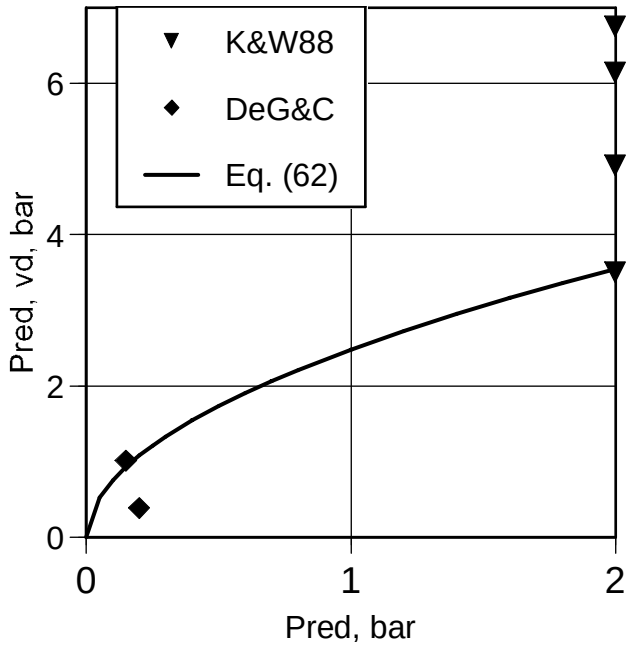

Figure 19. Effect of vent duct (3 m ≤ L_d ≤ 6 m) on P_{red}. Experimental points and Eq. (62).

5.2 Explosion pressures without a vent duct

Unfortunately, the maximum explosion pressure for enclosures without a vent duct P_{red} had been measured only in some test series. To overcome this paucity of data, the missing values of P_{red} were estimated by Russo and Di Benedetto (2007). First, they test the capabilities of the Bradley and Mitcheson (1978b) correlations Eqs. (15) to (19) and the Molkov correlations Eqs. (20) to (24) to predict the measured values of P_{red}. In Eq. (22) both sets of the parameters α and β for hydrocarbon-air mixtures were used. This calculation is now repeated.

5.2.1 Town gas-air mixtures

Kordylewski & Wach (1986, 1988) have measured P_{red} both without and with a vent duct. So, their results can be used to test the capabilities of existing correlations to predict the measured values of P_{red}. Note that the correlation for high-strength enclosures by Bartknecht Eq. (33) cannot be used for these tests with an initially open vent. The problem with this data is that the tests have been made with town gas-air mixtures and the dependence of S_0 and E on concentration is not known.

Russo and Di Benedetto (2007) use the values S_0 = 1.22 m/s and E = 6.64 for all concentrations of town gas. These values have been taken from Bradley and Mitcheson (1978) where they correspond to 25 % town gas concentration. The source of the value of S_0 is (Cubbage & Simmonds 1955). According to the latter authors, S_0 depends on the composition of town gas, but would be expected to be 1.07 to 1.22 m/s (3.5 to 4 ft/s).

Data on burning velocity is available for some German town gases. A town gas containing 54.5 % H_2 and 24.4 % CH_4 is reported to have a lower heating value of 17.54 MJ/m^3, a flammability range of 5.0–30.0 % and a fundamental burning velocity of 0.95 m/s (Joos 2006). A town gas whose composition satisfies the German standard DIN 3362 is reported to have a lower heating value of 15.6 MJ/m^3, a flammability range of 5.0–37.0 % and a fundamental burning velocity of 1.035 m/s. At stoichiometric concentration 21.4 % the burning velocity is 0.86 m/s (Janicka 2009).

Town gas is a volumetric fuel blend whose stoichiometric composition can be calculated as follows (Goodger 1977). Take one mole of the fuel blend consisting of

$$aC_xH_y + bH_2 + cCO + dO_2 + eN_2 + fCO_2 \quad (63)$$

The equation for stoichiometric combustion is

$$fuel + m_s\left(O_2 + 3.76N_2\right) \rightarrow n_1CO_2 + n_2H_2O + 3.76m_sN_2 \quad (64)$$

The stoichiometric amount of moles of oxygen per mole of fuel m_s is

$$m_s = \left(x + y/4\right)a + b/2 + c/2 - d \quad (65)$$

The stoichiometric concentration C_{st} is $1/(1 + 4.76m_s)$. The resulting values of C_{st} for town gas are given in Table 25.

The flammability limits of a gas mixture in air are usually estimated by the empirical mixing rule proposed by Le Chatelier already in 1891. According to him, the lower flammability limit of a mixture of combustible gases LFL_{mix} can be estimated using the formula

$$\frac{1}{LFL_{mix}} = \sum_{i=1}^{n} \frac{y_i}{LFL_i} \quad (66)$$

where y_i is the mole fraction of the ith component and LFL_i is the lower flammability limit of this component.

Mashuga and Crowl (2000) present a thermodynamic proof of Le Chatelier's mixing rule. According to them, Eq. (66) is valid provided that

— the product heat capacities are constant

— the number of moles of gas is constant

— the combustion kinetics of the pure species are independent and unchanged by the presence of other combustible species

— the adiabatic temperature rise at the flammability limit is the same for all species.

When these conditions are approximately satisfied, Eq. (66) will give results of satisfactory accuracy. Coward and Jones (1952) mention that Eq. (66) gives good results for mixtures of hydrogen, carbon monoxide and methane. This is also valid for mixtures of simpler paraffin hydrocarbons including natural gas. However, sometimes the differences between calculated and observed values are very large: e.g. for mixtures of hydrogen and hydrogen sulphide or methane and hydrogen sulphide in air.

Le Chatelier's rule is commonly used to estimate the upper flammability limit of gas mixtures although it does not give as good results as for the lower flammability limit.

The rule has been extended by Jones in 1926 to calculate the flammability limits of gas mixtures containing flammable gases, inert gases and oxygen. The procedure is as follows (Coward and Jones 1952):

1. Recalculate the composition of the mixture on an air-free basis by expressing the amount of each gas as a percentage of the total air-free mixture.
2. Dissect the air-free mixture into simpler mixtures, each of which contains only one flammable gas and part or all of an inert gas.
3. Read the flammability limits of each simple mixture from tables or curves.
4. Calculate the flammability limits of the air-free mixture inserting the mole fractions calculated at step 2 and the flammability limits calculated at step 3 into Eq. (64).
5. Deduce the flammability limits of the original mixture from those calculated at step 4.

Coward and Jones (1952) note that the choice of simple mixtures at step 2 must be done in such a way that the each of them is flammable. If this cannot be done due to an excessive amount of inert gas, the air-free mixture is non-flammable. Moreover, the air-free mixture may be flammable but when multiplied by the appropriate factor at step 5 the LFL may become greater than 100 %. In such a case the original mixture is non-flammable since it contains too much air already.

If the LFL of the mixture is less than 100 % and the UFL is greater than 100 %, the mixture is flammable without any dilution with air.

This method was applied to the town gas compositions in Table 25 and the resulting values of LFL and UFL are given in Table 25.

To evaluate the dimensionless parameter S in Eq. (10), the sound velocity in the unburned mixture c has to be calculated. In an ideal gas, the sound velocity is

$$c = \sqrt{\frac{\gamma_u RT}{M}} \qquad (67)$$

where γ_u is the ratio of specific heats C_p/C_v, R is the gas constant 8.314 J mol^{-1} K^{-1} and M is the molar mass [kg/mol]. Results of the calculation are presented in Table 32.

Table 32. Calculation of unburned mixture sound velocity

	McCann (1985)	K & W (1986)	K & W (1988)	DeG & C (1991)	P & L (1999)
fuel M, g/mol C, %	methane 16 9.5	town gas 13.3 20	town gas 13.8 18	propane 44 5.0	propane 44 4.0
M, g/mol γ_u	27.7 1.39	25.8 1.39	26.2 1.39	29.6 1.37	29.7 1.36
c, m/s	349	362	360	336	334

Russo and Di Benedetto (2007) use the values for γ_u and c given by Razus and Krause (2001). For 4.0 % propane-air mixtures the values are γ_u = 1.365 and c = 339 m/s and for 9.5 % methane-air mixtures γ_u = 1.38 and c = 353 m/s. For town gas-air mixtures they use the values γ_u = 1.4 and c = 408 m/s given by Razus and Krause (2001) for stoichiometric (29.5 %) hydrogen-air mixtures. This value of sound velocity is about 13 % larger than that in Table 32.

The expansion factor E of town gas-air mixtures can be calculated with the approximate method by Goodger (1977). At temperature above about 1800 K, the thermal energy contained in combustion products is sufficient to cause instability, giving rise to dissociation back towards CO and H_2, together with other species. The general combustion equation, on a molar basis, is written as

$$fuel + m(O_2 + 3.76N_2) \rightarrow n_1CO_2 + n_2H_2O + n_3CO + n_4H_2 + n_5O_2 + 3.76mN_2 \qquad (68)$$

The ratio n_1/n_3 is determined by the partial-equilibrium constant of the reaction $CO_2 \leftrightarrow CO + 0.5O_2$, and the ratio n_2/n_4 by the partial-equilibrium constant of the reaction $H_2O \leftrightarrow H_2 + 0.5O_2$. Further dissociation to radicals and atomic species is unlikely to be extensive, owing to the massive proportion of diluent nitrogen present.

The term n_5O_2 is frequently disregarded in the fuel-rich case. The ratio $(n_3 \cdot n_2)/(n_1 \cdot n_4)$ is determined by the partial-equilibrium constant of the water-gas reaction $CO + H_2O \leftrightarrow CO_2 + H_2$. In the fuel-weak case, the term n_3CO is frequently disregarded. Furthermore, since hydrogen is more reactive than carbon, it is common practice to disregard the minor term n_4H_2.

The method of Goodger (1977) is now applied to the compositions of town gas (Table 25) in the tests by Cubbage and Marshall (1972) and Kordylewski and Wach (1986), respectively, to calculate the ratio N_f/N_i and the adiabatic flame temperature T_{ad} at the concentrations used by the latter authors (Table 26). The amount of town gas is constant at 1 mol. When the values calculated for these quantities are inserted into Eq. (5), the corresponding values of the expansion factor E are found. The intermediate and final results of the calculation are given in Tables 33 and 34 and compared in Figure 20.

Table 33. Expansion factor of town gas-air mixtures, C & M (1972)

C, %	m	N_i	N_f	T_{ad}, K	E
10	1.891	10.000	9.739	1492	4.83
12	1.541	8.333	8.072	1701	5.48
14	1.291	7.143	6.883	1903	6.10
16	1.103	6.250	5.988	2029	6.69
18	0.957	5.556	5.315	2260	7.25
20	0.840	5.000	4.815	2295	7.42
22	0.745	4.545	4.458	2190	7.20
25	0.630	4.000	4.026	2036	6.87
30	0.490	3.333	3.499	1790	6.30

Table 34. Expansion factor of town gas-air mixtures, K & W (1986)

C, %	m	N_i	N_f	T_{ad}, K	E
10	1.891	10.000	9.749	1537	5.03
12	1.541	8.333	8.083	1751	5.70
14	1.291	7.143	6.894	1961	6.35
16	1.103	6.250	6.005	2147	6.92
18	0.957	5.556	5.336	2287	7.37
20	0.840	5.000	4.843	2300	7.47
22	0.745	4.545	4.481	2208	7.30
25	0.630	4.000	4.049	2058	6.99
30	0.490	3.333	3.522	1815	6.43

The calculated value for 25 % town gas-air mixture in the tests by Cubbage and Marshall (1972) E = 6.87 is 3.5 % larger than the value 6.64 used by Russo and Di Benedetto (2007). The latter value has been calculated by Sheppard (1971) from the composition of British town gas (Cubbage & Marshall 1972) in Table 25 (Bradley & Mitcheson 1978b). If this value of E is used to calculate burning velocity S_0 from the measured value of flame speed v_f = 9.0 m/s, the result is 1.31 m/s, which is 7 to 22 % higher than the value 1.07–1.22 m/s mentioned by Cubbage and Simmonds (1955).

The calculation method disregards the more extensive dissociation to atomic oxygen and hydrogen and to radicals OH and NO. For stoichiometric hydrocarbon gas-air mixtures, these reactions reduce T_{ad} by about 23 K or 1 % (Goodger 1977). On the other hand, dissociation has a smaller effect on E because it increases the final number of moles N_f. For the fuel-lean and fuel-rich mixtures in Tables 33 and 34, T_{ad} is lower and the more extensive dissociation need not be considered.

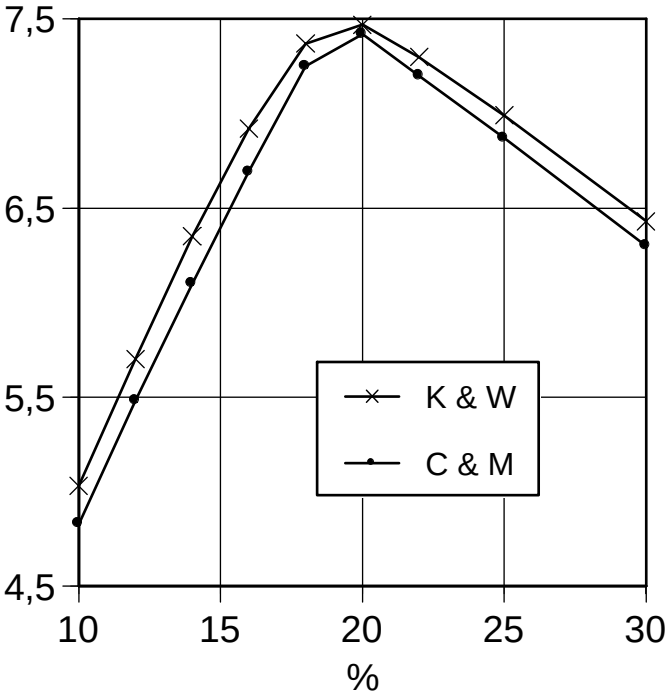

Figure 20. Expansion factors of town gas-air mixtures of Cubbage and Marshall (1972) and Kordylewski and Wach (1986)

The burning velocity of town gas-air mixtures can be calculated by dividing the measured values of flame speed v_f in Fig. 4 with the corresponding values of the expansion factor E. The values for concentrations missing from Table 33 are calculated by linear interpolation or, in the range 16 to 22 %, by interpolation wit a second degree polynomial. The results are presented in Table 35.

Table 35. Calculation of burning velocities of town gas-air mixtures

C, %	E	v_f, dP/dt	S_0, dP/dt	v_f, P_2	S_0, P_2
17	7.02	4.43	0.63	—	—
18	7.25	4.84	0.67	4.96	0.68
19	7.38	5.51	0.75	5.64	0.76
20	7.42	6.20	0.84	6.36	0.86
21	7.36	6.90	0.94	7.02	0.95
22	7.20	7.56	1.05	7.74	1.08
23	7.09	8.16	1.15	8.38	1.18
24	6.98	8.69	1.24	8.94	1.28
25	6.87	9.02	1.31	9.20	1.34
26	6.76	8.65	1.28	8.72	1.29
27	6.64	8.05	1.21	8.10	1.22
28	6.53	7.36	1.13	7.40	1.13
29	6.41	6.62	1.03	6.70	1.05
30	6.30	5.77	0.92	5.97	0.95

Another, although less accurate, method to extract values of S_0 from the test results by Cubbage and Simmonds (1955) is based on the measured explosion pressures presented in Fig. 3. The correlations for the prediction of the peak pressures P_1 and P_2, Eqs. (11) and (12), are based on data such as that in Fig. 3. However, they are expected to be somewhat conservative.

Because the experimental parameters in Eqs. (11) and (12), namely K, w and V are known, the equations can be inverted to give S_0 as functions of the peak pressures P_1 and P_2. Inserting $A_v = 0.836$ m^2, $A_c = 1.187$ m^2, w = 16.28 kg/m^2 and V = 1.47 m^3 gives $P_1 = 11.2S_0$ and $P_2 = 8.24S_0$. Since in this configuration $P_1 > P_2$, the test data gives the values of the first pressure peak P_1. The values of P_1 and S_0 are given in Table 36.

Table 36. Calculation of burning velocities of town gas-air mixtures

C, %	P_1, kPa	S_0, m/s	C, %	P_1, kPa	S_0, m/s
7	0.14	0.01	21	7.93	0.71
8	0.34	0.03	22	8.74	0.78
9	0.58	0.05	23	9.34	0.83
10	0.84	0.08	24	9.58	0.86
11	1.02	0.10	25	9.59	0.86
12	1.48	0.13	26	9.42	0.84
13	1.90	0.17	27	8.79	0.78
14	2.32	0.21	28	7.14	0.64
15	2.82	0.25	29	5.29	0.47
16	3.51	0.31	30	4.04	0.36
17	4.29	0.38	31	3.34	0.30
18	5.12	0.46	32	2.88	0.26
19	6.08	0.54	33	2.57	0.23
20	6.98	0.62	34	2.32	0.21
			35	2.06	0.18

The values of S_0 as a function of town gas concentration in Tables 34 and 35 are plotted in Figure 21.

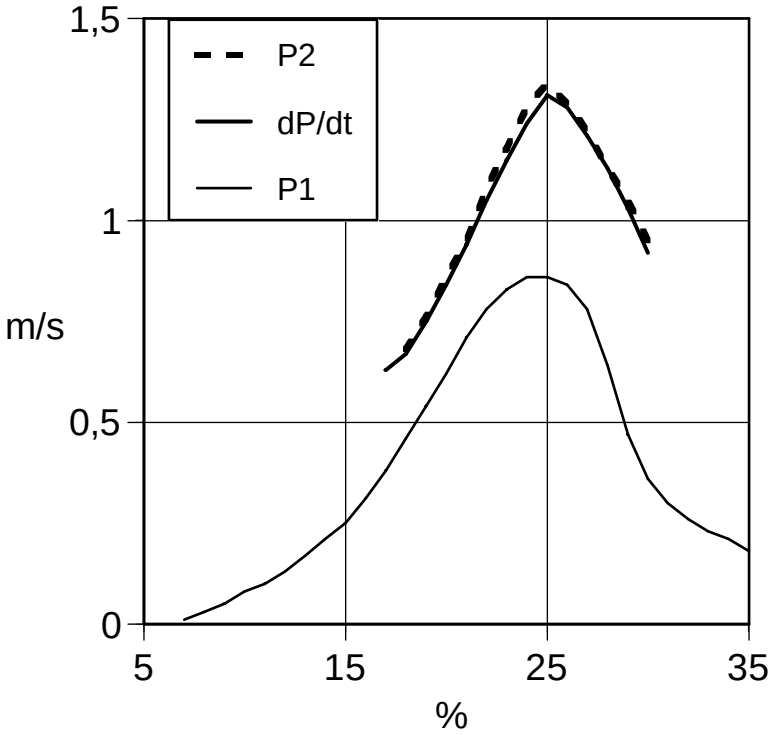

Figure 21. Burning velocity of town gas as a function of concentration.

The ratio of burning velocity derived from dP/dt to that derived from the measured values of P_1 using Eq. (11) is calculated in Table 37.

Cubbage and Simmonds (1955) conclude that the burning velocities calculated from the experimental values of flame speed as in Table 35 are 30 % higher than the expected values. Dividing the values in Table 35 by the factor 1.3 gives the value 1.0 m/s for the fundamental burning velocity.

For the validation of prediction methods of P_{red}, it is assumed that the fundamental burning velocity of the British town gas used in the tests by Cubbage and Marshall (1972) was 1.0 m/s. Thus, the values of S_0 at non-stoichiometric concentrations can be estimated by dividing the values in Table 35 by the factor 1.31 or the values in Table 36 by the factor 0.84. The readjusted burning velocity values are given in Table 37 and plotted in Figure 22.

Note that the readjusted values of S_0 calculated with the two methods differ the most at 30 % town gas-air mixture. The value based on dP/dt is 0.70 m/s whereas that based on P_1 is 0.42 m/s. Since the former method is presumably more accurate than the latter, the value 0.70 m/s will be used.

Table 37. Ratio of burning velocities calculated with two methods

C, %	S_0, P_1, m/s	S_0, dP/dt, m/s	ratio
17	0.38	0.63	0.60
18	0.46	0.67	0.69
19	0.54	0.75	0.72
20	0.62	0.84	0.74
21	0.71	0.94	0.76
22	0.78	1.05	0.74
23	0.83	1.15	0.72
24	0.86	1.24	0.69
25	0.86	1.31	0.66
26	0.84	1.28	0.66
27	0.78	1.21	0.64
28	0.64	1.13	0.57
29	0.47	1.03	0.46
30	0.36	0.92	0.39

The Bradley and Mitcheson correlations are now used to predict the values of P_{red} of the tests by Kordylewski and Wach (1986). Since in these tests the vent was initially uncovered, either Eq. (15) or Eq. (16) must be used, depending on the value of the ratio A/S. The value of the vent area A_v was $4.91 \cdot 10^{-4}$ m^2, the vessel surface A_s was 0.356 m^2 and the corresponding value of the dimensionless parameter A is $8.28 \cdot 10^{-4}$ m^2. Other parameter values used in the calculation are presented in Table 38 and the results in Table 39.

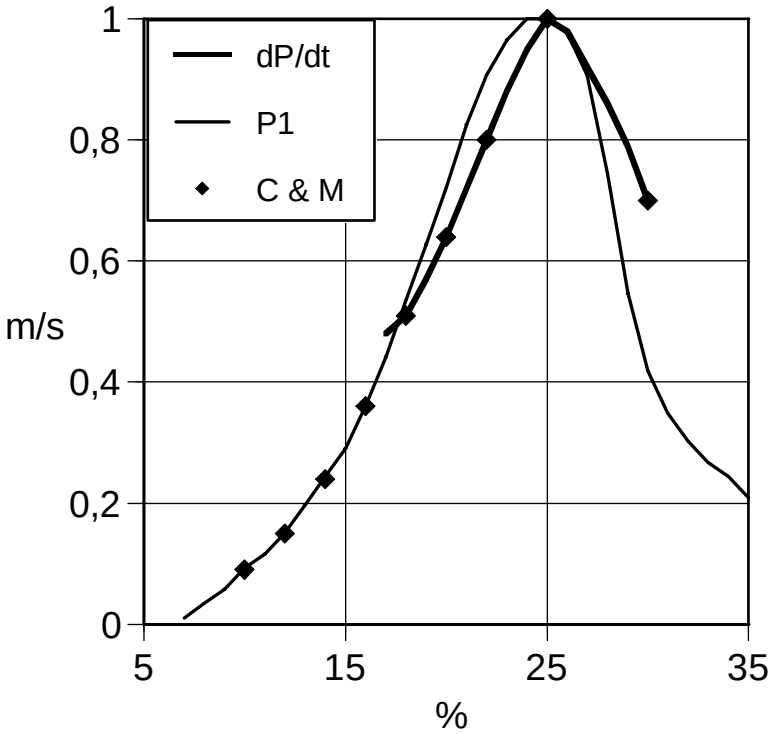

Figure 22. Readjusted values of S_0 used in the calculation.

Table 38. Parameters used in the calculation

C, %	E	S_0, m/s	M, g/mol	γ_u	c, m/s
10	5.03	0.09	27.4	1.395	352
12	5.70	0.15	27.1	1.394	354
14	6.35	0.24	26.8	1.393	356
16	6.92	0.36	26.5	1.392	358
18	7.37	0.51	26.2	1.391	360
20	7.47	0.64	25.8	1.390	362
22	7.30	0.80	25.5	1.389	364
25	6.99	1.00	25.1	1.387	367
30	6.43	0.70	24.3	1.385	373

Table 39. Predictions with the Bradley and Mitcheson method

C, %	S	A/S	P_{red}, bar	exp., bar	pred./exp
10	$1.03 \cdot 10^{-3}$	0.804	1.09	0	—
12	$1.99 \cdot 10^{-3}$	0.416	2.43	0.5	4.85
14	$3.61 \cdot 10^{-3}$	0.230	3.63	1.7	2.15
16	$5.95 \cdot 10^{-3}$	0.139	4.66	2.5	1.86
18	$9.02 \cdot 10^{-3}$	0.092	5.50	3.4	1.62
20	$1.14 \cdot 10^{-2}$	0.072	5.98	3.6	1.66
22	$1.38 \cdot 10^{-2}$	0.060	6.37	4.2	1.52
25	$1.63 \cdot 10^{-2}$	0.051	6.70	4.2	1.60
30	$1.02 \cdot 10^{-2}$	0.081	5.75	1.6	3.60

Since in each case the ratio A/S was lower than 0.84, Eq. (16) was used to calculate P_{red}. The Bradley and Mitcheson method is seen to give conservative predictions, overestimating the experimental value of P_{red} by at least a factor of 1.41. Near the flammability limits the ratio predicted/measured is larger.

The values of P_{red} predicted by the Molkov correlations Eqs. (20) to (25) for the tests by Kordylewski and Wach (1986) are now calculated. Both sets of empirical coefficients for hydrocarbon-air mixtures are used, namely the initial ones $\alpha = 0.9$ and $\beta = 1$ and the final ones $\alpha = 1.75$ and $\beta = 0.5$. The ratio of the specific heat capacities γ_b is set at 1.25. Predictions with the Molkov method are presented in Tables 40 and 41.

Table 40. Predictions with the Molkov method with $\alpha = 0.9$ and $\beta = 1$

C, %	Br	χ/μ	Br_t	P_{red}, bar	exp., bar	pred./exp.
10	6.03	2.01	1.18	0.70	0	—
12	3.15	1.68	0.78	1.70	0.5	3.4
14	1.75	1.48	0.52	2.70	1.7	1.59
16	1.07	1.37	0.36	3.45	2.5	1.38
18	0.71	1.30	0.26	4.00	3.4	1.18
20	0.56	1.27	0.21	4.30	3.6	1.20
22	0.46	1.25	0.17	4.55	4.2	1.09
25	0.39	1.24	0.15	4.75	4.2	1.13
30	0.63	1.29	0.22	4.25	1.6	2.65

Table 41. Predictions with the Molkov method with $\alpha = 1.75$ and $\beta = 0.5$

C, %	Br	χ/μ	Br_t	P_{red}, bar	exp., bar	pred./exp.
10	6.03	3.09	0.76	1.75	0	—
12	3.15	2.89	0.45	3.00	0.5	6.0
14	1.75	2.75	0.28	3.85	1.7	2.27
16	1.07	2.65	0.184	4.45	2.5	1.79
18	0.71	2.58	0.135	4.90	3.4	1.44
20	0.56	2.54	0.105	5.10	3.6	1.42
22	0.46	2.52	0.086	5.30	4.2	1.26
25	0.39	2.50	0.073	5.45	4.2	1.30
30	0.63	2.56	0.110	5.10	1.6	3.20

The tests by Kordylewski and Wach (1988) were made with 18 % town gas-air mixture in a 22 dm^3 vessel with a surface area A_s of 0.380 m^2 and three diameters of the circular vent: 21, 25 and 35 mm. The value of the dimensionless parameter S is taken from Table 39: $S = 9.02 \cdot 10^{-3}$. The predictions with Eq. (16) of the Bradley and Mitcheson method are given in Table 42.

Table 42. Predictions with the Bradley and Mitcheson method

d, mm	A	A/S	P_{red}, bar	exp., bar	pred./exp
21	$3.46 \cdot 10^{-4}$	0.038	7.3	4.2	1.75
25	$7.75 \cdot 10^{-4}$	0.086	5.6	3.0	1.90
35	$1.52 \cdot 10^{-3}$	0.169	4.25	2.0	2.15

Predictions with the Molkov method are presented in Tables 43 and 44.

Table 43. Predictions with the Molkov method with $\alpha = 0.9$ and $\beta = 1$

d, mm	Br	χ/μ	Br_t	P_{red}, bar	exp., bar	pred./exp.
21	0.467	1.27	0.176	4.55	4.2	1.08
25	0.663	1.31	0.242	4.10	3.0	1.37
35	1.299	1.42	0.435	3.10	2.0	1.54

Table 44. Predictions with the Molkov method with $\alpha = 1.75$ and $\beta = 0.5$

d, mm	Br	χ/μ	Br_t	P_{red}, bar	exp., bar	pred./exp.
21	0.467	2.55	0.087	5.30	4.2	1.26
25	0.663	2.60	0.122	4.95	3.0	1.66
35	1.299	2.71	0.228	4.20	2.0	2.10

The experimental values of P_{red} of tests with town gas-air mixtures with the calculated values of the ratio A/S are plotted in Figure 23.

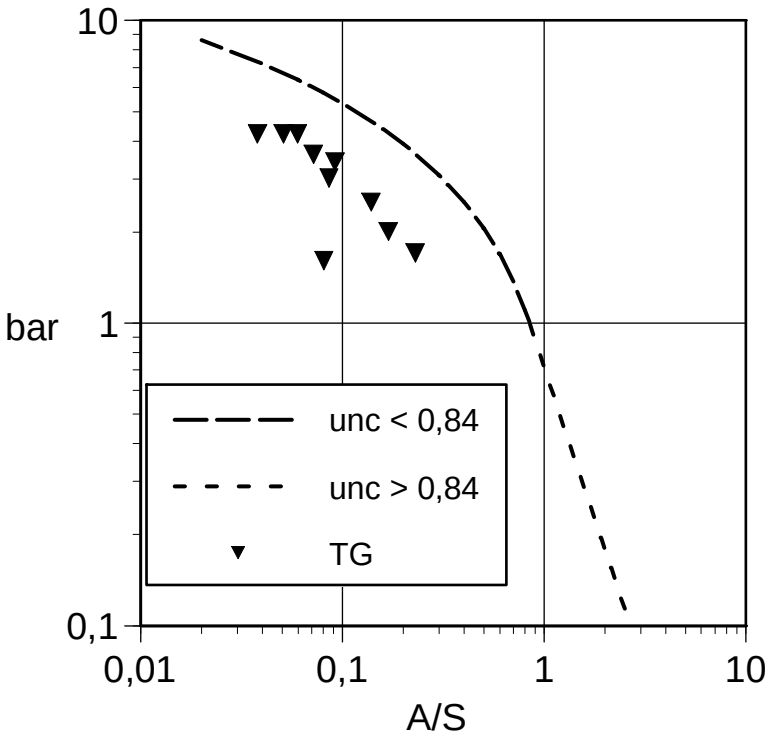

Figure 23. Values of the ratio A/S with the experimental values of P_{red}.

The experimental values of P_{red} of tests with town gas-air mixtures with the calculated values of Br_t are plotted in Figure 24. The values of Br_t calculated with the old parameter set $\alpha = 0.9$ and $\beta = 1$ are plotted with open symbols and those calculated with the new one $\alpha = 1.75$ and $\beta = 0.5$ with closed symbols.

To calculate the relative error, the gauge pressures in Tables 39 to 44 are converted into absolute pressures and inserted in Eq. (40). The results are presented in Table 45.

Table 45. Relative errors of the predictions (uncovered vent)

fuel	tests	Eq. (15)	$\alpha = 0.9$, $\beta = 1$	$\alpha = 1.75$, $\beta = 0.5$
town gas	11	73 %	33 %	63 %

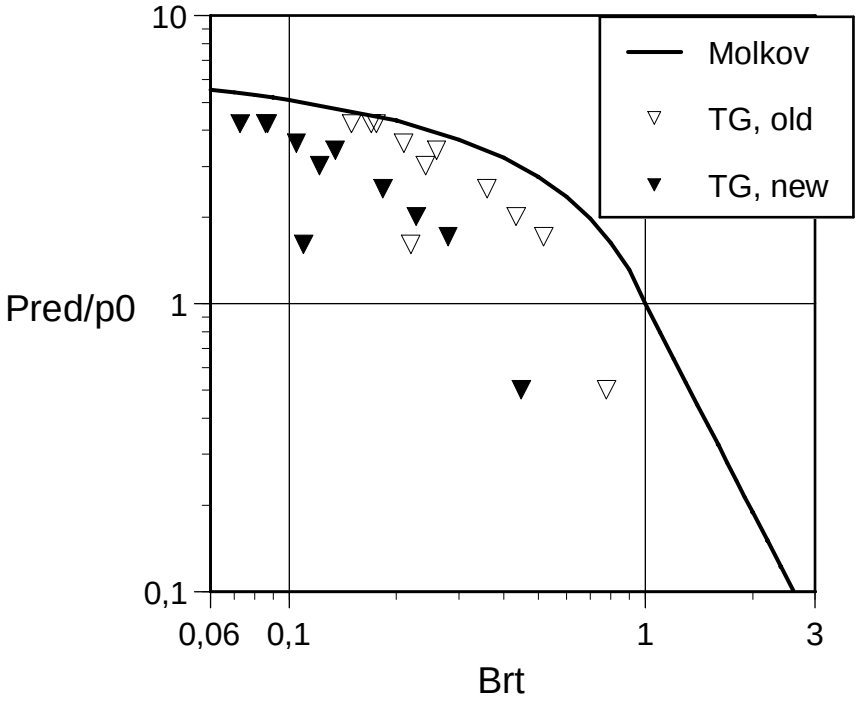

Figure 24. Values of Br_t with the experimental values of P_{red}/p_0.

5.2.2 Other gas-air mixtures

Other test series where P_{red} was measured were performed with 9.5 % methane-air (Table 24), 5 % propane-air (Table 28) and 4.9 % acetone-air mixture (Table 29). In the following, the predictions will be made with the values of S_0, E, c, γ_u and γ_b used by Bradley and Mitcheson (1978b) and Molkov (1999) to derive their respective correlations.

Of the test results of McCann et al. (1985) in Table 24, Russo and Di Benedetto (2007) use only those found with the smaller vessel with side of 0.18 m, probably because the tests with duct venting were done with this vessel. They assume that the vent was initially uncovered, which contradicts the description of the test apparatus. With $A_v = 0.01$ m^2 and $A_s = 6(0.18\text{ m})^2$, the dimensionless parameter A has the value $3.09 \cdot 10^{-2}$. With $S_0 = 0.43$ m/s, E = 7.52 and c = 349 m/s, the dimensionless parameter S has the value $8.03 \cdot 10^{-3}$. The ratio A/S is 3.85 and Eq. (15) gives $P_{red} = 0.048$ bar. If the value of $P_{red} = 0.079$ bar is valid, the ratio predicted to experimental is 0.61.

Predictions with the Molkov method with $S_0 = 0.38$ m/s, E = 7.4 and c = 354 m/s, $\gamma_u = 1.39$ and $\gamma_b = 1.25$ are presented in Table 46.

Table 46. Predictions with the Molkov method

α, β	Br	χ/μ	Br_t	P_{red}, bar	exp., bar	pred./exp
0.9, 1	43.0	3.577	5.734	0.0153	0.079	0.19
1.75, 0.5	43.0	3.581	5.728	0.0154	0.079	0.19

The larger vessel with side of 0.38 m had vent covers whose opening pressures P_{stat} are given in Table 24. The stated value of the vent coefficient K allows calculation of the vent area: $A_v = (0.38\text{ m})^2/18.4 = 7.85 \cdot 10^{-3}$ m^2. With a wall area A_s of $6(0.38\text{ m})^2$, the dimensionless parameter A has the value $0.6/(6 \times 18.4) =$

$5.43 \cdot 10^{-3}$. The ratio A/S is 0.77. Two correlations of the Bradley and Mitcheson method can be applied to this case, namely Eqs. (18) and (19). Eq. (18) is to be used when P_{red} is no larger than P_{stat} and Eq. (19) in the case $P_{red} > P_{stat}$. Thus, Eq. (19) is applied to the test with P_{stat} = 0.40 bar and Eq. (18) to the two remaining tests. The results of the calculation are given in Table 47.

Table 47. Predictions with the Bradley and Mitcheson method

P_{stat}, bar	P_1, bar	P_2, bar	P_{red}, bar	exp., bar	pred./exp
0.30	0.28	—	2.9	0.28	10
0.40	0.40	0.84	4.7	0.4	12
0.503	0.50	0.50	2.9	0.5	5.8

Predictions with the Molkov method are presented in Tables 48 and 49.

Table 48. Predictions with the Molkov method with α = 0.9 and β = 1

P_{stat}, bar	Br	χ/μ	Br_t	P_M	P_{red}, bar	exp., bar	pred./exp
0.30	7.38	2.24	1.58	0.335	0.49	0.28	1.75
0.40	7.38	2.21	1.60	0.320	0.53	0.4	1.30
0.503	7.38	2.17	1.63	0.310	0.57	0.5	1.15

Table 49. Predictions with the Molkov method with α = 1.75 and β = 0.5

P_{stat}, bar	Br	χ/μ	Br_t	P_M	P_{red}, bar	exp., bar	pred./exp
0.30	7.38	1.07	0.85	0.850	1.25	0.28	4.5
0.40	7.38	1.09	0.82	0.820	1.35	0.4	3.4
0.503	7.38	1.11	0.79	0.785	1.45	0.5	2.9

The tests by DeGood and Chatrathi (1991) in Table 28 were performed with 5 % propane-air mixture. Bradley and Mitcheson (1978b) give the values S_0 = 0.38 m/s, E = 7.97. Inserting these parameter values and c = 339 m/s, V = 2.6 m^3, A_v = 0.56 m^2 and A_s = 11.2 m^2 gives $A = 3.0 \cdot 10^{-2}$, $S = 7.8 \cdot 10^{-3}$ and A/S = 3.84. In these tests, P_{stat} was 0.10 bar and P_{red} 0.20 bar for central ignition. Because $P_{red} > P_{stat}$, Eq. (19) is used with the result P_{red} = 0.38 bar. The ratio predicted / experimental is 1.9.

Predictions with the Molkov method with S_0 = 0.29 m/s, E = 7.9, c = 338 m/s, γ_u = 1.365 and γ_b = 1.25 are presented in Table 50.

Table 50. Predictions with the Molkov method

α, β	Br	χ/μ	Br_t	P_M	P_{red}, bar	exp., bar	pred./exp
0.9, 1	48.3	7.13	3.37	0.054	0.063	0.20	0.32
1.75, 0.5	48.3	6.95	3.45	0.051	0.060	0.20	0.30

The tests by Molkov et al. (1993) in Table 29 were performed with stoichiometric (4.9 %) acetone-air mixture. For the smaller 0.027 m^3 vessel, insertion of S_0 = 0.29 m/s, E = 7.96, c = 322 m/s, V = 0.027 m^3, $A_v = 1.96 \cdot 10^{-3}$ m^2 and A_s = 0.498 m^2 gives $A = 2.36 \cdot 10^{-3}$, $S = 6.21 \cdot 10^{-3}$ and A/S = 0.381. In this test, P_{stat} was 0.22 bar and P_{red} 0.6 bar. Because $P_{red} > P_{stat}$, Eq. (19) is used with the result P_{red} = 6.75 bar. The ratio predicted / experimental is 11.

Predictions with the Molkov method (γ_u = 1.36, γ_b = 1.25) are presented in Table 51.

Table 51. Predictions with the Molkov method

α, β	Br	χ/μ	Br_t	P_M	P_{red}, bar	exp., bar	pred./exp
0.9, 1	3.36	1.69	0.994	1.02	1.37	0.6	2.3
1.75, 0.5	3.36	2.87	0.584	2.41	3.24	0.6	5.4

For the larger 2 m^3 vessel, insertion of S_0 = 0.315 m/s, E = 7.96, c = 329 m/s, V = 2 m^3, $A_v = 3.14 \cdot 10^{-2}$ m^2 and A_s = 9.6 m^2 gives $A = 1.96 \cdot 10^{-3}$, $S = 6.66 \cdot 10^{-3}$ and A/S = 0.295. In this test, P_{stat} was 0.14 bar and P_{red} 3.0 bar. Because $P_{red} > P_{stat}$, Eq. (19) is used with the result P_{red} = 10.6 bar. The ratio predicted / experimental is 3.5.

Predictions with the Molkov method are presented in Table 52.

Table 52. Predictions with the Molkov method

α, β	Br	χ/μ	Br_t	P_M	P_{red}, bar	exp., bar	pred./exp
0.9, 1	2.87	2.69	0.533	2.62	3.18	3.0	1.05
1.75, 0.5	2.87	4.69	0.306	3.68	4.47	3.0	1.5

The experimental values of P_{red} with the calculated values of Br_t are plotted in Figure 25. The values of Br_t calculated with α = 0.9 and β = 1 are plotted with open symbols and those calculated with α = 1.75 and β = 0.5 with closed symbols.

To calculate the relative error, the gauge pressures in the text above and in Tables 46 to 52 are converted into absolute pressures and inserted in Eq. (40). The results are presented in Table 53.

Table 53. Relative errors of the predictions (covered vent)

fuel	tests	Eq. (19)	α = 0.9, β = 1	α = 1.75, β = 0.5
CH_4, C_3H_8, C_3H_6O	6	164 %	14 %	58 %

5.2.3 Prediction of P_{red}

The values of P_{red} in the tests by Molkov et al. (1993) and Ponizy and Leyer (1999a, 1999b) where tests were made only with a duct are now estimated with the Bradley and Mitcheson (1978b) method Eqs. (15) to (19) and Molkov method Eqs. (20) to (25).

The values of P_{red} have already been predicted for those tests by Molkov et al. (1993) where they were measured. Now a prediction is made for the remaining tests in Table 29. The predictions made with the Bradley and Mitcheson method for the 27 dm^3 and 10 m^3 vessels are presented in Tables 54 and 55, respectively.

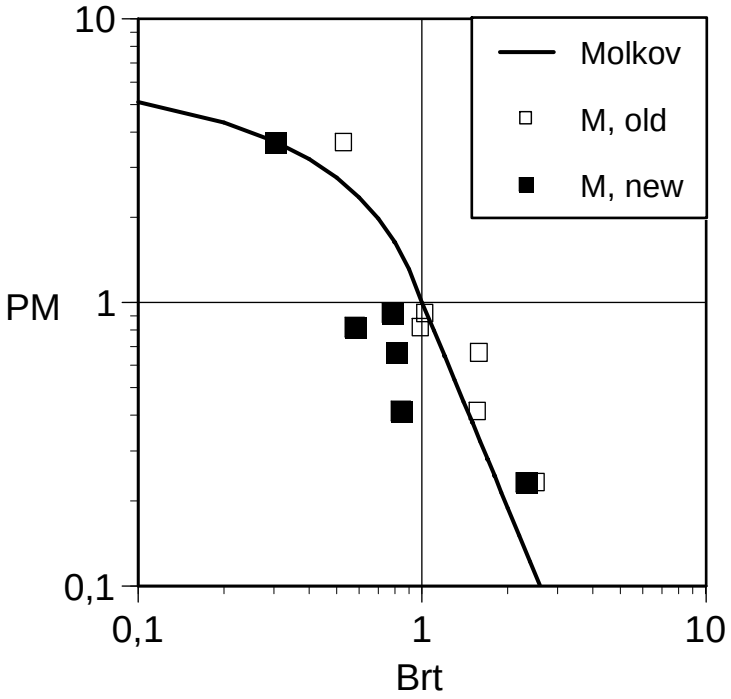

Figure 25. Values of Br_t with the experimental values of P_M in tests with a covered vent.

Table 54. Predictions with the Bradley and Mitcheson method

P_{stat}, bar	Eq. (18), bar	Eq. (19), bar	$P_{red, vd}$, bar
0.19	4.8	8.7	5.0†
0.24	4.8	9.5	3.5–4.4
1.64	4.8	12.6	1.9
1.41	4.8	18.5	4.4†

Table 55. Predictions with the Bradley and Mitcheson method

P_{stat}, bar	Eq. (18), bar	Eq. (19), bar	$P_{red, vd}$, bar
0.1	3.9	3.9	4.1
0.05	3.2	2.5	2.8

The Bradley and Mitcheson method is obviously inapplicable to the present problem. Except for one test with the 10 m^3 vessel, the predicted values of P_{red} are larger than the measured values of $P_{red, vd}$.

Predictions with the Molkov method are presented in Tables 56 and 57 for the 27 dm^3, and in Tables 58 and 59 for the 10 m^3 vessel.

Table 56. Predictions with the Molkov method with $\alpha = 0.9$ and $\beta = 1$

P_{stat}, bar	Br	χ/μ	Br_t	P_M	P_{red}, bar	$P_{red, vd}$, bar
0.19	3.36	1.70	0.988	1.035	1.34	5.0†
0.24	3.36	1.68	0.997	1.009	1.39	3.5–4.4
1.64	3.36	1.39	1.209	0.634	2.69	1.9
1.41	3.36	1.43	1.178	0.675	2.50	4.4†

Table 57. Predictions with the Molkov method with $\alpha = 1.75$ and $\beta = 0.5$

P_{stat}, bar	Br	χ/μ	Br_t	P_M	P_{red}, bar	$P_{red, vd}$, bar
0.19	3.36	2.89	0.581	2.43	3.25	5.0†
0.24	3.36	2.86	0.587	2.40	3.15	3.5–4.4
1.64	3.36	2.36	0.711	1.94	8.2	1.9
1.41	3.36	2.42	0.693	2.01	7.4	4.4†

Table 58. Predictions with the Molkov method with $\alpha = 0.9$ and $\beta = 1$

P_{stat}, bar	Br	χ/μ	Br_t	P_M	P_{red}, bar	$P_{red, vd}$, bar
0.1	6.10	4.04	0.755	1.787	2.06	4.1
0.05	6.10	4.28	1.816	1.581	1.70	2.8

Table 59. Predictions with the Molkov method with $\alpha = 1.75$ and $\beta = 0.5$

P_{stat}, bar	Br	χ/μ	Br_t	P_M	P_{red}, bar	$P_{red, vd}$, bar
0.1	6.99	6.19	0.492	2.79	3.20	4.1
0.05	6.99	6.40	0.546	2.56	2.75	2.8

The tests by Ponizy and Leyer (1999a) with stoichiometric 4.0 % propane-air were performed in a 3.66 dm^3 cylindrical vessel with a length to diameter ratio L/D of 3.7. The internal surface area A_s was 0.154 m^2. The vent with a diameter of 16, 21, 36 or 53 mm was initially uncovered. The experimental values of $P_{red, vd}$ are given in Table 30.

The parameter values for 4.0 % propane-air used by Bradley and Mitcheson (1978b) are $S_0 = 0.46$ m/s, E = 7.98 and c = 334 m/s. Hence, $S = 9.6 \cdot 10^{-3}$. The predicted values of P_{red} are given in Table 60.

Table 60. Predictions with the Bradley and Mitcheson method

d, mm	A_v, m^2	A	A/S	Eq. (16), bar	$P_{red, vd}$, bar
16	$2.01 \cdot 10^{-4}$	$3.46 \cdot 10^{-4}$	0.0815	5.75	1.17–1.45
21	$3.46 \cdot 10^{-4}$	$1.35 \cdot 10^{-3}$	0.140	4.65	1.45–1.92
36	$1.02 \cdot 10^{-3}$	$3.97 \cdot 10^{-3}$	0.413	2.45	1.55–1.92
53	$2.21 \cdot 10^{-3}$	$8.61 \cdot 10^{-3}$	0.896	0.87	2.11

The tests by Ponizy and Leyer (1999b) were performed the same 3.66 dm^3 vessel with a vent diameter of 36 mm. In addition to an initially open vent ($P_{stat} = 0$), covered vents with several values of P_{stat} were used. Test results with a 1.7 m duct are presented in Table 31. The predicted values of P_{red} are given in Table 61.

Table 61. Predictions with the Bradley and Mitcheson method

ignition	P_{stat}, bar	Eq. (18), bar	Eq. (19), bar	$P_{red, vd}$, bar
centre	0.3	4.5	9.2	2.16
centre	0.91	4.5	14.0	2.66
centre	2.3	4.5	19.8	3.37
rear	0.32	4.5	9.5	1.88
rear	0.83	4.5	13.5	1.81
near vent	1.11	4.5	15.1	1.27
near vent	2.24	4.5	19.6	2.24

The Bradley and Mitcheson method is obviously inapplicable to the present problem. Except for one test with a 53 mm diameter vent, the predicted values of P_{red} are larger than the measured values of $P_{red, vd}$.

Predictions with the Molkov method are presented in Tables 62 and 63 for the tests by Ponizy and Leyer (1999a), and in Tables 64 and 65 for the tests by Ponizy and Leyer (1999b). The parameter values by Molkov (1999) for 4.0 % propane-air have been used: S_0 = 0.335 m/s, E = 7.9, c = 339 m/s, γ_u = 1.365 and γ_b = 1.25.

Table 62. Predictions with the Molkov method with α = 0.9 and β = 1

d, mm	A_v, m^2	Br	χ/μ	Br_t	P_{red}, bar	$P_{red, vd}$, bar
16	$2.01 \cdot 10^{-4}$	1.20	1.19	0.496	2.81	1.45–1.92
21	$3.46 \cdot 10^{-4}$	2.06	1.31	0.781	1.72	1.17–1.55
36	$1.02 \cdot 10^{-3}$	6.06	1.73	1.74	0.27	1.27–1.92
53	$2.21 \cdot 10^{-3}$	13.1	2.23	2.94	0.08	2.11

Table 63. Predictions with the Molkov method with α = 1.75 and β = 0.5

d, mm	A_v, m^2	Br	χ/μ	Br_t	P_{red}, bar	$P_{red, vd}$, bar
16	$2.01 \cdot 10^{-4}$	1.20	2.29	0.260	3.99	1.45–1.92
21	$3.46 \cdot 10^{-4}$	2.06	2.39	0.423	3.11	1.17–1.55
36	$1.02 \cdot 10^{-3}$	6.06	2.65	1.14	0.75	1.27–1.92
53	$2.21 \cdot 10^{-3}$	13.1	2.91	2.24	0.15	2.11

Table 64. Predictions with the Molkov method with α = 0.9 and β = 1

ignition	P_{stat}, bar	χ/μ	Br_t	P_M	P_{red}, bar	$P_{red, vd}$, bar
centre	0	1.73	1.74	0.263	0.27	2.01
centre	0.3	1.64	1.84	0.231	0.35	2.16
centre	0.91	1.49	2.02	0.184	0.49	2.66
centre	2.3	1.28	2.36	0.127	0.76	3.37
rear	0.32	1.63	1.85	0.229	0.35	1.88
rear	0.83	1.51	2.00	0.189	0.47	1.81
near vent	1.11	1.45	2.08	0.178	0.53	1.27
near vent	2.24	1.28	2.35	0.129	0.73	2.24

Table 65. Predictions with the Molkov method with α = 1.75 and β = 0.5

ignition	P_{stat}, bar	χ/μ	Br_t	P_M	P_{red}, bar	$P_{red, vd}$, bar
centre	0	2.65	1.14	0.736	0.75	2.01
centre	0.3	2.51	1.20	0.645	0.96	2.16
centre	0.91	2.29	1.32	0.515	1.37	2.66
centre	2.3	1.96	1.54	0.355	2.13	3.37
rear	0.32	2.50	1.20	0.639	0.98	1.88
rear	0.83	2.31	1.30	0.529	1.32	1.81
near vent	1.11	2.23	1.35	0.484	1.49	1.27
near vent	2.24	1.97	1.53	0.360	2.10	2.24

5.3 Evaluation of correlations for $P_{red, vd}$

The evaluation of different methods for the calculation of $P_{red, vd}$ by Russo and Di Benedetto (2007) is now reviewed and updated. These authors use the test data by McCann et al. (1985) in Table 24, Kordylewski and Wach (1986) in Table 26, Kordylewski and Wach (1988) in Table 27, DeGood and Chatrathi (1991) in Table 28 and Molkov et al. (1993) in Table 29.

In addition, the data by Cubbage and Marshall (1972) in Table 23 is used although in these tests the gas-air mixture was contained by a polythene bag with a volume of 0.5 dm^3 located at the centre of the 136 dm^3 vessel. They say that the results in Table 23 were made consistent with the results of other test series by multiplying the measured values of P_{red} without and with a duct, respectively, by a factor of 60.

This is said to be the ratio of the volume of the exploding pocket to the vessel volume, which is obviously not the case. The inverse of the said ratio is 272. The ratio of the vessel volume to that of the gas-air mixture after combustion in constant pressure is 272/7.48 = 36.4. Maybe the combustion in a closed vessel partially filled with gas-air mixture has been modelled to find a correction factor.

5.3.1 Predicted and experimental values of P_{red}

The methods evaluated by Russo and Di Benedetto (2007) are

— Runes' method as in NFPA 68 (2002 edition), Eq. (30)

— Bradley and Mitcheson method, Eq. (17)

— Bradley and Mitcheson method, Eq. (19)

— Molkov method, Eqs. (20) to (24) with $\alpha = 0.9$ and $\beta = 1$

— Molkov method, Eqs. (20) to (24) with $\alpha = 1.75$ and $\beta = 0.5$.

The relative errors were calculated with Eq. (40) with the results given in Table 66.

Table 66. Relative errors of the methods to estimate P_{red}

method	relative error, %
Runes, Eq. (30)	419
Bradley and Mitcheson, Eq. (17)	3077
Bradley and Mitcheson, Eq. (19)	11
Molkov (1999) with $\alpha = 0.9$ and $\beta = 1$ "old"	46
Molkov (1999) with $\alpha = 1.75$ and $\beta = 0.5$ "new"	66

The comparison of predicted and experimental values of P_{red} is presented in Figure 26. The values of absolute pressure p_{red} in the original figure have been converted to gauge pressure P_{red}.

The experimental values of p_{red} along with the parameter values in Table 1 of Russo and Di Benedetto (2007) were used to identify the tests of which predicted values were calculated. Thus, there were 1 data point from tests by McCann et al.

(1985) (Table 24), 13 data points from tests by Kordylewski and Wach (1986, 1988) (Tables 26 and 27), 2 data points from tests by DeGood and Chatrathi (1991) (Table 28), and 1 data point from tests by Molkov et al. (1993) (Table 29). Also, one data point represented the test by Cubbage and Marshall (1972) (Table 23) with the absolute pressures multiplied by the factor 60.

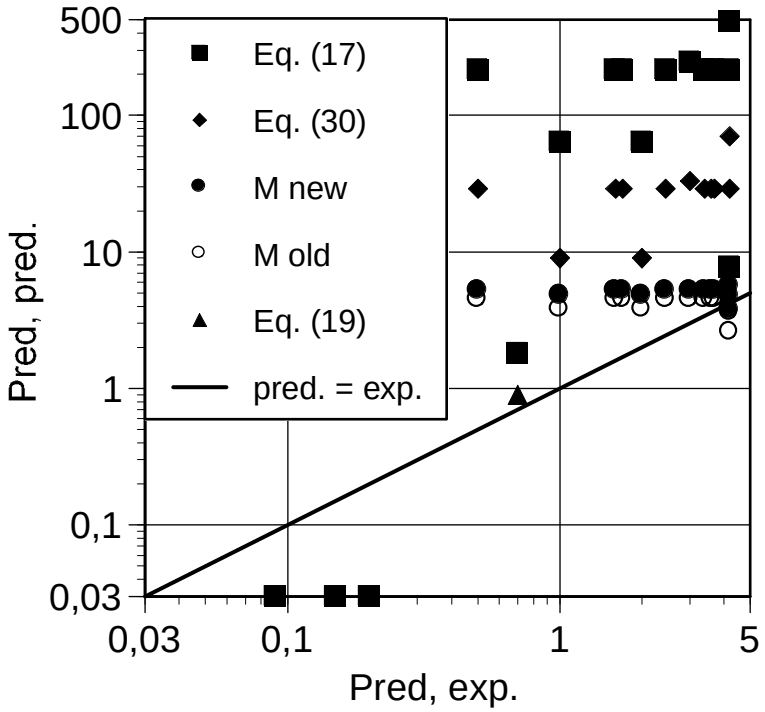

Figure 26. Comparison of predicted and experimental values of P_{red} (Russo and Di Benedetto 2007).

Russo and Di Benedetto (2007) give the values of all the parameters used in the prediction except the enclosure wall area A_s. Most data points (13 out of 18) come from the town gas-air experiments by Kordylewski and Wach (1986, 1988). The parameters used for town gas-air mixtures are: C_S = 0.037 bar$^{1/2}$, S_0 = 1.22 m/s, E = 6.64 and c = 408 m/s. The value C_S = 0.037 bar$^{1/2}$ is recommended by NFPA 68 (2002 edition) for methane-air mixtures and its use for much more reactive town gas-air mixtures cannot be justified. The value of sound velocity 408 m/s has been calculated for a hydrogen-air meixure and is 13 % larger than that in Table 32.

The values of S_0 and E for 25 % town gas concentration were used in the models to cover the entire range of concentrations from 10 to 30 %. This is somewhat misleading, since the variation in P_{red} in the tests is mainly caused by the changes in S_0 and E and not any parameters (such as ignition position) that cannot be accounted for.

To check the calculation, the values of A_s used when applying Eqs. (17) and (30) to the experiments by Kordylewski and Wach (1986, 1988) are recovered in Table 67.

It is seen from Table 67 that these authors have replaced the actual surface area A_s by the quantity $V^{2/3}$. Although A_s is proportional to $V^{2/3}$, it is much larger. In the case of a spherical vessel it is 4.84 times the surface area. The idea of setting A_s equal to $V^{2/3}$ is probably due to mixing up Eq. (20) with Eqs. (17) and (30).

Table 67. The values of A_s used for town gas tests

V, m^3 d, mm A_v, m^2	0.020 25 $4.91 \cdot 10^{-4}$ m^2	0.022 35 $9.62 \cdot 10^{-4}$ m^2	0.022 25 $4.91 \cdot 10^{-4}$ m^2	0.022 21 $3.46 \cdot 10^{-4}$ m^2
Eq. (30), bar calc. A_s, m^2	29 0.071	9 0.078	34 0.077	70 0.078
Eq. (17), bar A/S calc. A_s, m^2	215 0.241 0.073	63 0.445 0.077	245 0.226 0.077	485 0.160 0.077
actual A_s, m^2 $V^{2/3}$, m^2	0.356 0.0737	0.380 0.0785	0.380 0.0785	0.380 0.0785

Next, the values of P_{red} in the tests by McCann et al. (1985) with 9.5 % methane-air, and DeGood and Chatrathi (1991) with 5 % propane-air mixture are predicted with Eqs. (30) and (17) using the incorrect and correct values of A_s, respectively. The parameter values used for methane-air mixtures are C_S = 0.037 $bar^{1/2}$, S_0 = 0.44 m/s, E = 7.48 and c = 353 m/s, and those for propane-air mixtures C_S = 0.045 $bar^{1/2}$, S_0 = 0.46 m/s, E = 7.9 and c = 339 m/s. This calculation is presented in Table 68.

Table 68. The values of A_s used for methane and propane tests

V, m^3 A_v, m^2	$5.64 \cdot 10^{-3}$ m^2 0.01 m^2	$5.64 \cdot 10^{-3}$ m^2 0.01 m^2	2.6 0.56 m^2	2.6 0.56 m^2
A_s, m^2 Eq. (30), bar	$V^{2/3}$ 0.014	0.194 0.52	$V^{2/3}$ 0.023	11.2 0.81
A S A/S Eq. (17), bar	0.189 $8.08 \cdot 10^{-3}$ 23.4 0.023	$3.16 \cdot 10^{-2}$ $8.08 \cdot 10^{-3}$ 3.91 0.82	0.192 $9.36 \cdot 10^{-3}$ 20.6 0.029	$3.25 \cdot 10^{-2}$ $9.36 \cdot 10^{-3}$ 3.47 1.03
R&DiB, bar	≈ 0.03	≈ 0.03	≈ 0.03	≈ 0.03

Although the results by Russo and Di Benedetto (2007) cannot be extracted accurately from the original figure, it is obvious that the incorrect assumption $A_s = V^{2/3}$ has been made also for these tests.

Next, the predictions of P_{red} in the town gas-air tests with the Molkov method are recalculated. The parameters used for town gas-air mixtures are: S_0 = 1.22 m/s, E = 6.64, c = 408 m/s, γ_u = 1.4 and γ_b = 1.25. Predictions with the Molkov method of the test results by Kordylewski and Wach (1986, 1988) are presented in Tables 69 and 71.

Table 69. Predictions with the Molkov method with α = 0.9 and β = 1

V, m^3	d, mm	Br	χ/μ	Br_t	P_{red}, bar	R&DiB, bar
0.020	25	0.375	1.23	0.137	4.85	4.8
0.022	21	0.248	1.22	0.092	5.25	?
0.022	25	0.352	1.24	0.128	4.9	4.8
0.022	35	0.690	1.31	0.237	4.15	4.1

Table 70. Predictions with the Molkov method with α = 1.75 and β = 0.5

V, m^3	d, mm	Br	χ/μ	Br_t	P_{red}, bar	R&DiB, bar
0.020	25	0.375	2.49	0.068	5.5	5.5
0.022	21	0.248	2.43	0.045	5.8	5.6
0.022	25	0.352	2.51	0.063	5.55	5.5
0.022	35	0.690	2.60	0.120	5.0	5.0

Considering the accuracy of reading the values of P_{red} in Fig. 5 by Russo and Di Benedetto (2007), they are equal to those calculated with Eqs. (20) to (24).

5.3.2 Bartknecht correlations

Next, Russo and Di Benedetto (2007) present a plot (Figure 6) which compares experimental values of $P_{red,vd}$ with those predicted using the Bartknecht correlations for gas explosions. For those tests where P_{red} was not measured, predictions were made with the Molkov method. According to the figure caption, the values of P_{red} were predicted for the Molkov et al. (1993) (Table 29) and the Ponizy and Layer (1999a, 1999b) (Tables 30 and 31) tests. They do not, however, mention which one of the parameter sets α = 0.9 and β = 1 and α = 1.75 and β = 0.5 was used in the calculation.

Repeating the calculation with both parameter sets and the erroneous assumption (that P' in Eqs. (39) and (40) is $P_{red, vd}$) gives two plots of which the one with the parameter set α = 0.9 and β = 1 (Figure 27) is similar to Fig. 6 of Russo and Di Benedetto (2007).

A comparison of the predictions of $P_{red, vd}$ and the experimental values calculated with the same method of the Molkov et al. (1993) tests to the respective data points in Fig. 6 of Russo and Di Benedetto (2007) proves that the latter were calculated from the measured values of P_{red} in Table 29. This contradicts the statement in the figure caption.

The data points corresponding to the Kordylewski and Wach (1986) tests have been calculated from the measured values of P_{red} in Table 26 except for the test with 10 % town gas-air mixture for which a zero overpressure was reported. This is not a surprising test result considering the low value of S_0 at 10 % concentration (0.09 m/s in Table 38). Russo and Di Benedetto (2007), however, resolve this problem by predicting P_{red} with the Molkov method. Neglecting the dependence of S_0 on concentration and using the value S_0 = 1.22 m/s leads to a far too high prediction for $P_{red, vd}$ seen as an outlier in Fig. 27.

Russo and Di Benedetto (2007) calculate the relative error of the data points in Figure 27 as 44 %. They conclude that the Bartknecht correlations were unable to give conservative predictions for almost all the conditions investigated. Conservative predictions were given only for Ponizy and Layer (1999a) tests with small values of vent diameter (16 and 21 mm). The high value of relative error is related to the inability of the correlations to account for the effect of duct length, diameter and vessel volume.

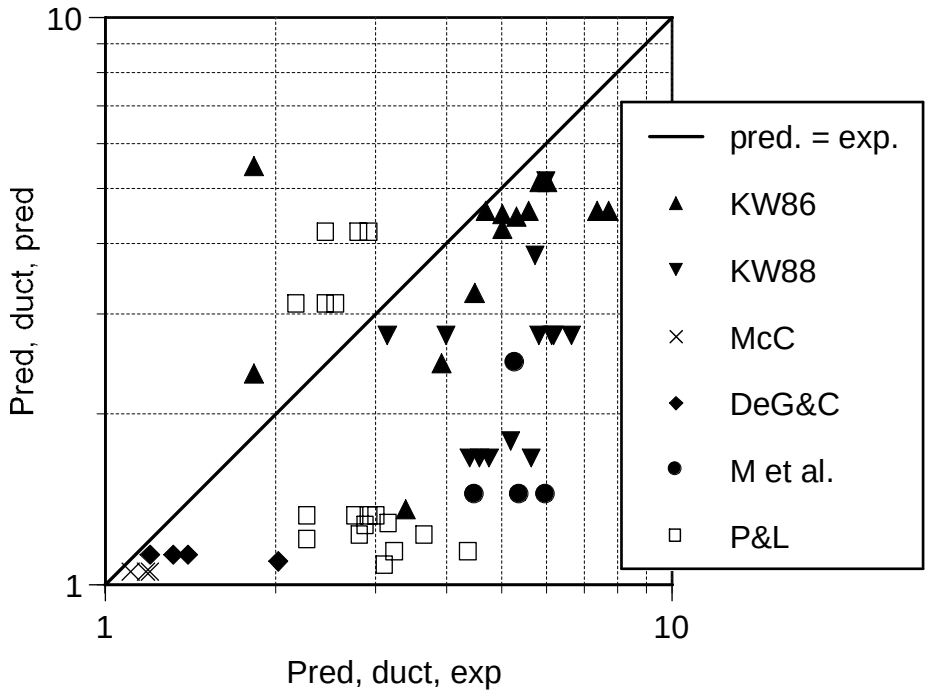

Figure 27. Figure 6 of Russo and Di Benedetto (2007) redrawn with α = 0.9 and β = 1 (in bar absolute pressure).

Figure 27 is now redrawn using the Bartknecht correlations for gas explosions, Eqs. (61) and (62) and the predicted values of P_{red} for the tests by Ponizy and Layer (1999a, 1999b) (Tables 62 to 65). The predictions for $P_{red, vd}$ are presented in Tables 71 to 77 and denoted by "gas". Predicted values calculated using the selection criterion in NFPA 68 (2007) are given in brackets when they differ from those of the original criterion by Bartknecht (1993).

Russo and Di Benedetto (2007) do not mention Bartknecht correlations for dust explosions, Eqs. (44) and (45). In the inverted form they are (Bartknecht 1993)

$$P_{red,vd} = 1.84 P_{red}^{0.654} \quad (69)$$

and

$$P_{red,vd} = 3.00 P_{red}^{0.4776} \quad (70)$$

The predictions for $P_{red, vd}$ by Eqs. (69) and (70) are presented in Tables 71 to 77 and denoted by "dust". In Tables 76 and 77, the parameter set α = 0.9 and β = 1 and the set α = 1.75 and β = 0.5 are called "old" and "new", respectively.

Table 71. Predicted $P_{red, vd}$ for the tests by McCann et al. (1985)

P_{red}, bar	L_d, m	$P_{red, vd}$, gas, bar	$P_{red, vd}$, dust, bar	exp., bar
0.079	0.105	0.14	0.35	0.10
0.079	0.30	0.14	0.35	0.19
0.079	0.50	0.14 (0.67)	0.35	0.17

Table 72. Predicted $P_{red, vd}$ for the tests by Kordylewski and Wach (1986)

%	P_{red}, bar	L_d, m	$P_{red, vd}$, gas, bar	$P_{red, vd}$, dust, bar	exp., bar
12	0.5	2.5	0.68 (1.73)	1.17	2.38
14	1.7	2.5	1.96 (3.26)	2.60	2.91
16	2.5	2.5	2.73 (3.98)	3.35	3.47
18	3.4	2.5	3.56 (4.67)	4.10	4.0
20	3.6	2.5	3.74 (4.81)	4.25	4.3
22	4.2	2.5	4.27 (5.20)	4.70	4.82
25	4.2	2.5	4.27 (5.20)	4.70	5.0
30	1.6	2.5	1.86 (3.16)	2.50	0.82
20	3.7	0.04	3.83	4.33	3.68
20	3.7	0.17	3.83 (4.87)	4.33	3.68
20	3.7	0.3	3.83 (4.87)	4.33	6.71
20	3.7	0.61	3.83 (4.87)	4.33	6.36
20	3.7	1.26	3.83 (4.87)	4.33	4.57
20	3.7	2.5	3.83 (4.87)	4.33	4.0

Table 73. Predicted $P_{red, vd}$ for the tests by Kordylewski and Wach (1988)

D_d, mm	P_{red}, bar	L_d, m	$P_{red, vd}$, gas, bar	$P_{red, vd}$, dust, bar	exp., bar
35	2.0	0.16	2.25 (3.55)	2.90	3.0
35	2.0	0.32	2.25 (3.55)	2.90	4.82
35	2.0	0.54	2.25 (3.55)	2.90	5.65
35	2.0	0.8	2.25 (3.55)	2.90	4.82
35	2.0	1.4	2.25 (3.55)	2.90	5.13
35	2.0	1.75	2.25 (3.55)	2.90	5.18
35	2.0	2.8	2.25 (3.55)	2.90	3.0
35	2.0	3.5	3.55	4.18	4.64
35	2.0	4.91	3.55	4.18	3.57
35	2.0	6.14	3.55	4.18	3.75
35	2.0	6.75	3.55	4.18	3.39
21	4.2	2.5	4.27 (5.20)	4.70	5.0
25	3.0	2.5	3.19 (4.37)	3.77	4.73
35	1.0	2.5	1.24 (2.48)	1.84	4.2

Table 74. Predicted $P_{red, vd}$ for the tests by DeGood and Chatrathi (1991)

ignition	P_{red}, bar	L_d, m	$P_{red, vd}$, gas, bar	$P_{red, vd}$, dust, bar	exp., bar
centre	0.20	1	0.31	0.64	0.185
centre	0.20	2	0.31	0.64	0.300
centre	0.20	3	0.31 (1.08)	0.64	0.385
bottom	0.15	3	0.24 (0.93)	0.53	1.01

Table 75. Predicted $P_{red, vd}$ for the tests by Molkov et al. (1993)

V, m^3	D_d, mm	P_{red}, bar	L_d, m	$P_{red, vd}$, gas, bar	$P_{red, vd}$, dust, bar	exp., bar
0.027	50	0.6	1.83	0.80 (1.90)	1.32	5.0
0.027	50	0.6	2.35	0.80 (1.90)	1.32	3.5–4.4
2	200	3.0	4	4.37 (4.37)	5.07	4.3

Table 76. Predictions of $P_{red, vd}$, gas explosions, Ponizy and Leyer (1999a)

D_d, mm	L_d, m	P_{red}, old, bar	old, bar	P_{red}, new, bar	new, bar	exp., bar
16	0.6	2.81	3.02 (4.23)	3.99	4.08 (5.07)	1.45
21	0.6	1.72	1.98 (3.28)	3.11	3.29 (4.46)	1.17
36	0.6	0.27	0.40 (1.26)	0.75	0.97 (2.14)	1.27
16	1.1	2.81	3.02 (4.23)	3.99	4.08 (5.07)	1.80
21	1.1	1.72	1.98 (3.28)	3.11	3.29 (4.46)	1.45
36	1.1	0.27	0.40 (1.26)	0.75	0.97 (2.14)	1.92
16	2.6	2.81	3.02 (4.23)	3.99	4.08 (5.07)	1.92
21	2.6	1.72	1.98 (3.28)	3.11	3.29 (4.46)	1.55
36	2.6	0.27	0.40 (1.26)	0.75	0.97 (2.14)	1.92
53	2.6	0.08	0.14 (0.67)	0.15	0.24 (0.93)	2.11

Table 77. Predictions of $P_{red, vd}$, gas explosions, Ponizy and Leyer (1999b)

ign.	L_d, m	P_{stat}, bar	P_{red}, old, bar	old, bar	P_{red}, new, bar	new, bar	exp., bar
c	1.7	0	0.27	0.40 (1.26)	0.75	0.97 (2.14)	2.01
c	1.7	0.3	0.35	0.50 (1.44)	0.96	1.20 (2.43)	2.16
c	1.7	0.91	0.49	0.67 (1.72)	1.37	1.63 (2.92)	2.66
c	1.7	2.3	0.76	0.98 (2.15)	2.13	2.38 (3.67)	3.37
r	1.7	0	0.27	0.40 (1.26)	0.75	0.97 (2.14)	1.76
r	1.7	0.32	0.35	0.50 (1.44)	0.98	1.22 (2.45)	1.88
r	1.7	0.83	0.47	0.65 (1.68)	1.32	1.57 (2.86)	1.81
nv	1.7	1.11	0.53	0.72 (1.79)	1.49	1.75 (3.05)	1.27
nv	1.7	2.24	0.73	0.95 (2.11)	2.10	2.35 (3.64)	2.24

Table 78. Predictions of $P_{red, vd}$, dust explosions, Ponizy and Leyer (1999a)

D_d, mm	L_d, m	P_{red}, old, bar	old, bar	P_{red}, new, bar	new, bar	exp., bar
16	0.6	2.81	3.62	3.99	4.62	1.45
21	0.6	1.72	2.62	3.11	3.86	1.17
36	0.6	0.27	0.78	0.75	1.52	1.27
16	1.1	2.81	3.62	3.99	4.62	1.80
21	1.1	1.72	2.62	3.11	3.86	1.45
36	1.1	0.27	0.78	0.75	1.52	1.92
16	2.6	2.81	3.62	3.99	4.62	1.92
21	2.6	1.72	2.62	3.11	3.86	1.55
36	2.6	0.27	0.78	0.75	1.52	1.92
53	2.6	0.08	0.34	0.15	0.53	2.11

Table 79. Predictions of $P_{red, vd}$, dust explosions, Ponizy and Leyer (1999b)

ign.	L_d, m	P_{stat}, bar	P_{red}, old, bar	old, dust, bar	P_{red}, new, bar	new, dust, bar	exp., bar
c	1.7	0	0.27	0.78	0.75	1.52	2.01
c	1.7	0.3	0.35	0.93	0.96	1.79	2.16
c	1.7	0.91	0.49	1.15	1.37	2.26	2.66
c	1.7	2.3	0.76	1.54	2.13	3.02	3.37
r	1.7	0	0.27	0.78	0.75	1.52	1.76
r	1.7	0.32	0.35	0.93	0.98	1.82	1.88
r	1.7	0.83	0.47	1.12	1.32	2.21	1.81
nv	1.7	1.11	0.53	1.21	1.49	2.39	1.27
nv	1.7	2.24	0.73	1.52	2.10	2.99	2.24

Predictions of Eqs. (61) and (62) with the original selection criterion are plotted in Figures 28 and 29 and with the criterion of NFPA 68 (2007) in Figures 30 and 31. Predictions of Eqs. (69) and (70) are plotted in Figures 32 and 33. Parameter set $\alpha = 0.9$ and $\beta = 1$ was used to plot Figs. 28, 30 and 32, and the set $\alpha = 1.75$ and $\beta = 0.5$ Figs. 29, 31 and 33.

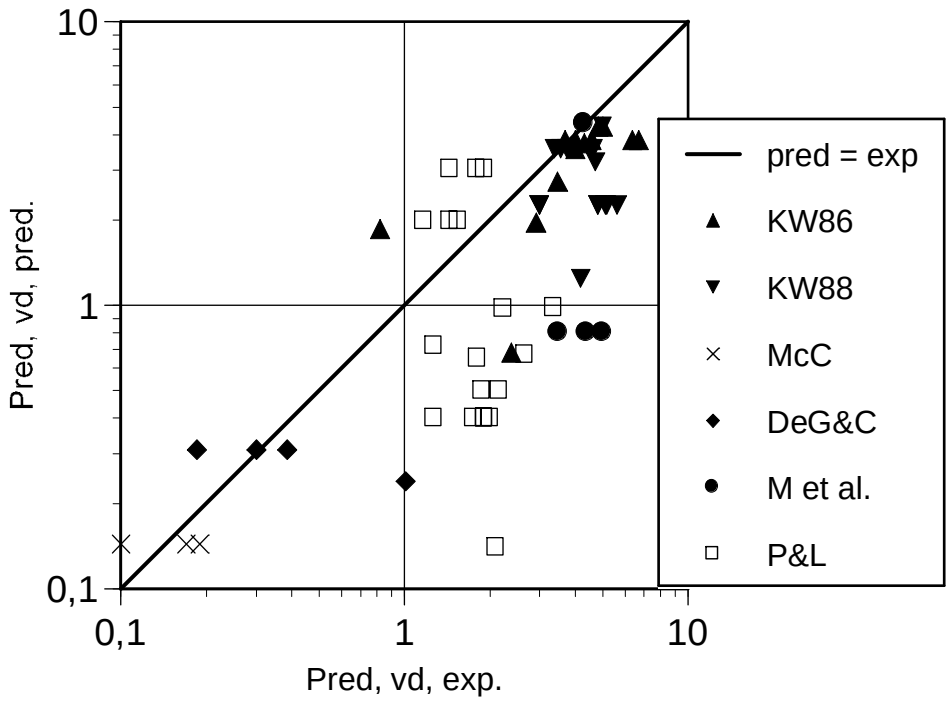

Figure 28. Experimental values of $P_{red, vd}$ compared with those predicted with Eqs. (61) and (62) with the original selection criterion. Parameter set $\alpha = 0.9$ and $\beta = 1$ was used for the tests of Ponizy and Layer (1999a, 1999b).

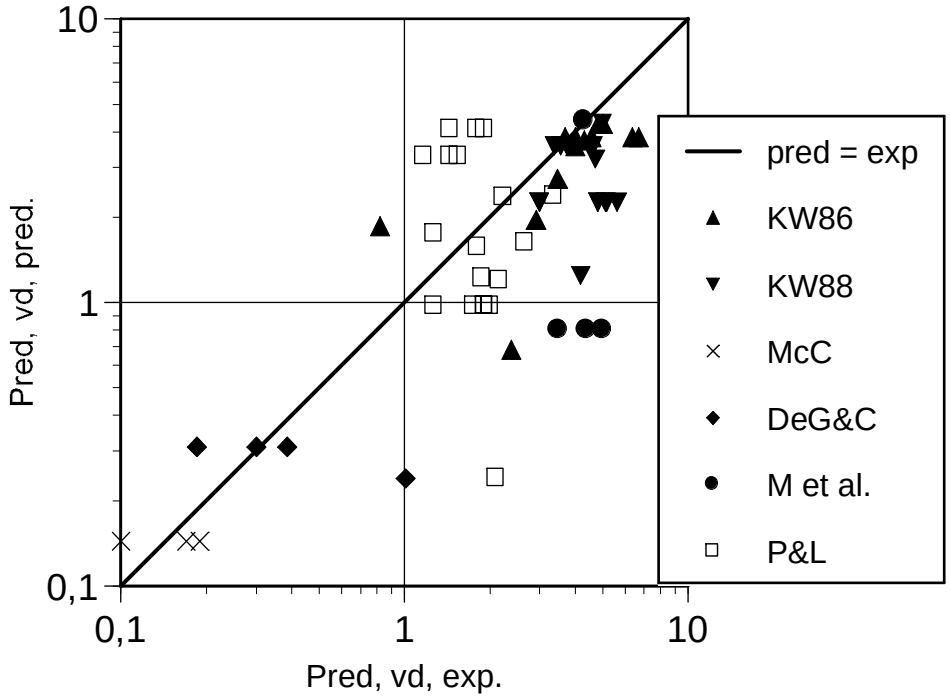

Figure 29. Experimental values of $P_{red,\,vd}$ compared with those predicted with Eqs. (61) and (62) with the original selection criterion. Parameter set α = 1.75 and β = 0.5 was used for the tests of Ponizy and Layer (1999a, 1999b).

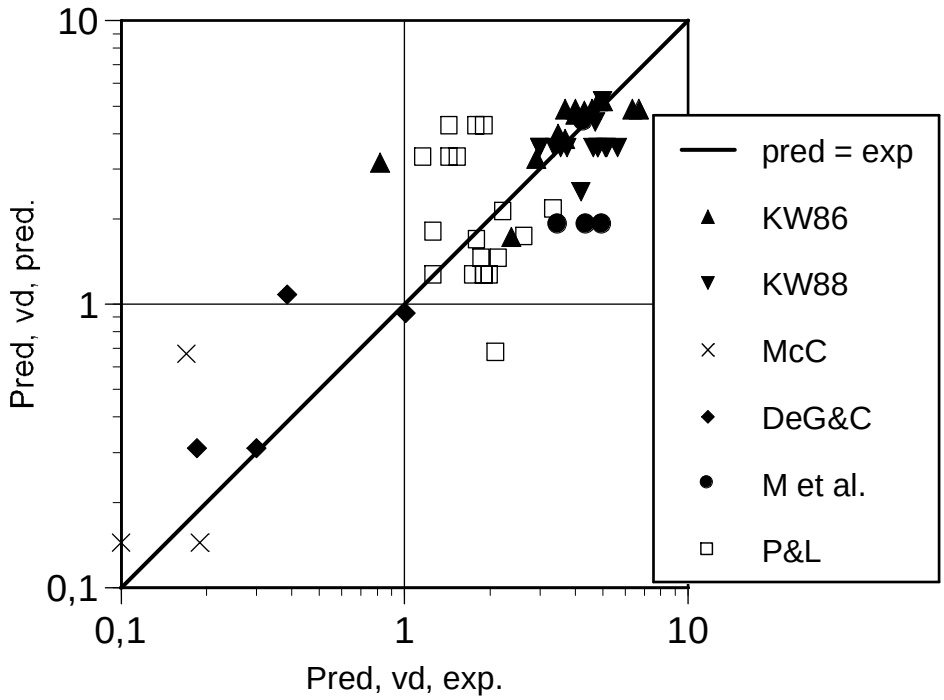

Figure 30. Experimental values of $P_{red,\,vd}$ compared with those predicted with Eqs. (61) and (62) with the criterion of NFPA 68 (2007). Parameter set α = 0.9 and β = 1 was used for the tests of Ponizy and Layer (1999a, 1999b).

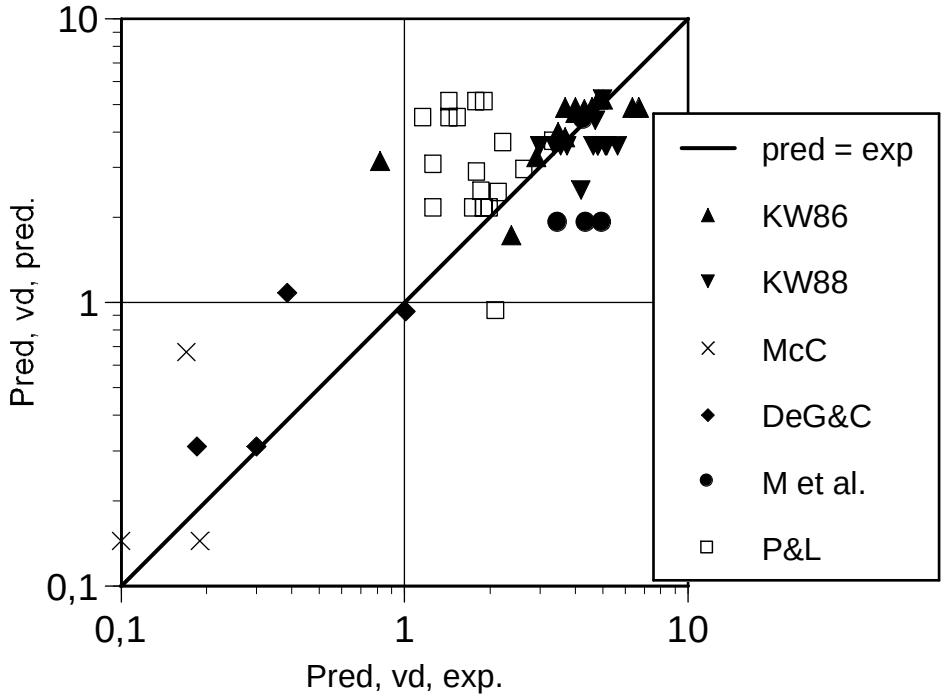

Figure 31. Experimental values of $P_{red,\,vd}$ compared with those predicted with Eqs. (61) and (62) with the criterion of NFPA 68 (2007). Parameter set $\alpha = 1.75$ and $\beta = 0.5$ was used for the tests of Ponizy and Layer (1999a, 1999b).

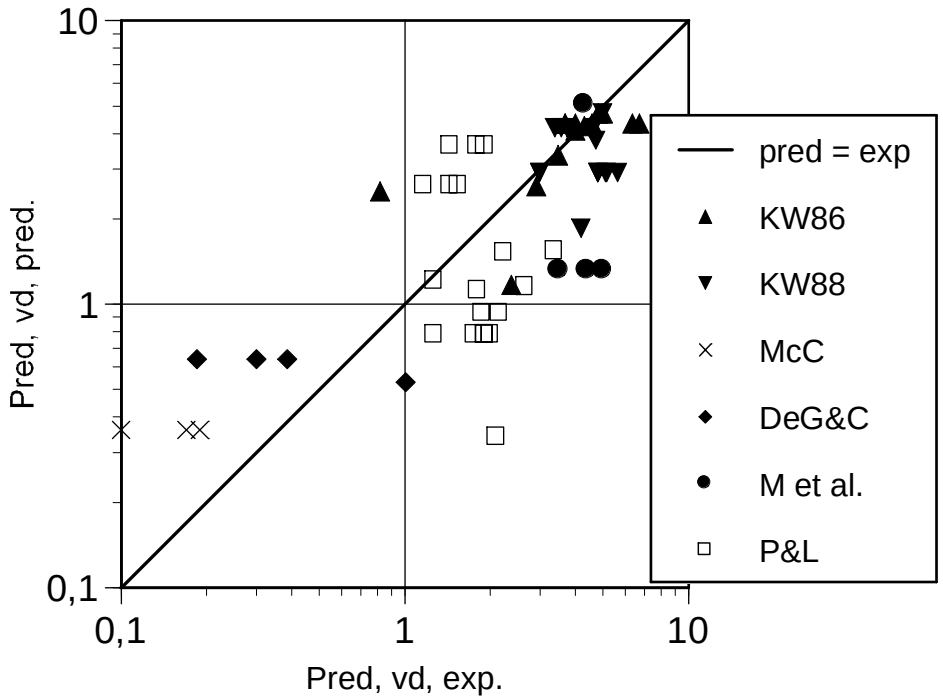

Figure 32. Experimental values of $P_{red,\,vd}$ compared with those predicted with Eqs. (69) and (70). Parameter set $\alpha = 0.9$ and $\beta = 1$ was used for the tests of Ponizy and Layer (1999a, 1999b).

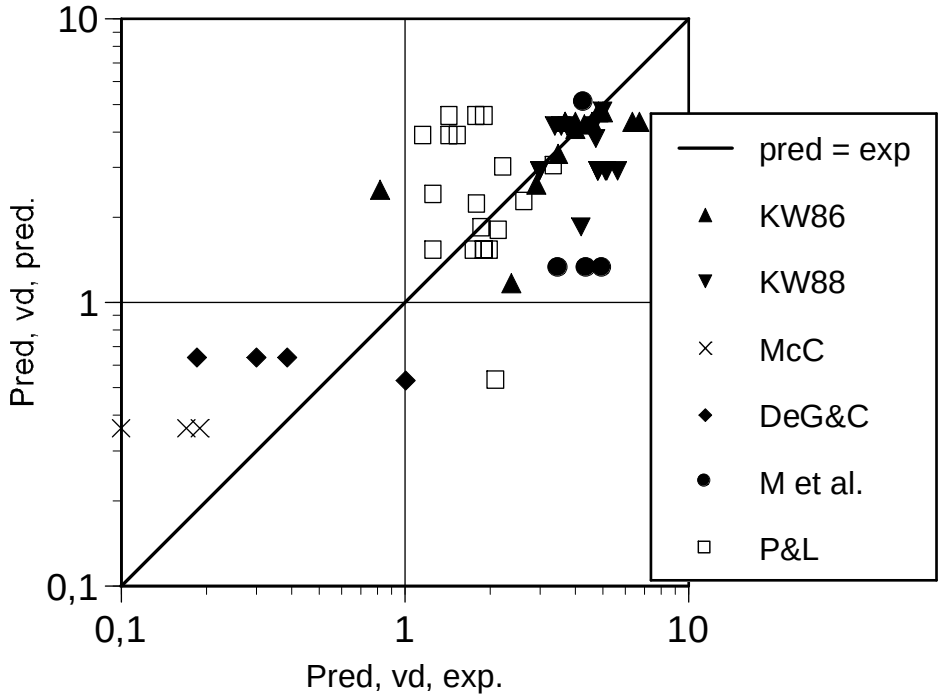

Figure 33. Experimental values of $P_{red, vd}$ compared with those predicted with Eqs. (69) and (70). Parameter set $\alpha = 1.75$ and $\beta = 0.5$ was used for the tests of Ponizy and Layer (1999a, 1999b).

The relative errors were calculated with Eq. (40) and the results are given in Table 71.

Table 80. Relative errors of the predictions, Bartknecht correlations

method	tests	experiment	old	new
gas				
K & W	28	23.0 % (19.5 %)	—	—
the others	11	24.0 % (23.0 %)	—	—
P & L	19	—	44.5 % (40.5 %)	44.0 % (56.0 %)
together	58	—	30.5 % (27.0 %)	30.0 % (32.0 %)
dust				
K & W	28	20.5 %	—	—
the others	11	20.0 %	—	—
P & L	19	—	42.5 %	45.0 %
together	57	—	27.5 %	28.5 %

5.3.3 VDI 3673

Russo and Di Benedetto (2007) validate the method of VDI 3673 Eqs. (47) and (48) with the same data set. This validation is now repeated. Predicted values for the tests with measured P_{red} are calculated in Tables 81 to 83. Cases where L_s calculated with Eq. (47) is lower than duct length L_d are denoted with an asterisk (*).

Table 81. Predicted $P_{red, vd}$ for the tests by McCann et al. (1985)

P_{red}, bar	L_s, m	L_d, m	$P_{red, vd}$, bar	exp., bar
0.079	11.5	0.105	0.12	0.10
0.079	11.5	0.30	0.21	0.19
0.079	11.5	0.50	0.29	0.17

Table 82. Predicted $P_{red, vd}$ for the tests by Kordylewski and Wach (1986)

%	P_{red}, bar	L_s, m	L_d, m	$P_{red, vd}$, bar	exp., bar
12	0.5	5.90	2.5	0.51	2.38
14	1.7	3.75	2.5	1.74	2.91
16	2.5	3.25	2.5	2.56	3.47
18	3.4	2.90	2.5	3.48	4.0
20	3.6	2.84	2.5	3.69	4.3
22	4.2	2.68	2.5	4.30	4.82
25	4.2	2.68	2.5	4.30	5.0
30	1.6	3.84	2.5	1.64	0.82
20	3.7	2.81	0.04	3.70	3.68
20	3.7	2.81	0.17	3.71	3.68
20	3.7	2.81	0.3	3.71	6.71
20	3.7	2.81	0.61	3.72	6.36
20	3.7	2.81	1.26	3.75	4.57
20	3.7	2.81	2.5	3.79	4.0

Table 83. Predicted $P_{red, vd}$ for the tests by Kordylewski and Wach (1988)

D_d, mm	P_{red}, bar	L_s, m	L_d, m	$P_{red, vd}$, bar	exp., bar
35	2.0	3.53	0.16	2.01	3.0
35	2.0	3.53	0.32	2.02	4.82
35	2.0	3.53	0.54	2.03	5.65
35	2.0	3.53	0.8	2.04	4.82
35	2.0	3.53	1.4	2.07	5.13
35	2.0	3.53	1.75	2.09	5.18
35	2.0	3.53	2.8	2.14	3.0
35	2.0	3.53	3.5	2.18	4.64
35	2.0	3.53	4.91	2.18*	3.57
35	2.0	3.53	6.14	2.18*	3.75
35	2.0	3.53	6.75	2.18*	3.39
21	4.2	2.68	2.5	4.25	5.0
25	3.0	3.04	2.5	3.07	4.73
35	1.0	4.56	2.5	1.06	4.2

Table 84. Predicted $P_{red, vd}$ for the tests by DeGood and Chatrathi (1991)

ignition	P_{red}, bar	L_s, m	L_d, m	$P_{red, vd}$, bar	exp., bar
centre	0.20	8.3	1	0.53	0.185
centre	0.20	8.3	2	0.85	0.300
centre	0.20	8.3	3	1.17	0.385
bottom	0.15	9.2	3	0.88	1.01

Table 85. Predicted $P_{red, vd}$ for the tests by Molkov et al. (1993)

V, m^3	D_d, mm	P_{red}, bar	L_s, m	L_d, m	$P_{red, vd}$, bar	exp., bar
0.027	50	0.6	5.5	1.83	0.67	5.0
0.027	50	0.6	5.5	2.35	0.69	3.5–4.4
2	200	3.0	3.04	4	3.28*	4.3

Russo and Di Benedetto (2007) use the following parameter values for 4 % propane-air mixture S_0 = 0.46 m/s, E = 7.90 and c = 339 m/s. Values of P_{red} are predicted for the tests by Ponizy and Leyer (1999a, 1999b) with Eqs. (20) to (24) and the parameter set α = 0.9 and β = 1. The calculation is repeated with the results in Tables 86 and 87.

Table 86. Predictions of P_{red} for the tests by Ponizy and Leyer (1999a)

d, mm	A_v, m^2	Br	χ/μ	Br_t	P_{red}, bar
16	$2.01 \cdot 10^{-4}$	0.87	1.14	0.379	3.35
21	$3.46 \cdot 10^{-4}$	1.50	1.24	0.603	2.37
36	$1.02 \cdot 10^{-3}$	4.42	1.58	1.39	0.46
53	$2.21 \cdot 10^{-3}$	9.57	2.00	2.38	0.126

Table 87. Predictions of P_{red} for the tests by Ponizy and Leyer (1999b)

ignition	P_{stat}, bar	χ/μ	Br_t	P_{red}, bar
centre	0	1.58	1.39	0.46
centre	0.3	1.49	1.47	0.59
centre	0.91	1.36	1.61	0.84
centre	2.3	1.17	1.88	1.31
rear	0.32	1.49	1.48	0.60
rear	0.83	1.38	1.60	0.81
near vent	1.11	1.33	1.66	0.91
near vent	2.24	1.17	1.87	1.29

Using the values of P_{red}, predictions for $P_{red, vd}$ are made in Tables 88 and 89.

Table 88. Predictions of $P_{red, vd}$ for the tests by Ponizy and Leyer (1999a)

D_d, mm	P_{red}, bar	L_s, m	L_d, m	$P_{red, vd}$, bar	exp., bar
16	3.35	2.92	0.6	3.40	1.45
21	2.37	3.32	0.6	2.44	1.17
36	0.46	6.1	0.6	0.51	1.27
16	3.35	2.92	1.1	3.45	1.80
21	2.37	3.32	1.1	2.49	1.45
36	0.46	6.1	1.1	0.55	1.92
16	3.35	2.92	2.6	3.57	1.92
21	2.37	3.32	2.6	2.63	1.55
36	0.46	6.1	2.6	0.65	1.92
53	0.126	9.8	2.6	0.28	2.11

Table 89. Predictions of $P_{red, vd}$ for the tests by Ponizy and Leyer (1999b)

ignition	P_{stat}, bar	P_{red}, bar	L_s, m	L_d, m	$P_{red, vd}$, bar	exp., bar
centre	0	0.46	6.1	1.7	0.59	2.01
centre	0.3	0.59	5.6	1.7	0.75	2.16
centre	0.91	0.84	4.7	1.7	1.06	2.66
centre	2.3	1.31	3.4	1.7	1.63	3.37
rear	0	0.46	6.1	1.7	0.59	1.76
rear	0.32	0.60	7.0	1.7	0.76	1.88
rear	0.83	0.81	4.9	1.7	1.02	1.81
near vent	1.11	0.91	4.8	1.7	1.15	1.27
near vent	2.24	1.29	4.2	1.7	1.61	2.24

Predicted values of $P_{red, vd}$ are compared to experimental ones in Figure 34 which is similar to Fig. 8 of Russo and Di Benedetto (2007) except for the data points of Molkov et al. (1993) which these authors have calculated with P_{red} = 0.7 bar instead of 0.6 bar. They calculate the relative error of the data points in their Fig. 8 as 38 %. When only experimental points were used, the relative error was 29 %.

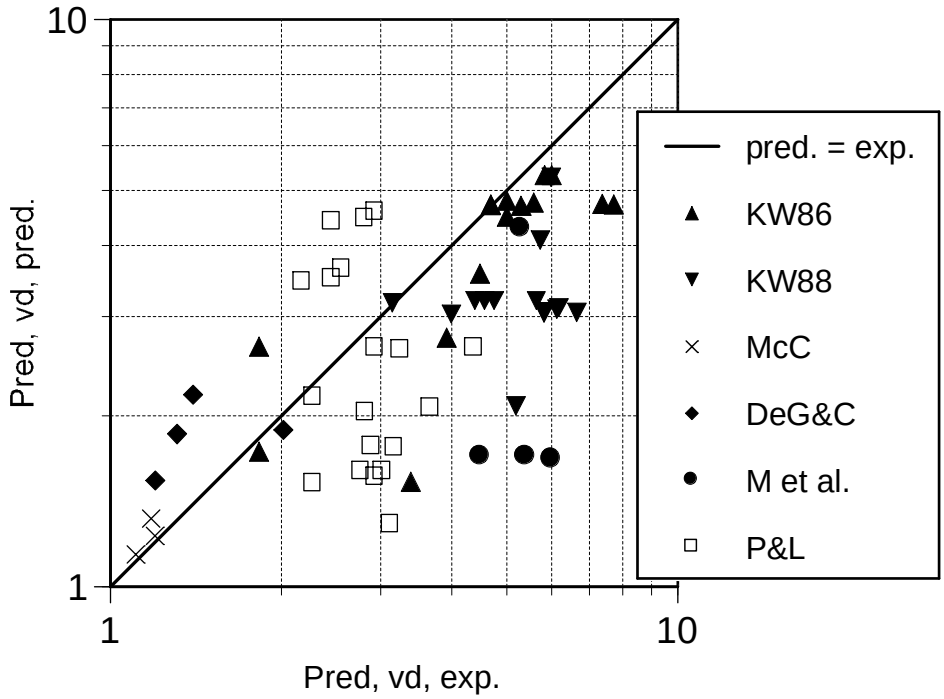

Figure 34. Figure 8 of Russo and Di Benedetto (2007) redrawn with α = 0.9 and β = 1 (in bar absolute pressure).

Predicted values of P_{red} for the tests by Ponizy and Layer (1999a, 1999b) in Tables 62 to 65 are now used to calculate the corresponding values of $P_{red, vd}$.

Table 90. Predicted $P_{red, vd}$ tests by Ponizy & Leyer (1999a) α = 0.9 and β = 1

D_d, mm	P_{red}, bar	L_s, m	L_d, m	$P_{red, vd}$, bar	exp., bar
16	2.81	3.11	0.6	2.86	1.45
21	1.72	3.73	0.6	1.78	1.17
36	0.27	7.4	0.6	0.30	1.27
16	2.81	3.11	1.1	2.90	1.80
21	1.72	3.73	1.1	1.82	1.45
36	0.27	7.4	1.1	0.32	1.92
16	2.81	3.11	2.6	3.02	1.92
21	1.72	3.73	2.6	1.93	1.55
36	0.27	7.4	2.6	0.39	1.92
53	0.08	11.6	2.6	0.18	2.11

Table 91. Predicted $P_{red, vd}$ tests by Ponizy & Leyer (1999b) α = 0.9 and β = 1

ignition	P_{stat}, bar	P_{red}, bar	L_s, m	L_d, m	$P_{red, vd}$, bar	exp., bar
centre	0	0.27	7.4	1.7	0.35	2.01
centre	0.3	0.35	6.7	1.7	0.45	2.16
centre	0.91	0.49	5.9	1.7	0.63	2.66
centre	2.3	0.76	5.1	1.7	0.96	3.37
rear	0	0.27	7.4	1.7	0.35	1.76
rear	0.32	0.35	7.0	1.7	0.45	1.88
rear	0.83	0.47	6.0	1.7	0.60	1.81
near vent	1.11	0.53	5.8	1.7	0.68	1.27
near vent	2.24	0.75	5.1	1.7	0.95	2.24

Table 92. Predicted $P_{red, vd}$ tests by Ponizy & Leyer (1999a) α = 1.75 and β = 0.5

D_d, mm	P_{red}, bar	L_s, m	L_d, m	$P_{red, vd}$, bar	exp., bar
16	4.0	2.74	0.6	4.04	1.45
21	3.11	3.00	0.6	3.18	1.17
36	0.75	5.1	0.6	0.83	1.27
16	4.0	2.74	1.1	4.09	1.80
21	3.11	3.00	1.1	3.24	1.45
36	0.75	5.1	1.1	0.88	1.92
16	4.0	2.74	2.6	4.22	1.92
21	3.11	3.00	2.6	3.42	1.55
36	0.75	5.1	2.6	1.05	1.92
53	0.15	9.3	2.6	0.32	2.11

Table 93. Predicted $P_{red, vd}$ tests by Ponizy & Leyer (1999b) α = 1.75 and β = 0.5

ignition	P_{stat}, bar	P_{red}, bar	L_s, m	L_d, m	$P_{red, vd}$, bar	exp., bar
centre	0	0.77	7.4	1.7	0.95	2.01
centre	0.3	0.98	6.7	1.7	1.21	2.16
centre	0.91	1.39	5.9	1.7	1.71	2.66
centre	2.3	2.17	3.4	1.7	2.63	3.37
rear	0	0.77	7.4	1.7	0.95	1.76
rear	0.32	1.00	7.0	1.7	1.23	1.88
rear	0.83	1.34	6.0	1.7	1.65	1.81
near vent	1.11	0.52	5.7	1.7	1.85	1.27
near vent	2.24	2.14	5.1	1.7	2.59	2.24

Predicted values in Tables 81 to 85 and those in Tables 90 and 91 and Tables 92 and 93 are plotted in Figs. 35 and 36, respectively.

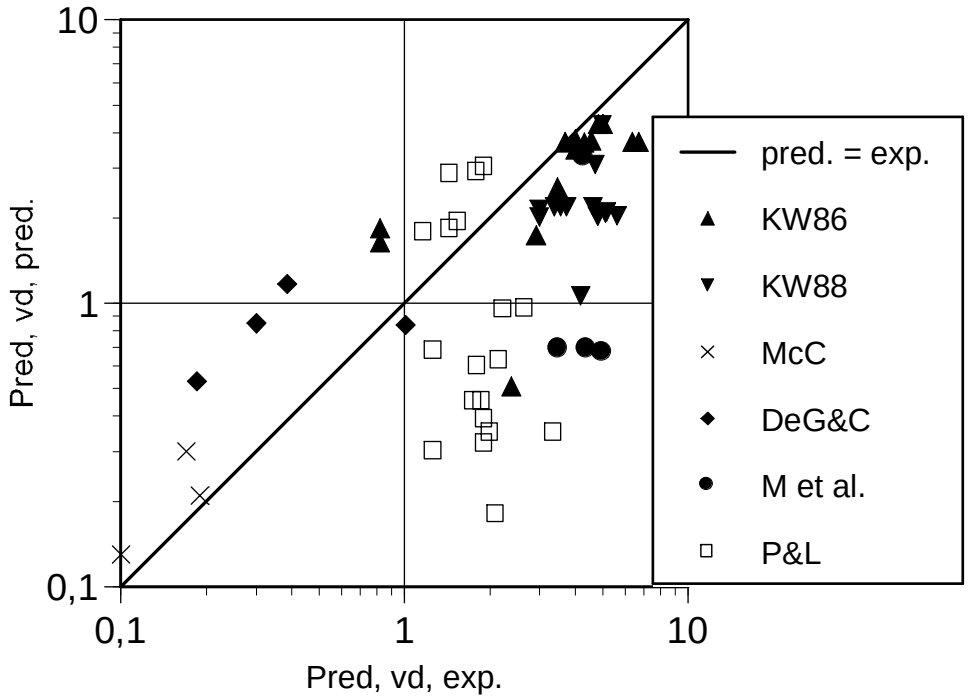

Figure 35. Experimental values of $P_{red,\,vd}$ compared with those predicted with Eqs. (47) and (48). Parameter set α = 0.9 and β = 1 was used for the tests of Ponizy and Layer (1999a, 1999b).

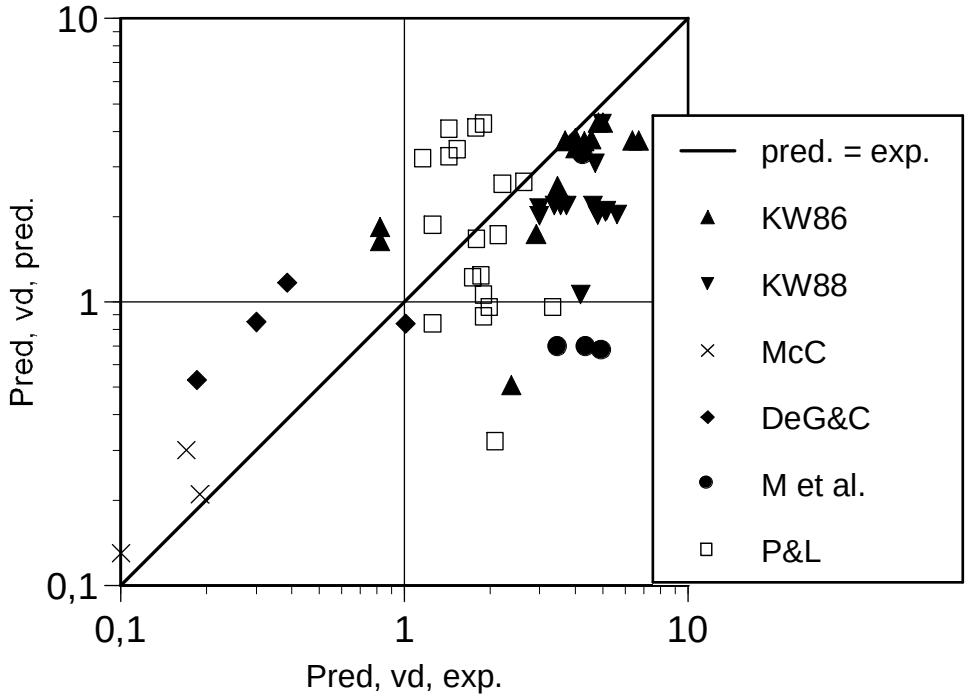

Figure 36. Experimental values of $P_{red,\,vd}$ compared with those predicted with Eqs. (47) and (48). Parameter set α = 1.75 and β = 0.5 was used for the tests of Ponizy and Layer (1999a, 1999b).

The relative errors were calculated with Eq. (40) and the results are given in Table 94.

Table 94. Relative errors of the predictions, VDI 3673

reference	tests	experiment	$\alpha = 0.9, \beta = 1$	$\alpha = 1.75, \beta = 0.5$
K & W	28	28.5 %	—	—
the others	11	34.0 %	—	—
P & L	19	—	43.5 %	42.5 %
together	57	—	34.5 %	34.0 %

5.3.4 NFPA 68 (2002)

Russo and Di Benedetto (2007) validate the method of NFPA 68 (2002 edition) Eqs. (46) and (51) with the same data set. They comply with the stated range of validity of Eq. (46) and exclude tests with $P_{red} > 2$ bar or $L_s < L_d$. The latter criterion, however, is not mentioned in the text. Predicted values of $P_{red, vd}$ for the tests with measured P_{red} are calculated in Tables 95 to 99.

Table 95. Predicted $P_{red, vd}$ for the tests by McCann et al. (1985)

P_{red}, bar	L_s, m	L_d, m	$P_{red, vd}$, bar	exp., bar
0.079	9.5	0.105	0.47	0.10
0.079	9.5	0.30	1.21	0.19
0.079	9.5	0.50	1.96	0.17

Table 96. Predicted $P_{red, vd}$ for the tests by Kordylewski and Wach (1986)

%	P_{red}, bar	L_s, m	L_d, m	$P_{red, vd}$, bar	exp., bar
12	0.5	4.87	2.5	0.99	2.38
14	1.7	3.09	2.5	3.36	2.91
30	1.6	3.16	2.5	3.16	0.82

Table 97. Predicted $P_{red, vd}$ for the tests by Kordylewski and Wach (1988)

D_d, mm	P_{red}, bar	L_s, m	L_d, m	$P_{red, vd}$, bar	exp., bar
35	2.0	2.91	0.16	2.23	3.0
35	2.0	2.91	0.32	2.47	4.82
35	2.0	2.91	0.54	2.79	5.65
35	2.0	2.91	0.8	3.17	4.82
35	2.0	2.91	1.4	4.05	5.13
35	2.0	2.91	1.75	4.56	5.18
35	2.0	2.91	2.8	6.10	3.0
35	1.0	3.76	2.5	2.83	4.2

Table 98. Predicted $P_{red, vd}$ for the tests by DeGood and Chatrathi (1991)

ignition	P_{red}, bar	L_s, m	L_d, m	$P_{red, vd}$, bar	exp., bar
centre	0.20	8.3	1	0.71	0.185
centre	0.20	8.3	2	1.22	0.300
centre	0.20	8.3	3	1.73	0.385
bottom	0.15	9.2	3	1.30	1.01

Table 99. Predicted $P_{red, vd}$ for the tests by Molkov et al. (1993)

V, m^3	D_d, mm	P_{red}, bar	L_s, m	L_d, m	$P_{red, vd}$, bar	exp., bar
0.027	50	0.6	4.55	1.83	1.98	5.0
0.027	50	0.6	4.55	2.35	2.37	3.5–4.4

The prediction of $P_{red, vd}$ for the tests by Ponizy and Layer (1999a, 1999b) is made with the predicted values of P_{red} in Tables 62 and 64. The results are presented in Tables 100 and 101 and plotted in Figure 37 along with those in Tables 95 to 99.

Table 100. Predictions of $P_{red, vd}$ for the tests by Ponizy and Leyer (1999a)

D_d, mm	P_{red}, bar	L_s, m	L_d, m	$P_{red, vd}$, bar	exp., bar
21	1.72	3.1	0.6	3.85	1.17
36	0.27	6.1	0.6	1.36	1.27
21	1.72	3.1	1.1	5.62	1.45
36	0.27	6.1	1.1	2.28	1.92
21	1.72	3.1	2.6	10.9	1.55
36	0.27	6.1	2.6	5.0	1.92
53	0.08	9.6	2.6	3.37	2.11

Table 101. Predictions of $P_{red, vd}$ for the tests by Ponizy and Leyer (1999b)

ignition	P_{stat}, bar	P_{red}, bar	L_s, m	L_d, m	$P_{red, vd}$, bar	exp., bar
centre	0	0.27	6.1	1.7	3.37	2.01
centre	0.3	0.35	5.6	1.7	4.37	2.16
centre	0.91	0.49	4.9	1.7	6.1	2.66
centre	2.3	0.76	4.2	1.7	9.5	3.37
rear	0	0.27	6.1	1.7	3.37	1.76
rear	0.32	0.35	5.6	1.7	4.37	1.88
rear	0.83	0.48	4.9	1.7	6.0	1.81
near vent	1.11	0.54	4.7	1.7	6.7	1.27
near vent	2.24	0.76	4.2	1.7	9.5	2.24

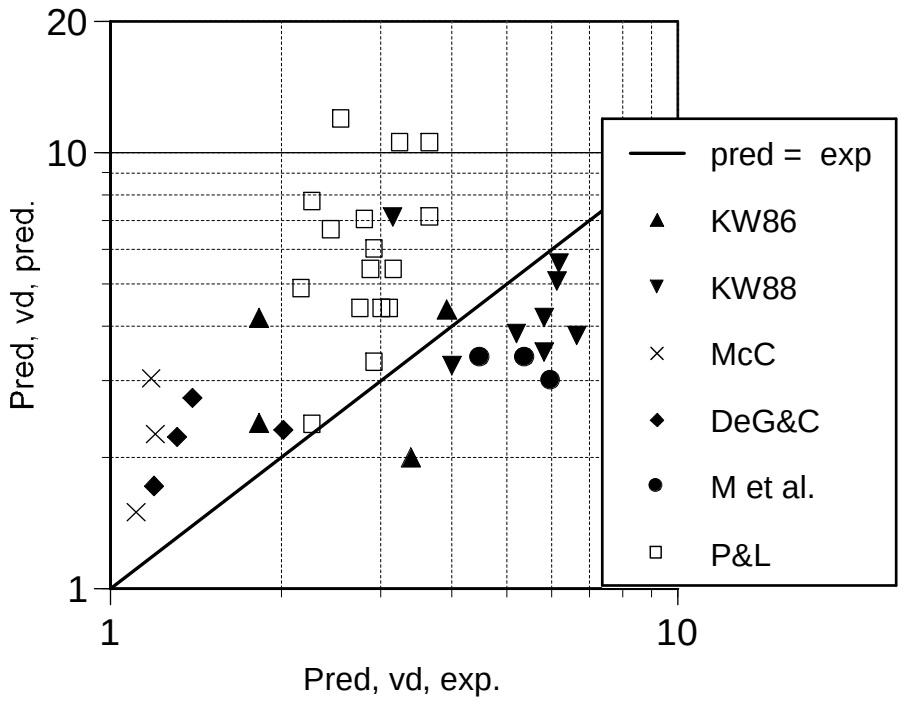

Figure 37. Comparison of $P_{red, vd}$ predicted with S_0 = 0.46 m/s, E = 7.90, c = 339 m/s, α = 0.9 and β = 1 with experimental values (in bar absolute pressure).

Russo and Di Benedetto (2007) calculate the relative error of the data points in their Fig. 9 as 56 %. Of course, this result is not comparable to those found for the other methods, since data points with high values of $P_{red, vd}$, have been omitted.

When Fig. 37 is compared to Fig. 9 of Russo and Di Benedetto (2007) it is found that the data points for the tests by McCann et al. (1985), Kordylewski and Wach (1988), DeGood and Chatrathi (1991), and Molkov et al. (1993) are the same. Some tests by Ponizy and Layer (1999b), particularly those with high predicted values of $P_{red,\ vd}$, have been omitted and the rest have somewhat lower value of $P_{red,\ vd}$ than in Tables 100 and 101 (Figure 38).

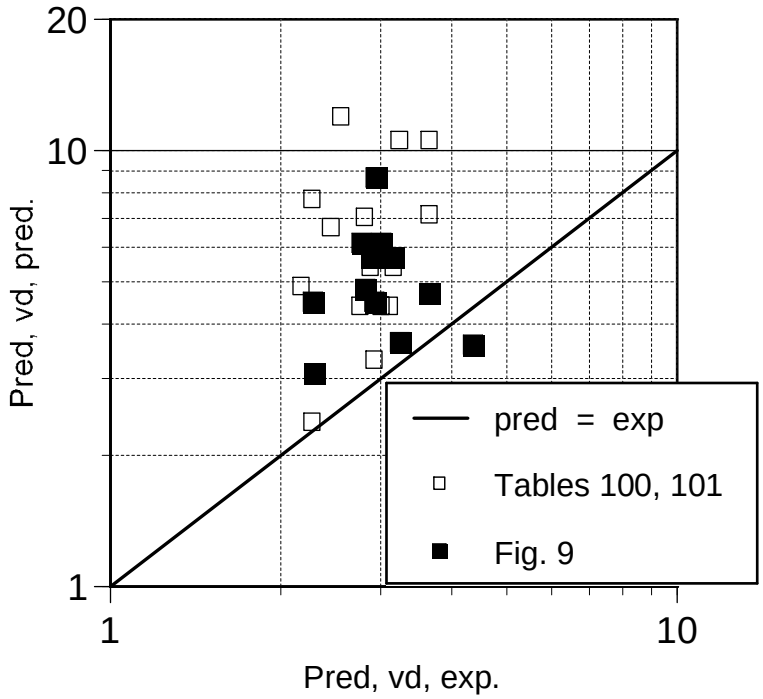

Figure 38. Comparison of $P_{red,\ vd}$ in Tables 100 and 101 with values in Fig. 9 of Russo and Di Benedetto (2007).

In fact, the discrepancy can be traced to lower values of P_{red} than in Tables 86 and 87. Inserting the values of A_v, V, L_d, D_d and $P_{red,\ vd}$ into Eq. (51) and solving for P_{red}, the values of P_{red} used to plot Fig. 9 of Russo and Di Benedetto (2007) can be calculated. This calculation is done in Tables 102 and 103.

Table 102. Calculation of P_{red} for the tests by Ponizy and Leyer (1999a)

D_d, mm	exp., bar	$P_{red,\ vd}$, bar	$P_{red,\ vd}/P_{red}$	P_{red}, bar
21	1.17	—	—	—
36	1.27	2.05	5.05	0.41
21	1.45	—	—	—
36	1.92	3.46	8.43	0.41
21	1.55	—	—	—
36	1.92	7.62	18.56	0.41
53	2.11	—	—	—

Table 103. Calculation of P_{red} for the tests by Ponizy and Leyer (1999b)

ignition	P_{stat}, bar	exp., bar	$P_{red, vd}$, bar	$P_{red, vd}/P_{red}$	P_{red}, bar
centre	0	2.01	5.09	12.5	0.41
centre	0.3	2.16	4.64	12.5	0.37
centre	0.91	2.66	3.66	12.5	0.29
centre	2.3	3.37	2.56	12.5	0.21
rear	0	1.76	5.09	12.5	0.41
rear	0.32	1.88	4.64	12.5	0.37
rear	0.83	1.81	3.78	12.5	0.30
near vent	1.11	1.27	3.46	12.5	0.28
near vent	2.24	2.24	2.60	12.5	0.21

It is seen from Table 102 that Russo and Di Benedetto (2007) have inserted in Eq. (51) the value of P_{red} = 0.41 bar for an initially open vent with diameter D_d = 36 mm. The value of Bradley number Br used by Russo and Di Benedetto (2007) can be found from the calculated values of P_{red} in Table 103. The turbulent Bradley number Br_t is found by inverting Eq. (23)

$$Br_t = \left(\frac{p_0}{P_{red}} \right)^{\frac{1}{2.4}} \tag{71}$$

Inserting Eqs. (20) and (22) into Eq. (21) and using the following parameter values: E = 7.9, c = 339 m/s, γ_u = 1.365, γ_b = 1.25, $A_v = 1.02 \cdot 10^{-3}$ m^2 and $V = 3.66 \cdot 10^{-3}$ m^3, leads to an equation for Br

$$f(Br) = \frac{Br}{\left(1 + \frac{1}{2} Br\right)^{0.4}} = \frac{2.62 Br_t}{\left(2 + \frac{P_{stat}}{p_0}\right)^{0.4}} \tag{72}$$

The values of function f(Br) corresponding to the values of P_{red} in Table 103 are calculated in Table 104.

Table 104. Calculation of f(Br) for the tests by Ponizy and Leyer (1999b)

ignition	P_{stat}, bar	exp., bar	P_{red}, bar	Br_t	f(Br)
centre	0	2.01	0.41	1.46	2.91
centre	0.3	2.16	0.37	1.52	2.86
centre	0.91	2.66	0.29	1.68	2.87
centre	2.3	3.37	0.21	1.94	2.86
rear	0	1.76	0.41	1.46	2.91
rear	0.32	1.88	0.37	1.52	2.85
rear	0.83	1.81	0.30	1.65	2.87
near vent	1.11	1.27	0.28	1.72	2.87
near vent	2.24	2.24	0.21	1.93	2.85

The mean of the values of f(Br) in Table 104 is 2.87 which corresponds to the value 4.64 of the Bradley number Br and the burning velocity S_0 = 0.44 m/s. On the other hand, if the stated value S_0 = 0.46 m/s has been used, the Bradley number is 5.05 and the value 7.0 has been given to the expansion coefficient E.

5.3.5 EN 14491

Eq. (47) is obviously incompatible with Eq. (51) and leads to high values of $P_{red, vd}$ that are unphysical. However, Eq. (50) can be used to calculate L_s even when values of $P_{red} > 2$ bar are investigated. This is the method of EN 14491. Values of $P_{red, vd}$ are calculated with Eqs. (50) and (51) using the predicted values of P_{red} for the tests by Ponizy and Layer (1999a, 1999b) in Tables 62 to 65. The results of the calculation are presented in Tables 105 to 113 and in Figures 39 and 40.

Table 105. Predicted $P_{red, vd}$ for the tests by McCann et al. (1985)

P_{red}, bar	L_s, m	L_d, m	$P_{red, vd}$, bar	exp., bar
0.079	1.3	0.105	0.47	0.10
0.079	1.3	0.30	1.21	0.19
0.079	1.3	0.50	1.96	0.17

Table 106. Predicted $P_{red, vd}$ for the tests by Kordylewski and Wach (1986)

%	P_{red}, bar	L_s, m	L_d, m	$P_{red, vd}$, bar	exp., bar
12	0.5	0.148	2.5	0.53*	2.38
14	1.7	0.094	2.5	1.76*	2.91
16	2.5	0.081	2.5	2.58*	3.47
18	3.4	0.073	2.5	3.50*	4.0
20	3.6	0.071	2.5	3.70*	4.3
22	4.2	0.067	2.5	4.31*	4.82
25	4.2	0.067	2.5	4.31*	5.0
30	1.6	0.096	2.5	1.66*	0.82
20	3.7	0.070	0.04	3.76	3.68
20	3.7	0.070	0.17	3.80*	3.68
20	3.7	0.070	0.3	3.80*	6.71
20	3.7	0.070	0.61	3.80*	6.36
20	3.7	0.070	1.26	3.80*	4.57
20	3.7	0.070	2.5	3.80*	4.0

Table 107. Predicted $P_{red, vd}$ for the tests by Kordylewski and Wach (1988)

D_d, mm	P_{red}, bar	L_s, m	L_d, m	$P_{red, vd}$, bar	exp., bar
35	2.0	0.127	0.16	2.19*	3.0
35	2.0	0.127	0.32	2.19*	4.82
35	2.0	0.127	0.54	2.19*	5.65
35	2.0	0.127	0.8	2.19*	4.82
35	2.0	0.127	1.4	2.19*	5.13
35	2.0	0.127	1.75	2.19*	5.18
35	2.0	0.127	2.8	2.19*	3.0
35	2.0	0.127	3.5	2.19*	4.64
35	2.0	0.127	4.91	2.19*	3.57
35	2.0	0.127	6.14	2.19*	3.75
35	2.0	0.127	6.75	2.19*	3.39
21	4.2	0.056	2.5	4.26*	5.0
25	3.0	3.04	2.5	3.08*	4.73
35	1.0	4.56	2.5	1.12*	4.2

Table 108. Predicted $P_{red, vd}$ for the tests by DeGood and Chatrathi (1991)

ignition	P_{red}, bar	L_s, m	L_d, m	$P_{red, vd}$, bar	exp., bar
centre	0.20	6.97	1	0.71	0.185
centre	0.20	6.97	2	1.22	0.300
centre	0.20	6.97	3	1.73	0.385
bottom	0.15	7.75	3	1.30	1.01

Table 109. Predicted $P_{red, vd}$ for the tests by Molkov et al. (1993)

V, m^3	D_d, mm	P_{red}, bar	L_s, m	L_d, m	$P_{red, vd}$, bar	exp., bar
0.027	50	0.6	0.276	1.83	0.81*	5.0†
0.027	50	0.6	0.276	2.35	0.81*	3.5–4.4
2	200	3.0	0.61	4	3.27*	4.3

Table 110. Predicted $P_{red, vd}$ tests by Ponizy & Leyer (1999a) α = 0.9 and β = 1

D_d, mm	P_{red}, bar	L_s, m	L_d, m	$P_{red, vd}$, bar	exp., bar
16	2.81	0.050	0.6	2.97*	1.45
21	1.72	0.078	0.6	2.00*	1.17
36	0.27	0.267	0.6	0.76*	1.27
16	2.81	0.050	1.1	2.97*	1.80
21	1.72	0.078	1.1	2.00*	1.45
36	0.27	0.267	1.1	0.76*	1.92
16	2.81	0.050	2.6	2.97*	1.92
21	1.72	0.078	2.6	2.00*	1.55
36	0.27	0.267	2.6	0.76*	1.92
53	0.08	0.62	2.6	0.86*	2.11

Table 111. Predicted $P_{red, vd}$ tests by Ponizy & Leyer (1999b) α = 0.9 and β = 1

ignition	P_{stat}, bar	P_{red}, bar	L_s, m	L_d, m	$P_{red, vd}$, bar	exp., bar
centre	0	0.27	0.267	1.7	0.76*	2.01
centre	0.3	0.35	0.242	1.7	0.92*	2.16
centre	0.91	0.49	0.214	1.7	1.20*	2.66
centre	2.3	0.76	0.182	1.7	1.69*	3.37
rear	0	0.27	0.267	1.7	0.76*	1.76
rear	0.32	0.35	0.250	1.7	0.92*	1.88
rear	0.83	0.48	0.216	1.7	1.18*	1.81
near vent	1.11	0.54	0.206	1.7	1.29*	1.27
near vent	2.24	0.76	0.182	1.7	1.69*	2.24

Table 112. Predicted $P_{red, vd}$ tests by Ponizy & Leyer (1999a) α = 1.75 and β = 0.5

D_d, mm	P_{red}, bar	L_s, m	L_d, m	$P_{red, vd}$, bar	exp., bar
16	4.0	0.044	0.6	4.19*	1.45
21	3.11	0.063	0.6	3.51*	1.17
36	0.75	0.181	0.6	1.68*	1.27
16	4.0	0.044	1.1	4.19*	1.80
21	3.11	0.063	1.1	3.51*	1.45
36	0.75	0.181	1.1	1.68*	1.92
16	4.0	0.044	2.6	4.19*	1.92
21	3.11	0.063	2.6	3.51*	1.55
36	0.75	0.181	2.6	1.68*	1.92
53	0.15	0.488	2.6	1.31*	2.11

Table 113. Predicted $P_{red, vd}$ tests by Ponizy & Leyer (1999b) $\alpha = 1.75$ and $\beta = 0.5$

ignition	P_{stat}, bar	P_{red}, bar	L_s, m	L_d, m	$P_{red, vd}$, bar	exp., bar
centre	0	0.75	0.183	1.7	1.68*	2.01
centre	0.3	0.96	0.167	1.7	2.04*	2.16
centre	0.91	1.37	0.146	1.7	2.72*	2.66
centre	2.3	2.13	0.124	1.7	3.92*	3.37
rear	0	0.75	0.183	1.7	1.68*	1.76
rear	0.32	0.98	0.166	1.7	2.08*	1.88
rear	0.83	1.32	0.148	1.7	2.64*	1.81
near vent	1.11	0.49	0.142	1.7	2.92*	1.27
near vent	2.24	2.10	0.125	1.7	3.87*	2.24

The relative errors were calculated with Eq. (40) and the results are given in Table 114.

Table 114. Relative errors of the predictions, EN 14491

reference	tests	experiment	$\alpha = 0.9$, $\beta = 1$	$\alpha = 1.75$, $\beta = 0.5$
K & W	28	26.5 %	—	—
the others	11	65.5 %	—	—
P & L	20	—	33.0 %	47.5 %
together	57	—	37.0 %	41.5 %

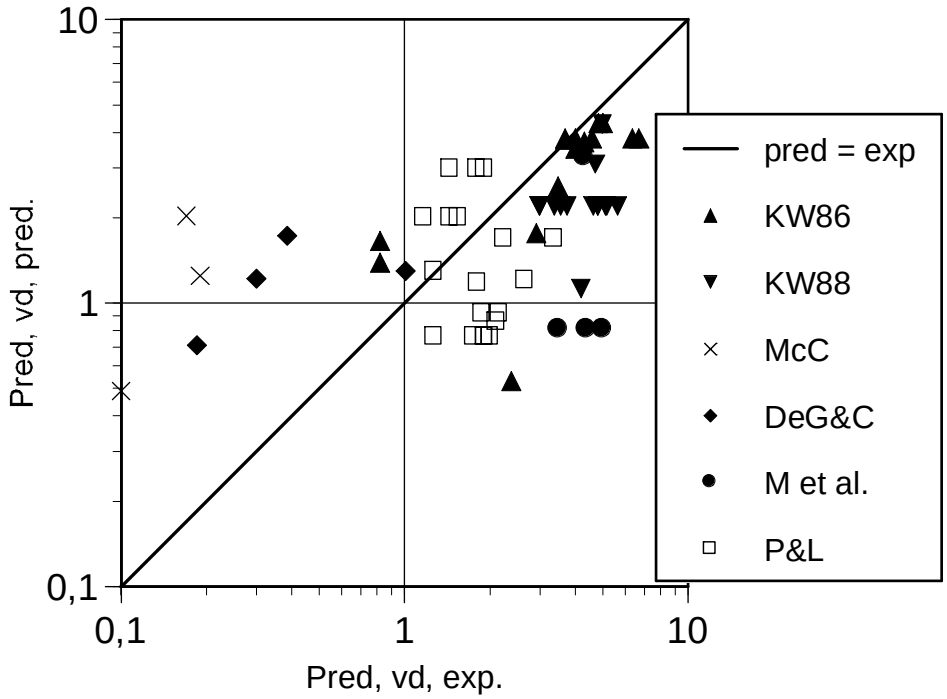

Figure 39. Experimental values of $P_{red, vd}$ compared with those predicted with Eqs. (50) and (51). Parameter set $\alpha = 0.9$ and $\beta = 1$ was used for the tests of Ponizy and Layer (1999a, 1999b).

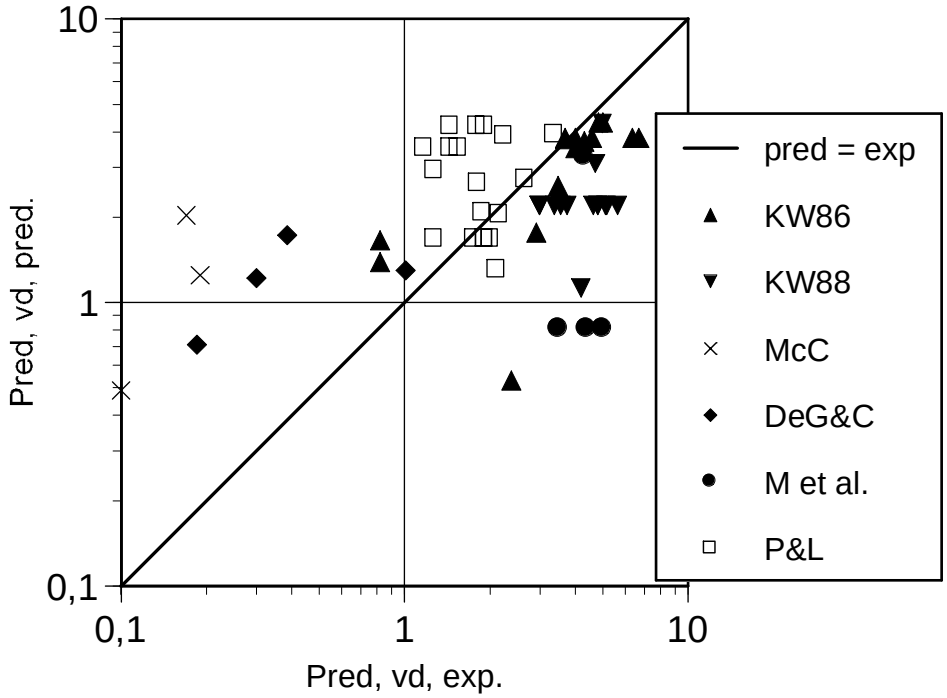

Figure 40. Experimental values of $P_{red,\,vd}$ compared with those predicted with Eqs. (50) and (51). Parameter set α = 1.75 and β = 0.5 was used for the tests of Ponizy and Layer (1999a, 1999b).

5.3.6 Tamanini model

Tamanini model Eqs. (56) to (59) differs from the Bartknecht correlations Eqs. (42) to (45) and Siwek correlations Eqs. (46) to (51) in that the value of the ratio $P_{red,\,vd}/P_{red}$ depends on the combustion properties of the mixture. Thus, the experimental values of this ratio, when available, cannot be used to validate the model. Russo and Di Benedetto (2007) resolve this problem by predicting the reduced pressure P_{red} corresponding to the area of an effective open vent A_{eff} in Eq. (56) with the Molkov method Eqs. (20) to (24) using the parameter set α = 0.9 and β = 1.

To apply the model, the values of the maximum overpressure P_m and gas deflagration index K_G for each mixture must be known. Russo and Di Benedetto (2007) use the values for optimum mixture measured by Bartknecht (1993) in a 5 dm^3 closed test vessel at room temperature using a 10 J spark as ignition source and given in Table 115. Bartknecht (1993) used a mixture of methane (40 %) and hydrogen (60 %) to simulate town gas. The values for acetone are based on measurements by Bartknecht and have been taken from NFPA 68.

Table 115. Values of P_m and K_G used by Russo and Di Benedetto (2007)

fuel	P_m, bar	K_G, bar·m/s
methane, natural gas	7.1	55
acetone	7.3	84
propane	7.9	100
town gas	7.1	140

Calculations by Russo and Di Benedetto (2007) are now repeated for the tests by McCann et al. (1985) with the parameters for 9.5 % methane-air mixture S_0 = 0.44 m/s, E = 7.48, c = 353 m/s, γ_u = 1.38 and γ_b = 1.18.

Table 116. Predicted $P_{red, vd}$ for the tests by McCann et al. (1985)

L_d, m	A_v/A_{eff}	Br	Br_t	$P_{red, vd}$, bar	exp., bar
0.105	1.10	32.4	4.85	0.023	0.10
0.30	1.30	27.5	4.38	0.029	0.19
0.50	1.50	23.9	4.01	0.036	0.17

The parameters for town gas-air mixtures test by Kordylewski and Wach (1986, 1988) were S_0 = 1.22 m/s, E = 6.64, c = 408 m/s, γ_u = 1.4 and γ_b = 1.25.

Table 117. Predicted $P_{red, vd}$ for the tests by Kordylewski and Wach (1986)

%	L_d, m	A_v/A_{eff}	Br	Br_t	$P_{red, vd}$, bar	exp., bar
10	2.5	2.62	0.143	0.054	5.67	0.82
12	2.5	2.62	0.143	0.054	5.67	2.38
14	2.5	2.62	0.143	0.054	5.67	2.91
16	2.5	2.62	0.143	0.054	5.67	3.47
18	2.5	2.62	0.143	0.054	5.67	4.0
20	2.5	2.62	0.143	0.054	5.67	4.3
22	2.5	2.62	0.143	0.054	5.67	4.82
25	2.5	2.62	0.143	0.054	5.67	5.0
30	2.5	2.62	0.143	0.054	5.67	0.82
20	0.04	1.03	0.365	0.133	4.87	3.68
20	0.17	1.11	0.338	0.124	4.95	3.68
20	0.3	1.20	0.314	0.116	5.02	6.71
20	0.61	1.40	0.269	0.100	5.17	6.36
20	1.26	1.82	0.206	0.077	5.40	4.57
20	2.5	2.62	0.143	0.054	5.67	4.0

Table 118. Predicted $P_{red, vd}$ for the tests by Kordylewski and Wach (1988)

D_d, mm	L_d, m	A_v/A_{eff}	Br	Br_t	$P_{red, vd}$, bar	exp., bar
35	0.16	1.11	0.621	0.216	4.27	3.0
35	0.32	1.22	0.565	0.198	4.39	4.82
35	0.54	1.37	0.504	0.178	4.53	5.65
35	0.8	1.54	0.448	0.160	4.66	4.82
35	1.4	1.95	0.354	0.128	4.91	5.13
35	1.75	2.19	0.315	0.115	5.03	5.18
35	2.8	2.91	0.237	0.088	5.29	3.0
35	3.5	3.38	0.204	0.076	5.35	4.64
35	4.91	4.34	0.159	0.060	5.61	3.57
35	6.14	5.18	0.133	0.050	5.73	3.75
35	6.75	5.60	0.123	0.046	5.78	3.39
21	2.5	2.50	0.127	0.048	5.76	5.0
25	2.5	2.56	0.176	0.066	5.53	4.73
35	2.5	2.70	0.256	0.094	5.22	4.2

The parameters used for tests with propane-air mixtures by DeGood and Chatrathi (1991) were S_0 = 0.46 m/s, E = 7.9, c = 339 m/s, γ_u = 1.365 and γ_b = 1.25.

Table 119. Predicted $P_{red,\,vd}$ for the tests by DeGood and Chatrathi (1991)

ignition	L_d, m	A_v/A_{eff}	Br	Br_t	$P_{red,\,vd}$, bar	exp., bar
centre	1	1.16	26.0	2.25	0.145	0.185
centre	2	1.33	22.8	2.07	0.175	0.300
centre	3	1.50	20.3	1.92	0.210	0.385
bottom	3	1.50	20.3	1.92	0.210	1.01

The parameters used for tests with acetone-air mixtures by Molkov et al. (1993) were E = 7.9, c = 339 m/s, γ_u = 1.365 and γ_b = 1.25. The values of S_0 calculated by Molkov for each test are used in the prediction.

Table 120. Predicted $P_{red,\,vd}$ for the tests by Molkov et al. (1993)

V, m^3	L_d, m	D_d, mm	A_v/A_{eff}	S_0, m/s	Br	Br_t	$P_{red,\,vd}$, bar	exp., bar
0.027	1.83	50	1.95	0.26	2.03	0.667	2.13	5.0†
0.027	2.35	50	2.22	0.28	1.66	0.570	2.50	4.4
0.027	2.35	50	2.22	0.28	1.66	0.570	2.50	3.5
0.027	2.35	50	2.22	0.29	1.60	0.670	2.11	1.9
0.027	1.83	50	1.95	0.29	1.82	0.731	1.90	4.4†
2	4	200	1.49	0.325	1.94	0.390	3.30	4.3
2	10	200	2.22	0.335	1.26	0.273	3.91	5.2
2	10	380	2.44	0.295	4.71	0.765	1.77	2.15
10	25	500	2.96	0.32	2.11	0.339	3.55	4.1
10	25	500	2.96	0.27	2.51	0.384	3.33	2.8

The parameters used for tests with propane-air mixtures by Ponizy & Leyer (1999a, 1999b) were S_0 = 0.46 m/s, E = 7.9, c = 339 m/s, γ_u = 1.365 and γ_b = 1.25.

Table 121. Predicted $P_{red,\,vd}$ for the tests by Ponizy & Leyer (1999a)

D_d, mm	L_d, m	A_v/A_{eff}	Br	Br_t	$P_{red,\,vd}$	Fig. 7	exp.
16	0.6	1.57	0.556	0.253	4.03	4.50	1.45
21	0.6	1.61	0.934	0.403	3.23	3.12	1.17
36	0.6	1.70	2.60	0.937	1.21	1.01	1.27
16	1.1	2.04	0.427	0.199	4.38	4.34	1.80
21	1.1	2.12	0.710	0.316	3.67	3.17	1.45
36	1.1	2.27	1.94	0.744	1.85	1.83	1.92
16	2.6	3.47	0.252	0.121	4.98	5.12	1.92
21	2.6	3.64	0.413	0.193	4.42	4.59	1.55
36	2.6	4.01	1.10	0.465	2.95	3.25	1.92
53	2.6	4.31	2.22	0.828	1.56	1.92	2.11

Table 122. Predicted $P_{red, vd}$ for the tests by Ponizy & Leyer (1999b)

ignition	P_{stat}, bar	A_v/A_{eff}	Br	Br_t	$P_{red, vd}$	Fig. 7	exp.
centre	0	2.97	1.49	0.598	2.39	2.41	2.01
centre	0.3	2.97	1.49	0.632	2.26	2.41	2.16
centre	0.91	2.97	1.49	0.694	2.03	2.50	2.66
centre	2.3	2.97	1.49	0.810	1.62	1.83	3.37
rear	0	2.97	1.49	0.598	2.39	2.51	1.76
rear	0.32	2.97	1.49	0.634	2.25	—	1.88
rear	0.83	2.97	1.49	0.686	2.06	2.20	1.81
near vent	1.11	2.97	1.49	0.713	1.96	2.14	1.27
near vent	2.24	2.97	1.49	0.806	1.61	1.83	2.24

The predicted and experimental values of $P_{red, vd}$ in Tables 116 to 122 are plotted in Figure 41.

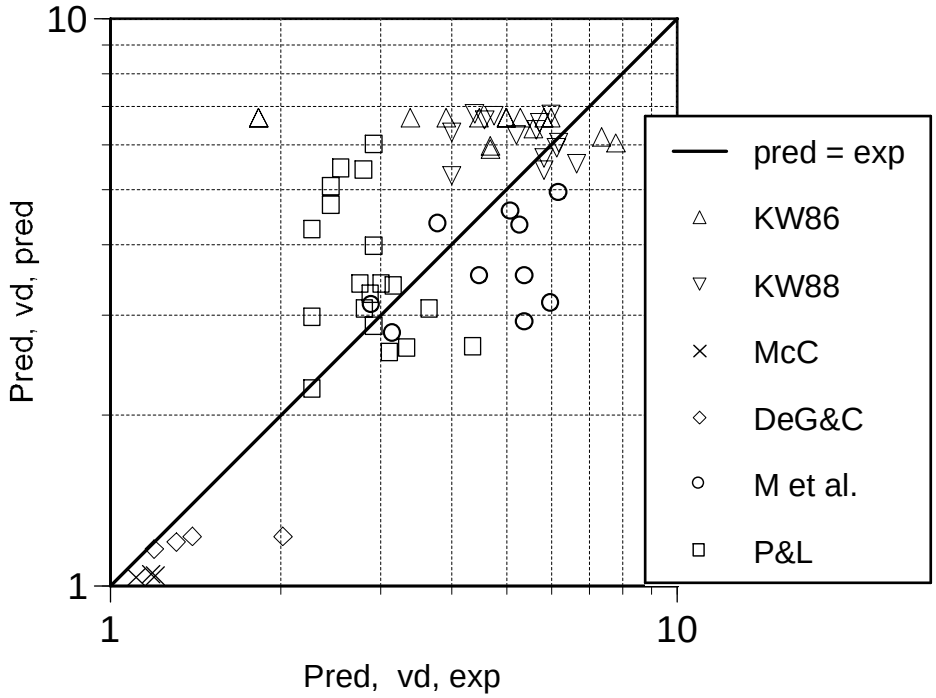

Figure 41. Comparison of $P_{red, vd}$ predicted with Tamanini model and Eqs. (20) to (24) with experimental values (in bar absolute pressure).

When Fig. 41 is compared to Fig. 7 of Russo and Di Benedetto (2007) it is found that the data points for the tests by McCann et al. (1985), Kordylewski and Wach (1988), and DeGood and Chatrathi (1991) are the same. The predicted values of $P_{red, vd}$ for the Molkov et al. (1993) tests in the 0.027 m^3 and 2 m^3 enclosures agree with those in Table 120. The predictions for the 10 m^3 enclosure, however, are about 20 % or 0.7 bar higher than in Table 120. Except for one case, the values in Fig. 7 of Russo and Di Benedetto (2007) are within ±15 % of the predictions in Tables 121 and 122. Russo and Di Benedetto (2007) calculate the relative error of the data points in their Fig. 7 as 39 %.

The values of P_m and K_G in Table 115 are based on measurements by Bartknecht who used them in the derivation of Eq. (33). Since vent dimensioning with Eq. (33) is done for optimal mixtures, the values of P_m and K_G have not been

measured for non-optimal mixtures. In the present data set, duct venting of non-optimal mixtures were investigated by Kordylewski and Wach (1986, 1988).

When Eqs. (57), (58) and (60) are inserted into Eq. (56) it is seen that the ratio A_v/A_{eff} for a straight duct with circular cross section is $1 + B(K_{St}/P_m)^{1/2}$ where B is a function of temperature as well as enclosure and duct dimensions. The ratio A_v/A_{eff} is seen to be weakly dependent on combustion properties of the flammable mixture. Thus, it is justified to evaluate the values of K_G and P_m approximately for non-optimal mixtures.

When the value of K_G of a flammable gas has not been measured, it can be approximated from a known value of another flammable gas by multiplying it with the ratio of respective fundamental burning velocities of the gases (NFPA 68)

$$K_{G,2} = \frac{S_{0,2}}{S_{0,1}} K_{G,1} \qquad (73)$$

A theoretical value for P_m can be calculated assuming adiabatic isochoric complete combustion. This value (P_{aicc}) is calculated by slightly modifying the approximate method by Goodger (1977). In the original method combustion at atmospheric pressure is assumed, enthalpy of the system remains constant and the adiabatic temperature T_{ad} is found by iteration using enthalpy tables.

In the modified method, internal energy remains constant and the values of P_{aicc} and T_{aicc} are found by iteration. At isochoric combustion, the change of internal energy is $\Delta h - V\Delta p$. Here V is the volume containing one mole of town gas and 4.76m moles of air at the initial temperature. The values of Δh are taken from the enthalpy tables. It is to be noted that the partial-equilibrium constants of the reactions $CO_2 \leftrightarrow CO + 0.5O_2$, and $H_2O \leftrightarrow H_2 + 0.5O_2$ are proportional to the square root of absolute pressure whereas that of the water-gas reaction is independent of pressure. The results of the calculation are presented in Table 123 and plotted in Figure 42.

Table 123. T_{aicc} and P_{aicc} of town gas-air mixtures, K & W (1986)

C, %	m	N_i	N_f	T_{aicc}, K	P_{aicc}, bar
10	1.891	10.000	9.750	1901	5.29
12	1.541	8.333	8.086	2143	6.05
14	1.291	7.143	6.902	2376	6.79
16	1.103	6.250	6.020	2552	7.38
18	0.957	5.556	5.370	2685	7.81
20	0.840	5.000	4.859	2719	7.97
22	0.745	4.545	4.481	2685	7.98
25	0.630	4.000	4.050	2506	7.61
30	0.490	3.333	3.522	2087	6.84

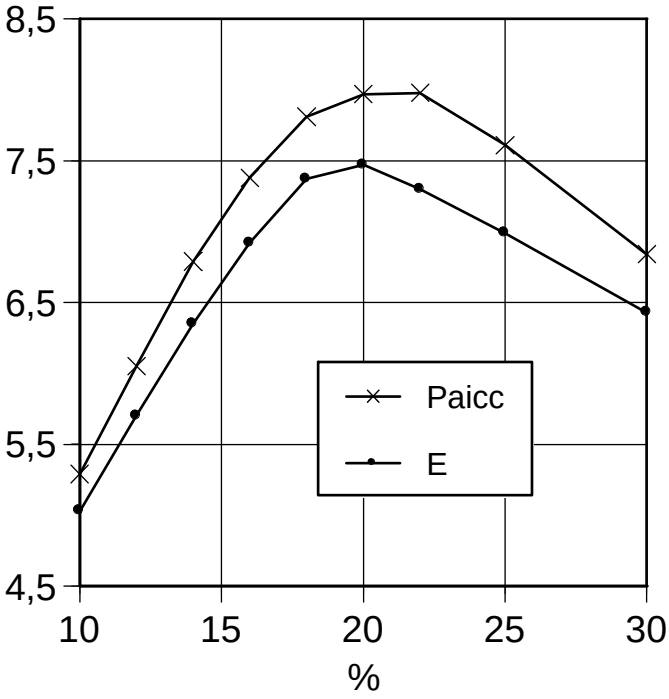

Figure 42. Adiabatic isochoric complete combustion pressure P_{aicc} [bar] and expansion factor E of town gas-air mixtures of Kordylewski & Wach (1986).

The experimental value of P_m, however, is always lower than P_{aicc}. Hot combustion products lose some heat to vessel wall by thermal radiation, resulting into a value of P_m that depends on the size of the vessel. An experimental value of a gas can be approximated from a known value of another flammable gas by multiplying it with the ratio of respective values of P_{aicc} of the gases (NFPA 68)

$$P_{m,2} = \frac{P_{aicc,2}}{P_{áicc,1}} P_{m,1} \qquad (74)$$

A prediction of $P_{red,\ vd}$ for the tests by Kordylewski and Wach (1986, 1988) is made using the parameter values for town gas-air mixtures in Tables 38 and 123, and Eqs. (73) and (74). Results of the calculation are presented in Tables 124 to 125.

Table 124. Predicted A_v/A_{eff} for the tests by Kordylewski and Wach (1986)

C, %	$S_{0,}$ m/s	K_G, bar·m/s	P_{aicc}, bar	P_m, bar	A_v/A_{eff}
10	0.09	13	5.29	4.94	1.60
12	0.15	21	6.05	5.64	1.71
14	0.24	34	6.79	6.33	1.85
16	0.36	50	7.38	6.89	1.99
18	0.51	71	7.81	7.29	2.15
20	0.64	90	7.97	7.44	2.28
22	0.80	112	7.98	7.45	2.43
25	1.00	140	7.61	7.10	2.63
30	0.70	98	6.84	6.38	2.44

Table 125. Predicted $P_{red, vd}$, Kordylewski and Wach (1986), α = 0.9 and β = 1

C, %	A_v/A_{eff}	γ_u	c, m/s	Br	Br_t	$P_{red, vd}$, bar	exp., bar
10	1.60	1.395	352	3.776	0.841	1.52	0.82
12	1.71	1.394	354	1.843	0.515	2.73	2.38
14	1.85	1.393	356	0.946	0.310	3.71	2.91
16	1.99	1.392	358	0.536	0.195	4.41	3.47
18	2.15	1.391	360	0.329	0.128	4.92	4.0
20	2.28	1.390	362	0.245	0.097	5.20	4.3
22	2.43	1.389	364	0.190	0.075	5.48	4.82
25	2.63	1.387	367	0.148	0.058	5.63	5.0
30	2.44	1.385	373	0.255	0.094	5.23	0.82

Table 126. Predicted $P_{red, vd}$, Kordylewski and Wach (1986), α = 0.9 and β = 1

C, %	L, m	A_v/A_{eff}	Br	Br_t	$P_{red, vd}$, bar	exp., bar
20	0.04	1.02	0.547	0.206	4.33	3.68
20	0.17	1.09	0.513	0.195	4.41	3.68
20	0.3	1.15	0.484	0.185	4.48	6.71
20	0.61	1.31	0.425	0.164	4.63	6.36
20	1.26	1.64	0.339	0.132	4.88	4.57
20	2.5	2.28	0.245	0.097	5.20	4.0

Table 127. Predicted $P_{red, vd}$, Kordylewski and Wach (1988) α = 0.9 and β = 1

D_d, mm	L_d, m	A_v/A_{eff}	Br	Br_t	$P_{red, vd}$, bar	exp., bar
35	0.16	1.08	1.206	0.409	3.21	3.0
35	0.32	1.15	1.126	0.385	3.32	4.82
35	0.54	1.26	1.032	0.358	3.46	5.65
35	0.8	1.38	0.939	0.329	3.60	4.82
35	1.4	1.49	0.873	0.309	3.71	5.13
35	1.75	1.55	0.706	0.256	4.02	5.18
35	2.8	2.34	0.554	0.206	4.34	3.0
35	3.5	2.68	0.485	0.182	4.50	4.64
35	4.91	3.36	0.387	0.147	4.76	3.57
35	6.14	3.95	0.329	0.127	4.93	3.75
35	6.75	4.24	0.306	0.118	5.00	3.39
21	2.5	2.06	0.227	0.089	5.28	5.0
25	2.5	2.10	0.315	0.122	4.97	4.73
35	2.5	2.20	0.591	0.218	4.25	4.2

Table 128. Predicted $P_{red, vd}$, Kordylewski and Wach (1986), α = 1.75 and β = 0.5

C, %	A_v/A_{eff}	γ_u	c, m/s	Br	Br_t	$P_{red, vd}$, bar	exp., bar
10	1.60	1.395	352	3.776	0.504	2.78	0.82
12	1.71	1.394	354	1.843	0.279	3.88	2.38
14	1.85	1.393	356	0.946	0.159	4.67	2.91
16	1.99	1.392	358	0.536	0.097	5.20	3.47
18	2.15	1.391	360	0.329	0.063	5.56	4.0
20	2.28	1.390	362	0.245	0.048	5.76	4.3
22	2.43	1.389	364	0.190	0.037	5.92	4.82
25	2.63	1.387	367	0.148	0.029	6.06	5.0
30	2.44	1.385	373	0.255	0.046	5.79	0.82

Table 129. Predicted $P_{red, vd,}$ Kordylewski and Wach (1986), α = 1.75 and β = 0.5

C, %	L, m	A_v/A_{eff}	Br	Br_t	$P_{red, vd}$, bar	exp., bar
20	0.04	1.02	0.547	0.103	5.14	3.68
20	0.17	1.09	0.513	0.097	5.20	3.68
20	0.3	1.15	0.484	0.092	5.25	6.71
20	0.61	1.31	0.425	0.081	5.29	6.36
20	1.26	1.64	0.339	0.065	5.47	4.57
20	2.5	2.28	0.245	0.048	5.76	4.0

Table 130. Predicted $P_{red, vd}$, Kordylewski and Wach (1988), α = 1.75 and β = 0.5

D_d, mm	L_d, m	A_v/A_{eff}	Br	Br_t	$P_{red, vd}$, bar	exp., bar
35	0.16	1.08	1.206	0.213	4.29	3.0
35	0.32	1.15	1.126	0.200	4.37	4.82
35	0.54	1.26	1.032	0.184	4.42	5.65
35	0.8	1.38	0.939	0.169	4.59	4.82
35	1.4	1.49	0.873	0.158	4.68	5.13
35	1.75	1.55	0.706	0.129	4.91	5.18
35	2.8	2.34	0.554	0.103	5.14	3.0
35	3.5	2.68	0.485	0.091	5.26	4.64
35	4.91	3.36	0.387	0.073	5.45	3.57
35	6.14	3.95	0.329	0.063	5.57	3.75
35	6.75	4.24	0.306	0.058	5.62	3.39
21	2.5	2.06	0.227	0.044	5.82	5.0
25	2.5	2.10	0.315	0.060	5.60	4.73
35	2.5	2.20	0.591	0.109	5.08	4.2

The predictions of $P_{red, vd}$ for the tests by McCann et al. (1985) with 9.5 % methane-air mixture are made using the parameter values by Molkov (1999): S_0 = 0.38 m/s, E = 7.4, c = 343 m/s, γ_u = 1.39 and γ_b = 1.25.

Table 131. Predicted $P_{red, vd}$, McCann et al. (1985), α = 0.9 and β = 1

L_d, m	A_v/A_{eff}	Br	Br_t	$P_{red, vd}$, bar	exp., bar
0.105	1.10	37.7	5.33	0.018	0.10
0.30	1.29	32.3	4.84	0.023	0.19
0.50	1.50	27.8	4.41	0.029	0.17

Table 132. Predicted $P_{red, vd}$, McCann et al. (1985), α = 1.75 and β = 0.5

L_d, m	A_v/A_{eff}	Br	Br_t	$P_{red, vd}$, bar	exp., bar
0.105	1.10	37.7	5.17	0.020	0.10
0.30	1.29	32.3	4.53	0.027	0.19
0.50	1.50	27.8	3.98	0.037	0.17

The predictions of $P_{red, vd}$ for tests with 5.0 % propane-air mixture by DeGood and Chatrathi (1991) are made using the parameter values by Molkov (1999): S_0 = 0.29 m/s, E = 7.9, c = 338 m/s, γ_u = 1.365 and γ_b = 1.25.

Table 133. Predicted $P_{red, vd}$, DeGood and Chatrathi (1991), α = 0.9 and β = 1

ignition	L_d, m	A_v/A_{eff}	Br	Br_t	P_M	$P_{red, vd}$, bar	exp., bar
centre	1	1.16	41.2	2.99	0.072	0.085	0.185
centre	2	1.33	36.1	2.76	0.088	0.10	0.300
centre	3	1.50	32.1	2.56	0.105	0.12	0.385
bottom	3	1.50	32.1	2.56	0.105	0.12	1.01

Table 134. Predicted $P_{red, vd}$, DeGood and Chatrathi (1991), α = 1.75 and β = 0.5

ignition	L_d, m	A_v/A_{eff}	Br	Br_t	P_M	$P_{red, vd}$, bar	exp., bar
centre	1	1.16	41.2	2.96	0.074	0.085	0.185
centre	2	1.33	36.1	2.65	0.096	0.11	0.300
centre	3	1.50	32.1	2.39	0.124	0.14	0.385
bottom	3	1.50	32.1	2.39	0.124	0.14	1.01

The predictions of $P_{red, vd}$ for tests with acetone-air mixtures by (1993) are made using the parameter values E = 7.9, c = 339 m/s, γ_u = 1.365 and γ_b = 1.25. The values of S_0 calculated by Molkov for each test are used in the prediction.

Table 135. Predicted $P_{red, vd}$, Molkov et al. (1993), α = 0.9 and β = 1

V, m^3	L_d, m	D_d, mm	A_v/A_{eff}	P_{stat}, bar	Br	Br_t	$P_{red, vd}$, bar	exp., bar
0.027	1.83	50	1.95	0.19	2.03	0.667	2.75	5.0†
0.027	2.35	50	2.22	0.24	1.66	0.570	3.44	4.4
0.027	2.35	50	2.22	0.24	1.66	0.570	3.44	3.5
0.027	2.35	50	2.22	1.64	1.60	0.671	8.9	1.9
0.027	1.83	50	1.95	1.41	1.82	0.728	7.1	4.4†
2	4	200	1.49	0.14	1.94	0.390	4.00	4.3
2	10	200	2.22	0.14	1.26	0.273	4.75	5.2
2	10	380	2.44	0.14	4.71	0.765	2.15	2.15
10	25	500	2.96	0.1	2.11	0.339	4.09	4.1
10	25	500	2.96	0.05	2.51	0.384	3.58	2.8

Table 136. Predicted $P_{red, vd}$, Molkov et al. (1993), α = 1.75 and β = 0.5

V, m^3	L_d, m	D_d, mm	A_v/A_{eff}	P_{stat}, bar	Br	Br_t	$P_{red, vd}$, bar	exp., bar
0.027	1.83	50	1.95	0.19	2.03	0.366	4.42	5.0†
0.027	2.35	50	2.22	0.24	1.66	0.306	5.13	4.4
0.027	2.35	50	2.22	0.24	1.66	0.306	5.13	3.5
0.027	2.35	50	2.22	1.64	1.60	0.359	14.6	1.9
0.027	1.83	50	1.95	1.41	1.82	0.394	12.1	4.4†
2	4	200	1.49	0.14	1.94	0.213	5.21	4.3
2	10	200	2.22	0.14	1.26	0.143	5.82	5.2
2	10	380	2.44	0.14	4.71	0.476	3.52	2.15
10	25	500	2.96	0.1	2.11	0.187	5.14	4.1
10	25	500	2.96	0.05	2.51	0.216	4.59	2.8

The predictions of $P_{red, vd}$ for tests with 4.0 % propane-air mixtures by Ponizy & Leyer (1999a, 1999b) are made using the parameter values by Molkov (1999): S_0 = 0.335 m/s, E = 7.9, c = 339 m/s, γ_u = 1.365 and γ_b = 1.25.

Table 137. Predicted $P_{red, vd}$, Ponizy & Leyer (1999a), α = 0.9 and β = 1

D_d, mm	L_d, m	A_v/A_{eff}	Br	Br_t	$P_{red, vd}$, bar	exp., bar
16	0.6	1.57	0.763	0.337	3.56	1.45
21	0.6	1.61	1.260	0.521	2.70	1.17
36	0.6	1.70	3.83	1.254	0.59	1.27
16	1.1	2.04	0.586	0.266	3.96	1.80
21	1.1	2.12	0.958	0.412	3.19	1.45
36	1.1	2.27	2.86	1.007	1.00	1.92
16	2.6	3.47	0.345	0.163	4.64	1.92
21	2.6	3.64	0.557	0.254	4.03	1.55
36	2.6	4.01	1.62	0.642	2.22	1.92
53	2.6	4.31	3.05	1.058	0.88	2.11

Table 138. Predicted $P_{red, vd}$, Ponizy & Leyer (1999a), α = 1.75 and β = 0.5

D_d, mm	L_d, m	A_v/A_{eff}	Br	Br_t	$P_{red, vd}$, bar	exp., bar
16	0.6	1.57	0.763	0.171	4.52	1.45
21	0.6	1.61	1.260	0.272	3.92	1.17
36	0.6	1.70	3.83	0.753	1.82	1.27
16	1.1	2.04	0.586	0.133	4.88	1.80
21	1.1	2.12	0.958	0.211	4.30	1.45
36	1.1	2.27	2.86	0.578	2.47	1.92
16	2.6	3.47	0.345	0.080	5.37	1.92
21	2.6	3.64	0.557	0.127	4.93	1.55
36	2.6	4.01	1.62	0.344	3.53	1.92
53	2.6	4.31	3.05	0.613	2.33	2.11

Table 139. Predicted $P_{red, vd}$, Ponizy & Leyer (1999b), α = 0.9 and β = 1

ignition	P_{stat}, bar	A_v/A_{eff}	Br	Br_t	P_M	$P_{red, vd}$, bar	exp., bar
centre	0	2.97	1.31	0.774	1.72	1.74	2.01
centre	0.3	2.97	1.31	0.818	1.57	2.35	2.16
centre	0.91	2.97	1.31	0.898	1.31	3.48	2.66
centre	2.3	2.97	1.31	1.049	0.89	5.34	3.37
rear	0	2.97	1.31	0.774	1.72	1.74	1.76
rear	0.32	2.97	1.31	0.821	1.56	2.39	1.88
rear	0.83	2.97	1.31	0.888	1.34	3.35	1.81
near vent	1.11	2.97	1.31	0.922	1.24	3.81	1.27
near vent	2.24	2.97	1.31	1.043	0.90	5.27	2.24

Table 140. Predicted $P_{red, vd}$, Ponizy & Leyer (1999b), α = 1.75 and β = 0.5

ignition	P_{stat}, bar	A_v/A_{eff}	Br	Br_t	P_M	$P_{red, vd}$, bar	exp., bar
centre	0	2.97	1.31	0.282	3.81	3.86	2.01
centre	0.3	2.97	1.31	0.298	3.72	5.6	2.16
centre	0.91	2.97	1.31	0.328	3.57	9.4	2.66
centre	2.3	2.97	1.31	0.383	3.29	19.7	3.37
rear	0	2.97	1.31	0.282	3.81	3.86	1.76
rear	0.32	2.97	1.31	0.299	3.72	5.7	1.88
rear	0.83	2.97	1.31	0.324	3.58	8.9	1.81
near vent	1.11	2.97	1.31	0.336	3.52	10.8	1.27
near vent	2.24	2.97	1.31	0.380	3.30	19.2	2.24

The predicted and experimental values of $P_{red, vd}$ in Tables 125 to 130 and Tables 133 to 141 are plotted in Figures 43 and 44. The very low predictions for the tests by McCann et al. (1985) in Tables 131 and 132 have been left out for the sake of clarity.

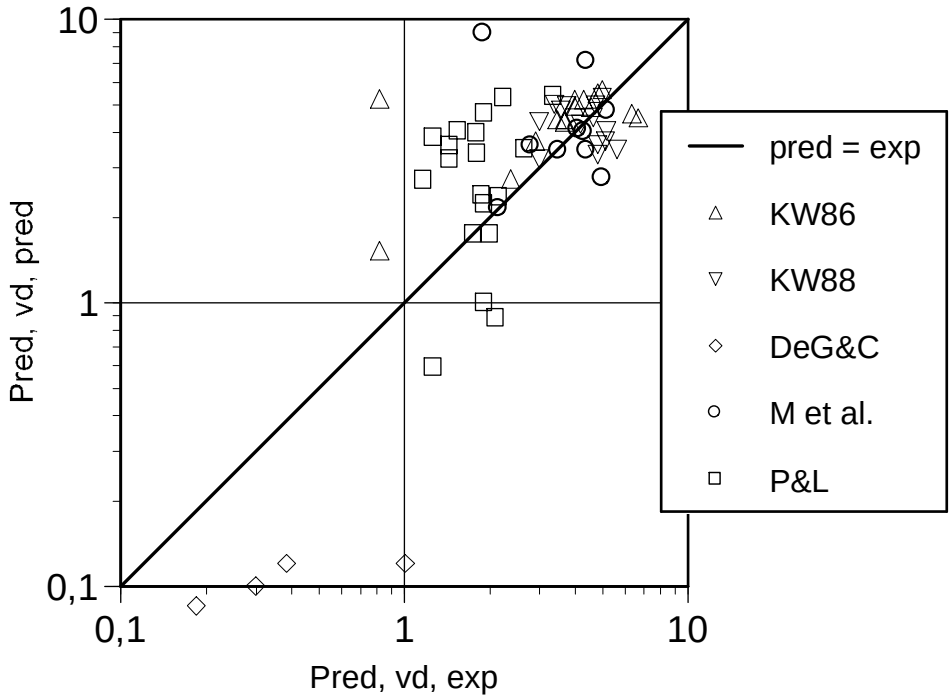

Figure 43. Comparison of $P_{red, vd}$ predicted with Tamanini model and Eqs. (20) to (25) using α = 0.9 and β = 1 with experimental values.

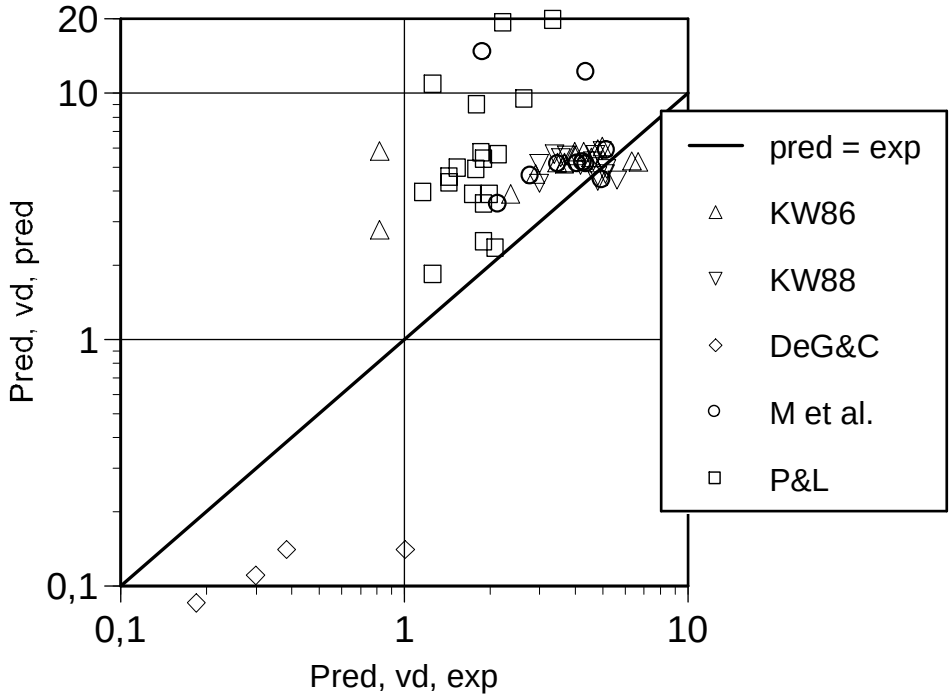

Figure 44. Comparison of $P_{red, vd}$ predicted with Tamanini model and Eqs. (20) to (25) using α = 1.75 and β = 0.5 with experimental values.

The relative errors of data in Tables 125 to 140 were calculated with Eq. (40) and the results are given in Table 141.

Table 141. Relative errors of the predictions, Tamanini

reference	tests	R & Di B	$\alpha = 0.9, \beta = 1$	$\alpha = 1.75, \beta = 0.5$
K & W	29	46.0 %	27.5 %	38.0 %
the others	17	36.5 %	29.5 %	52.5 %
P & L	19	28.5 %	50.5 %	155.5 %
together	65	39.0 %	34.5 %	76.0 %

It is seen from Table 141 that the use of values of S_0, E, K_G and P_m dependent on town gas concentration in the tests by Kordylewski and Wach (1986, 1988) reduces the average error of the Tamanini method from 46.0 % (Russo and Di Benedetto 2007) to 27.5 %. On the other hand, when the values of S_0, E by Molkov (1999) are used and the effect of P_{stat} on P_{red} is estimated with Eqs. (20) to (25), the average error of tests with other fuels increases from 32.0 % to 40.5 %.

5.3.7 NFPA 68 (2007)

The method by Ural is now validated with the experimental data from duct vented gas explosions. The method requires the values of the maximum overpressure P_m and gas deflagration index K_G for each mixture. The values of P_m and K_G in Tables 115 and 124 are used for this purpose. The values of P_{red} are calculated with Eq. (37) and, in case of enclosures with $L/D \geq 2$, Eq. (38). Thus, unlike in the Tamanini method, no outside correlations are needed.

The predictions for the tests by McCann et al. (1985) with 9.5 % methane-air mixture are made with P_m = 7.1 bar, K_G = 55 bar·m/s. Since the test vessel was cubical, Eq. (38) was not used. The results are presented in Table 142.

Table 142. Predicted $P_{red, vd}$ for the tests by McCann et al. (1985)

L_d, m	$A_v/A_{v, vd}$	$P_{red, vd}$, bar	exp., bar
0.105	1.86	0.003	0.10
0.30	2.44	0.006	0.19
0.50	2.84	0.008	0.17

The predictions for the tests by Kordylewski and Wach (1986, 1988) with town gas-air mixtures are made with the values of K_G and P_m in Table 124. Since the test vessel was spherical, Eq. (38) was not used. The results are presented in Tables 143 to 145.

Table 143. Predicted A_v/A_{eff} for the tests by Kordylewski and Wach (1986)

C, %	K_G, bar·m/s	$A_v/A_{v, vd}$	P_m, bar	$P_{red, vd}$, bar	exp., bar
10	13	1.81	4.94	0.30	0.82
12	21	1.77	5.64	0.79	2.38
14	34	1.74	6.33	1.85	2.91
16	50	1.72	6.89	3.20	3.47
18	71	1.71	7.29	4.60	4.0
20	90	1.70	7.44	5.45	4.3
22	112	1.69	7.45	6.00	4.82
25	140	1.68	7.10	6.15	5.0
30	98	1.69	6.38	4.90	0.82

Table 144. Predicted $P_{red, vd}$ for the tests by Kordylewski and Wach (1986)

K_G, bar·m/s	L, m	$A_v/A_{v, vd}$	P_m, bar	$P_{red, vd}$, bar	exp., bar
90	0.04	1.02	7.44	3.69	3.68
90	0.17	1.06	7.44	3.86	3.68
90	0.3	1.11	7.44	4.01	6.71
90	0.61	1.21	7.44	4.33	6.36
90	1.26	1.40	7.44	4.83	4.57
90	2.5	1.70	7.44	5.45	4.0

Table 145. Predicted $P_{red, vd}$ for the tests by Kordylewski and Wach (1988)

D_d, mm	L_d, m	K_G	$A_v/A_{v, vd}$	P_m, bar	$P_{red, vd}$, bar	exp., bar
35	0.16	71	1.05	7.29	1.19	3.0
35	0.32	71	1.09	7.29	1.27	4.82
35	0.54	71	1.14	7.29	1.36	5.65
35	0.8	71	1.19	7.29	1.47	4.82
35	1.4	71	1.31	7.29	1.70	5.13
35	1.75	71	1.37	7.29	1.81	5.18
35	2.8	71	1.53	7.29	2.15	3.0
35	3.5	71	1.64	7.29	2.35	4.64
35	4.91	71	1.83	7.29	2.71	3.57
35	6.14	71	1.98	7.29	2.99	3.75
35	6.75	71	2.05	7.29	3.12	3.39
21	2.5	71	1.78	7.29	5.9	5.0
25	2.5	71	1.70	7.29	4.83	4.73
35	2.5	71	1.49	7.29	2.06	4.2

The predictions for the tests by DeGood and Chatrathi (1991) with propane-air are made with P_m = 7.9 bar, K_G = 100 bar·m/s. The ratio L/D of the test vessel was 2.3 and Eq. (38) was used. The results are presented in Table 146.

Table 146. Predicted $P_{red, vd}$ for the tests by DeGood and Chatrathi (1991)

ignition	L_d, m	$A_v/A_{v, vd}$	$P_{red, vd}$, bar	exp., bar
centre	1	1.68	0.05	0.185
centre	2	1.98	0.07	0.300
centre	3	2.20	0.09	0.385
bottom	3	2.20	0.09	1.01

The predictions for the tests by Molkov et al. (1993) with acetone-air are made with P_m = 7.3 bar, K_G = 84 bar·m/s. Eq. (38) was used for the two larger test vessels with L/D > 2. The results are presented in Table 147.

Table 147. Predicted $P_{red, vd}$ for the tests by Molkov et al. (1993)

V, m^3	L/D	D_d, mm	L_d, m	P_{stat}, bar	$A_v/A_{v, vd}$	$P_{red, vd}$, bar	exp., bar
0.027	1	50	1.83	0.19	1.49	1.60	5.0†
0.027	1	50	2.35	0.24	1.58	1.80	4.4
0.027	1	50	2.35	0.24	1.58	1.80	3.5
0.027	1	50	2.35	1.64	1.48	5.40	1.9
0.027	1	50	1.83	1.41	1.40	4.75	4.4†
2	2.6	200	4	0.14	1.23	2.05	4.3
2	2.6	200	10	0.14	1.48	2.60	5.2
2	2.6	200	10	0.14	1.93	0.75	2.15
10	3.4	500	25	0.1	1.84	1.5	4.1
10	3.4	500	25	0.05	1.84	1.45	2.8

The predictions for the tests by Ponizy and Leyer (1999b) with propane-air are made with P_m = 7.9 bar, K_G = 100 bar·m/s. The ratio L/D of the test vessel was 3.7 and Eq. (38) was used. The results are presented in Tables 148 and 149.

Table 148. Predicted $P_{red, vd}$ for the tests by Ponizy & Leyer (1999a)

D_d, mm	L_d, m	$A_v/A_{v, vd}$	$P_{red, vd}$, bar	exp., bar
16	0.6	1.47	4.3	1.45
21	0.6	1.35	2.05	1.17
36	0.6	1.52	0.80	1.27
16	1.1	1.60	4.6	1.80
21	1.1	1.57	2.5	1.45
36	1.1	1.78	0.90	1.92
16	2.6	2.17	5.7	1.92
21	2.6	2.11	3.55	1.55
36	2.6	2.39	1.20	1.92
53	2.6	2.98	0.70	2.11

Table 149. Predicted $P_{red, vd}$ for the tests by Ponizy & Leyer (1999b)

ignition	P_{stat}, bar	$A_v/A_{v, vd}$	$P_{red, vd}$, bar	exp., bar
centre	0	2.05	1.05	2.01
centre	0.3	1.99	1.30	2.16
centre	0.91	1.88	2.35	2.66
centre	2.3	1.75	5.35	3.37
rear	0	2.05	1.05	1.76
rear	0.32	1.99	1.35	1.88
rear	0.83	1.90	2.20	1.81
near vent	1.11	1.86	2.85	1.27
near vent	2.24	1.75	5.25	2.24

The predicted and experimental values of $P_{red, vd}$ in Tables 143 to 149 are plotted in Figure 45. The very low predictions for the tests by McCann et al. (1985) and DeGood and Chatrathi (1991) in Table 142 have been left out for the sake of clarity.

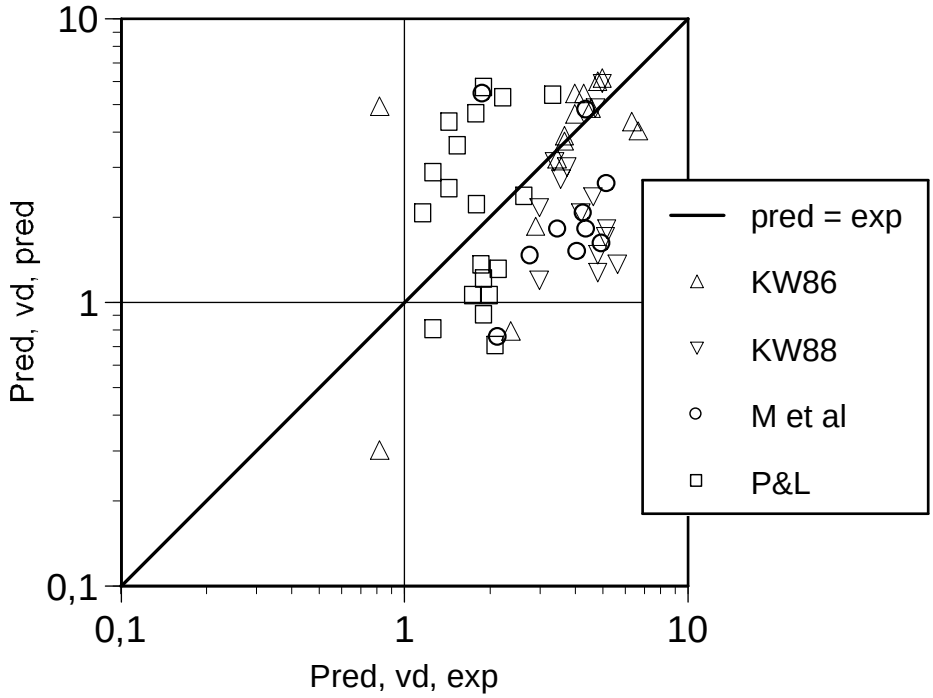

Figure 45. Comparison of $P_{red,\ vd}$ predicted with NFPA 68 (2007) model with experimental values. The data points corresponding to the tests by McCann et al. (1985) and DeGood and Chatrathi (1991) have been omitted.

The relative errors of data in Tables 142 to 149 were calculated with Eq. (40) and the results are given in Table 150.

Table 150. Relative errors of the predictions, NFPA 68 (2007)

reference	tests	rel. error
K & W	29	34.0 %
the others	17	36.5 %
P & L	19	50.5 %
together	65	39.5 %

5.4 Discussion

As seen from Fig. 26, the application by Russo and Di Benedetto (2007) of Runes' method Eq. (30) to town gas tests overestimated P_{red} by a factor ranging from 6 to 20. It is to be noted that the value of the parameter C_S = 0.037 $bar^{1/2}$ was recommended by NFPA 68 for methane-air, and is too low for more reactive town gas-air mixtures. To correct the error of replacing A_s by $V^{2/3}$, the values of P_{red} have to be multiplied by the factor A_s^2/V^3. In case of a spherical vessel, this factor is 4.84^2 = 23.4 and with other vessel shapes still larger. So, after the correction the predictions by Eq. (30) exceed the experimental values by two orders of magnitude.

NFPA 68 recommends the use of Runes' method for low-strength enclosures such as buildings. Obviously it is unsuitable for small high-strength enclosures such as the spherical vessels used in the tests by Kordylewski and Wach (1986, 1988).

In Eq. (17) by Bradley and Mitcheson (1978b) P_{red} is also proportional to A_s^2. Correcting the error replacing A_s by $V^{2/3}$ implies multiplying the values of P_{red} by

the factor A_s^2/V^3. However, the applicability of Eq. (17) to these tests is not obvious.

Russo and Di Benedetto (2007) misquote the Bartknecht correlations as giving the value of $P_{red, vd}$ as a function of P_{red}. Their Fig. 6 redrawn as Fig. 27 of the present report shows that they have calculated the relative error of the misquoted correlations. When the correlations are used in the correct way and the values of P_{red} in the tests of Ponizy and Layer (1999a, 1999b) are predicted with Eqs. (20) to (25) and the parameters values of propane-air used by Molkov, the relative error of 44 % by Russo and Di Benedetto (2007) is reduced to 30 %.

The evaluation of the method of VDI 3673 by Russo and Di Benedetto (2007) was found to be flawless. However, the use of Eqs. (20) to (25) and the parameters values of propane-air by Molkov to predict the values of P_{red} in the tests of Ponizy and Layer (1999a, 1999b) reduces the relative error of 38 % by Russo and Di Benedetto (2007) to 34 %.

The evaluation of the method of NFPA 68 (2002) by Russo and Di Benedetto (2007) is met with difficulties due to the obvious incompatibility of Eq. (46) with Eq. (51), leading to high, unphysical values of $P_{red, vd}$. They partially resolve this incompatibility by imposing the stated validity of Eq. (46) $P_{red} \leq 2.0$ bar. They also exclude all tests with $L_s > L_d$ and tests where the method results in high, unphysical values of $P_{red, vd}$. The latter exclusion is not mentioned in the text but seen in their Fig. 9. The relative error of the reduced data set is given as 56 %. Of course, this result is not comparable to those found for the other methods.

When the evaluation of the method of NFPA 68 (2002) was repeated it was found that Russo and Di Benedetto (2007) have not used the values $S_0 = 0.46$ m/s and E = 7.9 in the modelling of the tests by Ponizy and Layer (1999a, 1999b). Probably, either the set $S_0 = 0.44$ m/s and E = 7.9 or the set $S_0 = 0.46$ m/s and E = 7.0 has been used.

Russo and Di Benedetto (2007) have not validated the method of EN 14491, probably because the paper was submitted in September 2004 and the standard was published in March 2006. The relative error of this method was calculated at 37 %.

Tamanini model Eqs. (56) to (59) differs from the Bartknecht correlations Eqs. (42) to (45) and Siwek correlations Eqs. (46) to (51) in that the value of the ratio $P_{red, vd}/P_{red}$ depends on the combustion properties of the mixture. Thus, the experimental values of this ratio, when available, cannot be used to validate the model. Russo and Di Benedetto (2007) resolve this problem by predicting the reduced pressure P_{red} corresponding to the area of an effective open vent A_{eff} in Eq. (56) with the Molkov method Eqs. (20) to (24) using the parameter set $\alpha = 0.9$ and $\beta = 1$.

To apply the model, the values of the maximum overpressure P_m and gas deflagration index K_G for each mixture must be known. Russo and Di Benedetto (2007) use the values of P_m and K_G based on measurements by Bartknecht who used them in the derivation of Eq. (33). Since vent dimensioning with Eq. (33) is done for optimal mixtures, the values of P_m and K_G are not known for non-optimal

mixtures. For the other correlations considered, the non-optimality of the mixture was accounted for in the value of P_{red}. In the present data set, duct venting of non-optimal mixtures were investigated by Kordylewski and Wach (1986, 1988).

Since the ratio A_v/A_{eff} in the Tamanini method is weakly dependent on combustion properties of the flammable mixture, the values of K_G and P_m were evaluated approximately for non-optimal mixtures. The use of values of S_0, E, K_G and P_m dependent on town gas concentration in the tests by Kordylewski and Wach (1986, 1988) reduced the average error from 46.0 % estimated by Russo and Di Benedetto (2007) to 27.0 %. On the other hand, when the values of S_0, E by Molkov (1999) were used and the effect of P_{stat} on P_{red} was estimated with Eqs. (20) to (25), the average error of tests with other fuels increased from 33.0 % to 42.5 %.

The use of the method by Ural in NFPA 68 (2007) also required the values of K_G and P_m. As for the Tamanini method, values of S_0, E, K_G and P_m dependent on town gas concentration in the tests by Kordylewski and Wach (1986, 1988) were used. The values of P_{red} were calculated with experimental correlations for dust explosions Eqs. (37) and (38). Unlike for other methods, the form of the enclosure was accounted for when the length to diameter ratio L/D exceeded 2. The method was self-contained and no outside correlations were required.

In Table 151, the relative errors found in this report are compared to those found by Russo and Di Benedetto (2007). These authors have used the set of parameters $\alpha = 0.9$, $\beta = 1$ with Eq. (22), whereas both parameter sets by Molkov have been used in the present study. The predictions using the parameter set $\alpha = 1.75$, $\beta = 0.5$ in Table 151 are written in brackets. The latter set leads to larger relative errors for all the methods validated in this study. The effect of the parameter set on the relative error is particularly large with Tamanini method because the values of P_{red} were predicted with the Molkov method for all the tests and not only for the tests by Ponizy and Leyer.

Table 151. Relative errors of the predictions

method	R & Di B	this report
gas explosions		
Bartknecht	44 %	30.5 % (30.0 %)
NFPA 68 (2007)	—	27.0 % (32.0 %)
dust explosions		
Bartknecht	—	27.5 % (28.5 %)
VDI 3673	38 %	35 % (35.0 %)
NFPA 68 (2002)	56 %	—
EN 14491	—	37 % (41.5 %)
Tamanini	39 %	34.5 % (76.0 %)
NFPA 68 (2007)	—	39.5 %

When the set of parameters $\alpha = 0.9$, $\beta = 1$ was used, the methods were found to have comparable accuracies with the relative error ranging from 27.0 to 37.0 %. For those methods where comparison with the results by Russo and Di Benedetto (2007) is possible, that is VDI 3673 and Tamanini, a few per cent lower values have been found in the present study because of

— the use of values of S_0, E by Molkov for propane-air mixture

— the use of Eq. (25) for the tests with $P_{stat} > 0$

— the use of values of S_0, E, K_G and P_m dependent on town gas concentration (only with Tamanini method).

For the Bartknecht method, the results cannot be directly compared since Russo and Di Benedetto (2007) have misquoted the correlations. The NFPA 68 (2002) result by Russo and Di Benedetto (2007) is not comparable with other results by these authors since a lower number of data points was used to calculate the relative error.

6 New engineering correlations

Di Benedetto, Russo and Salzano have derived two engineering correlations for ducted venting. The first one is an extension of the correlation by Yao (1974). The second one is an extension of the Molkov method Eqs. (20) to (25).

6.1 Extension of Yao correlation

Yao (1974) developed a generalised mathematical model of low-pressure venting. The model describes a spherical vessel with an open vent containing a homogenous gas mixture at atmospheric pressure p_0 and ignited at the centre. The reduced pressure P_{red} was assumed to be no higher than 0.69 bar so that vent flow would be subsonic.

With minor modifications, the model was used to simulate gas explosion in an enclosure with an initially closed vent opening at a low pressure. When the vent opens, the flame front area is assumed to increase suddenly by the turbulence factor χ. The value of the discharge coefficient C_d is to be chosed based on the geometry of the vent opening. Yao (1974) defines a dimensionless venting parameter α as

$$\alpha = \frac{\sqrt{2} C_d A_v R}{S_0 V E^{7/6}} \left(\frac{p_0}{\rho_0} \right)^{1/2} \qquad (75)$$

where R [m] is the radius of the vessel and ρ_0 [kg/m^3] is the density of unburned mixture at the initial pressure p_0 and temperature T_0. For a cubical enclosure of side s, R = s/2 and R/V = 1/(2s^2) = 1/(2A_c). For a cylindrical enclosure with L/D < 3, R/V can be set equal to 1/(2A_c) where A_c is the cross section of the cylinder.

Yao (1974) presents his findings as two sets of correlation relating P_{red} and α, with the turbulence factor χ as a parameter. Figures 46 and 47 show the correlations for initially open and closed vent, respectively.

Yao (1974) presents a simplified formula to cover the curves in Fig. 47

$$\frac{P_{red}}{p_0} = 2{,}59 \frac{\chi^{1{,}35}}{\alpha^2} \qquad (76)$$

Eq. (76) is stated to be valid for L/D < 3, 2 < χ < 4 and 4 < E < 10. The range of P_{stat} is not explicitly stated, but in the tests by Yao (1974) it was no larger than 0.2 bar.

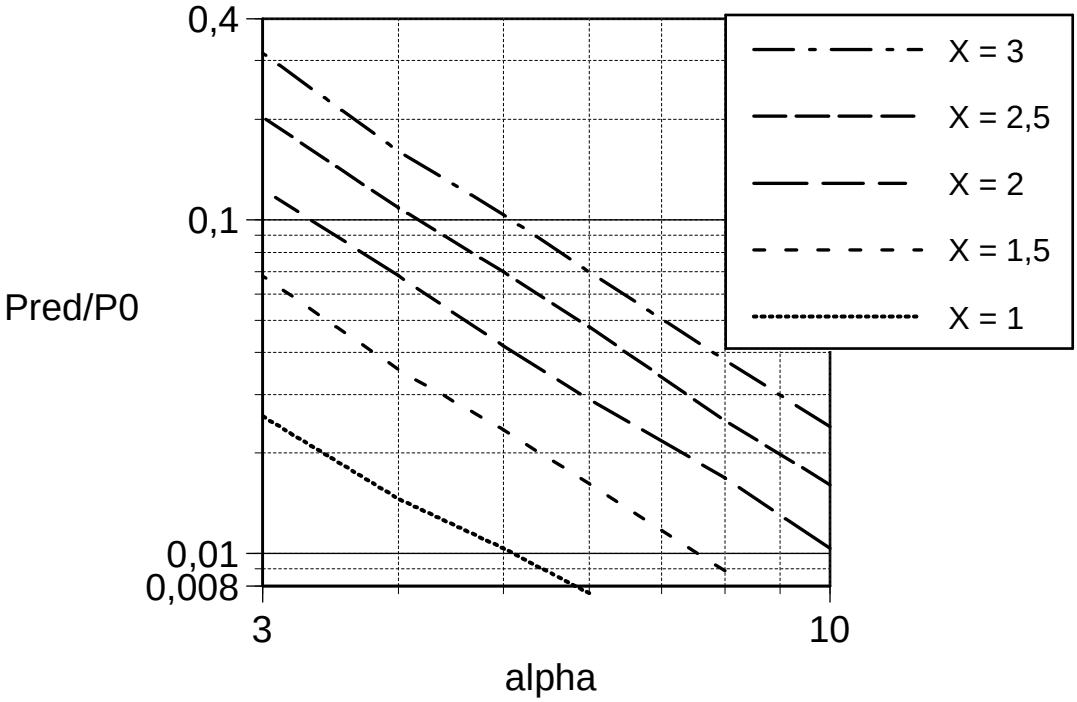

Figure 46. Correlation of scaled explosion overpressure P_{red}/p_0 versus venting parameter α for initially open vent (Yao 1974, redrawn).

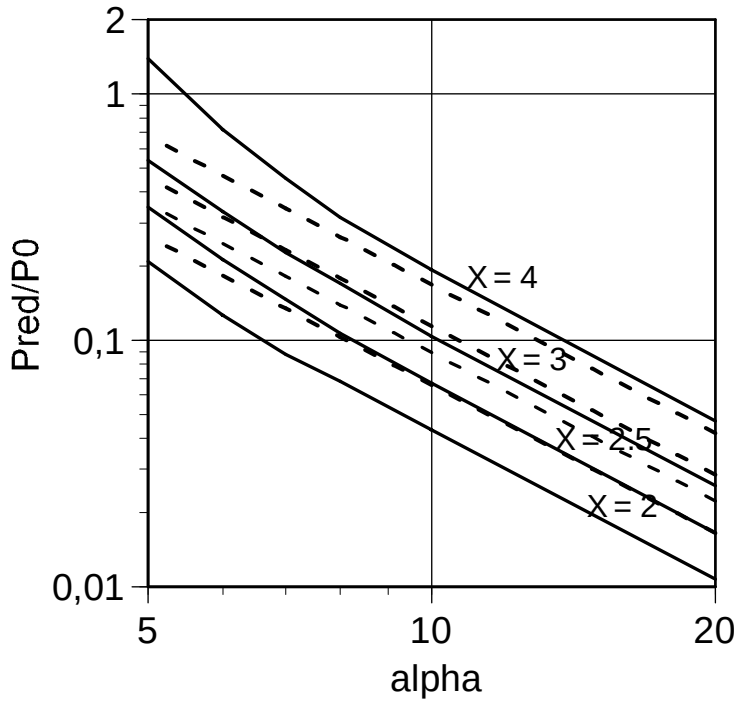

Figure 47. Correlation of scaled explosion overpressure P_{red}/p_0 versus venting parameter α for closed vent. Curves by Yao (1974) have been drawn with solid line. Curves representing Eq. (76) have been drawed with dashed line.

Di Benedetto, Russo and Salzano (2007) derive an equation analogous to Eq. (23) by inserting Eq. (75) into Eq. (76)

$$\frac{P_{red}}{p_0} = \frac{1}{br_t^2} \qquad (77)$$

where br_t is defined as

$$br_t = 1.38\frac{E-1}{E^{7/6}}\frac{A}{S} \tag{78}$$

where the dimensionless quantities A and S are defined by Eqs. (13) and (14), respectively. Note that Di Benedetto, Russo and Salzano (2007) call the ratio A/S Bradley number Br and the quantity br_t turbulent Bradley number Br_t. Eq. (78) is derived as follows. The ideal gas equation can be written as

$$\frac{p}{\rho} = \frac{RT}{M} \tag{79}$$

where R is the universal gas constant 8.314 J mol^{-1} K^{-1} and M the molar mass [kg/mol]. For a stoichiometric propane-air mixture M = 0.0297 kg/mol (Table 32). Insert this value of M and T = 293 K into Eq. (79). The resulting value of $(p_0/\rho_0)^{1/2}$ is 287 m/s.

Assume a cubical enclosure with $A_s/A_c = 6$. Eq. (75) can be written as

$$\alpha = \frac{3\sqrt{2}C_d A_v}{S_0 A_s}\frac{287}{E^{7/6}} \tag{80}$$

Insert Eq. (76) into Eq. (77) and solve br_t

$$br_t = \frac{0.62}{\chi^{0.675}}\alpha = \frac{0.62\cdot 287\cdot 3\sqrt{2}}{\chi^{0.675}c}\frac{C_d A_v}{A_s}\frac{c}{S_0(E-1)}\frac{E-1}{E^{7/6}} = \frac{2.26}{\chi^{0.675}}\frac{E-1}{E^{7/6}}\frac{A}{S} \tag{81}$$

where c is the sound velocity in the unburned mixture, c = 334 m/s (Table 32) and $C_d = 0.65$ as used by Di Benedetto, Russo and Salzano (2007).

Eq. (81) is also valid for spherical vessels and cylindrical vessels with L/D = 1 since $R/V = 3/A_s$ for these vessel forms. Insertion of $\chi = 2$ into Eq. (81) gives a value of 1.41 to the numerical coefficient. In other words, Di Benedetto, Russo and Salzano (2007) have used this value of χ instead of $\chi = 4$ which they claim to have used.

As in the extension of the Molkov method in Sec. 6.2, Di Benedetto, Russo and Salzano (2007) assume that the ratio of turbulent Bradley numbers for duct vented and simply vented vessel can be correlated with three dimensionless groups

$$\frac{br_{t,vd}}{br_t} = \frac{(\chi/\mu)}{(\chi/\mu)_{vd}} = \phi\left(\mathrm{Re}_f, A/S, L_d/D_d\right) = a\,\mathrm{Re}_f^b\left(\frac{A}{S}\right)^c\left(\frac{L_d}{D_d}\right)^d \tag{82}$$

where Re_f is the flame Reynolds number

$$\mathrm{Re}_f = \frac{S_0 V^{1/3}}{\nu} \tag{83}$$

where ν [m^2/s] is the kinematic viscosity of the unburned mixture. A similar correlation is derived for $P_{red,\,vd}/p_0$. It is assumed that Eq. (77) also relates $P_{red,\,vd}$ to $br_{t,\,vd}$

$$\frac{P_{red,vd}}{p_0} = \frac{1}{br_{t,vd}^2} \tag{84}$$

Then Eq. (78) is inserted in Eq. (82) and the resulting equation in Eq. (84)

$$\frac{P_{red,vd}}{p_0} = \left(\frac{br_t}{br_{t,vd}}\right)^2\frac{1}{br_t^2} = \frac{1}{(1.38a)^2}\frac{E^{7/3}}{(E-1)^2}\mathrm{Re}_f^{-2b}\left(\frac{A}{S}\right)^{-2(c+1)}\left(\frac{L_d}{D_d}\right)^{-2d} \tag{85}$$

The ratio $E^{7/3}/(E-1)^2$ is approximately 2.6 for the values of E in question.

Di Benedetto, Russo and Salzano (2007) proceed to calculate experimental values ϕ_{exp} by inserting the measured values of $P_{red, vd}$ in Eq. (84) and dividing the resulting $b_{t, vd}$ by the theoretical value of br_t from Eq. (78). They use the data by Kordylewski and Wach (1986, 1988), DeGood and Chatrathi (1991), Molkov et al. (1993) and Ponizy and Leyer (1999a, 1999b). The resulting correlation for ϕ is

$$\phi = 4.29\,\mathrm{Re}_f^{-0.25}\left(\frac{A}{S}\right)^{0.70}\left(\frac{L_d}{D_d}\right)^{-0.006} \quad (86)$$

and for $P_{red, vd}/p_0$

$$\frac{P_{red,vd}}{p_0} = 0.081\mathrm{Re}_f^{0.8}\left(\frac{A}{S}\right)^{-0.36}\left(\frac{L_d}{D_d}\right)^{0.026} \quad (87)$$

However, the parameters of Eq. (87) are inconsistent with those of Eq. (86). Besides when the respective values of Re_f, A/S and L_d/D_d of the test data set are inserted, the average error of Eq. (86) is 322 % and Eq. (87) yields high, unphysical values of $P_{red, vd}$.

The best thing to do is to fit the parameters a, b, c and d to the test data. The experimental value of $br_{t, vd}$ is calculated by inserting the measured $P_{red,vd}$ into Eq. (84) and solving for $br_{t, vd}$. The predicted value of br_t is calculated from Eq. (78). The calculation of ϕ_{exp} is presented in Tables 152 to 158.

Table 152. Values of ϕ_{exp} for the tests by McCann et al. (1985)

$P_{red, vd}$, bar	$br_{t,vd}$	A/S	br_t	ϕ_{exp}	L_d, m
0.07	3.80	3.85	3.29	1.156	0.105
0.11	3.04	3.85	3.29	0.922	0.30
0.13	2.79	3.85	3.29	0.848	0.50

Table 153. Values of ϕ_{exp} for the tests by Kordylewski and Wach (1986)

C, %	$P_{red, vd}$, bar	$br_{t,vd}$	A/S	br_t	ϕ_{exp}	L_d, m
10	0.82	1.111	0.869	0.734	1.51	2.5
12	2.38	0.652	0.450	0.383	1.70	2.5
14	2.91	0.590	0.248	0.212	2.78	2.5
16	3.47	0.540	0.150	0.128	4.22	2.5
18	4.0	0.503	0.099	0.084	5.97	2.5
20	4.3	0.485	0.078	0.067	7.26	2.5
22	4.82	0.458	0.065	0.055	8.29	2.5
25	5.0	0.450	0.055	0.047	9.58	2.5
30	0.82	1.111	0.088	0.075	14.8	2.5
20	3.68	0.525	0.078	0.067	7.84	0.04
20	3.68	0.525	0.078	0.067	7.84	0.17
20	6.71	0.389	0.078	0.067	5.81	0.3
20	6.36	0.399	0.078	0.067	5.97	0.61
20	4.57	0.471	0.078	0.067	7.04	1.26
20	4.0	0.503	0.078	0.067	7.52	2.5

Table 154. Values of ϕ_{exp} for the tests by Kordylewski and Wach (1988)

$P_{red,\ vd}$, bar	$br_{t,vd}$	A/S	br_t	ϕ_{exp}	D_d, mm	L_d, m
3.0	0.581	0.182	0.156	3.72	35	0.16
4.82	0.458	0.182	0.156	2.94	35	0.32
5.65	0.423	0.182	0.156	2.71	35	0.54
4.82	0.458	0.182	0.156	2.94	35	0.8
5.13	0.444	0.182	0.156	2.85	35	1.4
5.18	0.442	0.182	0.156	2.83	35	1.75
3.0	0.581	0.182	0.156	3.72	35	2.8
4.64	0.467	0.182	0.156	3.00	35	3.5
3.57	0.533	0.182	0.156	3.41	35	4.91
3.75	0.520	0.182	0.156	3.33	35	6.14
3.39	0.547	0.182	0.156	3.50	35	6.75
5.0	0.450	0.066	0.056	7.94	21	2.5
4.73	0.463	0.093	0.080	5.81	25	2.5
4.2	0.491	0.182	0.156	3.15	35	2.5

Table 155. Values of ϕ_{exp} for the tests by DeGood and Chatrathi (1991)

ignition	$P_{red,\ vd}$, bar	$br_{t,vd}$	A/S	br_t	ϕ_{exp}
centre	0.185	2.340	5.49	4.69	0.50
centre	0.300	1.838	5.49	4.69	0.39
centre	0.385	1.622	5.49	4.69	0.35
bottom	1.01	1.001	5.49	4.69	0.21

Table 156. Values of ϕ_{exp} for the tests by Molkov et al. (1993)

V, m^3	L_d, m	D_d, mm	$P_{red,\ vd}$, bar	$br_{t,vd}$	A/S	br_t	ϕ_{exp}
0.027	1.83	50	5.0†	0.450	0.458	0.388	1.16
0.027	2.35	50	4.4	0.480	0.425	0.361	1.33
0.027	2.35	50	3.5	0.538	0.425	0.361	1.49
0.027	2.35	50	1.9	0.730	0.410	0.348	2.10
0.027	1.83	50	4.4†	0.480	0.410	0.348	1.38
2	4	200	4.3	0.485	0.311	0.264	1.84
2	10	200	5.2	0.441	0.301	0.256	1.72
2	10	380	2.15	0.686	1.230	1.051	0.65
10	25	500	4.1	0.497	1.609	1.375	0.36
10	25	500	2.8	0.601	1.907	1.630	0.37

Table 157. Values of ϕ_{exp} for the tests by Ponizy & Leyer (1999a)

D_d, mm	L_d, m	$P_{red, vd}$	$br_{t,vd}$	A/S	br_t	ϕ_{exp}
16	0.6	1.45	0.836	0.124	0.106	7.89
21	0.6	1.17	0.930	0.214	0.183	5.08
36	0.6	1.27	0.893	0.630	0.538	1.66
16	1.1	1.80	0.750	0.124	0.106	7.08
21	1.1	1.45	0.836	0.214	0.183	4.57
36	1.1	1.92	0.726	0.630	0.538	1.35
16	2.6	1.92	0.726	0.124	0.106	6.85
21	2.6	1.55	0.808	0.214	0.183	4.42
36	2.6	1.92	0.726	0.630	0.538	1.35
53	2.6	2.11	0.693	1.366	1.107	0.63

Table 158. Values of ϕ_{exp} for the tests by Ponizy & Leyer (1999b)

ignition	P_{stat}, bar	$P_{red, vd}$	$br_{t,vd}$	A/S	br_t	ϕ_{exp}
centre	0	2.01	0.710	0.630	0.538	1.32
centre	0.3	2.16	0.685	0.630	0.538	1.27
centre	0.91	2.66	0.617	0.630	0.538	1.15
centre	2.3	3.37	0.548	0.630	0.538	1.02
rear	0	1.76	0.759	0.630	0.538	1.41
rear	0.32	1.88	0.734	0.630	0.538	1.36
rear	0.83	1.81	0.748	0.630	0.538	1.39
near vent	1.11	1.27	0.893	0.630	0.538	1.66
near vent	2.24	2.24	0.672	0.630	0.538	1.25

The parameters in Eq. (86) were readjusted so that the average error

$$\frac{1}{N}\sum_{1}^{N}\left|\phi_{pred}-\phi_{\exp}\right| \qquad (88)$$

was minimised. The SOLVER tool in Excel was used for this aim. To find out whether Eq. (86) contains a single printing error, the parameters were varied one by one. This procedure indicated that the parameters a and b were approximately correct but the value of the parameter c should be negative. Varying the parameters so that the average error is minimised gives the correlation for ϕ

$$\phi = 4.36\,\mathrm{Re}_f^{-0.232}\left(\frac{A}{S}\right)^{-0.866}\left(\frac{L_d}{D_d}\right)^{-0.017} \qquad (89)$$

The average error of Eq. (89) is 55.5 %.

The experimental values ϕ_{exp} and those predicted by the correlation Eq. (89) ϕ_{pred} are compared in Figure 48. In Fig. 48, the outlier with ϕ_{exp} = 14.8 corresponds to the test with 30 % town gas-air mixture by Kordylewski and Wach (1986). Fig. 48 is qualitatively similar to Fig. 1 of Di Benedetto, Russo and Salzano (2007) where experimental values and those predicted by Eq. (86) are compared. However, both variables in the latter Figure range from zero to unity and not from 0 to 10 as in Figure 48. This is probably an error.

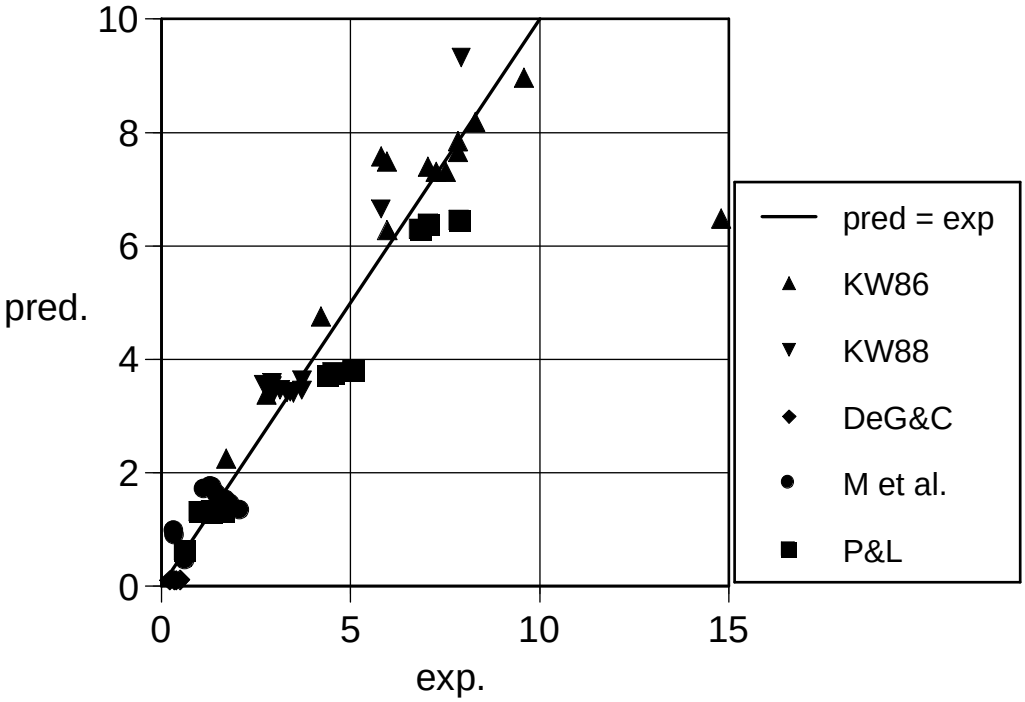

Figure 48. Experimental and predicted values of ϕ.

The resulting correlation for $P_{red,\,vd}/p_0$ is

$$\frac{P_{red,vd}}{p_0} = 0.072\,\mathrm{Re}_f^{0.464}\left(\frac{A}{S}\right)^{-0.268}\left(\frac{L_d}{D_d}\right)^{0.034} \qquad (90)$$

The relative error of Eq. (90) is 48 %. The parameters of the correlation for $P_{red,\,vd}/p_0$ were also found by minimising the relative error of this quantity. The result was

$$\frac{P_{red,vd}}{p_0} = 0.418\,\mathrm{Re}_f^{0.156}\left(\frac{A}{S}\right)^{-0.419}\left(\frac{L_d}{D_d}\right)^{0.053} \qquad (91)$$

Values of $P_{red,\,vd}$ predicted by the correlation Eq. (91) are given in Tables 159 to 165. They are compared with experimental values of $P_{red,\,vd}$ in Figure 49.

Table 159. Values of ϕ_{exp} for the tests by McCann et al. (1985)

L_d, m	Re_f	A/S	L_d/D_d	$P_{red,\,vd}$	exp., bar
0.3	4470	3.85	2.66	0.93	0.10
2.13	4470	3.85	18.9	1.03	0.19
12.2	4470	3.85	108	1.13	0.17

Table 160. Predicted $P_{red, vd}$ for the tests by Kordylewski and Wach (1986)

C, %	Re_f	A/S	L_d/D_d	$P_{red, vd}$	exp.
10	147	0.869	100	1.23	0.82
12	245	0.450	100	1.76	2.38
14	392	0.248	100	2.43	2.91
16	588	0.150	100	3.19	3.47
18	833	0.099	100	4.01	4.0
20	1046	0.078	100	4.58	4.3
22	1307	0.065	100	5.14	4.82
25	1634	0.055	100	5.70	5.0
30	1146	0.088	100	4.43	0.82
20	1046	0.078	1.6	3.68	3.68
20	1046	0.078	6.8	3.97	3.68
20	1046	0.078	12	4.10	6.71
20	1046	0.078	24.4	4.25	6.36
20	1046	0.078	50.4	4.42	4.57
20	1046	0.078	100	4.58	4.0

Table 161. Predicted $P_{red, vd}$ for the tests by Kordylewski and Wach (1988)

L_d, m	Re_f	A/S	L_d/D_d	$P_{red, vd}$	exp.	D_d, mm
0.16	1167	0.182	4.6	2.78	3.0	35
0.32	1167	0.182	9.1	2.88	4.82	35
0.54	1167	0.182	15.4	2.97	5.65	35
0.8	1167	0.182	22.9	3.03	4.82	35
1.4	1167	0.182	40	3.12	5.13	35
1.75	1167	0.182	50	3.16	5.18	35
2.8	1167	0.182	80	3.24	3.0	35
3.5	1167	0.182	100	3.27	4.64	35
4.91	1167	0.182	140	3.33	3.57	35
6.14	1167	0.182	175	3.37	3.75	35
6.75	1167	0.182	192	3.39	3.39	35
2.5	700	0.066	119	4.68	5.0	21
2.5	833	0.093	100	4.12	4.73	25
2.5	1167	0.182	71.4	3.22	4.2	35

Table 162. Predicted $P_{red, vd}$ for the tests by DeGood and Chatrathi (1991)

ignition	Re_f	A/S	L_d/D_d	$P_{red, vd}$	exp.
centre	16000	5.49	1.18	0.93	0.185
centre	16000	5.49	2.37	0.97	0.30
centre	16000	5.49	3.56	0.99	0.385
bottom	16000	5.49	3.56	0.99	1.01

Table 163. Predicted $P_{red, vd}$ for the tests by Molkov et al. (1993)

V, m^3	L_d, m	D_d, mm	Re_f	A/S	L_d/D_d	$P_{red, vd}$	exp.
0.027	1.83	50	850	0.458	36.6	2.01	5.0
0.027	2.35	50	915	0.433	47	2.11	4.4
0.027	2.35	50	915	0.474	47	2.03	3.5
0.027	2.35	50	948	0.590	47	1.86	1.9
0.027	1.83	50	948	0.433	36.6	2.09	4.4
2	4	200	2125	0.437	20	2.29	4.3
2	10	200	2190	0.404	50	2.49	5.2
2	10	380	7325	1.23	26.3	1.83	2.15
10	25	500	10460	0.445	50	3.06	4.1
10	25	500	8825	0.515	50	2.80	2.8

Table 164. Predicted $P_{red, vd}$ for the tests by Ponizy & Leyer (1999a)

D_d, mm	L_d, m	Re_f	A/S	L_d/D_d	$P_{red, vd}$	exp.
16	0.6	350	0.124	37.5	3.03	1.45
21	0.6	460	0.214	28.6	2.48	1.17
36	0.6	788	0.630	16.7	1.67	1.27
16	1.1	350	0.124	68.8	3.12	1.8
21	1.1	460	0.214	52.4	2.56	1.45
36	1.1	788	0.630	30.6	1.72	1.92
16	2.6	350	0.124	163	3.27	1.92
21	2.6	460	0.214	124	2.68	1.55
36	2.6	788	0.630	72.2	1.80	1.92
53	2.6	1160	1.366	49.1	1.35	2.11

Table 165. Predicted $P_{red, vd}$ for the tests by Ponizy & Leyer (1999b)

ignition	P_{stat}, bar	Re_f	A/S	L_d/D_d	$P_{red, vd}$	exp.
centre	0	788	0.630	47.2	1.76	2.01
centre	0.3	788	0.630	47.2	1.76	2.16
centre	0.91	788	0.630	47.2	1.76	2.66
centre	2.3	788	0.630	47.2	1.76	3.37
rear	0	788	0.630	47.2	1.76	1.76
rear	0.32	788	0.630	47.2	1.76	1.88
rear	0.83	788	0.630	47.2	1.76	1.81
near vent	1.11	788	0.630	47.2	1.76	1.27
near vent	2.24	788	0.630	47.2	1.76	2.24

The relative error of Eq. (91) is calculated in Table 166.

Table 166. Relative errors of the predictions of Eq. (91)

reference	tests	rel. error
K & W	29	21.0%
the others	17	40.5 %
P & L	19	25.5 %
together	65	27.5 %

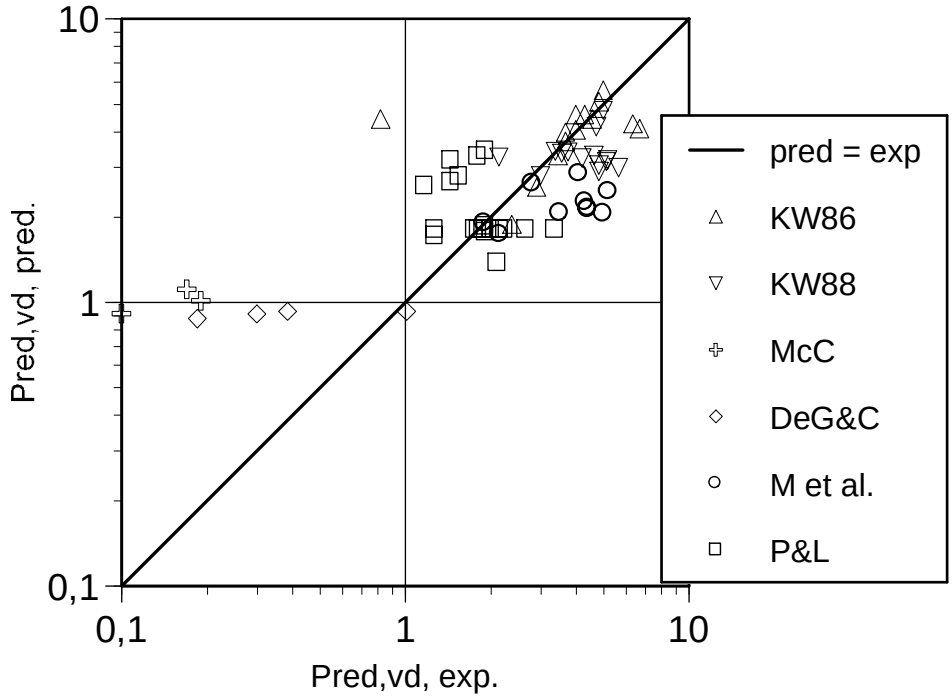

Figure 49. Comparison of values of explosion overpressure $P_{red,\,vd}$ predicted with Eq. (91) with experimental ones.

Di Benedetto, Russo and Salzano (2007) present a plot showing the experimental values of scaled explosion absolute pressure $p_{red,\,vd}/p_0$ as a function of the predicted values of $br_{t,\,vd} = \phi \cdot br_t$ where ϕ is calculated from Eq. (86) and br_t from Eq. (78). This plot is redrawn as Figure 50 by using Eq. (89) instead of Eq. (86).

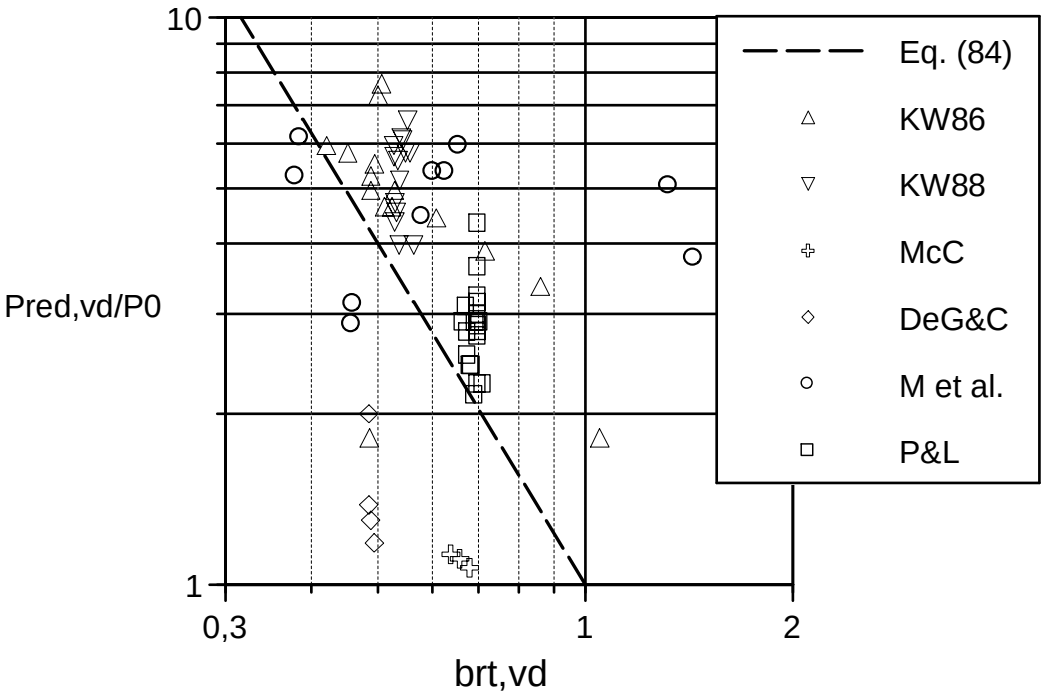

Figure 50. Experimental values of scaled explosion absolute pressure $p_{red,\,vd}/p_0$ and predicted values of $br_{t,\,vd}$.

The data points in Fig. 50 are qualitatively similar to Fig. 3 of Di Benedetto, Russo and Salzano (2007). However, the values of $br_{t,\,vd}$ have been calculated

with Eq. (84) which connects scaled explosion overpressure $P_{red, vd}/p_0$ with $br_{t, vd}$. This error has been corrected in Figure 51.

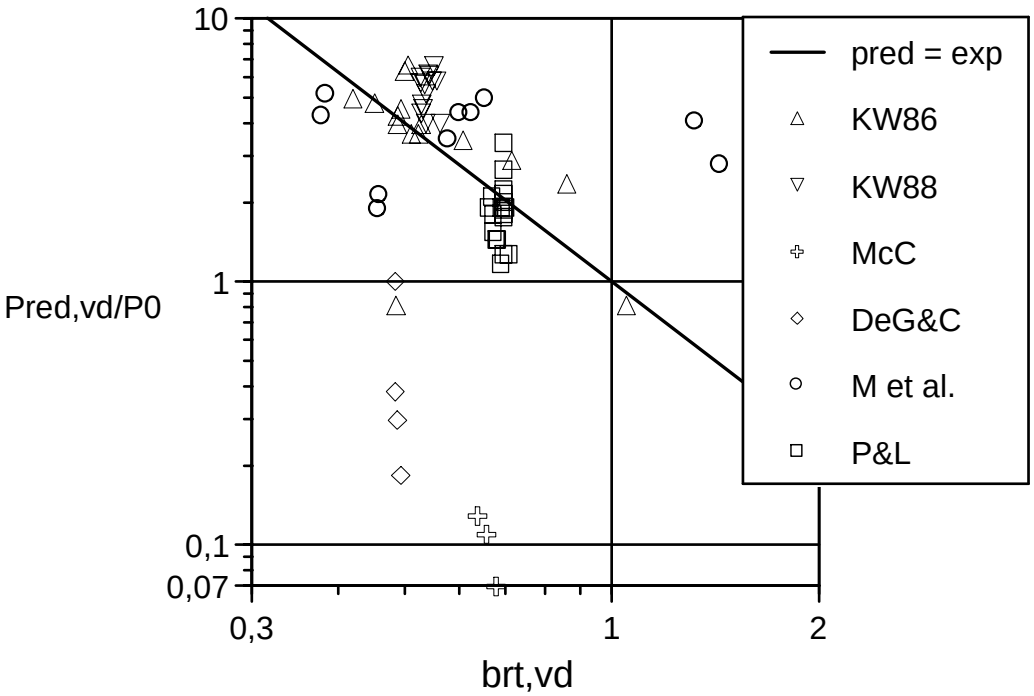

Figure 51. Experimental values of scaled explosion overpressure $P_{red, vd}/p_0$ and predicted values of $br_{t, vd}$.

The parameters a, b, c and d of Eq. (82) can also be fitted by using experimental values for P_{red} when available. Thus, the values of br_t are calculated by inserting the measured values of P_{red} into Eq. (77) and solving for br_t. This is done for the tests of McCann et al. (1985), Kordylewski and Wach (1986, 1988) and DeGood and Chatrathi (1991) in Tables 167 to 170.

Table 167. Values of ϕ_{exp} for the tests by McCann et al. (1985)

P_{red}, bar	br_t	$P_{red, vd}$, bar	$br_{t,vd}$	ϕ_{exp}	L_d, m
0.079	3.58	0.07	3.80	1.061	0.105
0.079	3.58	0.11	3.04	0.849	0.30
0.079	3.58	0.13	2.79	0.779	0.50

Table 168. Values of ϕ_{exp} for the tests by Kordylewski and Wach (1986)

C, %	P_{red}, bar	br_t	$P_{red, vd}$, bar	$br_{t,vd}$	ϕ_{exp}	L_d, m
12	0.5	1.424	2.38	0.652	0.458	2.5
14	1.7	0.772	2.91	0.590	0.764	2.5
16	2.5	0.658	3.47	0.540	0.821	2.5
18	3.4	0.546	4.0	0.503	0.921	2.5
20	3.6	0.531	4.3	0.485	0.913	2.5
22	4.2	0.491	4.82	0.458	0.933	2.5
25	4.2	0.491	5.0	0.450	0.916	2.5
30	1.6	0.796	0.82	1.111	1.396	2.5
20	3.7	0.274	3.68	0.525	1.916	0.04
20	3.7	0.274	3.68	0.525	1.916	0.17
20	3.7	0.274	6.71	0.389	1.420	0.3
20	3.7	0.274	6.36	0.399	1.456	0.61
20	3.7	0.274	4.57	0.471	1.719	1.26
20	3.7	0.274	4.0	0.503	1.836	2.5

Table 169. Values of ϕ_{exp} for the tests by Kordylewski and Wach (1988)

P_{red}, bar	br_t	$P_{red, vd}$, bar	$br_{t,vd}$	ϕ_{exp}	D_d, mm	L_d, m
2.0	0.712	3.0	0.581	0.816	35	0.16
2.0	0.712	4.82	0.458	0.643	35	0.32
2.0	0.712	5.65	0.423	0.594	35	0.54
2.0	0.712	4.82	0.458	0.643	35	0.8
2.0	0.712	5.13	0.444	0.624	35	1.4
2.0	0.712	5.18	0.442	0.621	35	1.75
2.0	0.712	3.0	0.581	0.816	35	2.8
2.0	0.712	4.64	0.467	0.656	35	3.5
2.0	0.712	3.57	0.533	0.749	35	4.91
2.0	0.712	3.75	0.520	0.790	35	6.14
2.0	0.712	3.39	0.547	0.768	35	6.75
4.2	0.491	5.0	0.450	0.632	21	2.5
3.0	0.581	4.73	0.463	0.650	25	2.5
1.0	1.007	4.2	0.491	0.690	35	2.5

Table 170. Values of ϕ_{exp} for the tests by DeGood and Chatrathi (1991)

P_{red}, bar	br_t	$P_{red, vd}$, bar	$br_{t,vd}$	ϕ_{exp}	ignition	L_d, m
0.20	2.25	0.185	2.340	1.040	centre	1
0.20	2.25	0.300	1.838	0.817	centre	2
0.20	2.25	0.385	1.622	0.721	centre	3
0.15	2.60	1.01	1.001	0.445	bottom	3

Varying the parameters of Eq. (86) so that the average error is minimised gives the correlation for ϕ

$$\phi = 6.97\,\mathrm{Re}_f^{-0.211}\left(\frac{A}{S}\right)^{-0.004}\left(\frac{L_d}{D_d}\right)^{-0.103} \qquad (92)$$

The average error of Eq. (92) is 72.5 %.

The resulting correlation for $P_{red,\,vd}/p_0$ is

$$\frac{P_{red,vd}}{p_0} = 0.028\,\mathrm{Re}_f^{0.422}\left(\frac{A}{S}\right)^{-0.836}\left(\frac{L_d}{D_d}\right)^{0.206} \quad (93)$$

The relative error of Eq. (93) is 54.5 %. The parameters of the correlation for $P_{red,\,vd}/p_0$ were also found by minimising the relative error of this quantity. The result was

$$\frac{P_{red,vd}}{p_0} = 0.550\,\mathrm{Re}_f^{0.119}\left(\frac{A}{S}\right)^{-0.411}\left(\frac{L_d}{D_d}\right)^{0.053} \quad (94)$$

Values of $P_{red,\,vd}$ predicted by the correlation Eq. (94) are given in Tables 171 to 177. They are compared with experimental values of $P_{red,\,vd}$ in Figure 52.

Table 171. Values of $P_{red,\,vd}$ for the tests by McCann et al. (1985)

L_d, m	Re_f	A/S	L_d/D_d	$P_{red,\,vd}$	exp., bar
0.3	4470	3.85	2.66	0.91	0.10
2.13	4470	3.85	18.9	1.01	0.19
12.2	4470	3.85	108	1.11	0.17

Table 172. Predicted $P_{red,\,vd}$ for the tests by Kordylewski and Wach (1986)

C, %	Re_f	A/S	L_d/D_d	$P_{red,\,vd}$	exp.
12	245	0.450	100	1.88	2.38
14	392	0.248	100	2.54	2.91
16	588	0.150	100	3.28	3.47
18	833	0.099	100	4.05	4.0
20	1046	0.078	100	4.59	4.3
22	1307	0.065	100	5.09	4.82
25	1634	0.055	100	5.60	5.0
30	1146	0.088	100	4.42	0.82
20	1046	0.078	1.6	3.68	3.68
20	1046	0.078	6.8	3.97	3.68
20	1046	0.078	12	4.10	6.71
20	1046	0.078	24.4	4.25	6.36
20	1046	0.078	50.4	4.42	4.57
20	1046	0.078	100	4.59	4.0

Table 173. Predicted $P_{red, vd}$ for the tests by Kordylewski and Wach (1988)

L_d, m	Re_f	A/S	L_d/D_d	$P_{red, vd}$	exp.	D_d, mm
0.16	1167	0.182	4.6	2.79	3.0	35
0.32	1167	0.182	9.1	2.89	4.82	35
0.54	1167	0.182	15.4	2.97	5.65	35
0.8	1167	0.182	22.9	3.04	4.82	35
1.4	1167	0.182	40	3.13	5.13	35
1.75	1167	0.182	50	3.17	5.18	35
2.8	1167	0.182	80	3.25	3.0	35
3.5	1167	0.182	100	3.29	4.64	35
4.91	1167	0.182	140	3.35	3.57	35
6.14	1167	0.182	175	3.39	3.75	35
6.75	1167	0.182	192	3.40	3.39	35
2.5	700	0.066	119	4.74	5.0	21
2.5	833	0.093	100	4.16	4.73	25
2.5	1167	0.182	71.4	3.23	4.2	35

Table 174. Predicted $P_{red, vd}$ for the tests by DeGood and Chatrathi (1991)

ignition	Re_f	A/S	L_d/D_d	$P_{red, vd}$	exp.
centre	16000	5.49	1.18	0.88	0.185
centre	16000	5.49	2.37	0.91	0.30
centre	16000	5.49	3.56	0.93	0.385
bottom	16000	5.49	3.56	0.93	1.01

Table 175. Predicted $P_{red, vd}$ for the tests by Molkov et al. (1993)

V, m^3	L_d, m	D_d, mm	Re_f	A/S	L_d/D_d	$P_{red, vd}$	exp.
0.027	1.83	50	850	0.458	36.6	2.05	5.0
0.027	2.35	50	915	0.433	47	2.15	4.4
0.027	2.35	50	915	0.474	47	2.07	3.5
0.027	2.35	50	948	0.590	47	1.90	1.9
0.027	1.83	50	948	0.433	36.6	2.13	4.4
2	4	200	2125	0.437	20	2.26	4.3
2	10	200	2190	0.404	50	2.46	5.2
2	10	380	7325	1.23	26.3	1.74	2.15
10	25	500	10460	0.445	50	2.85	4.1
10	25	500	8825	0.515	50	2.63	2.8

Table 176. Predicted $P_{red, vd}$ for the tests by Ponizy & Leyer (1999a)

D_d, mm	L_d, m	Re_f	A/S	L_d/D_d	$P_{red, vd}$	exp.
16	0.6	350	0.124	37.5	3.16	1.45
21	0.6	460	0.214	28.6	2.57	1.17
36	0.6	788	0.630	16.7	1.71	1.27
16	1.1	350	0.124	68.8	3.27	1.8
21	1.1	460	0.214	52.4	2.66	1.45
36	1.1	788	0.630	30.6	1.77	1.92
16	2.6	350	0.124	163	3.42	1.92
21	2.6	460	0.214	124	2.78	1.55
36	2.6	788	0.630	72.2	1.85	1.92
53	2.6	1160	1.366	49.1	1.38	2.11

Table 177. Predicted $P_{red, vd}$ for the tests by Ponizy & Leyer (1999b)

ignition	P_{stat}, bar	Re_f	A/S	L_d/D_d	$P_{red, vd}$	exp.
centre	0	788	0.630	47.2	1.81	2.01
centre	0.3	788	0.630	47.2	1.81	2.16
centre	0.91	788	0.630	47.2	1.81	2.66
centre	2.3	788	0.630	47.2	1.81	3.37
rear	0	788	0.630	47.2	1.81	1.76
rear	0.32	788	0.630	47.2	1.81	1.88
rear	0.83	788	0.630	47.2	1.81	1.81
near vent	1.11	788	0.630	47.2	1.81	1.27
near vent	2.24	788	0.630	47.2	1.81	2.24

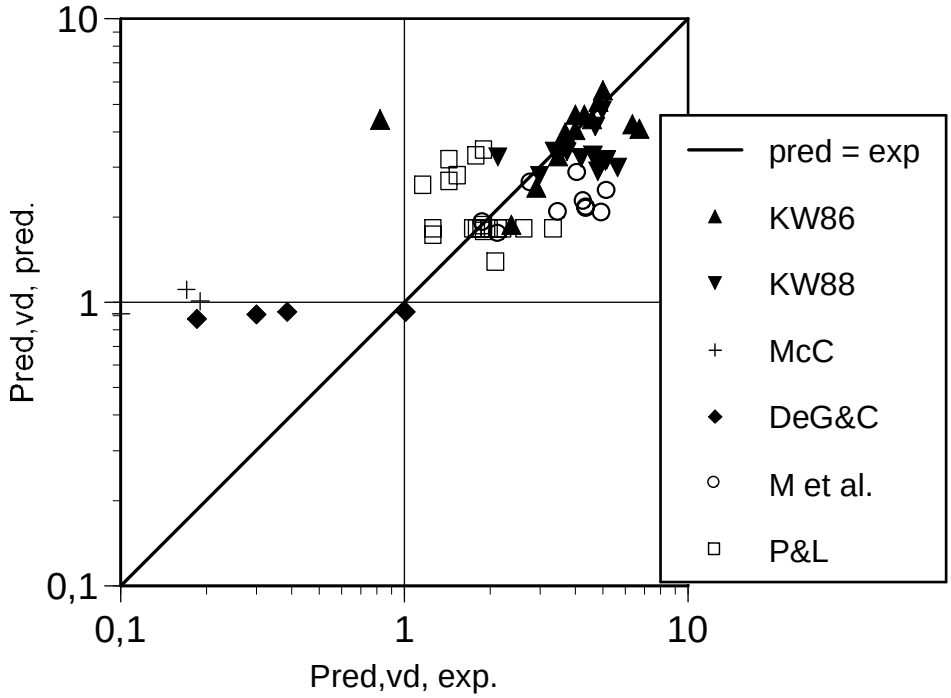

Figure 52. Comparison of values of explosion overpressure $P_{red, vd}$ predicted with Eq. (92) with experimental ones.

The relative error of Eq. (92) is calculated in Table 179.

Table 179. Relative errors of the predictions of Eq. (92)

reference	tests	rel. error
K & W	28	20.5%
the others	17	40.0 %
P & L	19	26.5 %
together	64	27.5 %

The obvious limitation of the extended Yao correlation is that it does not consider the effect of P_{stat} on P_{red} and $P_{red, vd}$. Di Benedetto, Russo and Salzano (2008) pursue their quest for a method to predict $P_{red, vd}$ by extending the Molkov method, where P_{stat} is included in the definition of P_M Eq. (27).

6.2 Extension of Molkov method

6.2.1 Method

Di Benedetto, Russo and Salzano (2008) have used all the test data of duct vented gas explosions with central ignition to perform a sensitivity analysis and derive two empirical correlations. The tests where the ignition location is not mentioned, that is, those by Cubbage and Marshall (1972), and McCann et al. (1985), and the tests with noncentral ignition, that is, one of the four tests by DeGood and Chatrathi (1991), all tests by Ponizy and Leyer (1999a) and five of the nine tests by Ponizy and Leyer (1999b), were excluded. Their methodology is based on the assumption that the duct vented explosions are well represented by the turbulent Bradley number Br_t, which quantifies the intensification of both turbulisation and frictional effects in a simple vented vessel.

In the presence of a duct, they assume that the intense burn-up occurring in the sections of the duct filled by unburned mixture affects both flame turbulisation and frictional effects. More precisely, it gives rise to additional reduction of the vent area, thus affecting the discharge flow and the parameter μ. Moreover, the resulting flow from the duct to the vessel, due to high local values of pressure in the duct entrance, produces turbulisation of the mixture in the vessel, affecting the parameter χ. The quantification of these two effects, the discharge flow reduction and the flame turbulisation, is still obtained by means of evaluation of the ratio χ/μ.

For the sake of describing duct vented explosion phenomena, they define a ducted turbulent Bradley number $Br_{t,\,vd}$, which takes into account the effect of the duct. $Br_{t,\,vd}$ is defined by Eq. (22) where the ratio χ/μ now refers to the ducted system. Br_t is the turbulent Bradley number of the unducted system also defined by Eq. (22) with the ratio χ/μ referring to the unducted system. The ratio of the two numbers $Br_{t,\,vd} / Br_t$ was expected to be a function of the reactivity of the flammable mixture and geometrical properties of the ducted vessel configuration

$$\frac{Br_{t,vd}}{Br_t} = \frac{(\chi/\mu)}{(\chi/\mu)_{vd}} = f(reactivity, geometry) \qquad (95)$$

Experimental values of $P_{red,\,vd}$ and P_{stat} were inserted into Eq. (27) and the corresponding values of $Br_{t,\,vd}$ were solved from Eq. (23) or Eq. (41). Di Benedetto, Russo and Salzano (2008) quote Eq. (41) as a part of the Molkov method although it is their own modification of Eq. (24) and validated only with data from tests at initially elevated pressures. Besides, Eq. (41) is based on the data in Fig. 11 where an erroneous definition for P_M has been used to plot the data points corresponding to the tests by Pegg et al. (1992).

Note that the replacement of Eq. (24) by Eq. (41) is also inconsistent with the derivation of the Molkov method. The "universal correlation" Eqs. (23) and (24) is based on simulations of simply vented gas explosions with the model by Molkov et al. (1993). The only correlation partially based on test data is Eq. (22).

The values of Br_t were calculated with Eqs. (20) to (22) using the parameter set α = 1.75, β = 0.5 and inserting values of S_0 and E calculated with the CHEMKIN software (Russo 2008). Then the values of the ratio f for each test were found with

Eq. (95). Once the values of f were found, Di Benedetto, Russo and Salzano (2008) tried to correlate them with the respective values of reactivity and geometrical parameters. To this end, the following power law equation was adopted

$$f = a\left(\frac{P_m}{p_0}\right)^b S_0^c V^e L_d^g D_d^h \quad (96)$$

The values of the parameters a, b, c, e, g, and h were found with regression analysis ($R^2 = 0.42$) with the result

$$f = 3.0 \cdot 10^5 \left(\frac{P_m}{p_0}\right)^{-4.0} S_0^{-0.1} V^{-0.4} L_d^{-1.6} D_d^{3.7} \quad (97)$$

Based on a sensitivity analysis, they concluded that the duct vented vessel can be described by six variables, namely D_d, L_d, S_0, P_m, V and density ρ. Since there are six variables and three dimensions (length, time and mass), three dimensionless groups can be derived

$$\frac{Br_{t,vd}}{Br_t} = \frac{(\chi/\mu)}{(\chi/\mu)_{vd}} = f(\mathrm{Re}_f, \frac{P_m}{p_0}, \frac{L_d}{D_d}) \quad (98)$$

Density ρ is included in Re_f which contains kinematic viscosity since $\nu = \mu/\rho$, where μ is the dynamic viscosity of the unburned mixture. They also note that ignition position affects $P_{red, vd}$, which is not accounted for in any of the correlations. Since only tests with central ignition were included, the effect of ignition position was not considered in the derivation.

Re_f accounts for flame acceleration due to the presence of the venting section. The ratio P_m/p_0 accounts for the entity of back-flow induced by the duct burn-up, which causes a sudden increase of the pressure. The ratio L_d/D_d accounts for the effect of the burn-up, which causes the reduction of the vent area. Again a power law equation was adopted for f

$$\frac{Br_{t,vd}}{Br_t} = \frac{(\chi/\mu)}{(\chi/\mu)_{vd}} = k\,\mathrm{Re}_f^l \left(\frac{P_m}{p_0}\right)^m \left(\frac{L_d}{D_d}\right)^n \quad (99)$$

The values of the parameters k, l, m, and n were found by the least squares method with the result

$$\frac{Br_{t,vd}}{Br_t} = 5\,\mathrm{Re}_f^{-0.1} \left(\frac{P_m}{p_0}\right)^{-0.1} \left(\frac{L_d}{D_d}\right)^{-0.5} \quad (100)$$

The validity of Eq. (100) is limited by the range of the test data

- $5 \le P_m/p_0 \le 10$
- $1 \le L_d/D_d \le 200$
- $1000 < Re_f < 65\,000$
- $V \le 10\ m^3$
- central ignition.

They found that only the data of ducts longer than 1 m could be regressed by Eq. (99) because ducted venting with $L_d \le 1$ m behaved as simply vented vessel with f = 1. The accuracy of Eq. (100) was estimated by comparing the predicted values of the reduced pressure with test data and found to be satisfactory.

6.2.2 Predicted $Br_{t, vd}$ vs. experimental P_M

Di Benedetto, Russo and Salzano (2008) validated Eq. (100) in the following way. For those tests where P_{red} was measured, the values of P_M were calculated by inserting P_{red} and P_{stat} into Eq. (25). The values of P_M were inserted into Eq. (23) or Eq. (24) and the corresponding values of Br_t were solved. For those tests where P_{red} was not measured, the values of Br_t were calculated with Eqs. (20) to (22) using the parameter values $\alpha = 1.75$, $\beta = 0.5$. The corresponding values of P_M were calculated with Eq. (23) or Eq. (24). The values of Br_t found in either way were multiplied by the values of f calculated from Eq. (100) to get predicted values of $Br_{t, vd}$.

The result was presented as a scatter plot consisting of experimental values of P_M as a function of predicted values of $Br_{t, vd}$. A curve representing the universal correlation by Molkov, Eqs. (23) and (24), was also drawn to represent perfect predictions ie. the values of $Br_{t, vd}$ corresponding to the experimental values of P_M. This plot, Fig. 6 in Di Benedetto, Russo and Salzano (2008), is now reproduced.

In this Figure, there are eight test points represented by closed symbols, which stand for medium scale test vessels. There are three tests with a 2.6 m^3 vessel and central ignition by DeGood and Chatrathi (1991), so the remaining five tests must be those by Molkov et al. (1993). Since P_{red} was measured only for one test with the 2 m^3 vessel and noncentral ignition, and none with the 10 m^3 vessel, it can be concluded that Di Benedetto, Russo and Salzano (2008) have used predicted values of Br_t for the tests by Molkov et al. (1993) as a starting point.

Di Benedetto, Russo and Salzano (2008) do not give the values of S_0 and P_m calculated with the CHEMKIN software. Instead, the values calculated above are used in the present calculation. In Tables 179 to 186, the values of $Br_{t, vd}$ and P_M are calculated also for those tests that were excluded from the derivation of Eq. (100). The results are plotted in Figure 53.

Table 179. Predicted $Br_{t, vd}$ for the tests by McCann et al. (1985)

P_{red}, bar	Br_t	L_d, m	f	$Br_{t, vd}$	$P_{red, vd}$, bar	P_M
0.079	2.90	0.105	1.84	5.34	0.10	0.099
0.079	2.90	0.30	1.09	3.16	0.19	0.188
0.079	2.90	0.50	0.84	2.44	0.17	0.168

Table 180. Predicted $Br_{t, vd}$ for the tests by Kordylewski and Wach (1986)

C, %	P_{red}, bar	Br_t	$S_{0,}$ m/s	P_m, bar	f	$Br_{t, vd}$	$P_{red, vd,}$ bar	P_M
12	0.5	1.342	0.15	5.64	0.191	0.257	2.38	2.35
14	1.7	0.787	0.24	6.33	0.181	0.142	2.91	2.87
16	2.5	0.571	0.36	6.89	0.172	0.098	3.47	3.43
18	3.4	0.369	0.51	7.29	0.165	0.061	4.0	3.95
20	3.6	0.330	0.64	7.44	0.161	0.053	4.3	4.24
22	4.2	0.226	0.80	7.45	0.157	0.036	4.82	4.76
25	4.2	0.226	1.00	7.10	0.155	0.035	5.0	4.24
30	1.6	0.816	0.70	6.38	0.162	0.132	0.82	0.81

Table 181. Predicted $Br_{t, vd}$ for the tests by Kordylewski and Wach (1986)

P_{red}, bar	Br_t	$S_{0,}$ m/s	P_m, bar	L_d, m	f	$Br_{t, vd}$	$P_{red, vd}$, bar	P_M
3.7	0.311	0.64	7.44	0.04	1.273	0.396	3.68	3.63
3.7	0.311	0.64	7.44	0.17	0.617	0.192	3.68	3.63
3.7	0.311	0.64	7.44	0.3	0.465	0.145	6.71	6.62
3.7	0.311	0.64	7.44	0.61	0.326	0.102	6.36	6.28
3.7	0.311	0.64	7.44	1.26	0.227	0.071	4.57	4.51
3.7	0.311	0.64	7.44	2.5	0.161	0.050	4.0	3.95

Table 182. Predicted $Br_{t, vd}$ for the tests by Kordylewski and Wach (1988)

P_{red}, bar	Br_t	D_d, mm	L_d, m	f	$Br_{t, vd}$	$P_{red, vd}$, bar	P_M
2.0	0.702	35	0.16	0.769	0.540	3.0	2.96
2.0	0.702	35	0.32	0.544	0.382	4.82	4.76
2.0	0.702	35	0.54	0.419	0.294	5.65	5.58
2.0	0.702	35	0.8	0.344	0.241	4.82	4.76
2.0	0.702	35	1.4	0.260	0.183	5.13	5.06
2.0	0.702	35	1.75	0.233	0.163	5.18	5.11
2.0	0.702	35	2.8	0.184	0.129	3.0	2.96
2.0	0.702	35	3.5	0.165	0.115	4.64	4.58
2.0	0.702	35	4.91	0.139	0.097	3.57	3.52
2.0	0.702	35	6.14	0.124	0.087	3.75	3.70
2.0	0.702	35	6.75	0.118	0.083	3.39	3.35
4.2	0.226	21	2.5	0.151	0.034	5.0	4.94
3.0	0.453	25	2.5	0.165	0.075	4.73	4.67
1.0	1.005	35	2.5	0.195	0.196	4.2	4.15

Table 183. Predicted $Br_{t, vd}$ for the tests by DeGood and Chatrathi (1991)

ignition	P_{red}, bar	Br_t	L_d, m	f	$Br_{t, vd}$	$P_{red, vd}$, bar	P_{stat}, bar	P_M
centre	0.20	2.085	1	1.352	2.82	0.185	0.1	0.159
centre	0.20	2.085	2	0.956	1.99	0.300	0.1	0.257
centre	0.20	2.085	3	0.780	1.63	0.385	0.1	0.330
bottom	0.15	2.351	3	0.780	1.84	1.01	0.1	0.866

Table 184. Predicted $Br_{t, vd}$, Molkov et al. (1993), α = 1.75 and β = 0.5

Br_t	V, m^3	L_d, m	S_0, m/s	f	$Br_{t, vd}$	$P_{red, vd}$, bar	P_{stat}, bar	P_M
0.642	0.027	1.83	0.26	0.289	0.186	5.0†	0.19	3.81
0.605	0.027	2.35	0.28	0.253	0.153	4.4	0.24	3.16
0.605	0.027	2.35	0.28	0.253	0.153	3.5	0.24	2.51
0.711	0.027	2.35	0.29	0.252	0.179	1.9	1.64	0.44
0.693	0.027	1.83	0.29	0.286	0.198	4.4†	1.41	1.17
0.297	2	4	0.325	0.332	0.097	4.3	0.14	3.50
0.289	2	10	0.335	0.209	0.059	5.2	0.14	4.23
1.019	2	10	0.295	0.291	0.317	2.15	0.14	1.75
0.793	10	25	0.32	0.199	0.095	4.1	0.1	3.51
0.817	10	25	0.27	0.203	0.111	2.8	0.05	2.57

Table 185. Predicted $Br_{t, vd}$, Ponizy & Leyer (1999a), α = 1.75 and β = 0.5

Br_t	D_d, mm	L_d, m	f	$Br_{t, vd}$	$P_{red, vd}$, bar	P_M
0.256	16	0.6	0.295	0.076	1.45	1.43
0.423	21	0.6	0.338	0.143	1.17	1.15
1.12	36	0.6	0.443	0.496	1.27	1.25
0.256	16	1.1	0.218	0.056	1.80	1.78
0.423	21	1.1	0.250	0.106	1.45	1.43
1.12	36	1.1	0.327	0.366	1.92	1.90
0.256	16	2.6	0.142	0.036	1.92	1.90
0.423	21	2.6	0.162	0.069	1.55	1.53
1.12	36	2.6	0.213	0.239	1.92	1.90
2.22	53	2.6	0.258	0.573	2.11	2.08

Table 186. Predicted $Br_{t, vd,}$ Ponizy & Leyer (1999b), α = 1.75 and β = 0.5

ignition	Br_t	f	$Br_{t, vd}$	$P_{red, vd}$, bar	P_{stat}, bar	P_M
centre	1.02	0.259	0.264	2.01	0	1.98
centre	1.18	0.259	0.306	2.16	0.3	1.45
centre	1.30	0.259	0.337	2.66	0.91	1.00
centre	1.52	0.259	0.394	3.37	2.3	0.56
rear	1.02	0.259	0.264	1.76	0	1.74
rear	1.19	0.259	0.308	1.88	0.32	1.23
rear	1.29	0.259	0.334	1.81	0.83	1.81
near vent	1.35	0.259	0.344	1.27	1.11	0.413
near vent	1.51	0.259	0.391	2.24	2.24	0.384

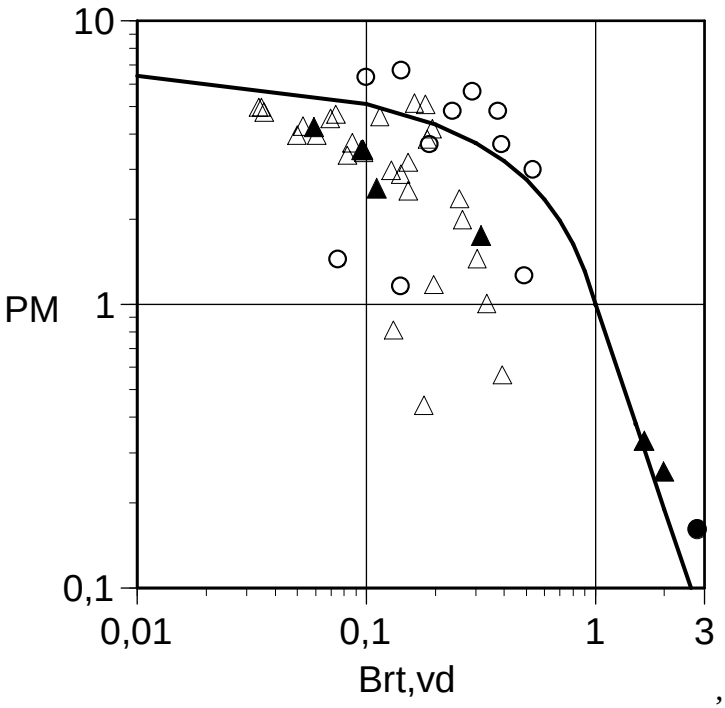

Figure 53. Experimental values of P_M plotted as a function of predicted values of $Br_{t, vd}$ for tests with central ignition. Circles and triangles represent data points with $L_d \leq 1$ m and $L_d > 1$ m, respectively. Tests with laboratory and medium scale vessel are represented by open and closed symbols, respectively. The curve is the universal correlation by Molkov, Eqs. (23) and (24).

Fig. 53 is qualitatively but not exactly similar to Fig. 6 in Di Benedetto, Russo and Salzano (2008). This Figure shows that Eq. (100) gives conservative predictions for practically all tests with $L_d > 1$ m. For seven of the nine tests with $L_d \leq 1$ m, the method underestimates $P_{red, vd}$. This is consistant with the statement of Di Benedetto, Russo and Salzano (2008) that Eq. (100) is not valid for $L_d \leq 1$ m. To get a conservative prediction, the existence of a duct shorter than 1 m should be neglected.

Fig. 53 also shows that for some of the tests with $L_d > 1$ m, Eq. (100) overestimates the experimental values of P_M by a factor up to ten. To study this feature more closely, the data points are plotted using different symbols for different series of tests. Tests with $L_d > 1$ m are plotted in Figure 54 and those with $L_d \leq 1$ m in Figure 55.

It is seen from Fig. 54 that Eq. (100) overestimates P_M somewhat for the tests by Kordylewski & Wach (1986, 1988), where P_{red} was measured. On the other hand, the values of P_M for some tests by Molkov et al. (1993), and Ponizy and Layer (1999b) are substantially overestimated. Fig. 55 shows that the values of P_M for seven of the eight tests by Kordylewski & Wach (1986, 1988) are slightly underestimated.

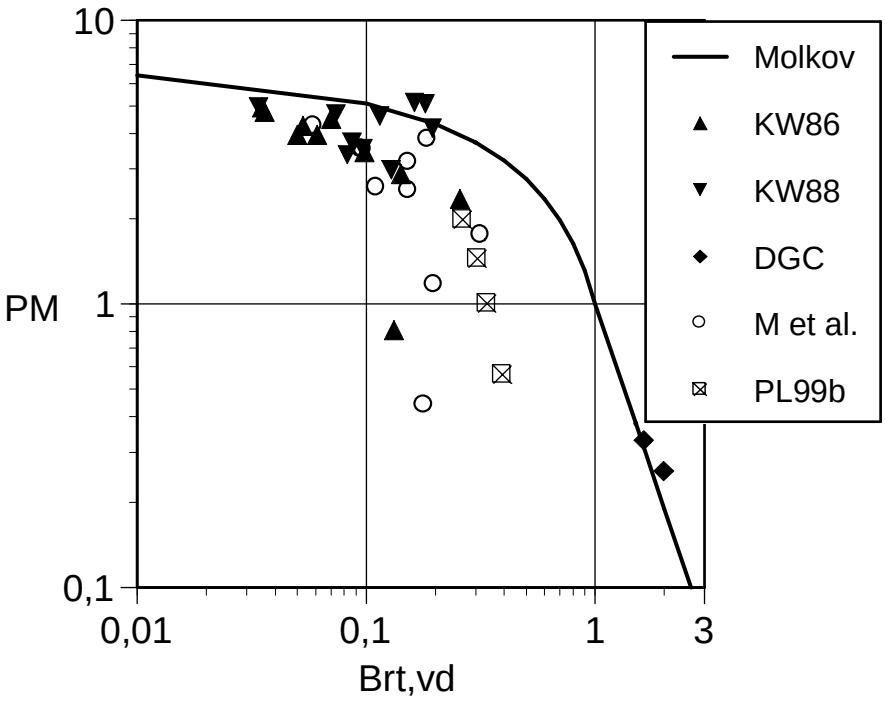

Figure 54. Experimental values of P_M plotted as a function of predicted values of $Br_{t, vd}$ for tests with central ignition and $L_d > 1$ m.

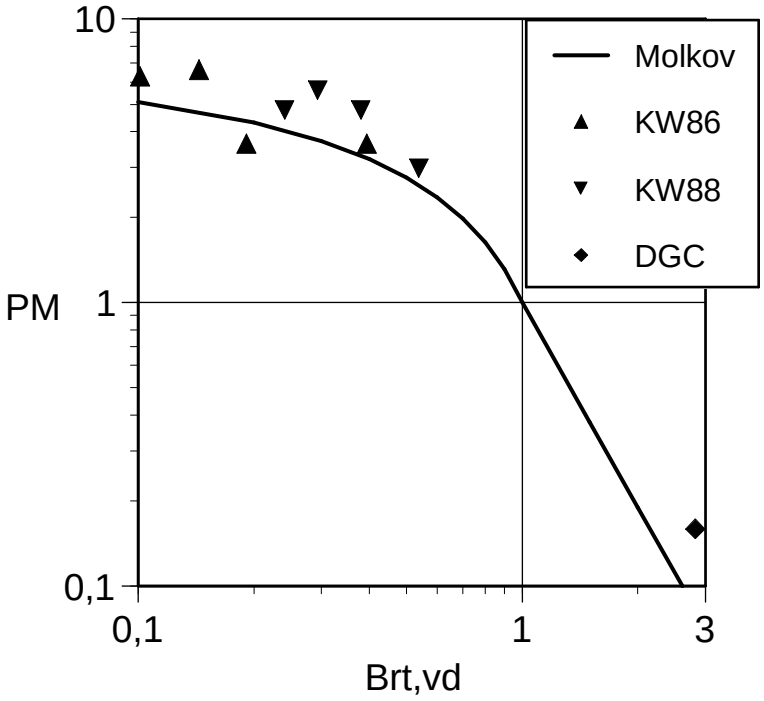

Figure 55. Experimental values of P_M plotted as a function of predicted values of $Br_{t,\,vd}$ for tests with central ignition and $L_d \leq 1$ m.

6.2.3 Predicted vs. experimental ratio of $Br_{t,\,vd}$ / Br_t

The validity of the assumption by Di Benedetto, Russo and Salzano (2008) that duct vented explosions are well represented by $Br_{t,\,vd}$ is now investigated by calculating the experimental values of the ratio $Br_{t,\,vd}/Br_t$. For those tests where P_{red} was measured, the values of Br_t and $Br_{t,\,vd}$ are calculated inserting P_{red} or $P_{red,\,vd}$ into Eq. (25) and solving Br_t either from Eq. (23) or Eq. (24). In Tables 186 to 190, the values of the ratio $Br_{t,\,vd}/Br_t$ are compared to the predictions of Eq. (100).

Table 187. Experimental $Br_{t,\,vd}/Br_t$ for the tests by McCann et al. (1985)

P_{red}, bar	Br_t	$P_{red,\,vd}$, bar	$Br_{t,\,vd}$	$Br_{t,\,vd}/Br_t$	L_d, m	f
0.079	2.90	0.10	2.62	0.905	0.105	1.84
0.079	2.90	0.19	2.01	0.694	0.30	1.09
0.079	2.90	0.17	2.10	0.725	0.50	0.84

Table 188. Experimental $Br_{t,\,vd}/Br_t$ for the tests by Kordylewski and Wach (1986)

C, %	P_{red}, bar	Br_t	$P_{red,\,vd}$, bar	$Br_{t,\,vd}$	$Br_{t,\,vd}/Br_t$	$S_{0,}$ m/s	P_m, bar	f
12	0.5	1.342	2.38	0.601	0.448	0.15	5.64	0.191
14	1.7	0.787	2.91	0.473	0.601	0.24	6.33	0.181
16	2.5	0.571	3.47	0.355	0.622	0.36	6.89	0.172
18	3.4	0.369	4.0	0.259	0.701	0.51	7.29	0.165
20	3.6	0.330	4.3	0.211	0.639	0.64	7.44	0.161
22	4.2	0.226	4.82	0.140	0.618	0.80	7.45	0.157
25	4.2	0.226	5.0	0.118	0.524	1.00	7.10	0.155
30	1.6	0.816	0.82	1.092	1.338	0.70	6.38	0.162

Table 189. Experimental $Br_{t,\,vd}/Br_t$ for the tests by Kordylewski and Wach (1986)

P_{red}, bar	Br_t	$P_{red,\,vd}$, bar	$Br_{t,\,vd}$	$Br_{t,\,v}/Br_t$	$S_{0,}$ m/s	P_m, bar	L_d, m	f
3.7	0.311	3.68	0.315	1.01	0.64	7.44	0.04	1.273
3.7	0.311	3.68	0.315	1.01	0.64	7.44	0.17	0.617
3.7	0.311	6.71	0.004	0.013	0.64	7.44	0.3	0.465
3.7	0.311	6.36	0.014	0.047	0.64	7.44	0.61	0.326
3.7	0.311	4.57	0.172	0.553	0.64	7.44	1.26	0.227
3.7	0.311	4.0	0.259	0.832	0.64	7.44	2.5	0.161

Table 190. Experimental $Br_{t,\,vd}/Br_t$ for the tests by Kordylewski and Wach (1988)

P_{red}, bar	Br_t	$P_{red,\,vd}$, bar	$Br_{t,\,vd}$	$Br_{t,\,v}/Br_t$	D_d, mm	L_d, m	f
2.0	0.702	3.0	0.453	0.645	35	0.16	0.769
2.0	0.702	4.82	0.140	0.199	35	0.32	0.544
2.0	0.702	5.65	0.056	0.080	35	0.54	0.419
2.0	0.702	4.82	0.140	0.199	35	0.8	0.344
2.0	0.702	5.13	0.104	0.148	35	1.4	0.260
2.0	0.702	5.18	0.099	0.141	35	1.75	0.233
2.0	0.702	3.0	0.453	0.645	35	2.8	0.184
2.0	0.702	4.64	0.163	0.232	35	3.5	0.165
2.0	0.702	3.57	0.336	0.479	35	4.91	0.139
2.0	0.702	3.75	0.302	0.430	35	6.14	0.124
2.0	0.702	3.39	0.371	0.528	35	6.75	0.118
4.2	0.226	5.0	0.118	0.524	21	2.5	0.151
3.0	0.453	4.73	0.151	0.333	25	2.5	0.165
1.0	1.004	4.2	0.226	0.225	35	2.5	0.195

Table 191. Experimental $Br_{t,\,vd}/Br_t$ for the tests by DeGood and Chatrathi (1991)

ignition	P_{red}, bar	Br_t	$P_{red,\,vd}$, bar	P_M	$Br_{t,\,vd}$	$Br_{t,\,v}/Br_t$	L_d, m	f
centre	0.20	2.085	0.185	0.159	2.154	1.033	1	1.352
centre	0.20	2.085	0.300	0.257	1.761	0.845	2	0.956
centre	0.20	2.085	0.385	0.330	1.587	0.761	3	0.780
bottom	0.15	2.351	1.01	0.866	1.062	0.452	3	0.780

The experimental values of $B_{rt,\,vd}/Br_t$ for tests with central ignition are plotted with the values predicted with Eq. (100) in Figures 56 and 57 for tests with $L_d > 1$ m and $L_d \leq 1$ m, respectively. In Fig. 56, the predicted values are seen to be close to the experimental ones for two of the three data points corresponding to the tests by DeGood and Chatrathi (1991).

For the data points corresponding to the tests by Kordylewski and Wach (1986, 1988), however, little correlation is seen to exist between the experimental and predicted values of $B_{rt,\,vd}/Br_t$. Concerning those tests by Kordylewski and Wach (1986) where only the concentration was varied, this is a consequence of the weak dependence of f on concentration: f is proportional to $(S_0 \cdot P_m)^{-0.1}$.

Somewhat better correlation is seen to exist in Fig. 57 which, however, represents the tests with $L_d \leq 1$ m that are outside the stated validity of Eq. (100).

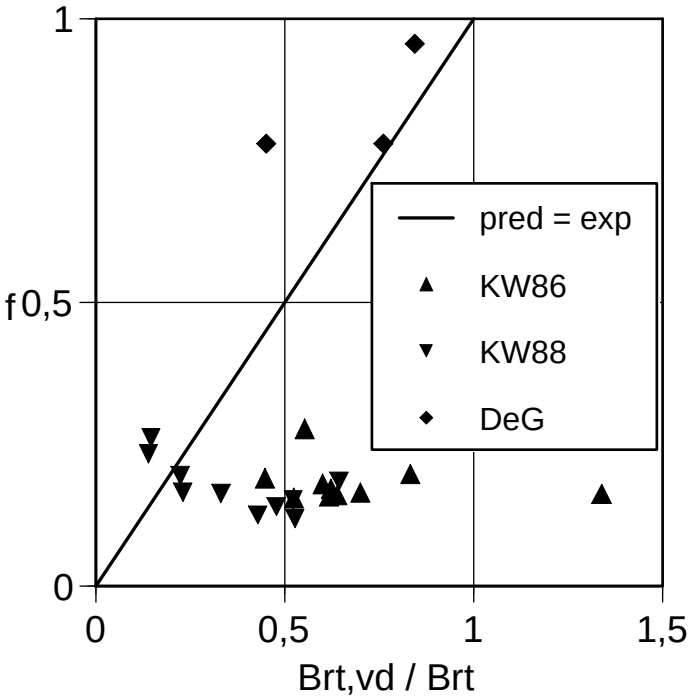

Figure 56. Experimental values of $B_{rt,\,vd}$ /Br_t and those predicted with Eq. (100) for tests with central ignition and L_d > 1 m.

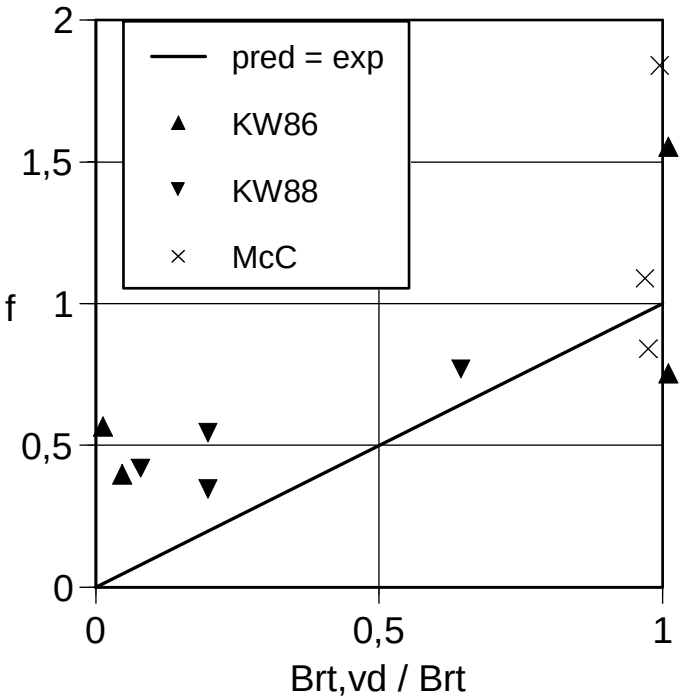

Figure 57. Experimental values of $B_{rt,\,vd}$ /Br_t and those predicted with Eq. (100) for tests with central ignition and $L_d \leq 1$ m.

For the tests by Molkov et al. (1993), and Ponizy and Leyer (1999a, 1999b), the value of Br_t is calculated from Eqs. (20) to (22) with the both parameter sets α = 0.9, β = 1 and α = 1.75, β = 0.5. The values are presented in Tables 191 to 196 and plotted in Figures 58 and 59.

Table 192. Predicted $Br_{t, vd}/Br_t$, Molkov et al. (1993), α = 0.9 and β = 1

Br_t	$P_{red, vd}$, bar	P_{stat}, bar	P_M	$Br_{t, vd}$	$Br_{t, vd}/Br_t$	V, m^3	L_d, m	f
1.073	5.0†	0.19	3.81	0.283	0.264	0.027	1.83	0.289
1.024	4.4	0.24	3.16	0.410	0.400	0.027	2.35	0.253
1.024	3.5	0.24	2.51	0.560	0.547	0.027	2.35	0.253
1.209	1.9	1.64	0.44	1.408	1.165	0.027	2.35	0.252
1.178	4.4†	1.41	1.17	0.944	0.801	0.027	1.83	0.286
0.520	4.3	0.14	3.50	0.340	0.654	2	4	0.331
0.508	5.2	0.14	4.23	0.213	0.419	2	10	0.209
1.384	2.15	0.14	1.75	0.766	0.553	2	10	0.291
0.733	4.1	0.1	3.51	0.338	0.461	10	25	0.199
0.817	2.8	0.05	2.57	0.545	0.667	10	25	0.203

Table 193. Predicted $Br_{t, vd}/Br_t$, Molkov et al. (1993), α = 1.75 and β = 0.5

Br_t	$P_{red, vd}$, bar	P_{stat}, bar	P_M	$Br_{t, vd}$	$Br_{t, vd}/Br_t$	V, m^3	L_d, m	f
0.642	5.0†	0.19	3.81	0.283	0.440	0.027	1.83	0.289
0.605	4.4	0.24	3.16	0.410	0.677	0.027	2.35	0.253
0.605	3.5	0.24	2.51	0.560	0.926	0.027	2.35	0.253
0.711	1.9	1.64	0.44	1.408	1.980	0.027	2.35	0.252
0.693	4.4†	1.41	1.17	0.944	1.362	0.027	1.83	0.286
0.297	4.3	0.14	3.50	0.340	1.145	2	4	0.331
0.289	5.2	0.14	4.23	0.213	0.737	2	10	0.209
1.019	2.15	0.14	1.75	0.766	0.752	2	10	0.291
0.475	4.1	0.1	3.51	0.338	0.712	10	25	0.199
0.547	2.8	0.05	2.57	0.545	0.996	10	25	0.203

Table 194. Predicted $Br_{t, vd}/Br_t$, Ponizy & Leyer (1999a), α = 0.9 and β = 1

Br_t	$P_{red, vd}$, bar	$Br_{t, vd}$	$Br_{t, v}/Br_t$	D_d, mm	L_d, m	f
0.496	1.45	0.861	1.74	16	0.6	0.295
0.781	1.17	0.949	1.22	21	0.6	0.338
1.74	1.27	0.917	0.526	36	0.6	0.443
0.496	1.80	0.758	1.53	16	1.1	0.218
0.781	1.45	0.861	1.10	21	1.1	0.250
1.74	1.92	0.724	0.415	36	1.1	0.327
0.496	1.92	0.724	1.46	16	2.6	0.142
0.781	1.55	0.831	1.06	21	2.6	0.162
1.74	1.92	0.724	0.415	36	2.6	0.213
2.94	2.11	0.672	0.229	53	2.6	0.258

Table 195. Predicted $Br_{t, vd}/Br_t$, Ponizy & Leyer (1999a), α = 1.75 and β = 0.5

Br_t	$P_{red, vd}$, bar	$Br_{t, vd}$	$Br_{t, v}/Br_t$	D_d, mm	L_d, m	f
0.260	1.45	0.861	3.31	16	0.6	0.295
0.429	1.17	0.949	2.21	21	0.6	0.338
1.14	1.27	0.917	0.807	36	0.6	0.443
0.260	1.80	0.758	2.92	16	1.1	0.218
0.429	1.45	0.861	2.01	21	1.1	0.250
1.14	1.92	0.724	0.637	36	1.1	0.327
0.260	1.92	0.724	2.78	16	2.6	0.142
0.429	1.55	0.831	1.94	21	2.6	0.162
1.14	1.92	0.724	0.637	36	2.6	0.213
2.24	2.11	0.672	0.299	53	2.6	0.258

Table 196. Predicted $Br_{t, vd}/Br_{t,}$ Ponizy & Leyer (1999b), α = 0.9 and β = 1

ignition	P_{stat}, bar	Br_t	$P_{red, vd}$, bar	P_M	$Br_{t, vd}$	$Br_{t, v}/Br_t$	f
centre	0	1.744	2.01	1.98	0.699	0.401	0.259
centre	0.3	1.843	2.16	1.45	0.857	0.465	0.259
centre	0.91	2.023	2.66	1.00	0.999	0.494	0.259
centre	2.3	2.362	3.37	0.562	1.27	0.538	0.259
rear	0	1.744	1.76	1.74	0.769	0.441	0.259
rear	0.32	1.849	1.88	1.23	0.925	0.500	0.259
rear	0.83	2.000	1.81	1.81	1.09	0.571	0.259
near vent	1.11	2.077	1.27	0.413	1.45	0.696	0.259
near vent	2.24	2.349	2.24	0.384	1.49	0.634	0.259

Table 197. Predicted $Br_{t, vd}/Br_{t,}$ Ponizy & Leyer (1999b), α = 1.75 and β = 0.5

ignition	P_{stat}, bar	Br_t	$P_{red, vd}$, bar	P_M	$Br_{t, vd}$	$Br_{t, v}/Br_t$	f
centre	0	1.136	2.01	1.98	0.699	0.615	0.259
centre	0.3	1.201	2.16	1.45	0.857	0.714	0.259
centre	0.91	1.318	2.66	1.00	0.999	0.758	0.259
centre	2.3	1.539	3.37	0.562	1.27	0.826	0.259
rear	0	1.136	1.76	1.74	0.769	0.677	0.259
rear	0.32	1.205	1.88	1.23	0.925	0.768	0.259
rear	0.83	1.304	1.81	0.728	1.09	0.838	0.259
near vent	1.11	1.353	1.27	0.413	1.45	1.068	0.259
near vent	2.24	1.530	2.24	0.384	1.49	0.974	0.259

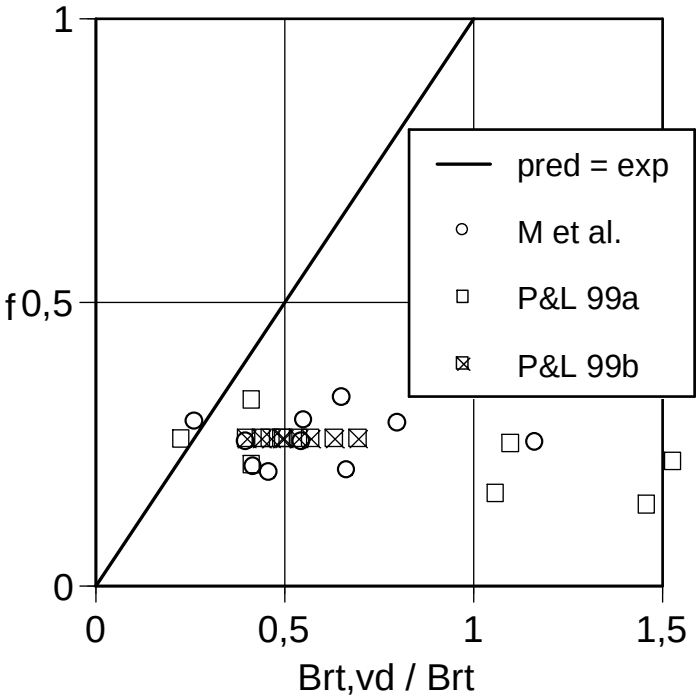

Figure 58. Experimental values of $B_{rt,\ vd}$ /Br_t calculated with Eqs. (20) to (25) using α = 0.9 and β = 1 and those predicted with Eq. (100).

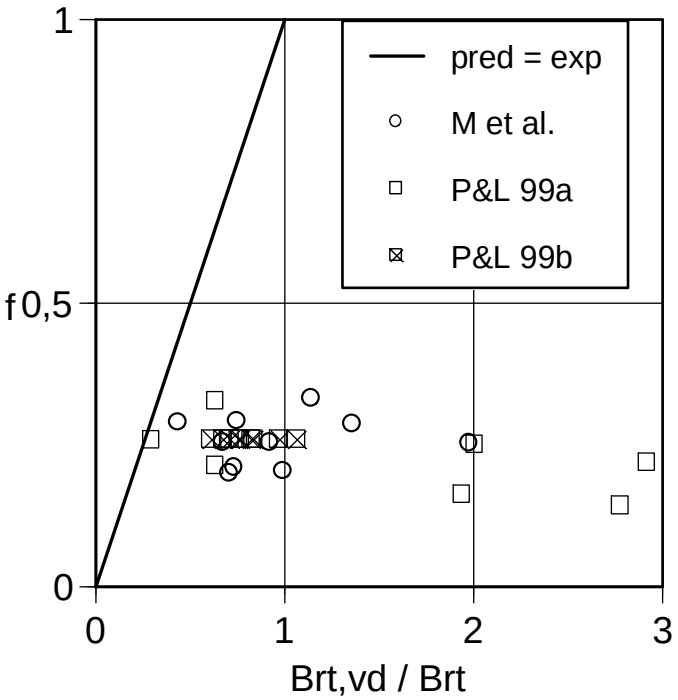

Figure 59. Experimental values of $B_{rt,\ vd}$ /Br_t calculated with Eqs. (20) to (25) using α = 1.75 and β = 0.5 and those predicted with Eq. (100).

With either parameter set, there is no correlation between experimental values of $B_{rt,\ vd}$ /Br_t and those predicted by Eq. (100).

6.2.4 Predicted vs. experimental values of $P_{red,\ vd}$

In Tables 197 to 207, the values of $P_{red,\ vd}$ predicted by Eq. (100) are compared to the experimental ones. All tests irrespective of ignition location and duct length are considered.

Table 198. Predicted $P_{red, vd}$ for the tests by McCann et al. (1985)

P_{red}, bar	Br_t	L_d, m	f	$Br_{t, vd}$	$P_{red, vd}$, bar	exp., bar
0.079	2.90	0.105	1.84	5.33	0.02	0.10
0.079	2.90	0.30	1.09	3.16	0.06	0.19
0.079	2.90	0.50	0.84	2.43	0.12	0.17

Table 199. Predicted $P_{red, vd}$ for the tests by Kordylewski and Wach (1986)

C, %	P_{red}, bar	Br_t	$S_{0,}$ m/s	P_m, bar	f	$Br_{t, vd}$	$P_{red, vd}$, bar	exp., bar
10	—	0.933	0.09	4.94	0.204	0.190	4.44	0.82
12	0.5	1.342	0.15	5.64	0.191	0.257	4.01	2.38
14	1.7	0.787	0.24	6.33	0.181	0.142	4.80	2.91
16	2.5	0.571	0.36	6.89	0.172	0.098	5.19	3.47
18	3.4	0.369	0.51	7.29	0.165	0.061	5.59	4.0
20	3.6	0.330	0.64	7.44	0.161	0.053	5.69	4.3
22	4.2	0.226	0.80	7.45	0.157	0.036	5.94	4.82
25	4.2	0.226	1.00	7.10	0.155	0.035	5.95	5.0
30	1.6	0.816	0.70	6.38	0.162	0.132	4.88	0.82

Table 200. Predicted $P_{red, vd}$ for the tests by Kordylewski and Wach (1986)

L_d, m	P_{red}, bar	Br_t	$S_{0,}$ m/s	P_m, bar	f	$Br_{t, vd}$	$P_{red, vd}$, bar	exp., bar
0.04	3.7	0.311	0.64	7.44	1.273	0.396	3.26	3.68
0.17	3.7	0.311	0.64	7.44	0.617	0.192	4.43	3.68
0.3	3.7	0.311	0.64	7.44	0.465	0.145	4.78	6.71
0.61	3.7	0.311	0.64	7.44	0.326	0.102	5.16	6.36
1.26	3.7	0.311	0.64	7.44	0.227	0.071	5.48	4.57
2.5	3.7	0.311	0.64	7.44	0.161	0.050	5.73	4.0

Table 201. Predicted $P_{red, vd}$ for the tests by Kordylewski and Wach (1988)

D_d, mm	L_d, m	f	P_{red}, bar	Br_t	$Br_{t, vd}$	$P_{red, vd}$, bar	exp., bar
35	0.16	0.769	2.0	0.702	0.540	2.63	3.0
35	0.32	0.544	2.0	0.702	0.382	3.34	4.82
35	0.54	0.419	2.0	0.702	0.294	3.80	5.65
35	0.8	0.344	2.0	0.702	0.241	4.11	4.82
35	1.4	0.260	2.0	0.702	0.183	4.50	5.13
35	1.75	0.233	2.0	0.702	0.163	4.64	5.18
35	2.8	0.184	2.0	0.702	0.129	4.91	3.0
35	3.5	0.165	2.0	0.702	0.115	5.03	4.64
35	4.91	0.139	2.0	0.702	0.097	5.19	3.57
35	6.14	0.124	2.0	0.702	0.087	5.30	3.75
35	6.75	0.118	2.0	0.702	0.083	5.34	3.39
21	2.5	0.151	4.2	0.226	0.034	5.97	5.0
25	2.5	0.165	3.0	0.453	0.075	5.43	4.73
35	2.5	0.195	1.0	1.004	0.196	4.40	4.2

Table 202. Predicted $P_{red, vd}$ for the tests by DeGood and Chatrathi (1991)

ignition	P_{red}, bar	Br_t	L_d, m	f	$Br_{t, vd}$	P_M	$P_{red, vd}$, bar	exp., bar
centre	0.20	2.085	1	1.352	2.82	0.083	0.10	0.185
centre	0.20	2.085	2	0.956	1.99	0.191	0.22	0.300
centre	0.20	2.085	3	0.780	1.63	0.311	0.315	0.385
bottom	0.15	2.351	3	0.780	1.83	0.233	0.27	1.01

Table 203. Predicted $P_{red, vd}$, Molkov et al. (1993), α = 0.9 and β = 1

V, m^3	L_d, m	P_{stat}, bar	S_0, m/s	f	Br_t	$Br_{t, vd}$	P_M	$P_{red, vd}$, bar	exp., bar
0.027	1.83	0.19	0.26	0.289	1.073	0.310	3.66	4.80	5.0†
0.027	2.35	0.24	0.28	0.253	1.024	0.259	3.95	5.50	4.4
0.027	2.35	0.24	0.28	0.253	1.024	0.259	3.95	5.50	3.5
0.027	2.35	1.64	0.29	0.252	1.209	0.305	3.69	15.8	1.9
0.027	1.83	1.41	0.29	0.286	1.178	0.337	3.52	13.2	4.4†
2	4	0.14	0.325	0.331	0.520	0.172	4.51	5.55	4.3
2	10	0.14	0.335	0.209	0.508	0.106	5.05	6.21	5.2
2	10	0.14	0.295	0.291	1.384	0.403	3.19	3.93	2.15
10	25	0.1	0.32	0.199	0.733	0.146	4.71	5.50	4.1
10	25	0.05	0.27	0.203	0.817	0.166	4.56	4.97	2.8

Table 204. Predicted $P_{red, vd}$, Molkov et al. (1993), α = 1.75 and β = 0.5

V, m^3	L_d, m	P_{stat}, bar	S_0, m/s	f	Br_t	$Br_{t, vd}$	P_M	$P_{red, vd}$, bar	exp., bar
0.027	1.83	0.19	0.26	0.289	0.642	0.186	4.42	5.79	5.0†
0.027	2.35	0.24	0.28	0.253	0.605	0.153	4.65	6.48	4.4
0.027	2.35	0.24	0.28	0.253	0.605	0.153	4.65	6.48	3.5
0.027	2.35	1.64	0.29	0.252	0.711	0.179	4.46	19.2	1.9
0.027	1.83	1.41	0.29	0.286	0.693	0.198	4.33	16.0	4.4†
2	4	0.14	0.325	0.331	0.297	0.098	5.12	6.30	4.3
2	10	0.14	0.335	0.209	0.289	0.060	5.52	6.80	5.2
2	10	0.14	0.295	0.291	1.019	0.297	3.73	4.59	2.15
10	25	0.1	0.32	0.199	0.475	0.095	5.16	6.02	4.1
10	25	0.05	0.27	0.203	0.547	0.111	5.00	5.44	2.8

Table 205. Predicted $P_{red, vd}$, Ponizy & Leyer (1999a), α = 0.9 and β = 1

D_d, mm	L_d, m	f	Br_t	$Br_{t, vd}$	P_M	$P_{red, vd}$, bar	exp., bar
16	0.6	0.295	0.496	0.146	4.71	4.77	1.45
21	0.6	0.338	0.781	0.264	3.92	3.97	1.17
36	0.6	0.443	1.74	0.773	1.73	1.75	1.27
16	1.1	0.218	0.496	0.108	5.03	5.09	1.80
21	1.1	0.250	0.781	0.195	4.35	4.41	1.45
36	1.1	0.327	1.74	0.570	2.47	2.50	1.92
16	2.6	0.142	0.496	0.070	5.41	5.48	1.92
21	2.6	0.162	0.781	0.127	4.87	4.93	1.55
36	2.6	0.213	1.74	0.371	3.34	3.39	1.92
53	2.6	0.258	2.94	0.758	1.78	1.80	2.11

Table 206. Predicted $P_{red, vd}$, Ponizy & Leyer (1999a), α = 1.75 and β = 0.5

D_d, mm	L_d, m	f	Br_t	$Br_{t, vd}$	P_M	$P_{red, vd}$, bar	exp., bar
16	0.6	0.295	0.260	0.077	5.34	5.41	1.45
21	0.6	0.338	0.429	0.145	5.72	4.78	1.17
36	0.6	0.443	1.14	0.503	2.74	2.78	1.27
16	1.1	0.218	0.260	0.057	5.57	5.64	1.80
21	1.1	0.250	0.429	0.107	5.04	5.10	1.45
36	1.1	0.327	1.14	0.371	3.34	3.39	1.92
16	2.6	0.142	0.260	0.037	5.85	5.92	1.92
21	2.6	0.162	0.429	0.069	5.42	5.49	1.55
36	2.6	0.213	1.14	0.242	4.05	4.10	1.92
53	2.6	0.258	2.24	0.579	2.43	2.47	2.11

Table 207. Predicted $P_{red, vd}$, Ponizy & Leyer (1999b), α = 0.9 and β = 1

ignition	P_{stat}, bar	f	Br_t	$Br_{t, vd}$	P_M	$P_{red, vd}$, bar	exp., bar
centre	0	0.263	1.74	0.459	2.94	2.97	2.01
centre	0.3	0.263	1.84	0.485	2.82	4.2	2.16
centre	0.91	0.263	2.02	0.532	2.62	6.95	2.66
centre	2.3	0.263	2.36	0.621	2.27	13.8	3.37
rear	0	0.263	1.74	0.459	2.94	2.97	1.76
rear	0.32	0.263	1.85	0.486	2.82	4.3	1.88
rear	0.83	0.263	2.00	0.526	2.65	6.6	1.81
near vent	1.11	0.263	2.08	0.546	2.56	7.9	1.27
near vent	2.24	0.263	2.35	0.618	2.28	13.1	2.24

Table 208. Predicted $P_{red, vd}$, Ponizy & Leyer (1999b), α = 1.75 and β = 0.5

ignition	P_{stat}, bar	f	Br_t	$Br_{t, vd}$	P_M	$P_{red, vd}$, bar	exp., bar
centre	0	0.263	1.14	0.299	3.72	3.77	2.01
centre	0.3	0.263	1.20	0.316	3.63	5.4	2.16
centre	0.91	0.263	1.32	0.347	3.47	9.2	2.66
centre	2.3	0.263	1.54	0.405	3.18	19.1	3.37
rear	0	0.263	1.14	0.299	3.72	3.77	1.76
rear	0.32	0.263	1.20	0.317	3.62	5.55	1.88
rear	0.83	0.263	1.30	0.343	3.49	8.65	1.81
near vent	1.11	0.263	1.35	0.356	3.42	10.5	1.27
near vent	2.24	0.263	1.53	0.402	3.19	18.6	2.24

The predicted and experimental values of $P_{red, vd}$ in Tables 197 to 207 are plotted in Figures 60 and 61.

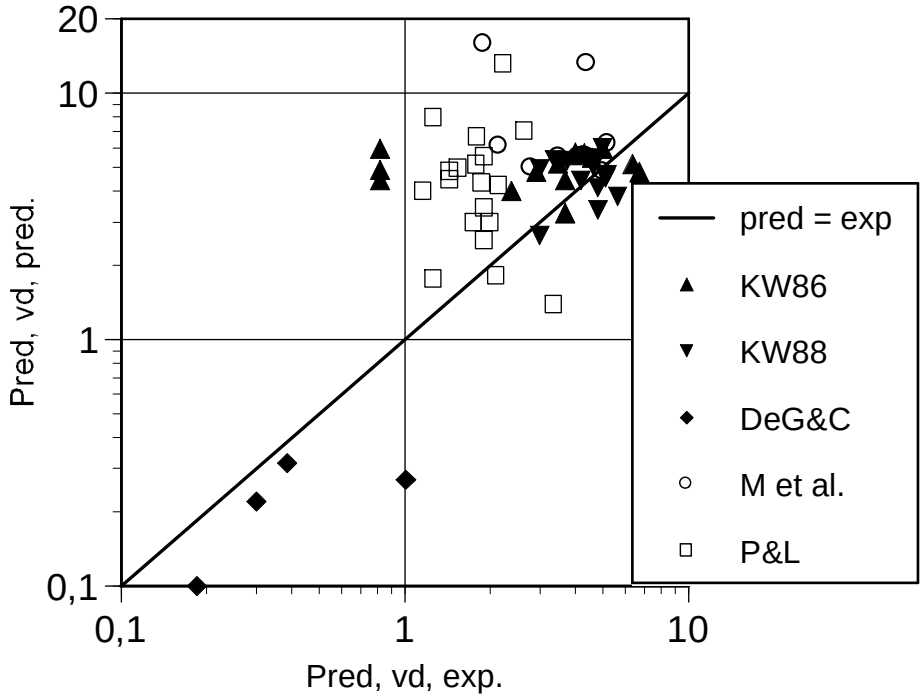

Figure 60. Comparison of $P_{red,\,vd}$ predicted with Eq. (100) and Eqs. (20) to (25) using α = 0.9 and β = 1 with experimental values.

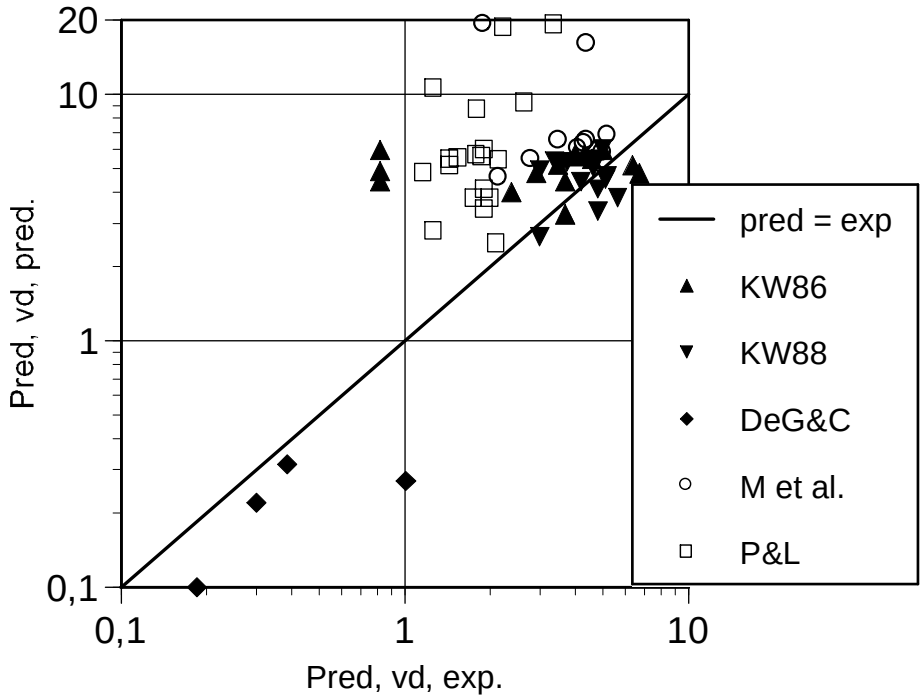

Figure 61. Comparison of $P_{red,\,vd}$ predicted with Eq. (100) and Eqs. (20) to (25) using α = 1.75 and β = 0.5 with experimental values.

The relative errors of data in Tables 197 to 207 were calculated with Eq. (40) and the results are given in Table 209. Since the predictions of $P_{red,\,vd}$ for the tests by Molkov et al. (1993), and Ponizy and Leyer (1999b) with $P_{stat} > 0.24$ bar are very high and even unphysical, the relative error has also been calculated for the tests with $P_{stat} \leq 0.24$ bar.

Table 209. Relative errors of the predictions with Eq. (100)

reference	tests	experiment	$\alpha = 0.9$, $\beta = 1$	$\alpha = 1.75$, $\beta = 0.5$
K & W	28	32.0 %	—	—
the others	7	11.0 %	—	—
M et al.	10	—	96.0 %	117.5 %
P & L	19	—	107.0 %	166.0 %
all tests	64	—	62.0 %	83.0 %
K & W	28	32.0 %	—	—
the others	7	11.0 %	—	—
M et al. , $P_{stat} \leq 0.24$ bar	8	—	39.5 %	49.5 %
P & L, $P_{stat} \leq 0.24$ bar	12	—	77.5 %	103.0 %
$P_{stat} \leq 0.24$ bar	55	—	40.5 %	47.5 %

6.2.5 Comparison of the relative errors of predictions

The accuracy of Eq. (100) is now compared to that of the other correlations. When the correlations by Bartknecht, of VDI 3673 and EN 14491 were validated, the predictions of $P_{red, vd}$ for the Molkov et al. (1993) tests were based on the experimental values of P_{red} measured with the 0.027 and 2 m^3 vessels and given in Table 29. In Tables 210 to 215, the predicted values of $P_{red, vd}$ are calculated starting from values of P_{red} predicted with Eqs. (21) to (25) and both sets of parameters: $\alpha = 0.9$, $\beta = 1$, and $\alpha = 1.75$, $\beta = 0.5$.

Table 210. Predicted $P_{red, vd}$, $\alpha = 0.9$ and $\beta = 1$, Bartknecht

V, m^3	L_d, m	P_{stat}, bar	Br_t	P_M	P_{red}, bar	gas, bar	dust, bar	exp., bar
0.027	1.83	0.19	1.073	0.844	1.28	1.53 (2.82)	2.16	5.0†
0.027	2.35	0.24	1.024	0.945	1.32	1.57 (2.86)	2.21	4.4
0.027	2.35	0.24	1.024	0.945	1.32	1.57 (2.86)	2.21	3.5
0.027	2.35	1.64	1.209	0.634	2.72	2.94 (4.16)	3.54	1.9
0.027	1.83	1.41	1.178	0.675	2.18	2.43 (3.71)	3.06	4.4†
2	4	0.14	0.520	2.673	3.29	4.59	5.30	4.3
2	10	0.14	0.508	2.724	3.35	4.63	5.35	5.2
2	10	0.14	1.384	0.458	0.46	1.67	2.07	2.15
10	25	0.1	0.733	1.863	2.17	3.70	4.34	4.1
10	25	0.05	0.817	1.577	1.72	3.28	3.89	2.8

Table 211. Predicted $P_{red, vd}$, $\alpha = 1.75$ and $\beta = 0.5$, Bartknecht

V, m^3	L_d, m	P_{stat}, bar	Br_t	P_M	P_{red}, bar	gas, bar	dust, bar	exp., bar
0.027	1.83	0.19	0.642	2.19	2.87	3.07 (4.28)	3.67	5.0†
0.027	2.35	0.24	0.605	2.33	3.25	3.42 (4.56)	3.98	4.4
0.027	2.35	0.24	0.605	2.33	3.25	3.42 (4.56)	3.98	3.5
0.027	2.35	1.64	0.711	1.94	10.1	9.1 (8.2)	8.35	1.9
0.027	1.83	1.41	0.693	2.01	7.5	7.0 (7.0)	6.87	4.4†
2	4	0.14	0.297	3.73	4.59	5.45	6.21	4.3
2	10	0.14	0.289	3.82	4.71	5.52	6.29	5.2
2	10	0.14	1.019	0.96	1.18	2.70	3.25	2.15
10	25	0.1	0.475	2.86	3.34	4.62	5.34	4.1
10	25	0.05	0.547	2.56	2.79	4.21	4.90	2.8

Table 212. Predicted $P_{red, vd}$, α = 0.9 and β = 1, VDI 3673

V, m^3	P_{stat}, bar	P_{red}, bar	L_s, m	L_d, m	$P_{red, vd}/P_{red}$	$P_{red, vd}$, bar	exp., bar
0.027	0.19	1.28	4.17	1.83	1.115	1.43	5.0†
0.027	0.24	1.32	4.12	2.35	1.147	1.51	4.4
0.027	0.24	1.32	4.12	2.35	1.147	1.51	3.5
0.027	1.64	2.72	3.15	2.35	1.147	3.12	1.9
0.027	1.41	2.18	3.42	1.83	1.115	2.50	4.4†
2	0.14	3.29	2.94	4	1.087	3.59*	4.3
2	0.14	3.35	2.92	10	1.086	3.65*	5.2
2	0.14	0.46	6.06	10	2.397	0.98*	2.15
10	0.1	2.17	3.43	25	1.274	2.63*	4.1
10	0.05	1.72	3.73	25	1.298	2.13*	2.8

Table 213. Predicted $P_{red, vd}$, α = 1.75 and β = 0.5, VDI 3673

V, m^3	P_{stat}, bar	P_{red}, bar	L_s, m	L_d, m	$P_{red, vd}/P_{red}$	$P_{red, vd}$, bar	exp., bar
0.027	0.19	2.87	3.09	1.83	1.115	3.20	5.0†
0.027	0.24	3.25	2.95	2.35	1.147	3.73	4.4
0.027	0.24	3.25	2.95	2.35	1.147	3.73	3.5
0.027	1.64	10.1	1.94	2.35	1.121	11.3*	1.9
0.027	1.41	7.5	2.17	1.83	1.115	8.35	4.4†
2	0.14	4.59	2.60	4	1.077	4.91*	4.3
2	0.14	4.71	2.57	10	1.076	5.04*	5.2
2	0.14	1.18	4.29	10	1.992	2.07*	2.15
10	0.1	3.34	2.92	25	1.233	3.89*	4.1
10	0.05	2.79	3.12	25	1.249	3.31*	2.8

Table 214. Predicted $P_{red, vd}$, α = 0.9 and β = 1, EN 14491

V, m^3	P_{stat}, bar	P_{red}, bar	D_d, m	L_s, m	L_d, m	$P_{red, vd}/P_{red}$	$P_{red, vd}$, bar	exp., bar
0.027	0.19	1.28	0.05	0.208	1.83	1.260	1.61*	5.0†
0.027	0.24	1.32	0.05	0.206	2.35	1.258	1.66*	4.4
0.027	0.24	1.32	0.05	0.206	2.35	1.258	1.66*	3.5
0.027	1.64	2.72	0.05	0.158	2.35	1.197	3.26*	1.9
0.027	1.41	2.18	0.05	0.171	1.83	1.214	2.65*	4.4†
2	0.14	3.29	0.2	0.588	4	1.087	3.58*	4.3
2	0.14	3.35	0.2	0.584	10	1.086	3.64*	5.2
2	0.14	0.46	0.2	2.30	10	2.33	1.11*	2.15
10	0.1	2.17	0.5	1.72	25	1.274	2.76*	4.1
10	0.05	1.72	0.5	1.87	25	1.298	2.23*	2.8

Table 215. Predicted $P_{red, vd}$, α = 1.75 and β = 0.5, EN 14491

V, m^3	P_{stat}, bar	P_{red}, bar	D_d, m	L_s, m	L_d, m	$P_{red, vd}$ /P_{red}	$P_{red, vd}$, bar	exp., bar
0.027	0.19	2.87	0.05	0.154	1.83	1.193	3.43*	5.0†
0.027	0.24	3.25	0.05	0.148	2.35	1.185	3.85*	4.4
0.027	0.24	3.25	0.05	0.148	2.35	1.185	3.85*	3.5
0.027	1.64	10.1	0.05	0.097	2.35	1.121	11.3*	1.9
0.027	1.41	7.5	0.05	0.108	1.83	1.136	8.5*	4.4†
2	0.14	4.59	0.2	0.519	4	1.077	4.94*	4.3
2	0.14	4.71	0.2	0.514	10	1.076	5.07*	5.2
2	0.14	1.18	0.2	2.66	10	1.99	2.35*	2.15
10	0.1	3.34	0.5	1.46	25	1.233	4.12*	4.1
10	0.05	2.79	0.5	1.56	25	1.249	3.49*	2.8

Di Benedetto, Russo and Salzano (2008) state that Eq. (100) is only valid for ducts longer than 1 m. Nevertheless, Fig. 57 shows good correlation of predictions of Eq. (100) with experimental values. The values of the relative error are compared in Table 216 for all tests, for those with L_d > 1 m and those with $P_{stat} \leq$ 0.24 bar. In Table 217, only tests with central ignition have been included.

Table 216. Relative errors of the predictions, all ignition locations

method	all data	L_d > 1 m	$P_{stat} \leq$ 0.24 bar
gas explosions			
Bartknecht	29.5 % (32.5 %)	31.0 % (32.0 %)	27.5 % (30.0 %)
NFPA 68 (2007)	26.0 % (32.0 %)	25.0 % (32.0 %)	26.5 % (30.5 %)
dust explosions			
Bartknecht, dust	28.0 % (32.0 %)	29.0 % (34.0 %)	27.5 % (30.5 %)
VDI 3673	33.0 % (36.0 %)	34.5 % (36.5 %)	31.5 % (33.0 %)
EN 14491	35.0 % (42.5 %)	31.0 % (38.0 %)	35.5 % (44.5 %)
Tamanini	34.5 % (76.0 %)	36.0 % (88.0 %)	29.0 % (42.5 %)
NFPA 68 (2007)	39.5 %	37.5 %	39.5 %
Eq. (91)	27.5 %	25.5 %	28.5 %
Eq. (100)	62.0 % (83.0 %)	71.5 % (96.5 %)	40.5 % (47.5 %)

Table 217. Relative errors of the predictions, central ignition

method	all L_d	L_d > 1 m
gas explosions		
Bartknecht	27.0 % (29.0 %)	27.5 % (29.5 %)
NFPA 68 (2007)	20.5 % (23.5 %)	21.0 % (24.0 %)
dust explosions		
Bartknecht	23.5 % (26.0 %)	23.5 % (26.5 %)
VDI 3673	33.0 % (35.0 %)	33.5 % (36.0 %)
EN 14491	32.5 % (36.5 %)	32.5 % (37.5 %)
Tamanini	28.5 % (57.5 %)	30.0 % (65.5 %)
NFPA 68 (2007)	35.5 %	36.0 %
Eq. (91)	25.5 %	25.0 %
Eq. (100)	47.5 % (62.0 %)	53.5 % (71.5 %)

Table 216 shows that inclusion of tests with $L_d \leq$ 1 m results in a significant decrease of the average error of Eq. (100) when all ignition locations are included. When tests with P_{stat} > 0.24 bar are excluded, the average error decreases even

more. For the other methods, the effect of duct length L_d and vent opening pressure on the relative error is small. A comparison of Table 216 with Table 217 shows that exclusion of tests where ignition location was either not given or non-central results in significant decrease of the average error of Eq. (100) when all duct lengths are included. For the other methods, the effect of ignition location on the relative error is quite small.

The relative error of the Tamanini method with the parameter set $\alpha = 1.75$ and $\beta = 0.5$ shows similar behaviour as that of Eq. (100).

6.2.6 Dependence of $P_{red, vd}$ on P_{stat}

The reason for the poor accuracy of Tamanini method with the parameter set $\alpha = 1.75$ and $\beta = 0.5$ and Eq. (100) with both parameter sets is a consequence from very high and unphysical predictions of $P_{red, vd}$ for the tests by Molkov et al. (1993) and those by Ponizy and Leyer (1999b) with high values of P_{stat}. The values of $P_{red, vd}$ for all the tests by Ponizy and Leyer (1999b) predicted with the different methods are plotted as a function of P_{stat} in Figures 62 to 64.

It is seen from Figs. 62 to 64 that the measured values of $P_{red, vd}$ increase somewhat with increasing P_{stat} for all the three ignition locations. Obviously, the values of $P_{red, vd}$ depend on the ignition location but no method exists to take this into account. The methods of VDI 3673 and EN 14491 give good predictions for $P_{red, vd}$ with the parameter set $\alpha = 1.75$ and $\beta = 0.5$.

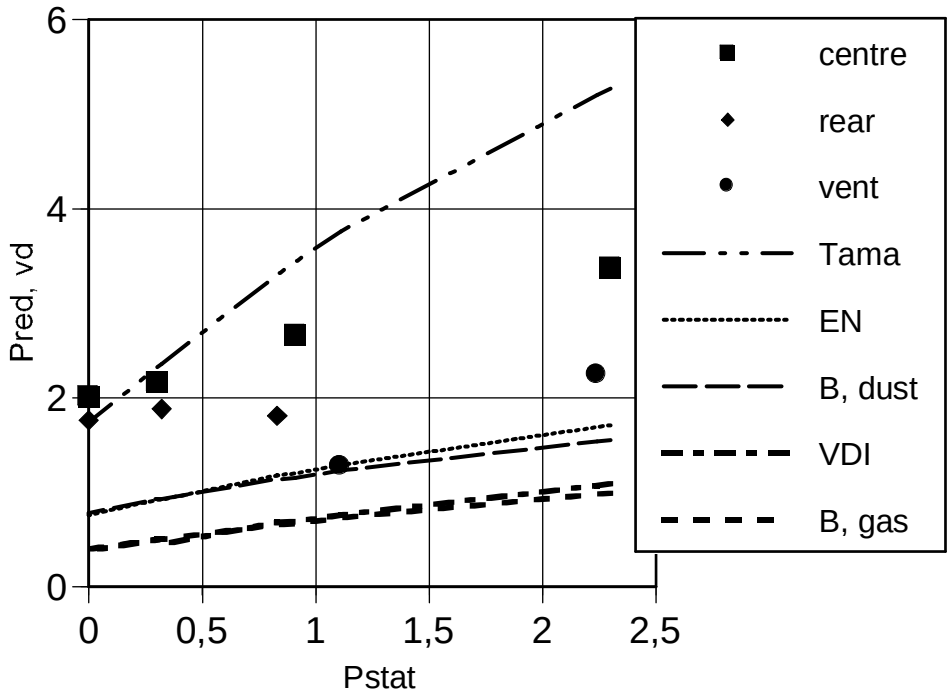

Figure 62. P_{red} predicted with Eqs. (20) to (25) using $\alpha = 0.9$ and $\beta = 1$ and $P_{red, vd}$ predicted with different methods for the tests by Ponizy and Leyer (1999b).

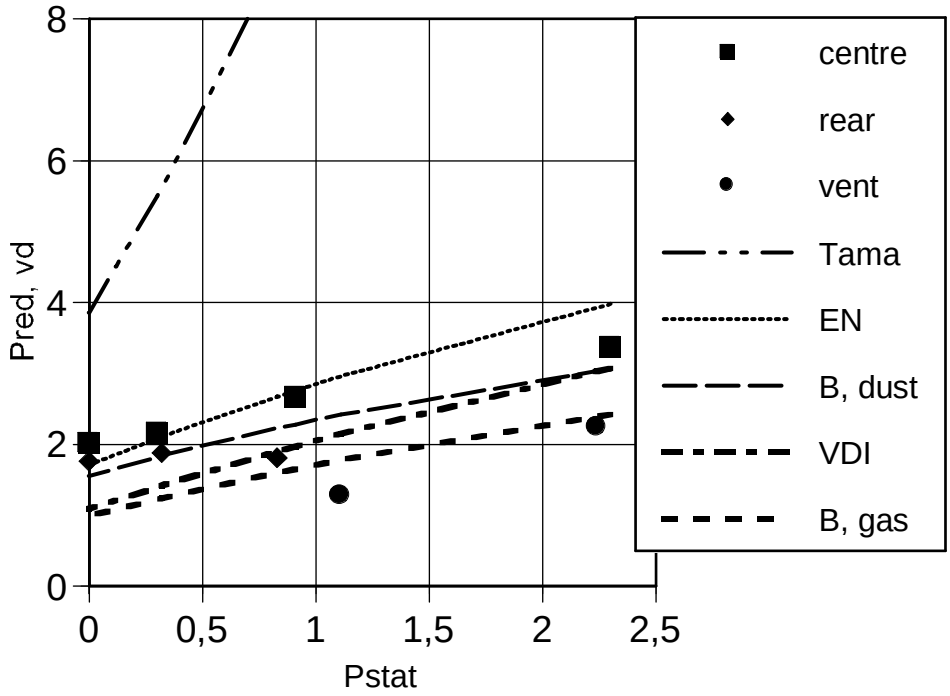

Figure 63. P_{red} predicted with Eqs. (20) to (25) using α = 1.75 and β = 0.5 and $P_{red, vd}$ predicted with different methods for the tests by Ponizy and Leyer (1999b).

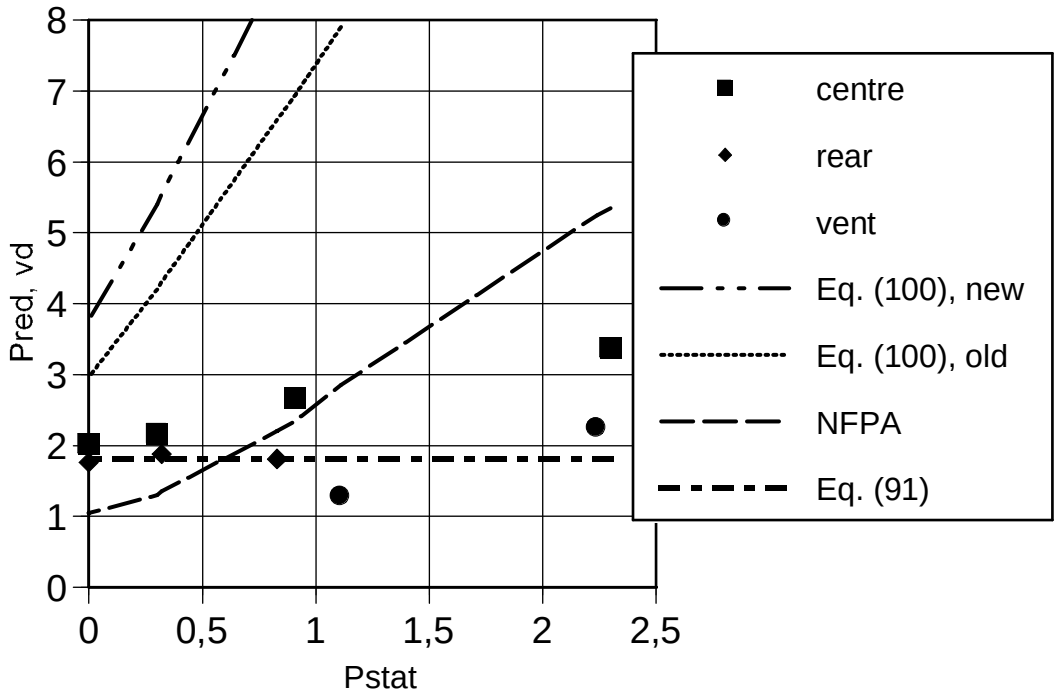

Figure 64. P_{red} predicted with Eqs. (20) to (25) and $P_{red, vd}$ predicted with different methods for the tests by Ponizy and Leyer (1999b).

The slopes of $P_{red, vd}$ predicted with the Bartknecht methods, VDI 3673 and EN 14491 are comparable to the experimental ones whereas that predicted with NFPA 68 (2007) is higher. The slope $P_{red, vd}$ predicted with Tamanini method depends on the parameter set used to predict P_{red}. Predictions with Tamanini method using the parameter set α = 1.75 and β = 0.5 and those with Eq. (100) overestimate the measured values for all P_{stat} and the slopes of the $P_{red, vd}$ curves are significantly higher than experimental ones.

The poor performance of Eq. (100) with high values of the vent opening pressure P_{stat} can be traced back to the basic assumption by Di Benedetto, Russo and Salzano (2008) that duct vented explosions are well represented by $Br_{t,\,vd}$. A corollary of this assumption is that the dependence of P_{red} on P_{stat} that is included in the value of Br_t is transferred via the value of $Br_{t,\,vd}$ to the value of $P_{red,\,vd}$. Relying on the validity of the assumption, they assume that the value of P_{stat} does not affect the ratio $Br_{t,\,vd}$ / Br_r.

From the equations of the Molkov method, it is easy to derive an equation relating $P_{red,\,vd}$ and P_{red}. The tests with unphysical predictions for $P_{red,\,vd}$ have values of P_{stat} > 0 and $Br_{t,\,vd}$ < 1. Define an auxiliary function $g(P_{stat})$ as

$$g(P_{stat}) = p_a\left(P_{stat} / p_a + 1\right)^{3/2} \tag{101}$$

The function $g(P_{stat})$ in the range $0 \le P_{stat} \le 2.5$ bar is plotted in Figure 65.

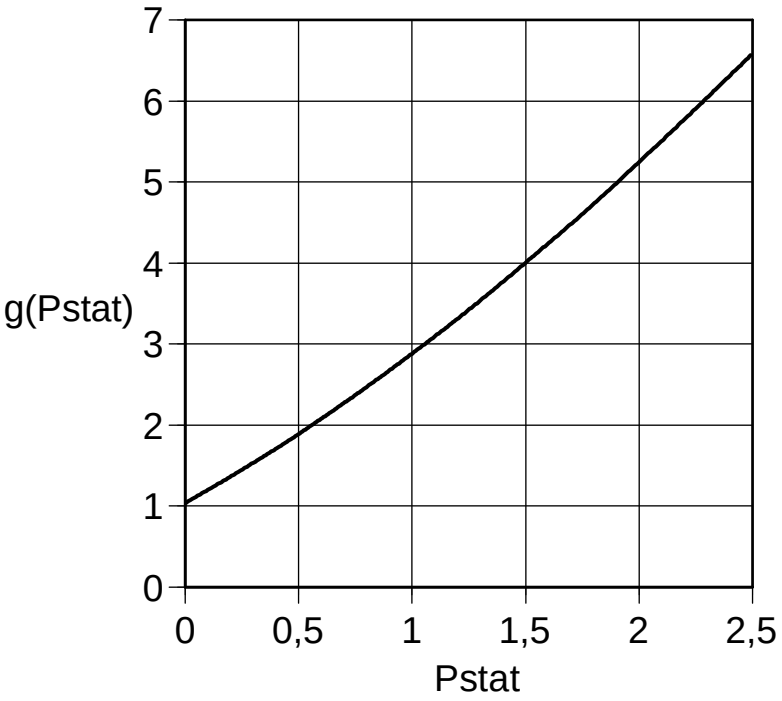

Figure 65. Function $g(P_{stat})$.

Eq. (27) can be written as

$$P_M = \frac{P_{red}}{g\left(P_{stat}\right)} \tag{102}$$

The value of Br_t can be smaller or larger than unity. When Br_t < 1, Eq. (102) is inserted in Eq. (24) and the turbulent Bradley number Br_t is solved

$$Br_t = \frac{1}{36}\left(7 - \frac{P_{red}}{g(P_{stat})}\right)^2 \tag{103}$$

According to the theory, $Br_{t,\,vd} = f \times Br_t$. The value of P_M for the ducted system $P_{M,vd}$ is found by inserting Eq. (102) in Eq. (24)

$$P_{M,vd} = 7\left(1 - f^{1/2}\right) + f^{1/2}\frac{P_{red}}{g\left(P_{stat}\right)} \tag{104}$$

Inserting $P_{M,vd} = P_{red,\,vd}/g(P_{stat})$ into Eq. (104) gives

$$P_{red,vd} = 7\left(1 - f^{1/2}\right) g\left(P_{stat}\right) + f^{1/2} P_{red} \quad (105)$$

When $Br_t > 1$, Eq. (102) is inserted in Eq. (23) and Br_t is solved

$$Br_t = \left[\frac{g\left(P_{stat}\right)}{P_{red}}\right]^{\frac{1}{2.4}} \quad (106)$$

The value of $P_{M.\,vd}$ is found by inserting Eq. (106) in Eq. (24)

$$P_{M,vd} = 7 - 6 f^{1/2} \left[\frac{g\left(P_{stat}\right)}{P_{red}}\right]^{\frac{1}{4.8}} \quad (107)$$

Inserting $P_{M,vd} = P_{red,\,vd}/g(P_{stat})$ into Eq. (107) gives

$$P_{red,vd} = g\left(P_{stat}\right)\left[7 - 6 f^{1/2}\left(\frac{g\left(P_{stat}\right)}{P_{red}}\right)^{\frac{1}{4.8}}\right] \quad (108)$$

Thus, the theory predicts that $P_{red,\,vd}$ is proportional (for $Br_t > 1$) or contains a term that is proportional (for $Br_t < 1$) to the function $g(P_{stat})$. This is the cause of the high value of the slope of $P_{red,\,vd}$ in Fig. 64 which is not found in the test data.

7 Validation of methods with predicted values of P_{red}

So far, the different methods to predict $P_{red,\,vd}$ have been validated in the same way as Di Benedetto, Russo and Salzano (2008) have done, that is, with measured values of P_{red} when available and with predicted ones for those tests where P_{red} was not measured. Although P_{red} was measured for some test configurations by Molkov et al. (1993), predicted values were used for all tests by these authors.

Although this way of mixing experimental and predicted values of P_{red} was reasonable when deriving correlations, it is somewhat questionable when validating them. This has to do with the fact that when the methods are applied to practical vent duct design problems, the value of P_{red} is not known and must be predicted.

The Molkov method has been shown to give the best predictions for P_{red} and it would be applied to practical problems. The values of P_{red} predicted with this method have been presented in Tables 40 to 42 for the tests by Kordylewski and Wach (1986, 1988), in Table 46 for the tests by McCann et al. (1985), in Table 50 for the tests by DeGood and Chatrathi (1991), and in Tables 56 to 59 for the tests by Molkov et al. (1993). In the following, the parameter set $\alpha = 0.9$ and $\beta = 1$ and the set $\alpha = 1.75$ and $\beta = 0.5$ will be called "old" and "new", respectively.

The predictions of the Bartknecht correlations are presented in Tables 76 to 79, 209, 210 and 217 to 222. Predictions of Eqs. (61) and (62) with the original selection criterion are plotted in Figures 66 and 67 and with the criterion of NFPA 68 (2007) in Figures 68 and 69. Predictions of Eqs. (69) and (70) are plotted in Figures 70 and 71. The very low predictions for the tests by McCann et al. (1985) in Table 218 are not shown in the Figures for the sake of clarity.

Table 218. Predicted $P_{red, vd}$ for the tests by McCann et al. (1985)

L_d, m	P_{red}, old	old, gas	old, dust	P_{red}, new	new, gas	new, dust	exp., bar
0.105	0.015	0.03	0.12	0.015	0.03	0.12	0.10
0.30	0.015	0.03	0.12	0.015	0.03	0.12	0.19
0.50	0.015	0.03 (0.29)	0.12	0.015	0.03 (0.29)	0.12	0.17

Table 219. Predicted $P_{red, vd}$, gas explosions, Kordylewski and Wach (1986)

%	L_d, m	P_{red}, old	old	P_{red}, new	new	exp., bar
10	2.5	0.68	0.89 (2.03)	1.77	2.03 (3.33)	0.82
12	2.5	1.71	1.97 (3.27)	2.99	3.19 (4.37)	2.38
14	2.5	2.70	2.92 (4.14)	3.86	3.97 (4.98)	2.91
16	2.5	3.44	3.59 (4.80)	4.47	4.50 (5.38)	3.47
18	2.5	4.00	4.09 (5.08)	4.90	4.87 (5.64)	4.0
20	2.5	4.30	4.36 (5.27)	5.12	5.06 (5.77)	4.3
22	2.5	4.55	4.57 (5.42)	5.30	5.22 (5.87)	4.82
25	2.5	4.77	4.76 (5.56)	5.45	5.34 (5.95)	5.0
30	2.5	4.25	4.31 (5.24)	5.08	5.03 (5.74)	0.82
20	0.04	4.30	4.36	5.12	5.06	3.68
20	0.17	4.30	4.36 (5.27)	5.12	5.06 (5.77)	3.68
20	0.3	4.30	4.36 (5.27)	5.12	5.06 (5.77)	6.71
20	0.61	4.30	4.36 (5.27)	5.12	5.06 (5.77)	6.36
20	1.26	4.30	4.36 (5.27)	5.12	5.06 (5.77)	4.57
20	2.5	4.30	4.36 (5.27)	5.12	5.06 (5.77)	4.0

Table 220. Predicted $P_{red, vd}$, gas explosions, Kordylewski and Wach (1988)

D_d, mm	L_d, m	P_{red}, old	old	P_{red}, new	new	exp., bar
35	0.16	3.08	3.27 (4.43)	4.19	4.26 (5.20)	3.0
35	0.32	3.08	3.27 (4.43)	4.19	4.26 (5.20)	4.82
35	0.54	3.08	3.27 (4.43)	4.19	4.26 (5.20)	5.65
35	0.8	3.08	3.27 (4.43)	4.19	4.26 (5.20)	4.82
35	1.4	3.08	3.27 (4.43)	4.19	4.26 (5.20)	5.13
35	1.75	3.08	3.27 (4.43)	4.19	4.26 (5.20)	5.18
35	2.8	3.08	3.27 (4.43)	4.19	4.26 (5.20)	3.0
35	3.5	3.08	4.43	4.19	5.20	4.64
35	4.91	3.08	4.43	4.19	5.20	3.57
35	6.14	3.08	4.43	4.19	5.20	3.75
35	6.75	3.08	4.43	4.19	5.20	3.39
21	2.5	4.54	4.56 (5.42)	5.30	5.22 (5.87)	5.0
25	2.5	4.10	4.18 (5.14)	4.97	4.93 (5.68)	4.73
35	2.5	3.08	3.27 (4.43)	4.19	4.26 (5.20)	4.2

Table 221. Predicted $P_{red, vd}$, dust explosions, Kordylewski and Wach (1986)

%	L_d, m	P_{red}, old	old	P_{red}, new	new	exp., bar
10	2.5	0.68	1.43	1.77	2.67	0.82
12	2.5	1.71	2.61	2.99	3.77	2.38
14	2.5	2.70	3.52	3.86	4.53	2.91
16	2.5	3.44	4.13	4.47	4.90	3.47
18	2.5	4.00	4.56	4.90	5.20	4.0
20	2.5	4.30	4.78	5.12	5.35	4.3
22	2.5	4.55	4.96	5.30	5.48	4.82
25	2.5	4.77	5.11	5.45	5.58	5.0
30	2.5	4.25	4.74	5.08	5.33	0.82
20	0.04	4.30	4.78	5.12	5.31	3.68
20	0.17	4.30	4.78	5.12	5.31	3.68
20	0.3	4.30	4.78	5.12	5.31	6.71
20	0.61	4.30	4.78	5.12	5.31	6.36
20	1.26	4.30	4.78	5.12	5.31	4.57
20	2.5	4.30	4.78	5.12	5.31	4.0

Table 222. Predicted $P_{red, vd}$, dust explosions, Kordylewski and Wach (1988)

D_d, mm	L_d, m	P_{red}, old	old, dust	P_{red}, new	new, dust	exp., bar
35	0.16	3.08	3.99	4.19	4.70	3.0
35	0.32	3.08	3.99	4.19	4.70	4.82
35	0.54	3.08	3.99	4.19	4.70	5.65
35	0.8	3.08	3.99	4.19	4.70	4.82
35	1.4	3.08	3.99	4.19	4.70	5.13
35	1.75	3.08	3.99	4.19	4.70	5.18
35	2.8	3.08	3.99	4.19	4.70	3.0
35	3.5	3.08	5.28	4.19	5.95	4.64
35	4.91	3.08	5.28	4.19	5.95	3.57
35	6.14	3.08	5.28	4.19	5.95	3.75
35	6.75	3.08	5.28	4.19	5.95	3.39
21	2.5	4.54	4.95	5.30	5.48	5.0
25	2.5	4.10	4.63	4.97	5.25	4.73
35	2.5	3.08	3.84	4.19	4.75	4.2

Table 223. Predicted $P_{red, vd}$ for the tests by DeGood and Chatrathi (1991)

ign.	L_d, m	P_{red}, old	old, gas	old, dust	P_{red}, new	new, gas	new, dust	exp., bar
c	1	0.063	0.12	0.30	0.060	0.11	0.29	0.185
c	2	0.063	0.12	0.30	0.060	0.11	0.29	0.300
c	3	0.063	0.12 (0.60)	0.30	0.060	0.11 (0.58)	0.29	0.385
b	3	0.063	0.12 (0.60)	0.30	0.060	0.11 (0.58)	0.29	1.01

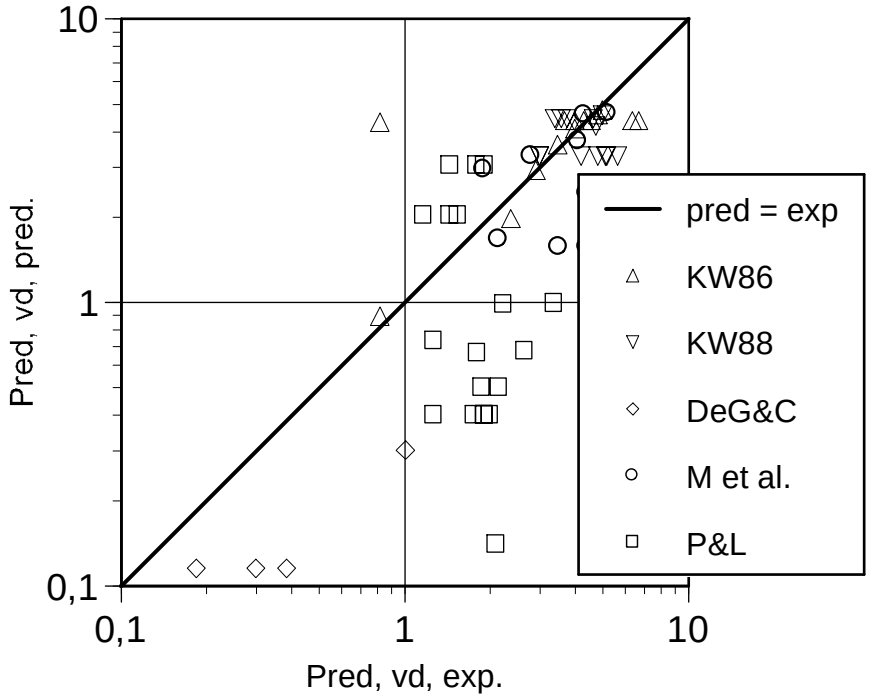

Figure 66. Experimental values of $P_{red,\,vd}$ compared with those predicted with Eqs. (61) and (62) with the original selection criterion. All values of P_{red} were predicted with $\alpha = 0.9$ and $\beta = 1$.

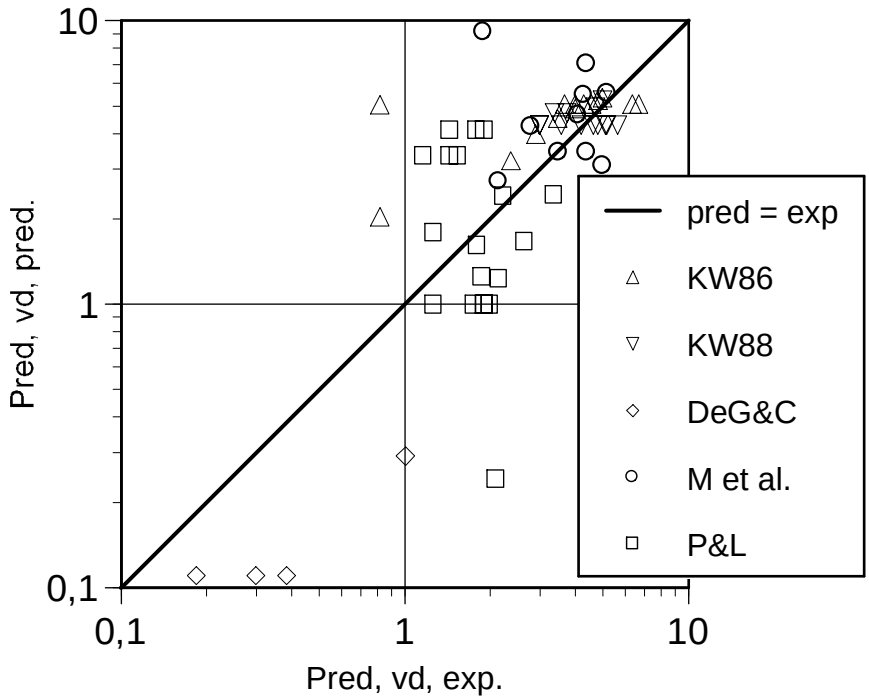

Figure 67. Experimental values of $P_{red,\,vd}$ compared with those predicted with Eqs. (61) and (62) with the original selection criterion. All values of P_{red} were predicted with $\alpha = 1.75$ and $\beta = 0.5$.

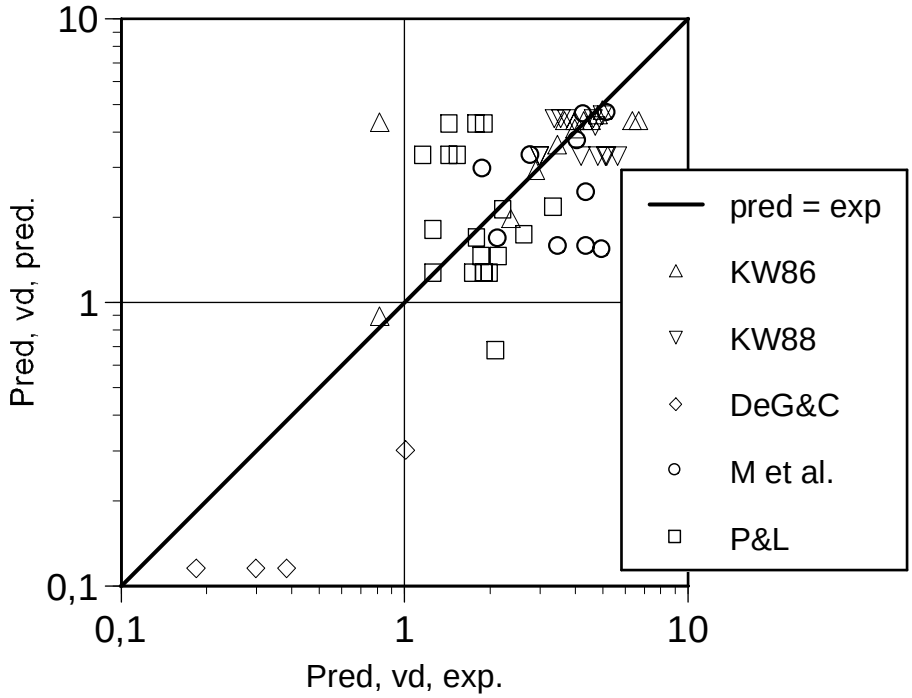

Figure 68. Experimental values of $P_{red,\,vd}$ compared with those predicted with Eqs. (61) and (62) with the criterion of NFPA 68 (2007). All values of P_{red} were predicted with $\alpha = 0.9$ and $\beta = 1$.

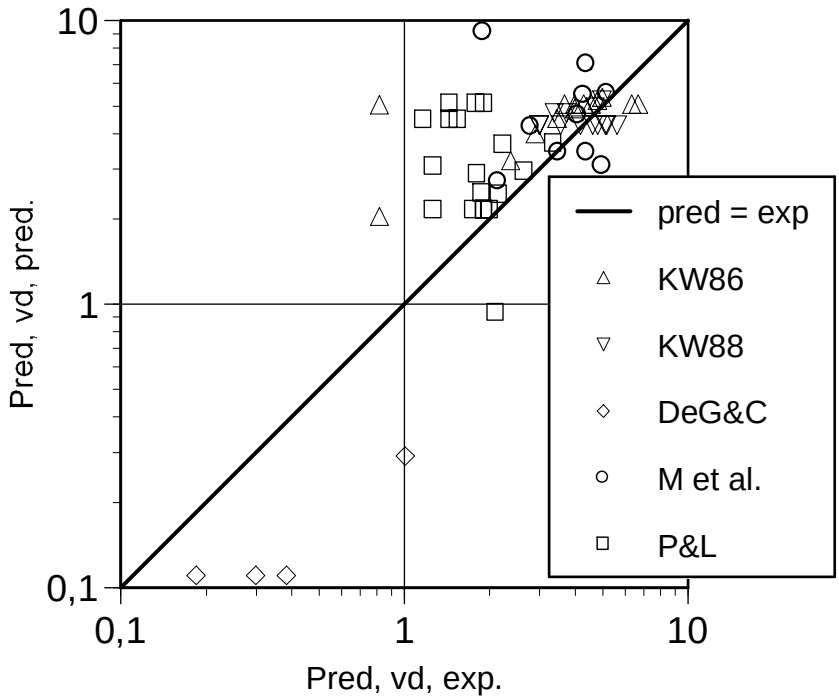

Figure 69. Experimental values of $P_{red,\,vd}$ compared with those predicted with Eqs. (61) and (62) with the criterion of NFPA 68 (2007). All values of P_{red} were predicted with $\alpha = 1.75$ and $\beta = 0.5$.

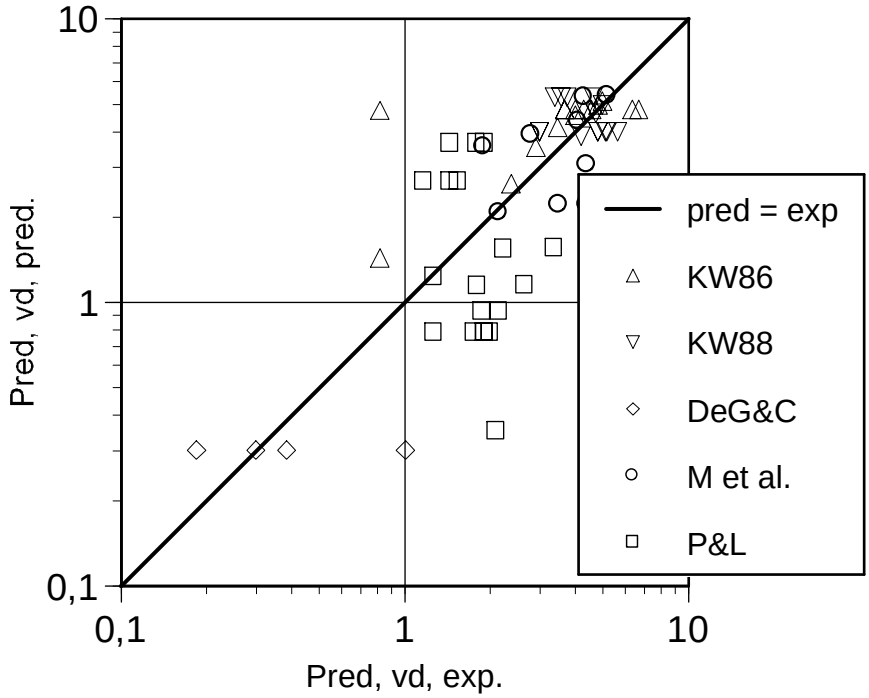

Figure 70. Experimental values of $P_{red,\,vd}$ compared with those predicted with Eqs. (69) and (70). All values of P_{red} were predicted with $\alpha = 0.9$ and $\beta = 1$.

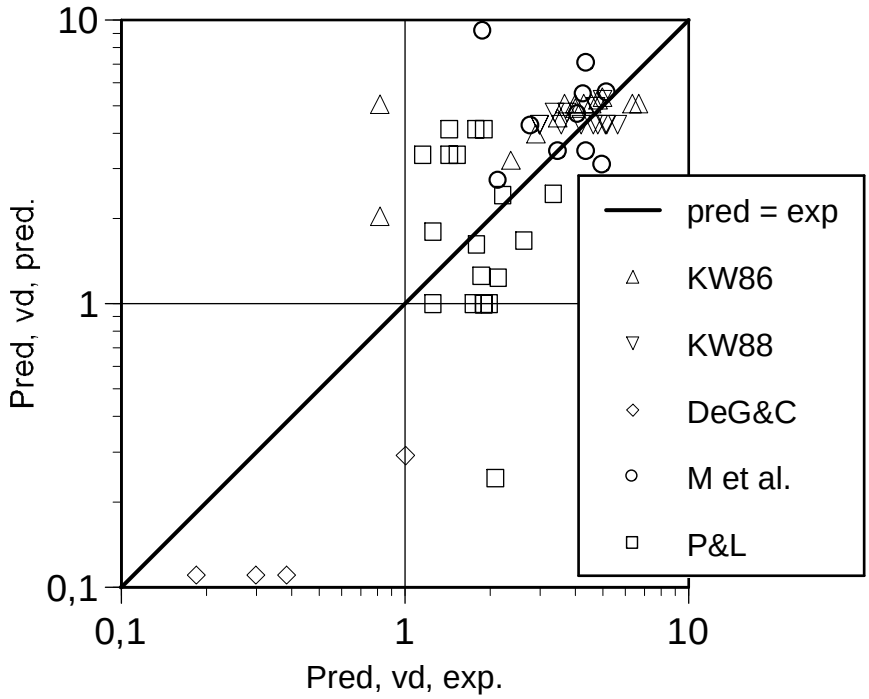

Figure 71. Experimental values of $P_{red,\,vd}$ compared with those predicted with Eqs. (69) and (70). All values of P_{red} were predicted with $\alpha = 1.75$ and $\beta = 0.5$.

The values of relative error in Tables 217 to 222 are presented in Table 224.

Table 224. Relative errors of the predictions, Bartknecht correlations

method	tests	$\alpha = 0.9, \beta = 1$	$\alpha = 1.75, \beta = 0.5$
gas exposions			
K & W	29	21.0 % (28.0 %)	29.0 % (39.5 %)
the others	7	15.0 % (12.0 %)	15.0 % (12.0 %)
M et al.	10	27.5 % (27.5 %)	44.0 % (44.0 %)
P & L	19	44.5 % (40.5 %)	44.0 % (56.0 %)
together	65	28.0 % (30.0 %)	34.0 % (42.0 %)
dust explosions			
K & W	29	25.0 %	35.5 %
the others	7	9.0 %	12.0 %
M et al.	10	25.5 %	47.5 %
P & L	19	42.5 %	45.0 %
together	65	28.5 %	37.5 %

The predictions of the VDI 3673 method are presented in Tables 90 to 93, 210, 212 and 224 to 227 and plotted in Figures 72 and 73. The very low predictions for the tests by McCann et al. (1985) in Table 225 are not shown in the Figures for the sake of clarity.

Table 225. Predicted $P_{red, vd}$ for the tests by McCann et al. (1985)

L_d, m	P_{red}, old, bar	$P_{red, vd}$, old, bar	P_{red}, new, bar	$P_{red, vd}$, new, bar	exp., bar
0.105	0.0153	0.024	0.0154	0.024	0.10
0.30	0.0153	0.040	0.0154	0.040	0.19
0.50	0.0153	0.056	0.0154	0.057	0.17

Table 226. Predicted $P_{red, vd}$ for the tests by Kordylewski and Wach (1986)

%	L_d, m	P_{red}, old, bar	$P_{red, vd}$, old, bar	P_{red}, new, bar	$P_{red, vd}$, new, bar	exp., bar
10	2.5	0.68	0.70	1.77	1.81	0.82
12	2.5	1.71	1.75	2.99	3.06	2.38
14	2.5	2.70	2.77	3.86	3.95	2.91
16	2.5	3.44	3.52	4.47	4.58	3.47
18	2.5	4.00	4.10	4.90	5.02	4.0
20	2.5	4.30	4.41	5.12	5.24*	4.3
22	2.5	4.55	4.66	5.30	5.43*	4.82
25	2.5	4.77	4.89	5.45	5.58*	5.0
30	2.5	4.25	4.35	5.08	5.20	0.82
20	0.04	4.30	4.30	5.12	5.12	3.68
20	0.17	4.30	4.31	5.12	5.13	3.68
20	0.3	4.30	4.31	5.12	5.14	6.71
20	0.61	4.30	4.33	5.12	5.15	6.36
20	1.26	4.30	4.35	5.12	5.18	4.57
20	2.5	4.30	4.41	5.12	5.24*	4.0

Table 227. Predicted $P_{red, vd}$ for the tests by Kordylewski and Wach (1988)

D_d, mm	L_d, m	P_{red}, old, bar	$P_{red, vd}$, old, bar	P_{red}, new, bar	$P_{red, vd}$, new, bar	exp., bar
35	0.16	3.08	3.09	4.19	4.21	3.0
35	0.32	3.08	3.11	4.19	4.22	4.82
35	0.54	3.08	3.12	4.19	4.25	5.65
35	0.8	3.08	3.14	4.19	4.28	4.82
35	1.4	3.08	3.19	4.19	4.34	5.13
35	1.75	3.08	3.22	4.19	4.38	5.18
35	2.8	3.08	3.30	4.19	4.48*	3.0
35	3.5	3.08	3.32*	4.19	4.48*	4.64
35	4.91	3.08	3.32*	4.19	4.48*	3.57
35	6.14	3.08	3.32*	4.19	4.48*	3.75
35	6.75	3.08	3.32*	4.19	4.48*	3.39
21	2.5	4.54	4.56	5.30	5.33*	5.0
25	2.5	4.10	4.14	4.97	5.01	4.73
35	2.5	3.08	3.16	4.19	4.30	4.2

Table 228. Predicted $P_{red, vd}$ for the tests by DeGood and Chatrathi (1991)

ignition	L_d, m	P_{red}, old, bar	$P_{red, vd}$, old, bar	P_{red}, new, bar	$P_{red, vd}$, new, bar	exp., bar
centre	1	0.063	0.17	0.060	0.16	0.185
centre	2	0.063	0.27	0.060	0.26	0.300
centre	3	0.063	0.37	0.060	0.36	0.385
bottom	3	0.063	0.37	0.060	0.36	1.01

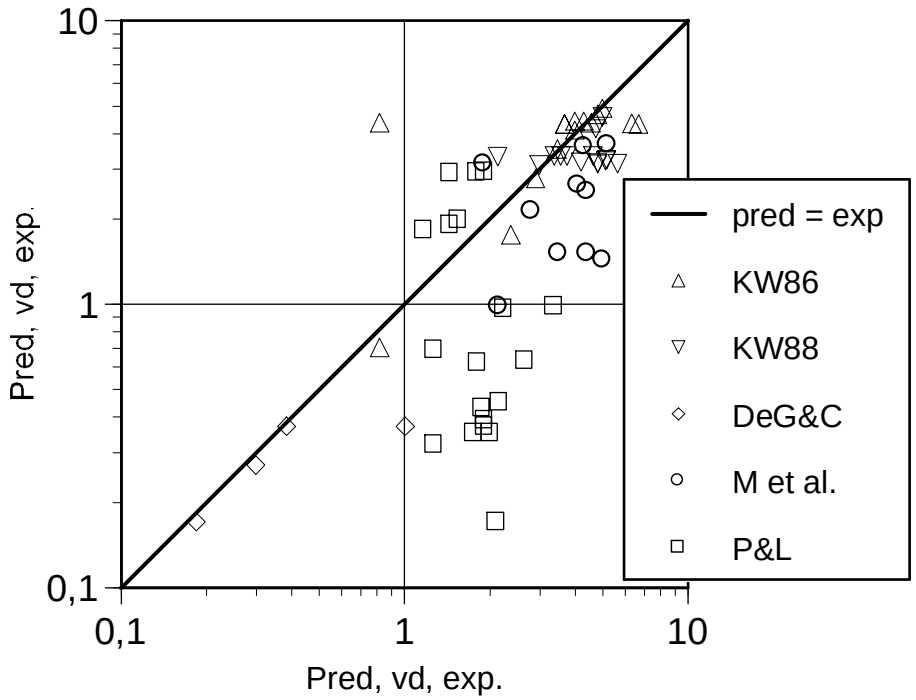

Figure 72. Experimental values of $P_{red, vd}$ compared with those predicted with Eqs. (47) and (48). All values of P_{red} were predicted with $\alpha = 0.9$ and $\beta = 1$.

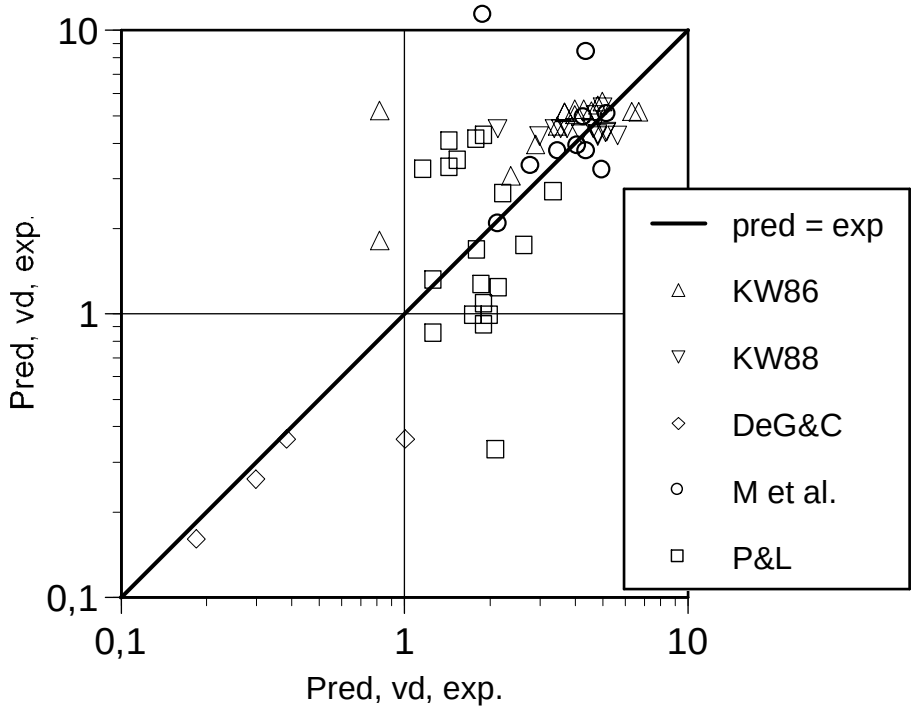

Figure 73. Experimental values of $P_{red,\,vd}$ compared with those predicted with Eqs. (47) and (48). All values of P_{red} were predicted with $\alpha = 1.75$ and $\beta = 0.5$.

Table 229. Relative errors of the predictions, VDI 3673

reference	tests	$\alpha = 0.9$, $\beta = 1$	$\alpha = 1.75$, $\beta = 0.5$
K & W	29	21.0 %	27.5 %
the others	7	9.5 %	9.5 %
M et al.	10	35.5 %	47.5 %
P & L	19	44.0 %	43.0 %
together	65	28.5 %	33.5 %

The predictions of the EN 14491 method are presented in Tables 110 to 113, 213, 214, and 229 to 232 and plotted in Figures 74 and 75. The very low predictions for the tests by McCann et al. (1985) in Table 230 are not shown in the Figures for the sake of clarity.

Table 230. Predicted $P_{red,\,vd}$ for the tests by McCann et al. (1985)

L_d, m	P_{red}, old, bar	$P_{red,\,vd}$, old, bar	P_{red}, new, bar	$P_{red,\,vd}$, new, bar	exp., bar
0.105	0.0153	0.09	0.0154	0.09	0.10
0.30	0.0153	0.23	0.0154	0.23	0.19
0.50	0.0153	0.38	0.0154	0.38	0.17

Table 231. Predicted $P_{red, vd}$ for the tests by Kordylewski and Wach (1986)

%	L_d, m	P_{red}, old, bar	$P_{red, vd}$, old, bar	P_{red}, new, bar	$P_{red, vd}$, new, bar	exp., bar
10	2.5	0.68	0.72*	1.77	1.83*	0.82
12	2.5	1.71	1.77*	2.99	3.08*	2.38
14	2.5	2.70	2.78*	3.86	3.96*	2.91
16	2.5	3.44	3.54*	4.47	4.58*	3.47
18	2.5	4.00	4.11*	4.90	5.02*	4.0
20	2.5	4.30	4.41*	5.12	5.24*	4.3
22	2.5	4.55	4.67*	5.30	5.43*	4.82
25	2.5	4.77	4.89*	5.45	5.58*	5.0
30	2.5	4.25	4.36*	5.08	5.20*	0.82
20	0.04	4.30	4.37	5.12	5.20	3.68
20	0.17	4.30	4.41*	5.12	5.24*	3.68
20	0.3	4.30	4.41*	5.12	5.24*	6.71
20	0.61	4.30	4.41*	5.12	5.24*	6.36
20	1.26	4.30	4.41*	5.12	5.24*	4.57
20	2.5	4.30	4.41*	5.12	5.24*	4.0

Table 232. Predicted $P_{red, vd}$ for the tests by Kordylewski and Wach (1988)

D_d, mm	L_d, m	P_{red}, old, bar	$P_{red, vd}$, old, bar	P_{red}, new, bar	$P_{red, vd}$, new, bar	exp., bar
35	0.16	3.08	3.32*	4.19	4.48*	3.0
35	0.32	3.08	3.32*	4.19	4.48*	4.82
35	0.54	3.08	3.32*	4.19	4.48*	5.65
35	0.8	3.08	3.32*	4.19	4.48*	4.82
35	1.4	3.08	3.32*	4.19	4.48*	5.13
35	1.75	3.08	3.32*	4.19	4.48*	5.18
35	2.8	3.08	3.32*	4.19	4.48*	3.0
35	3.5	3.08	3.32*	4.19	4.48*	4.64
35	4.91	3.08	3.32*	4.19	4.48*	3.57
35	6.14	3.08	3.32*	4.19	4.48*	3.75
35	6.75	3.08	3.32*	4.19	4.48*	3.39
21	2.5	4.54	4.60*	5.30	5.37*	5.0
25	2.5	4.10	4.20*	4.97	5.08*	4.73
35	2.5	3.08	3.32*	4.19	4.48*	4.2

Table 233. Predicted $P_{red, vd}$ for the tests by DeGood and Chatrathi (1991)

ignition	L_d, m	P_{red}, old, bar	$P_{red, vd}$, old, bar	P_{red}, new, bar	$P_{red, vd}$, new, bar	exp., bar
centre	1	0.063	0.18	0.060	0.17	0.185
centre	2	0.063	0.29	0.060	0.28	0.300
centre	3	0.063	0.41	0.060	0.39	0.385
bottom	3	0.063	0.41	0.060	0.39	1.01

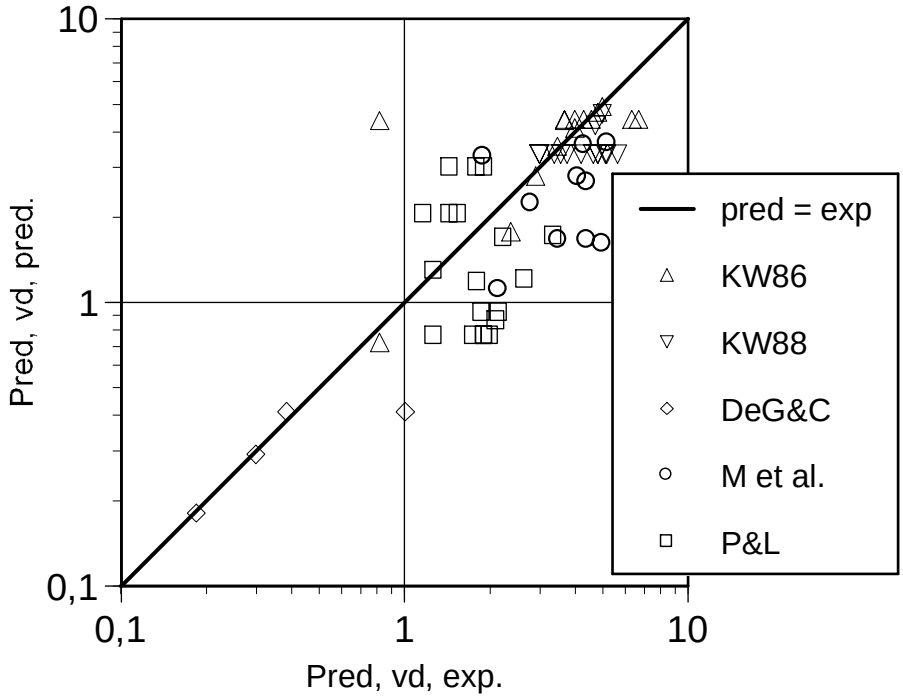

Figure 74. Experimental values of $P_{red,\,vd}$ compared with those predicted with Eqs. (50) and (51). All values of P_{red} were predicted with $\alpha = 0.9$ and $\beta = 1$.

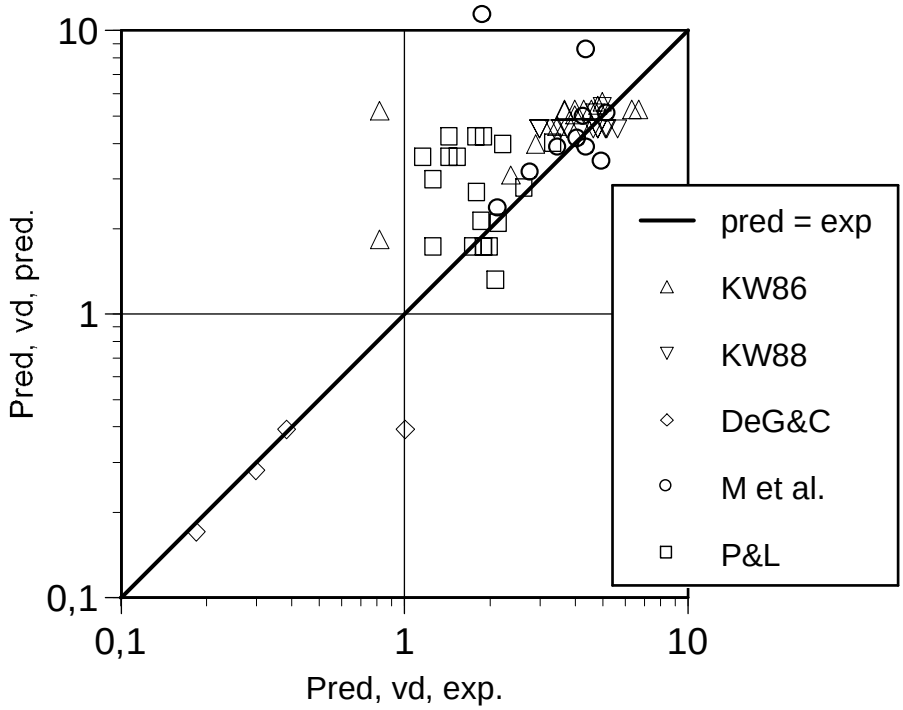

Figure 75. Experimental values of $P_{red,\,vd}$ compared with those predicted with Eqs. (50) and (51). All values of P_{red} were predicted with $\alpha = 1.75$ and $\beta = 0.5$.

Table 234. Relative errors of the predictions, EN 14491

reference	tests	$\alpha = 0.9$, $\beta = 1$	$\alpha = 1.75$, $\beta = 0.5$
K & W	29	20.5 %	27.5 %
the others	7	8.0 %	8.0 %
M et al.	10	34.0 %	48.0 %
P & L	19	33.5 %	42.0 %
together	65	25.0 %	33.0 %

The predictions of Eq. (100) are presented in Tables 203 to 208, and 235 to 238 and plotted in Figures 76 and 77. The very low predictions for the tests by McCann et al. (1985) in Table 235 are not shown in the Figures for the sake of clarity.

Table 235. Predicted $P_{red, vd}$ for the tests by McCann et al. (1985)

L_d, m	f	P_{red}, old, bar	$P_{red, vd}$, old, bar	P_{red}, new, bar	$P_{red, vd}$, new, bar	exp., bar
0.105	10.45	0.0153	0.004	0.0154	0.004	0.10
0.30	6.19	0.0153	0.013	0.0154	0.013	0.19
0.50	4.77	0.0153	0.024	0.0154	0.024	0.17

Table 236. Predicted $P_{red, vd}$ for the tests by Kordylewski and Wach (1986)

%	L_d, m	f	P_{red}, old, bar	$P_{red, vd}$, old, bar	P_{red}, new, bar	$P_{red, vd}$, new, bar	exp., bar
10	2.5	0.203	0.68	4.13	1.77	4.45	0.82
12	2.5	0.190	1.71	4.75	2.99	5.52	2.38
14	2.5	0.180	2.70	5.23	3.86	5.73	2.91
16	2.5	0.171	3.44	5.59	4.47	6.01	3.47
18	2.5	0.165	4.00	5.81	4.90	6.18	4.0
20	2.5	0.160	4.30	5.98	5.12	6.31	4.3
22	2.5	0.158	4.55	6.09	5.30	6.38	4.82
25	2.5	0.155	4.77	6.17	5.45	6.45	5.0
30	2.5	0.162	4.25	5.95	5.08	6.28	0.82
20	0.04	1.553	4.30	3.64	5.12	4.65	3.68
20	0.17	0.754	4.30	4.68	5.12	5.39	3.68
20	0.3	0.567	4.30	5.00	5.12	5.62	6.71
20	0.61	0.398	4.30	5.34	5.12	5.85	6.36
20	1.26	0.226	4.30	5.76	5.12	6.16	4.57
20	2.5	0.161	4.30	5.98	5.12	6.30	4.0

Table 237. Predicted $P_{red, vd}$ for the tests by Kordylewski and Wach (1988)

D_d, mm	L_d, m	f	P_{red}, old, bar	$P_{red, vd}$, old, bar	P_{red}, new, bar	$P_{red, vd}$, new, bar	exp., bar
35	0.16	0.768	3.08	3.52	4.19	4.50	3.0
35	0.32	0.543	3.08	4.09	4.19	4.91	4.82
35	0.54	0.418	3.08	4.45	4.19	5.18	5.65
35	0.8	0.344	3.08	4.70	4.19	5.36	4.82
35	1.4	0.260	3.08	5.01	4.19	5.58	5.13
35	1.75	0.232	3.08	5.13	4.19	5.67	5.18
35	2.8	0.184	3.08	5.34	4.19	5.82	3.0
35	3.5	0.164	3.08	5.44	4.19	5.89	4.64
35	4.91	0.139	3.08	5.57	4.19	5.99	3.57
35	6.14	0.124	3.08	5.66	4.19	6.05	3.75
35	6.75	0.118	3.08	5.69	4.19	6.07	3.39
21	2.5	0.151	4.54	6.08	5.30	6.38	5.0
25	2.5	0.162	4.10	5.87	4.97	6.22	4.73
35	2.5	0.194	3.08	5.30	4.19	5.79	4.2

Table 238. Predicted $P_{red, vd}$ for the tests by DeGood and Chatrathi (1991)

ignition	L_d, m	f	P_{red}, old, bar	$P_{red, vd}$, old, bar	P_{red}, new, bar	$P_{red, vd}$, new, bar	exp., bar
centre	1	1.352	0.063	0.06	0.060	0.07	0.185
centre	2	0.956	0.063	0.14	0.060	0.17	0.300
centre	3	0.780	0.063	0.23	0.060	0.28	0.385
bottom	3	0.780	0.063	0.23	0.060	0.28	1.01

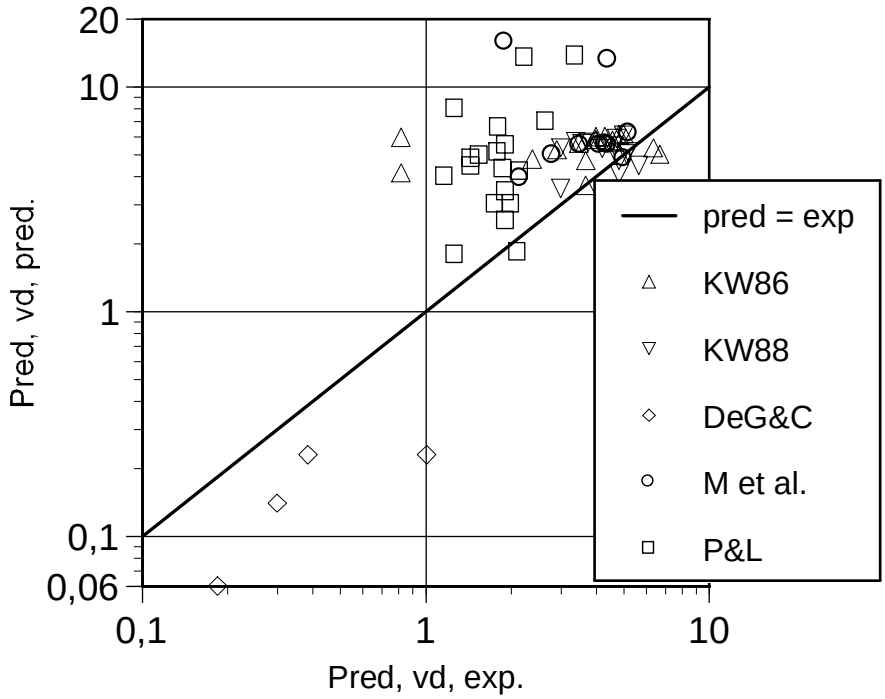

Figure 76. Experimental values of $P_{red, vd}$ compared with those predicted with Eq. (100). All values of P_{red} were predicted with $\alpha = 0.9$ and $\beta = 1$.

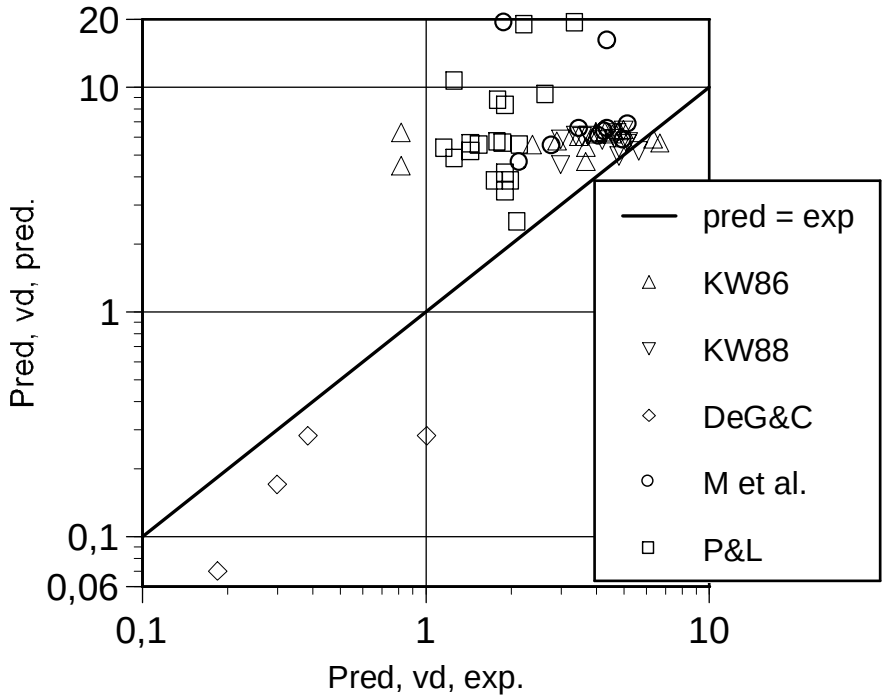

Figure 77. Experimental values of $P_{red, vd}$ compared with those predicted with Eq. (100). All values of P_{red} were predicted with $\alpha = 1.75$ and $\beta = 0.5$.

Table 239. Relative errors of the predictions, Eq. (100)

reference	tests	$\alpha = 0.9, \beta = 1$	$\alpha = 1.75, \beta = 0.5$
K & W	29	42.0 %	50.0 %
the others	7	15.5 %	14.0 %
M et al.	10	89.0 %	117.5 %
P & L	19	118.5 %	177.5 %
together	65	69.0 %	94.0 %

In Table 240, the relative errors of $P_{red,\,vd}$ calculated with predicted values of P_{red} are compared with those of Table 216 calculated with experimental and predicted values of P_{red}. It is seen that the use of only predicted values of P_{red} reduces the relative errors significantly for the methods of VDI 3673 and EN 14491. On the other hand, the already large relative errors of Eq. (100) are still increased when only predicted values of P_{red} are used. It is remarkable that with all the methods the use of the parameter set $\alpha = 0.9$, $\beta = 1$ to predict P_{red} leads to lower relative errors in $P_{red,\,vd}$ than the parameter set $\alpha = 1.75$, $\beta = 0.5$.

Table 240. Relative errors of the predictions

method	P_{red} exp. & pred.	P_{red} pred.
gas explosions		
Bartknecht	29.5 % (32.5 %)	27.5 % (34.5 %)
NFPA 68 (2007)	26.0 % (32.0 %)	30.0 % (42.0 %)
dust explosions		
Bartknecht	28.0 % (32.0 %)	28.5 % (37.5 %)
VDI 3673	33.0 % (36.0 %)	28.5 % (33.5 %)
EN 14491	35.0 % (42.5 %)	25.0 % (33.0 %)
Tamanini	—	35.5 % (76.5 %)
NFPA 68 (2007)	—	39.5 %
Eq. (91)	27.5 %	27.5 %
Eq. (100)	64.0 % (83.5 %)	69.0 % (94.0 %)

8 Proposed new method

Yao correlation for P_{red} Eq. (76) was derived assuming subcritical flow i.e. $P_{red} < 0.69$ bar and a constant C_d, and neglecting any dependence of P_{stat} on P_{red} and $P_{red,\,vd}$. Nevertheless, Table 240 shows that the extended Yao correlation with parameters found by minimising the relative error Eq. (91) is able to predict the test data equally well as the methods of Bartknecht and Siwek (VDI 3673 and EN 14491).

On the contrary, the extended Molkov method Eq. (100) produces significantly poorer predictions than any of the existing methods. This was shown to result from the use of Eq. (25) to include P_{stat} in Br_t and, consequently, in $Br_{t,vd}$. This problem, however, can be avoided by returning to an earlier version of the Molkov method where $P_M = P_{red}/p_0$ or $P_{red,\,vd}/p_0$. As mentioned in Sec. 3.5, the set of Eqs. (20) to (24) has the drawback that P_{red} decreases with increasing P_{stat}. This unphysical feature of the model, however, can be amended by complementing Eq. (99) with another term: the scaled absolute vent opening pressure (with an open vent, the added term is unity)

$$\frac{Br_{t,vd}}{Br_t} = \frac{(\chi/\mu)}{(\chi/\mu)_{vd}} = k\,\mathrm{Re}_f^{\,l}\left(\frac{P_m}{p_0}\right)^m\left(\frac{L_d}{D_d}\right)^n\left(\frac{p_{stat}}{p_0}\right)^o \qquad (109)$$

Values of the parameters in Eq. (109) are found in the same way as those of Eq. (99). First, for those tests where P_{red} was measured, the experimental values are inserted in Eqs. (23) or (24) and the corresponding values of Br_t are solved. For the tests by Molkov et al. (1993) and Ponizy and Leyer (1999a, 1999b), the values of Br_t are predicted with Eqs. (20) to (22) using both parameter sets: $\alpha = 0.9$, $\beta = 1$ (old) and $\alpha = 1.75$ and $\beta = 0.5$ (new). The experimental values of $P_{red,\,vd}$ are inserted in Eqs. (23) or (24) and the corresponding values of $Br_{t,\,vd}$ are solved.

The experimental values of $Br_{t,\,vd}/Br_t$ for the tests with $P_{stat} = 0$ by McCann et al. (1985), and Kordylewski and Wach (1986, 1988) are taken from Tables 186 to 189. The values of $Br_{t,\,vd}/Br_t$ for the tests with $P_{stat} = 0.1$ bar by DeGood and Chatrathi (1991) are calculated in Table 241. The values for the tests by Molkov et al. (1993) and Ponizy and Leyer (1999a, 1999b) are calculated in Tables 241 to 243.

Table 241. Experimental $Br_{t,\,vd}/Br_t$ for the tests by DeGood and Chatrathi (1991)

ignition	$P_{red,\,vd}$, bar	$Br_{t,\,vd}$	P_{red}, bar	Br_t	$Br_{t,vd}/Br_t$
centre	0.185	2.031	0.20	2.08	0.974
centre	0.300	1.660	0.20	2.08	0.796
centre	0.385	1.496	0.20	2.08	0.718
back	1.01	1.001	0.15	2.35	0.426

Table 242. Experimental $Br_{t,\,vd}/Br_t$ for the tests by Molkov et al. (1993)

V, m^3	L_d, m	$P_{red,\,vd}$, bar	$Br_{t,\,vd}$	Br_t, old	$Br_{t,vd}/Br_t$, old	Br_t, new	$Br_{t,vd}/Br_t$, new
0.027	1.83	5.0†	0.118	1.073	0.110	0.642	0.184
0.027	2.35	4.4	0.196	1.024	0.191	0.605	0.324
0.027	2.35	3.5	0.349	1.024	0.341	0.605	0.577
0.027	2.35	1.9	0.729	1.209	0.603	0.711	1.026
0.027	1.83	4.4†	0.196	1.178	0.166	0.693	0.283
2	4	4.3	0.211	0.520	0.406	0.297	0.710
2	10	5.2	0.097	0.508	0.191	0.289	0.335
2	10	2.15	0.661	1.384	0.477	1.019	0.649
10	25	4.1	0.242	0.733	0.330	0.475	0.510
10	25	2.8	0.498	0.817	0.610	0.547	0.911

Table 243. Experimental $Br_{t,vd}/Br_t$ for the tests by Ponizy & Leyer (1999a)

D_d, mm	L_d, m	$P_{red,vd}$, bar	$Br_{t,vd}$	Br_t, old	$Br_{t,vd}/Br_t$, old	Br_t, new	$Br_{t,vd}/Br_t$, new
16	0.6	1.45	0.861	0.496	1.74	0.260	3.31
21	0.6	1.17	0.949	0.781	1.22	0.429	2.21
36	0.6	1.27	0.917	1.74	0.526	1.14	0.807
16	1.1	1.80	0.758	0.496	1.53	0.260	2.92
21	1.1	1.45	0.861	0.781	1.10	0.429	2.01
36	1.1	1.92	0.724	1.74	0.415	1.14	0.637
16	2.6	1.92	0.724	0.496	1.46	0.260	2.78
21	2.6	1.55	0.831	0.781	1.06	0.429	1.94
36	2.6	1.92	0.724	1.74	0.415	1.14	0.637
53	2.6	2.11	0.672	2.94	0.229	2.24	0.299

Table 244. Experimental $Br_{t,vd}/Br_t$ for the tests Ponizy & Leyer (1999b)

ignition	P_{stat}, bar	$P_{red,vd}$, bar	$Br_{t,vd}$	Br_t, old	$Br_{t,vd}/Br_t$, old	Br_t, new	$Br_{t,vd}/Br_t$, new
centre	0	2.01	0.699	1,74	0.401	1.14	0.615
centre	0.3	2.16	0.658	1,84	0.357	1.20	0.543
centre	0.91	2.66	0.532	2,02	0.263	1.32	0.403
centre	2.3	3.37	0.375	2,36	0.159	1.54	0.244
rear	0	1.76	0.769	1,74	0.441	1.14	0.677
rear	0.32	1.88	0.735	1,85	0.398	1.20	0.610
rear	0.83	1.81	0.755	2,00	0.377	1.30	0.579
near vent	1.11	1.27	0.917	2,08	0.442	1.35	0.678
near vent	2.24	2.24	0.637	2,35	0.271	1.53	0.416

Parameters of Eq. (109) were fitted to the experimental values of $Br_{t,vd}/Br_t$ in Tables 186 to 189 and 240 to 243 using the values of Re_f, P_m, L_d/D_d and p_{stat}/p_0 given in Tables 244 to 250. When the values of P_{red} were predicted with the parameter set $\alpha = 0.9$, $\beta = 1$ (old) and the average error of $Br_{t,vd}/Br_t$ was minimised, the result was

$$\frac{Br_{t,vd}}{Br_t} = 0.646\,\mathrm{Re}_f^{-0.011}\left(\frac{P_m}{p_0}\right)^{0.254}\left(\frac{L_d}{D_d}\right)^{-0.144}\left(\frac{p_{stat}}{p_0}\right)^{-1.232} \qquad (110)$$

with the relative error of $P_{red,vd}$ equal to 26.0 %. When the relative error of $P_{red,vd}$ was minimised the result was

$$\frac{Br_{t,vd}}{Br_t} = 1.027\,\mathrm{Re}_f^{0.081}\left(\frac{P_m}{p_0}\right)^{-0.479}\left(\frac{L_d}{D_d}\right)^{-0.079}\left(\frac{p_{stat}}{p_0}\right)^{-0.500} \qquad (111)$$

with the relative error of $P_{red,vd}$ equal to 24.0 %.

When the values of P_{red} were predicted with the parameter set $\alpha = 1.75$, $\beta = 0.5$ (new) and the average error of $Br_{t,vd}/Br_t$ was minimised, the result was

$$\frac{Br_{t,vd}}{Br_t} = 0.497\,\mathrm{Re}_f^{-0.030}\left(\frac{P_m}{p_0}\right)^{0.432}\left(\frac{L_d}{D_d}\right)^{-0.098}\left(\frac{p_{stat}}{p_0}\right)^{-0.417} \qquad (112)$$

with the relative error of $P_{red,vd}$ equal to 24.5 %. When the relative error of $P_{red,vd}$ was minimised the result was

$$\frac{Br_{t,vd}}{Br_t} = 0.497\,\mathrm{Re}_f^{-0.030}\left(\frac{P_m}{p_0}\right)^{0.432}\left(\frac{L_d}{D_d}\right)^{-0.098}\left(\frac{p_{stat}}{p_0}\right)^{-0.417} \quad (113)$$

with the relative error of $P_{red,\,vd}$ equal to 24.5 %. The values of $P_{red,\,vd}$ predicted with Eqs. (111) and (113) are given in Tables 245 to 251 and plotted in Figures 78 and 79.

Table 245. Predicted $P_{red,\,vd}$ for the tests by McCann et al. (1985)

L_d, m	Re_f	P_m, bar	L_d/D_d	p_{stat}/p_0	$P_{red,\,vd}$, old	$P_{red,\,vd}$, new	exp., bar
0.3	4470	7.1	2.66	1.08	0.18	0.14	0.10
2.13	4470	7.1	18.9	1.08	0.26	0.22	0.19
12.2	4470	7.1	108	1.08	0.36	0.33	0.17

Table 246. Predicted $P_{red,\,vd}$ for the tests by Kordylewski and Wach (1986)

C, %	Re_f	P_m, bar	L_d/D_d	p_{stat}/p_0	$P_{red,\,vd}$, old	$P_{red,\,vd}$, new	exp., bar
12	245	5.64	100	1	2.17	1.81	2.38
14	392	6.33	100	1	3.35	2.97	2.91
16	588	6.89	100	1	3.92	3.54	3.47
18	833	7.29	100	1	4.54	4.22	4.0
20	1046	7.44	100	1	4.67	4.37	4.3
22	1307	7.45	100	1	5.07	4.85	4.82
25	1634	7.1	100	1	5.03	4.88	5.0
30	1146	6.38	100	1	3.12	2.96	0.82
20	1046	7.44	1.6	1	4.32	3.85	3.68
20	1046	7.44	6.8	1	4.47	4.08	3.68
20	1046	7.44	12	1	4.53	4.16	6.71
20	1046	7.44	24.4	1	4.60	4.26	6.36
20	1046	7.44	50.4	1	4.67	4.36	4.57
20	1046	7.44	100	1	4.74	4.45	4.0

Table 247. Predicted $P_{red,\,vd}$ for the tests by Kordylewski and Wach (1988)

L_d, m	Re_f	P_m, bar	L_d/D_d	p_{stat}/p_0	$P_{red,\,vd}$, old	$P_{red,\,vd}$, new	exp., bar
0.16	1167	7.29	4.6	1	3.06	2.50	3.0
0.32	1167	7.29	9.1	1	3.17	2.65	4.82
0.54	1167	7.29	15.4	1	3.25	2.76	5.65
0.8	1167	7.29	22.9	1	3.31	2.85	4.82
1.4	1167	7.29	40	1	3.39	2.96	5.13
1.75	1167	7.29	50	1	3.42	3.01	5.18
2.8	1167	7.29	80	1	3.49	3.10	3.0
3.5	1167	7.29	100	1	3.52	3.14	4.64
4.91	1167	7.29	140	1	3.57	3.21	3.57
6.14	1167	7.29	175	1	3.60	3.25	3.75
6.75	1167	7.29	192	1	3.61	3.27	3.39
2.5	700	7.29	119	1	5.12	4.85	5.0
2.5	833	7.29	100	1	4.26	3.90	4.73
2.5	1167	7.29	71.4	1	2.77	2.29	4.2

Table 248. Predicted $P_{red, vd}$ for the tests by DeGood and Chatrathi (1991)

ignition	Re_f	P_m, bar	L_d/D_d	p_{stat}/p_0	$P_{red, vd}$, old	$P_{red, vd}$, new	exp., bar
centre	16000	7.9	1.18	1.1	0.31	0.25	0.185
centre	16000	7.9	2.37	1.1	0.35	0.30	0.300
centre	16000	7.9	3.56	1.1	0.38	0.33	0.385
bottom	16000	7.9	3.56	1.1	0.28	0.25	1.01

Table 249. Predicted $P_{red, vd}$ for the tests by Molkov et al. (1993)

V, m^3	L_d, m	Re_f	P_m, bar	L_d/D_d	p_{stat}/p_0	$P_{red, vd}$, old	$P_{red, vd}$, new	exp., bar
0.027	1.83	850	7.3	36.6	1.19	2.75	3.25	5.0†
0.027	2.35	915	7.3	47	1.24	2.92	3.44	4.4
0.027	2.35	915	7.3	47	1.24	2.92	3.44	3.5
0.027	2.35	948	7.3	47	2.62	3.33	3.71	1.9
0.027	1.83	948	7.3	36.6	2.39	3.26	3.64	4.4†
2	4	2125	7.3	20	1.14	3.85	4.41	4.3
2	10	2190	7.3	50	1.14	3.99	4.56	5.2
2	10	7325	7.3	26.3	1.14	1.59	2.28	2.15
10	25	10460	7.3	50	1.1	3.09	3.90	4.1
10	25	8825	7.3	50	1.05	2.85	3.63	2.8

Table 250. Predicted $P_{red, vd}$ for the tests by Ponizy & Leyer (1999a)

D_d, mm	L_d, m	Re_f	P_m, bar	L_d/D_d	p_{stat}/p_0	$P_{red, vd}$, old	$P_{red, vd}$, new	exp., bar
16	0.6	350	7.9	37.5	1	4.18	4.48	1.45
21	0.6	460	7.9	28.6	1	3.36	3.71	1.17
36	0.6	788	7.9	16.7	1	1.27	1.48	1.27
16	1.1	350	7.9	68.8	1	4.25	4.56	1.80
21	1.1	460	7.9	52.4	1	3.44	3.81	1.45
36	1.1	788	7.9	30.6	1	1.41	1.65	1.92
16	2.6	350	7.9	163	1	4.34	4.66	1.92
21	2.6	460	7.9	124	1	3.57	3.94	1.55
36	2.6	788	7.9	72.2	1	1.60	1.87	1.92
53	2.6	1160	7.9	49.1	1	0.40	0.38	2.11

Table 251. Predicted $P_{red, vd}$ for the tests by Ponizy & Leyer (1999b)

ignition	Re_f	P_m, bar	L_d/D_d	p_{stat}/p_0	$P_{red, vd}$, old	$P_{red, vd}$, new	exp., bar
centre	788	7.9	47.2	1	1.50	1.76	2.01
centre	788	7.9	47.2	1.3	1.71	1.90	2.16
centre	788	7.9	47.2	1.9	1.96	2.07	2.66
centre	788	7.9	47.2	3.27	2.25	2.24	3.37
rear	788	7.9	47.2	1	1.50	1.76	1.76
rear	788	7.9	47.2	1.32	1.71	1.91	1.88
rear	788	7.9	47.2	1.82	1.93	2.05	1.81
near vent	788	7.9	47.2	2.25	2.11	2.18	1.27
near vent	788	7.9	47.2	3.21	2.24	2.24	2.24

Table 252. Relative errors of the predictions

gas	tests	$\alpha = 0.9, \beta = 1$	$\alpha = 1.75, \beta = 0.5$
K & W	28	18.0 %	19.0 %
the others	7	11.5 %	9.5 %
M et al	10	21.5 %	16.5 %
P & L	19	39.5 %	42.5 %
together	64	24.0 %	24.5 %

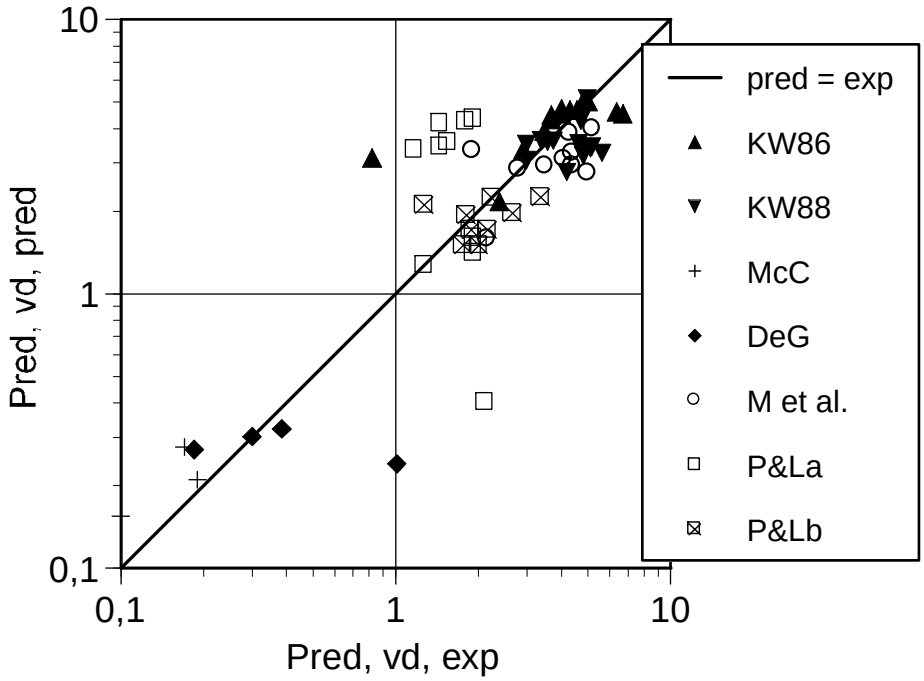

Figure 78. Experimental values of $P_{red,\,vd}$ compared with those predicted with Eq. (111). Values of P_{red} of Molkov et al. (1993), and Ponizy and Leyer (1999a, 1999b) were predicted with $\alpha = 0.9$ and $\beta = 1$.

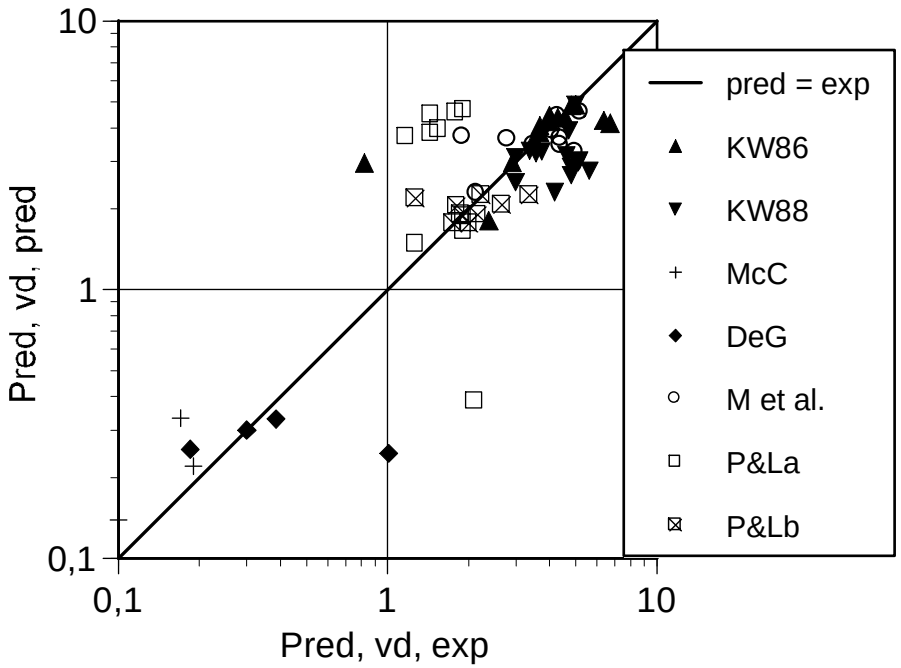

Figure 79. Experimental values of $P_{red,\,vd}$ compared with those predicted with Eq. (113). Values of P_{red} of Molkov et al. (1993), and Ponizy and Leyer (1999a, 1999b) were predicted with $\alpha = 1.75$ and $\beta = 0.5$.

The second way of fitting the parameters of Eq. (109) is to use predicted values for all data sets. The values of the ratio $Br_{t,\,vd}/Br_t$ are calculated in Tables 253 to 257 from Eqs. (23) and (24) using the values of P_{red} predicted with both parameter sets $\alpha = 0.9$, $\beta = 1$ (old) and $\alpha = 1{,}75$, $\beta = 0.5$ (new), and experimental values of $P_{red,\,vd}$.

Table 253. Experimental $Br_{t,\,vd}/Br_t$ for the tests by McCann et al. (1985)

$P_{red,\,vd}$, bar	$Br_{t,\,vd}$	P_{red}, bar, old	Br_t, old	$Br_{t,\,vd}/Br_t$, old	P_{red}, bar, new	Br_t, new	$Br_{t,\,vd}/Br_t$, new
0.10	2.62	0.0153	5.74	0.457	0.0154	5.72	0.459
0.19	2.01	0.0153	5.74	0.350	0.0154	5.72	0.351
0.17	2.10	0.0153	5.74	0.367	0.0154	5.72	0.368

Table 254. Experimental $Br_{t,\,vd}/Br_t$ for the tests by Kordylewski and Wach (1986)

C, %	$P_{red,\,vd}$, bar	$Br_{t,\,vd}$	P_{red}, old	Br_t, old	$Br_{t,vd}/Br_t$, old	P_{red}, new	Br_t, new	$Br_{t,\,vd}/Br_t$, new
10	0.82	1.092	0.68	1.181	0.925	1.77	0.767	1.425
12	2.38	0.601	1.71	0.784	0.767	2.99	0.455	1.320
14	2.91	0.473	2.70	0.522	0.906	3.86	0.283	1.673
16	3.47	0.355	3.44	0.361	0.983	4.47	0.186	1.907
18	4.0	0.259	4.00	0.259	1.000	4.90	0.130	1.991
20	4.3	0.211	4.30	0.211	1.000	5.12	0.105	2.004
22	4.82	0.140	4.55	0.175	0.800	5.30	0.087	1.610
25	5.0	0.118	4.77	0.146	0.808	5.45	0.073	1.616
30	0.82	1.092	4.25	0.219	7.726	5.08	0.110	15.44

Table 255. Experimental $Br_{t,\,vd}/Br_t$ for the tests by Kordylewski and Wach (1986)

$P_{red,\,vd}$, bar	$Br_{t,\,vd}$	P_{red}, old	Br_t, old	$Br_{t,vd}/Br_t$, old	P_{red}, new	Br_t, new	$Br_{t,\,vd}/Br_t$, new
3.68	0.315	4.30	0.211	1.493	5.12	0.105	2.992
3.68	0.315	4.30	0.211	1.493	5.12	0.105	2.992
6.71	0.004	4.30	0.211	0.019	5.12	0.105	0.038
6.36	0.014	4.30	0.211	0.069	5.12	0.105	0.138
4.57	0.172	4.30	0.211	0.816	5.12	0.105	1.635
4.0	0.259	4.30	0.211	1.227	5.12	0.105	2.458

Table 256. Experimental $Br_{t,\,vd}/Br_t$ for the tests by Kordylewski and Wach (1988)

$P_{red,\,vd}$, bar	$Br_{t,\,vd}$	P_{red}, old	Br_t, old	$Br_{t,vd}/Br_t$, old	P_{red}, new	Br_t, new	$Br_{t,\,vd}/Br_t$, new
3.0	0.453	3.08	0.436	1.040	4.19	0.228	1.988
4.82	0.140	3.08	0.436	0.321	4.19	0.228	0.613
5.65	0.056	3.08	0.436	0.025	4.19	0.228	0.247
4.82	0.140	3.08	0.436	0.321	4.19	0.228	0.613
5.13	0.104	3.08	0.436	0.239	4.19	0.228	0.457
5.18	0.099	3.08	0.436	0.227	4.19	0.228	0.434
3.0	0.453	3.08	0.436	1.040	4.19	0.228	1.988
4.64	0.163	3.08	0.436	0.374	4.19	0.228	0.715
3.57	0.336	3.08	0.436	0.771	4.19	0.228	1.473
3.75	0.302	3.08	0.436	0.694	4.19	0.228	1.326
3.39	0.371	3.08	0.436	0.851	4.19	0.228	1.627
5.0	0.118	4.54	0.176	0.672	5.30	0.087	1.734
4.73	0.151	4.10	0.242	0.623	4.97	0.122	0.807
4.2	0.226	3.08	0.436	0.520	4.19	0.228	1.007

Table 257. Experimental $Br_{t,\,vd}/Br_t$ for the tests by DeGood and Chatrathi (1991)

ignition	$P_{red,\,vd}$, bar	$Br_{t,\,vd}$	Br_t, old	$Br_{t,vd}/Br_t$, old	Br_t, new	$Br_{t,\,vd}/Br_t$, new
centre	0.185	2.031	3.37	0.603	3.45	0.589
centre	0.300	1.661	3.37	0.493	3.45	0.481
centre	0.385	1.497	3.37	0.444	3.45	0.434
back	1.01	1.001	3.37	0.297	3.45	0.293

Parameters of Eq. (109) were fitted to the experimental values of $Br_{t,\,vd}/Br_t$ in Tables 241 to 244 and 253 to 257 using the values of Re_f, P_m, L_d/D_d and p_{stat}/p_0 given in Tables 258 to 264. When the values of P_{red} were predicted with the parameter set $\alpha = 0.9$, $\beta = 1$ (old) and the average error of $Br_{t,\,vd}/Br_t$ was minimised, the result was

$$\frac{Br_{t,vd}}{Br_t} = 0.938\,\mathrm{Re}_f^{-0.348}\left(\frac{P_m}{p_0}\right)^{1.182}\left(\frac{L_d}{D_d}\right)^{-0.038}\left(\frac{p_{stat}}{p_0}\right)^{-1.787} \qquad (114)$$

with the relative error of $P_{red,\,vd}$ equal to 25.5 %. When the relative error of $P_{red,\,vd}$ was minimised the result was

$$\frac{Br_{t,vd}}{Br_t} = 0.958\,\mathrm{Re}_f^{-0.293}\left(\frac{P_m}{p_0}\right)^{1.130}\left(\frac{L_d}{D_d}\right)^{-0.087}\left(\frac{p_{stat}}{p_0}\right)^{-1.543} \qquad (115)$$

with the relative error of $P_{red,\,vd}$ equal to 23.0 %.

When the values of P_{red} were predicted with the parameter set $\alpha = 1.75$, $\beta = 0.5$ (new) and the average error of $Br_{t,\,vd}/Br_t$ was minimised, the result was

$$\frac{Br_{t,vd}}{Br_t} = 0.233\,\mathrm{Re}_f^{-0.481}\left(\frac{P_m}{p_0}\right)^{1.909}\left(\frac{L_d}{D_d}\right)^{0.270}\left(\frac{p_{stat}}{p_0}\right)^{-1.632} \qquad (116)$$

with the relative error of $P_{red,\,vd}$ equal to 37.5 %. When the relative error of $P_{red,\,vd}$ was minimised the result was

$$\frac{Br_{t,vd}}{Br_t} = 0.360\,\mathrm{Re}_f^{-0.364}\left(\frac{P_m}{p_0}\right)^{1.922}\left(\frac{L_d}{D_d}\right)^{0.027}\left(\frac{p_{stat}}{p_0}\right)^{-1.699} \quad (117)$$

with the relative error of $P_{red,\,vd}$ equal to 24.5 %. The values of $P_{red,\,vd}$ predicted with Eqs. (115) and (117) are given in Tables 258 to 264 and plotted in Figures 80 and 81.

Table 258. Predicted $P_{red,\,vd}$ for the tests by McCann et al. (1985)

L_d, m	Re_f	P_m, bar	L_d/D_d	p_{stat}/p_0	$P_{red,\,vd}$, old	$P_{red,\,vd}$, new	exp., bar
0.3	4470	7.1	2.66	1.08	0.05	0.04	0.10
2.13	4470	7.1	18.9	1.08	0.08	0.04	0.19
12.2	4470	7.1	108	1.08	0.11	0.04	0.17

Table 259. Predicted $P_{red,\,vd}$ for the tests by Kordylewski and Wach (1986)

C, %	Re_f	P_m, bar	L_d/D_d	p_{stat}/p_0	$P_{red,\,vd}$, old	$P_{red,\,vd}$, new	exp., bar
10	147	4.94	100	1	0.89	0.87	0.82
12	245	5.64	100	1	2.01	2.09	2.38
14	392	6.33	100	1	2.96	3.04	2.91
16	588	6.89	100	1	3.69	3.78	3.47
18	833	7.29	100	1	4.27	4.35	4.0
20	1046	7.44	100	1	4.60	4.68	4.3
22	1307	7.45	100	1	4.89	4.98	4.82
25	1634	7.1	100	1	5.20	5.32	5.0
30	1146	6.38	100	1	4.79	5.00	0.82
20	1046	7.44	1.6	1	4.11	4.81	3.68
20	1046	7.44	6.8	1	4.29	4.77	3.68
20	1046	7.44	12	1	4.36	4.75	6.71
20	1046	7.44	24.4	1	4.44	4.73	6.36
20	1046	7.44	50.4	1	4.52	4.70	4.57
20	1046	7.44	100	1	4.60	4.68	4.0

Table 260. Predicted $P_{red,\,vd}$ for the tests by Kordylewski and Wach (1988)

L_d, m	Re_f	P_m, bar	L_d/D_d	p_{stat}/p_0	$P_{red,\,vd}$, old	$P_{red,\,vd}$, new	exp., bar
0.16	1167	7.29	4.6	1	3.10	3.82	3.0
0.32	1167	7.29	9.1	1	3.22	3.79	4.82
0.54	1167	7.29	15.4	1	3.31	3.76	5.65
0.8	1167	7.29	22.9	1	3.37	3.75	4.82
1.4	1167	7.29	40	1	3.46	3.72	5.13
1.75	1167	7.29	50	1	3.50	3.71	5.18
2.8	1167	7.29	80	1	3.57	3.69	3.0
3.5	1167	7.29	100	1	3.60	3.68	4.64
4.91	1167	7.29	140	1	3.65	3.66	3.57
6.14	1167	7.29	175	1	3.69	3.65	3.75
6.75	1167	7.29	192	1	3.70	3.65	3.39
2.5	700	7.29	119	1	4.72	4.77	5.0
2.5	833	7.29	100	1	4.36	4.44	4.73
2.5	1167	7.29	71.4	1	3.55	3.69	4.2

Table 261. Predicted $P_{red,\,vd}$ for the tests by DeGood and Chatrathi (1991)

ignition	Re_f	P_m, bar	L_d/D_d	p_{stat}/p_0	$P_{red,\,vd}$, old	$P_{red,\,vd}$, new	exp., bar
centre	16000	7.9	1.18	1.1	0.31	0.32	0.185
centre	16000	7.9	2.37	1.1	0.35	0.30	0.300
centre	16000	7.9	3.56	1.1	0.39	0.30	0.385
bottom	16000	7.9	3.56	1.1	0.39	0.30	1.01

Table 262. Predicted $P_{red,\,vd}$ for the tests by Molkov et al. (1993)

V, m^3	L_d, m	Re_f	P_m, bar	L_d/D_d	p_{stat}/p_0	$P_{red,\,vd}$, old	$P_{red,\,vd}$, new	exp., bar
0.027	1.83	850	7.3	36.6	1.19	1.84	1.92	5.0†
0.027	2.35	915	7.3	47	1.24	2.23	2.28	4.4
0.027	2.35	915	7.3	47	1.24	2.23	2.28	3.5
0.027	2.35	948	7.3	47	2.62	4.14	4.35	1.9
0.027	1.83	948	7.3	36.6	2.39	3.94	4.18	4.4†
2	4	2125	7.3	20	1.14	3.70	4.03	4.3
2	10	2190	7.3	50	1.14	3.89	4.05	5.2
2	10	7325	7.3	26.3	1.14	2.53	2.54	2.15
10	25	10460	7.3	50	1.1	3.94	4.07	4.1
10	25	8825	7.3	50	1.05	3.56	3.61	2.8

Table 263. Predicted $P_{red,\,v}$ for the tests by Ponizy & Leyer (1999a)

D_d, mm	L_d, m	Re_f	P_m, bar	L_d/D_d	p_{stat}/p_0	$P_{red,\,vd}$, old	$P_{red,\,vd}$, new	exp., bar
16	0.6	350	7.9	37.5	1	2.24	2.25	1.45
21	0.6	460	7.9	28.6	1	1.18	1.20	1.17
36	0.6	788	7.9	16.7	1	0.22	0.19	1.27
16	1.1	350	7.9	68.8	1	2.37	2.22	1.80
21	1.1	460	7.9	52.4	1	1.33	1.15	1.45
36	1.1	788	7.9	30.6	1	0.25	0.18	1.92
16	2.6	350	7.9	163	1	2.54	2.16	1.92
21	2.6	460	7.9	124	1	1.54	1.09	1.55
36	2.6	788	7.9	72.2	1	0.30	0.17	1.92
53	2.6	1160	7.9	49.1	1	0.10	0.05	2.11

Table 264. Predicted $P_{red,\,vd}$ for the tests by Ponizy & Leyer (1999b)

ignition	Re_f	P_m, bar	L_d/D_d	p_{stat}/p_0	$P_{red,\,vd}$, old	$P_{red,\,vd}$, new	exp., bar
centre	788	7.9	47.2	1	0.27	0.18	2.01
centre	788	7.9	47.2	1.3	0.63	0.44	2.16
centre	788	7.9	47.2	1.9	1.85	1.62	2.66
centre	788	7.9	47.2	3.27	3.36	3.37	3.37
rear	788	7.9	47.2	1	0.27	0.18	1.76
rear	788	7.9	47.2	1.32	0.65	0.47	1.88
rear	788	7.9	47.2	1.82	1.70	1.45	1.81
near vent	788	7.9	47.2	2.25	2.43	2.30	1.27
near vent	788	7.9	47.2	3.21	3.32	3.32	2.24

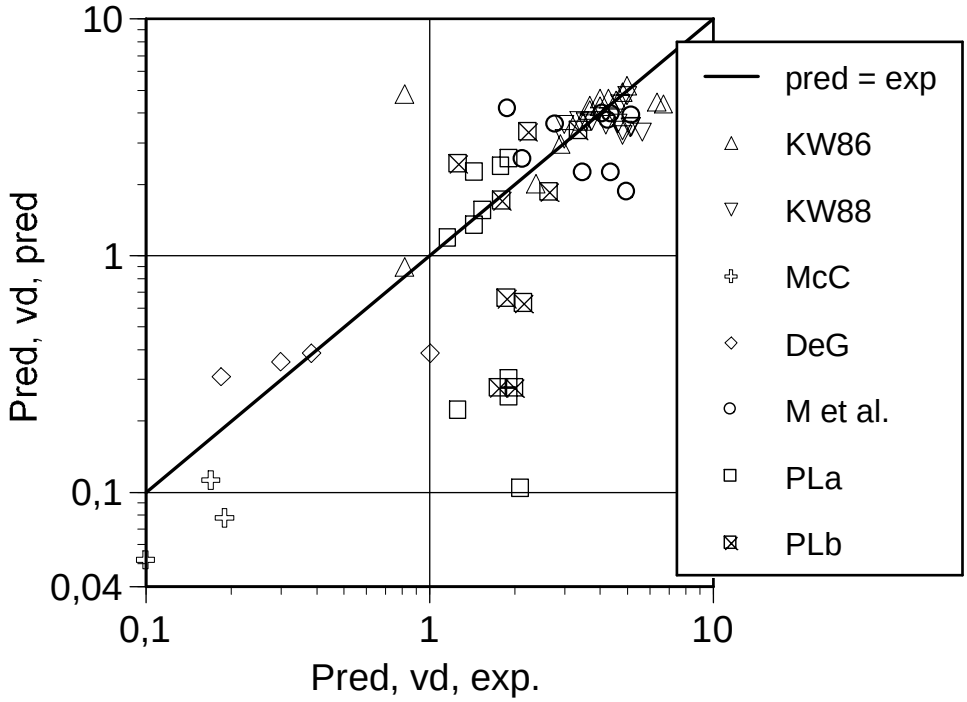

Figure 80. Experimental values of $P_{red,\,vd}$ compared with those predicted with Eq. (115). All values of P_{red} were predicted with $\alpha = 0.9$ and $\beta = 1$.

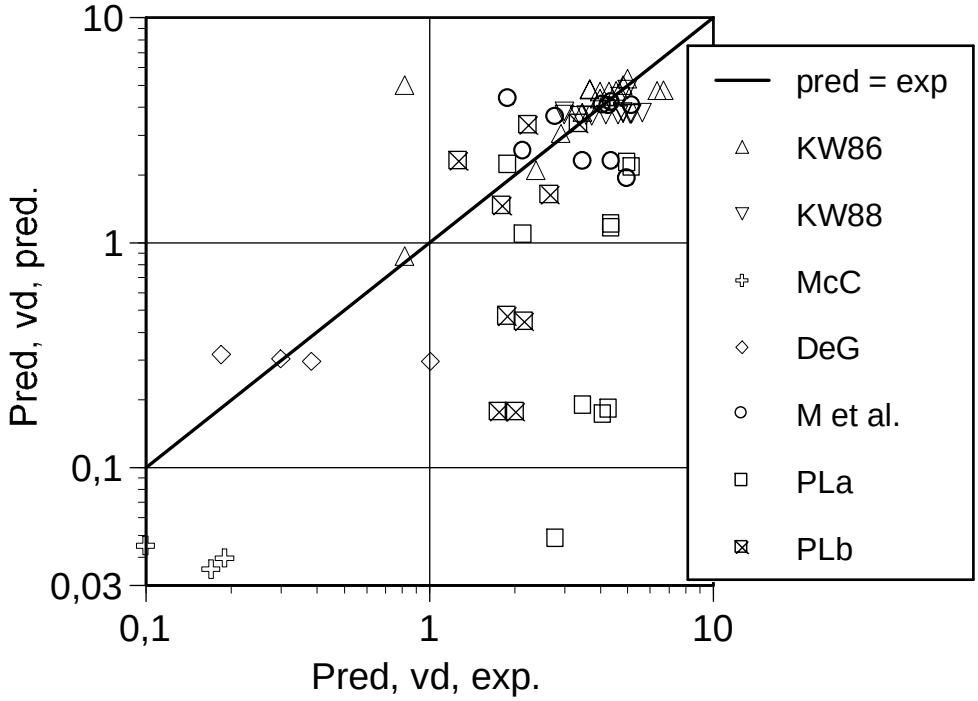

Figure 81. Experimental values of $P_{red,\,vd}$ compared with those predicted with Eq. (117). All values of P_{red} were predicted with $\alpha = 1.75$ and $\beta = 0.5$.

Table 265. Relative errors of the predictions, Eq. (115) and (117)

reference	tests	$\alpha = 0.9$, $\beta = 1$	$\alpha = 1.75$, $\beta = 0.5$
K & W	29	19.0 %	20.0 %
the others	7	9.0 %	11.5 %
M et al.	10	27.5 %	26.5 %
P & L	19	32.5 %	34.5 %
together	65	23.0 %	24.5 %

Table 266 summarises the calculated relative errors of the existing methods for gas and dust explosions and the new correlations. Of the methods included in the standards, the Bartknecht and Siwek correlations give the best predictions for $P_{red,\,vd}$ when the values of P_{red} are predicted with the old parameter set $\alpha = 0.9$, $\beta = 1$. The Bartknecht and Siwek (VDI 3673 and EN 14491) correlations for dust explosions are equally accurate as the Bartknecht correlations for gas explosions both in their original form and in the modified form of NFPA 68 (2007). The methods for dust explosions by Tamanini and Fischer and Ural are less accurate when applied to the present data base of duct vented gas explosions.

Table 266. Relative errors of the predictions

method	P_{red} exp. & pred.	P_{red} pred.	– outlier
gas explosions			
Bartknecht, gas	29.5 % (32.5 %)	28.0 % (34.0 %)	25.5 % (31.0 %)
NFPA 68 (2007)	26.0 % (32.0 %)	30.0 % (42.0 %)	28.0 % (38.5 %)
dust explosions			
Bartknecht, dust	28.0 % (32.0 %)	28.5 % (37.5 %)	25.5 % (36.0 %)
VDI 3673	33.0 % (36.0 %)	28.5 % (33.5 %)	26.0 % (31.0 %)
EN 14491	35.0 % (42.5 %)	25.0 % (33.0 %)	22.0 % (30.0 %)
Tamanini	—	35.5 % (76.5 %)	31.5 % (73.0 %)
NFPA 68 (2007)	—	39.5 %	36.5 %
new correlations			
Eq. (91)	27.5 %	27.5 %	25.0 %
Eq. (100)	62.0 % (83.0 %)	69.0 % (94.0 %)	65.5 % (90.5 %)
Eqs. (111), (113), (115) and (117)	24.0 % (24.5 %)	23.0 % (24.5 %)	20.0 % (21.0 %)

The extended Yao correlation Eq. (91) is about equally accurate as the Bartknecht and Siwek (VDI 3673 and EN 14491) correlations with values of P_{red} predicted with the old parameter set $\alpha = 0.9$, $\beta = 1$. The proposed correlation with different parameter sets Eqs. (111), (113), (115) and (117) has somewhat better accuracy than the existing ones. The extended Molkov method Eq. (100) has a significantly poorer accuracy than all the other methods. This is due to the inclusion of P_{stat} in the turbulent Bradley number $Br_{t\,,vd}$ which exaggerates the dependence of $P_{red,\,vd}$ on P_{stat}.

The tests with 30 % town gas-air mixture by Kordylewski and Wach (1986) differ from all the other tests in the present data base in that duct vented overpressure $P_{red,\,vd}$ is only about half the simply vented overpressure P_{red}. These tests are the only ones performed with a rich mixture near UFL. It is, however, very difficult to say whether the very rich mixture contributes to this behaviour of $P_{red,\,vd}$ or not. Anyway, the corresponding data point constitutes an outlier for all the correlations studied so far.

In Table 266, the relative errors with predicted values of P_{red} are also calculated without the outlier. It is seen that the relative error of 64 remaining data points is about 3.0 percent points lower than the value with 65 data points including the outlier. Removing the outlier, however, does not affect the ranking of the methods.

Another interesting point is the ability of the new correlations to predict the dependence of $P_{red, vd}$ on P_{stat}. In Figure 82, the values of $P_{red, vd}$ for the tests by Ponizy and Leyer (1999b) predicted with the new correlations are compared with each other.

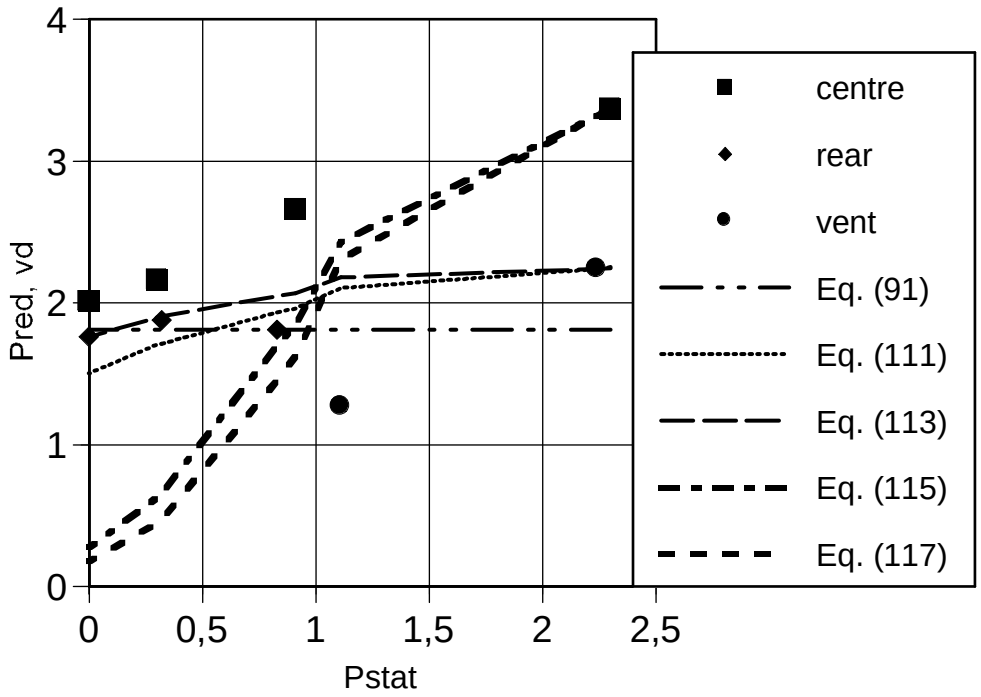

Figure 82. P_{red} predicted with Eqs. (20) to (25) and $P_{red, vd}$ predicted with different methods for the tests by Ponizy and Leyer (1999b).

The extended Yao correlation Eq. (91) is independent of the value of P_{stat} but nevertheless predicts quite well the measured values. The exponent of the term (p_{stat}/p_0) in the correlations derived with both experimental and predicted values of P_{red} Eqs. (111) and (113) is about –0.5 whereas in the correlations derived with predicted values of P_{red} Eqs. (115) and (117) it is about –1.5. The value –0.5 predicts the experimental values quite well although it underestimates $P_{red, vd}$ at high values of P_{stat}. The value –1.5 leads to an underestimation of $P_{red, vd}$ at low values of P_{stat}, which can also be seen in Figs. 80 and 81. Of course, with such a small number of tests with $P_{stat} > 0$, the correct value of the exponent remains an open issue.

9 Conclusions

The semi-empirical vent dimensioning methods by Bradley and Mitcheson and by Molkov are based on models of simply vented gas explosions. The validation of these methods with data of medium scale explosions shows that Molkov method with the "old" parameter set gives the best predictions for the tests with initially uncovered vent. For tests with covered vent, Bradley and Mitcheson method predicts test results equally well as Molkov method.

Since the phenomena contributing to overpressure generation in duct vented gas and dust explosions are poorly understood, no models for such explosions have been developed. The methods included in the standards are extensions of

empirical correlations for vent dimensioning of simply vented high-strength enclosures. Some of them are based exclusively on confidential test data.

The experimental data in the open literature of duct vented gas explosions consists mainly of tests with laboratory scale vessels, often with an initially open vent. Most test configurations are outside the range of validity of vent dimensioning of high-strength enclosures.

Russo and Di Benedetto resolved this problem by combining the empirical duct venting correlations by Bartknecht and Siwek with the semi-empirical Molkov method. The average relative errors of these methods proved to be comparable to each other and the "old" parameter set of the Molkov method gave the best predictions. The correlations for dust explosions gave equally accurate results as the one for gas explosions. The methods of Tamanini and Ural for dust explosions were somewhat less accurate than those by Bartknecht and Siwek.

Di Benedetto et al. used the same data of duct vented gas explosions to extend the correlation by Yao and the Molkov method. When the parameters of the previous correlation were recalculated, the resulting correlations predicted the test data equally well as the methods of Bartknecht and Siwek (VDI 3673 and EN 14491) together with Molkov method with the "old" parameter set. The Yao correlation, however, does not include any dependence on vent opening pressure.

The extension of the Molkov method turned out to give poor predictions because the inclusion of vent opening pressure in the turbulent Bradley number exaggerated the dependence of explosion overpressure on vent opening pressure. When the inclusion was not made but instead an explicit dependence on vent opening pressure was introduced, the resulting correlations had somewhat better accuracy than the existing ones.

Acknowledgement

The author is indebted to Paola Russo, Università di Salerno, for information on the method used to calculate town gas properties.

References

Bartknecht, W. 1981. Explosions. Course, prevention, protection. Berlin: Springer. Pp. 112–113. ISBN 3-540-10216-7.

Bartknecht, W. 1993. Explosionsschutz. Grundlagen und Anwendung. Berlin: Springer. Pp. 470–535. ISBN 3-540-55464-5.

Bosschaart, K. J. 2002. Analysis of the heat flux method for measuring burning velocities. Eindhoven: Technical University of Eindhoven. Dissertation. Pp. 65–76, Appendix D. alexandria.tue.nl/extra2/2003/0699.pdf

Bradley, D. & Mitcheson, A. 1978a. The venting of gaseous explosions in spherical vessels, I – theory. Combustion and Flame, Vol. 32, pp. 221–236. ISSN 0010-2180.

Bradley, D. & Mitcheson, A. 1978b. The venting of gaseous explosions in spherical vessels, II – theory and experiment. Combustion and Flame, Vol. 32, pp. 237–255. ISSN 0010-2180.

British Gas 1990. Review of the applicability of predictive methods to gas explosions in offshore modules. London: Department of Energy. 175 p. (Offshore Technology Report OTH 89 312.) ISBN 0-11-413314-X.

Catlin, C.A., Manos, A. & Tite, J. P. 1993. Mathematical modelling of confined explosions in empty cube and duct shaped enclosures. Transactions of the Institution of Chemical Engineers, Vol. 71, Part B, May, pp. 89–100. ISSN 0957-5820.

Chaineaux, J. & Dannin, E. 1992. Sizing of explosion vents for the protection of vessels in which gases are processed at p and T higher than ambient. In: Loss Prevention and Safety Promotion in the Process Industries, 7th International Symposium. Taormina, 4–8 May 1992. Pp. 60-1–60-30.

Cooper, M. G., Fairweather, M. & Tite, J. P. 1986. On the mechanisms of pressure generation in vented explosions. Combustion and Flame, Vol. 65, pp. 1–14. ISSN 0010-2180.

Coward, H. F. & Jones G. W. 1952. Limits of flammability of gases and vapors. Washington, DC: Bureau of Mines. 176 p. (Bulletin 503.)

Cubbage, P. A. & Marshall, M. R. 1972. Pressures generated in combustion chambers by the ignition of air-gas mixtures. Institution of Chemical Engineers, Symposium Series, No. 33. Pp. 24–31.

Cubbage, P. A. & Simmonds, W. A. 1955. An investigation of explosion reliefs for industrial drying ovens. I. Top relief in box ovens. Transactions of the Institute of Gas Engineers, Vol. 105, pp. 470–526.

DeGood, R. & Chatrathi, K. 1991. Comparative analysis of test work stydying factors influencing pressures developed in vented explosions. Journal of Loss Prevention in the Process Industries, Vol. 4, Oct., pp. 297–304. ISSN 0950-4230.

Di Benedetto, A., Salzano, E. & Russo, P. 2005. Prediction of pressure piling by semi-empirical correlations. Fire Safety Journal, Vol. 40, pp. 282–298. ISSN 0379-7112.

Di Benedetto, A., Russo, P. & Salzano, E. 2007. Gas explosions mitigation by ducted venting. Turkish Journal of Engineering and Environmental Sciences, Vol. 31, pp. 355–363. ISSN 1303-6157. http://journals.tubitak.gov.tr/engineering/issues/muh-07-31-6/muh-31-6-4-0711-4.pdf

Di Benedetto, A., Russo, P. & Salzano, E. 2008. The design of duct venting of gas explosions. Process Safety Progress, Vol. 27, No. 2, pp. 164–172. ISSN 1547-5913.

EN 14994. 2007. Gas explosion venting protective systems. Brussels: European Committee for Standardization. 27 p.

Ferrara G., Di Benedetto A., Salzano E. & Russo G. 2008. CFD analysis of gas explosions vented through relief pipes. Journal of Hazardous Materials, Vol. A137, No. 2, pp. 654–655. ISSN 0304-3894.

Gardner, D. J. & Hulme, G. 1995. A survey of current predictive methods for explosion hazard assessments in the UK offshore industry. London: Health and Safety Executive. P. 7. (Offshore Technology Report OTH 94 449.) ISBN 0-7176-0969-3.

Gelfand, B. E. 2000. Laminar and turbulent flame propagation in hydrogen-air-steam mixtures. Appendix A in: Flame acceleration and deflagration-to-detonation transition in nuclear safety. State-of the art report by a group of experts. Paris: Nuclear Energy Agency. 17 p. (NEA/CSNI/R(2000)7). http://www.galcit.caltech.edu/~jeshep/SOAR/

Goodger, E. M. 1977. Combustion calculations. Theory, worked examples and problems. London: Macmillan. 106 p. ISBN 0-333-21801-9.

Harris, R. J. 1983. The investigation and control of gas explosions in buildings and heating plant. London: E & FN Spon. 194 p. ISBN 0-419-13220-1.

Harrison, A. J. & Eyre, J. A. 1987. "External explosions" as a result of explosion venting. Combustion Science and Technology, Vol. 52, pp. 91–106. ISSN 0010-2202.

Janicka, J. 2009. Vormischflammen. Technische Universität Darmstadt. Pp. 7, 22. http://www.ekt.tu-darmstadt.de/media/fachgebiet_ekt/documents_1/vorlesungen_7/ws09_2/nva_08_vormischflammen_ws09.pdf

Joos, F. 2006. Technische Verbrennung: Verbrennungstechnik, Verbrennungs-modellierung. Berlin, Heidelberg: Springer. S. 288. ISBN: 978-3-540-34333-2.

Kordulewski, W. & Wach, J. 1986. Influence of ducting on the explosion pressure. Combustion and Flame, Vol. 66, pp. 77–79. ISSN 0010-2180.

Kordulewski, W. & Wach, J. 1988. Influence of ducting on explosion pressure: small scale experiments. Combustion and Flame, Vol. 71, pp. 51–61. ISSN 0010-2180.

Mashuga, C. V. & Crowl, D. A. 2000. Derivation of Le Chatelier's mixing rule for flammable limits. Process Safety Progress, Vol. 19, No. 2, pp. 112–117. ISSN 1066-8527.

McCann, D. P. J., Thomas, G. O. & Edwards, D. H. 1985. Gasdynamics of vented explosions. Part I: experimental studies. Combustion and Flame, Vol. 59, pp. 233–250. ISSN 0010-2180.

Metghalci, M. & Keck, J. C. 1982. Burning velocities of mixtures of air with methanol, isooctane, and indolene at high pressure and temperature. Combustion and Flame, Vol. 48, pp. 191–210. ISSN 0010-2180.

Milani, A. & Wünnig, J. G. 2007. Handbuch der Brennertechnik für Industrieöfen. Essen: Vulkan. 234 S. ISBN 978-3-8027-2938-6.

Moen, I. O. et al. 1982. Pressure development due to turbulent flame propagation in large-scale methane-air explosions. Combustion and Flame, Vol. 47, pp. 31–52. ISSN 0010-2180.

Molkov, V. V. 1994. Venting of deflagrations: dynamics of the process in systems with a duct and receiver. Fire Safety Science – Proceedings of the Fourth International Symposium, Ottawa. Pp. 1245–1254.

Molkov, V. V. 1999. Explosion safety engineering: NFPA 68 and improved vent sizing technology. Interflam '99. Proceedings of the 8th International Fire Science & Engineering Conference, Edinburgh, 29 June–1 July. Pp. 1129–1134.

Molkov, V. V. 2001. Unified correlations for vent sizing of enclosures at atmospheric and elevated pressures. Journal of Loss Prevention in the Process Industries, Vol. 14, pp. 567–574. ISSN 0950-4230.

Molkov, V., Baratov, A. & Korolchenko, A. 1993. Dynamics of gas explosions in vented vessels; review and progress. Progress in Astronautics and Aeronautics, Vol. 154, pp. 117–131. ISSN 0079-6050.

Molkov, V., Dobashi, R., Suzuki, M. & Hirano, T. 1999. Modeling of vented hydrogen-air deflagrations and correlations for vent sizing. Journal of Loss Prevention in the Process Industries, Vol. 12, pp. 147–156. ISSN 0950-4230.

Molkov, V., Dobashi, R., Suzuki, M. & Hirano, T. 2000. Venting of deflagrations: hydrocarbon-air and hydrogen-air systems. Journal of Loss Prevention in the Process Industries, Vol. 13, pp. 397–409. ISSN 0950-4230.

Moore, P. E. & Siwek, R. 2002. An update on the European explosion suppression and explosion venting standards. Process Safety Progress, Vol. 21, No. 1, pp. 74–84. ISSN 1066-8527.

NACA 1957. Basic considerations in the combustion of hydrocarbon fuels with air. Washington, DC: National Advisory Committee for Aeronautics. (Report 1300).

NFPA 68. 1998. Guide for venting of deflagrations. Quincy, MA: National Fire Protection Association. 56 p.

NFPA 68. 2002. Guide for venting of deflagrations. Quincy, MA: National Fire Protection Association. 62 p.

NFPA 68. 2007. Standard on explosion protection by deflagration venting. Quincy, MA: National Fire Protection Association. 82 p.

Pasman, H. J. & Groothuisen, T. M. & Gooijer, P. H. 1974. Design of pressure relief vents. Loss Prevention and Safety Promotion in the Process Industries. New York: Elsevier. Pp. 185–189.

Pegg, M. J., Amyotte, P. R. & Chippet, S. 1992. Confined and vented deflagrations of propane/air mixtures at initially elevated pressures. In: Loss Prevention and Safety Promotion in the Process Industries, 7th International Symposium. Taormina, 4–8 May 1992. Pp. 110-1–110-14.

Pichon, S. et al. 2009. The combustion chemistry of a fuel tracer: measured flame speeds and ignition delays and a detailed kinetic model for the oxidation of acetone. Combustion and Flame, Vol. 156, No. 2, pp. 494–504. ISSN 0010-2180.

Ponizy, B. & Leyer, J. C. 1999a. Flame dynamics in a vented vessel connected to a duct: 1. Mechanism of vessel-duct interaction. Combustion and Flame, Vol. 116, No. 1–2, pp. 259–271. ISSN 0010-2180.

Ponizy, B. & Leyer, J. C. 1999b. Flame dynamics in a vented vessel connected to a duct: 2. Influence of ignition site, membrane rupture, and turbulence. Combustion and Flame, Vol. 116, No. 1–2, pp. 272–281. ISSN 0010-2180.

Razus, D. M. & Krause, U. 2001. Comparison of empirical and semi-empirical calculation methods for venting of gas explosions. Fire Safety Journal, Vol. 36, No. 1, pp. 1–23. ISSN 0379-7112.

Runes, E. 1972. Explosion venting. Loss Prevention, Vol. 6, pp. 63–67.

Russo, P. & Di Benedetto, A. 2007. Effects of a duct on the venting of explosions – critical review. Trans IChemE, Part B, Process Safety and Environmental Protection, Vol. 85, No. B1, pp. 9–22. ISSN 0957-5820.

Russo, P. 2008. Email to R. Lautkaski, 24 October 2008.

Shepherd, J. E., Krok, J. C. & Lee, J. L. 1997. Jet A explosion experiments. Laboratory testing. Pasadena, CA. Pp. 27–28. (California Institute of Technology. Explosion Dynamics Laboratory Report FM97-5.)
http://caltechgalcitfm.library.caltech.edu/43/01/FM97-5.pdf

Sheppard, C. G. W. 1971. Electrical phenomena in flames. PhD thesis, University of Leeds. Reference of (Bradley & Mitcheson 1978b).

Singh, J. 1977. PhD Thesis. University of London. (British Library Ref. No. D24652/78). Reference of (Singh 1994).

Singh, J. 1994. Gas explosions in inter-connected vessels. Pressure piling. Transactions of the Institution of Chemical Engineers, Vol. 72, Part B, November, pp. 220–228. ISSN 0957-5820.

Siwek, R. 1996. Explosion venting technology. Journal of Loss Prevention in the Process Industries, Vol. 9, No. 1, pp. 81–90. ISSN 0950-4230.

Siwek, R. 1998. New findings on explosion venting. In: Loss Prevention and Safety Promotion in the Process Industries, 9th International Symposium. Barcelona, 4–7 May 1998. Pp. 580–589.

Siwek, R. & van Wingerden, K. 2006. Dust explosion venting: EN standard 14491 vs. VDI-guideline 3673. CISAP-2. 2nd International Conference on Safety and Environment in Process Industry. Naples, 21–24 May 2006. Chemical Engineering Transactions, Vol. 9. ISBN 88-90 1915-1-1.
http://www.fireex.eu/dbase/2006%20-%20Explosion%20venting%20EN-14491%20vs%20VDI-GL-3673.pdf

Solberg, D. M., Pappas, J. A. & Skramstad, E. 1980. Experimental investigations on flame acceleration and pressure rise phenomena in large scale vented gas

explosions. In: Loss Prevention and Safety Promotion in the Process Industries, 3rd International Symposium. Basle, 15–19 Sept. 1980. Pp. 16/1295–16/1303.

Tamanini, F. & Fischer, M. 2003. Mixed-mode venting of dust explosions. Fourth International Seminar on Fire and Explosion Hazards, Londonderry, UK, 8–12 September 2003. Pp. 725–734.

VDI 3673. 2002. Druckentlastung von Staubexplosionen. Pressure venting of dust explosions. Düsseldorf: Verein Deutscher Ingenieure. 44 p.

Ural, E. A. 2005. Dust explosion venting through ducts. AIChE 2005 Spring National Meeting 39th Annual Loss Prevention Symposium, Atlanta GA, April 11–13, 2005. Paper TG004-5.

Yao, C. 1974. Explosion venting of low-strength equipment and structures. Loss Prevention, Vol. 8, pp. 1–9.

Zalosh, R. G. 1970. Gas explosion tests in room-sized enclosures. Loss Prevention, Vol. 13, pp. 98–110

Nomenclature

a	parameter of Eq. (82)
A	Eq. (14)
A_c	cross-section of the enclosure, m^2
A_{eff}	effective vent area of duct vented enclosure, m^2
A_f	area of pear-shaped flame, m^2
A_f	area of spherical flame, m^2
A_s	internal surface area of the enclosure, m^2
A_v	vent area, m^2
A_{v1}	vent area of long enclosure, Eq. (38), m^2
$A_{v,vd}$	vent area of duct vented enclosure, m^2
b	parameter of Eq. (82)
br_t	turbulent Bradley number of simply vented enclosure, Eq. (78)
$br_{t,vd}$	turbulent Bradley number of duct vented enclosure
Br	Bradley number, Eq. (20)
Br_t	turbulent Bradley number of simply vented enclosure, Eq. (21)
$Br_{t,vd}$	turbulent Bradley number of duct vented enclosure
c	parameter of Eq. (82)
c	sound velocity, m/s
C	fuel concentration, %
C_d	discharge coefficient
C_p	molar heat capacity at constant pressure, J mol^{-1} K^{-1}
C_R	constant of Eq. (28)
C_S	constant of Eq. (30)
C_{st}	stoichiometric concentration, %
C_v	molar heat capacity at constant volume, J mol^{-1} K^{-1}
d	parameter of Eq. (82)
D	enclosure diameter, m
D_d	vent duct diameter, m
e	relative error, Eq. (39), %
e_{abs}	relative absolute error, Eq. (40), %
E	expansion factor, N_fT_f/N_iT_I
E_1	Eq. (53)
E_2	Eq. (54)
f	$Br_{t,\,vd}/Br_t$, Eq. (98)
f(Br)	Eq. (72)
g	auxiliary function, Eq. (101)
k	parameter of Eqs. (99) and (109)
K	vent coefficient, Eq. (1)
K_G	deflagration index of gas, bar·m/s
K_{St}	deflagration index of dust, bar·m/s
l	parameter of Eqs. (99) and (109)
L	enclosure length, m
L_1	room dimension, m
L_2	room dimension, m
L_d	vent duct length, m
LFL	lower flammability limit, %
LFL_i	lower flammability limit of component i, %
LFL_{mix}	lower flammability limit of mixture, %

L_s	vent duct length with maximum overpressure, m
m	parameter of Eqs. (99) and (109)
m	moles of oxygen per moles of fuel
m_s	moles of oxygen per moles of fuel in stoichiometric combustion
M	molar mass, g/mol
n	parameter of Eqs. (99) and (109)
n_{45}	number of 45° bends
n_{90}	number of 90° bends
N_f	final number of moles
N_i	initial number of moles
o	parameter of Eq. (109)
p_i	absolute pressure at flame arrival to secondary vessel, bar
p_k	maximum explosion absolute pressure in secondary vessel, bar
p_m	maximum explosion overpressure in a closed vessel, bar
p_{stat}	vent opening absolute pressure, bar
p_{red}	explosion absolute pressure, bar
$p_{red, exp}$	calculated explosion absolute pressure, bar
$p_{red, pred}$	predicted explosion absolute pressure, bar
p_0	initial absolute pressure, bar
P_{aicc}	adiabatic isochoric complete combustion pressure, bar
P_M	dimensionless explosion overpressure, Eq. (25)
$P_{M, vd}$	dimensionless explosion overpressure of a duct vented enclosure
P_{max}	maximum explosion overpressure in a closed vessel, bar
P_{red}	explosion overpressure of a simply vented enclosure, bar
$P_{red, exp}$	experimental explosion overpressure of a simply vented enclosure, bar
$P_{red, pred}$	predicted explosion overpressure of a simply vented enclosure, bar
$P_{red, vd}$	explosion overpressure of a duct vented enclosure, bar
P'_{red}	corresponding overpressure of a simply vented enclosure, Eqs. (42) and (43), bar
P_{stat}	vent opening overpressure, bar
P_1	first pressure peak of a simply vented enclosure, bar
P_2	second pressure peak of a simply vented enclosure, bar
P_3	third pressure peak of a simply vented enclosure, bar
P_4	fourth pressure peak of a simply vented enclosure, bar
R	vessel radius, m
R	gas constant, 8.314 J mol^{-1} K^{-1}
Re_f	flame Reynolds number, Eq. (83)
S	Eq. (13)
S_r	reference burning velocity, m/s
S_0	burning velocity, m/s
T_{ad}	adiabatic flame temperature at constant pressure, K
T_{aicc}	adiabatic flame temperature at constant volume, K
T_f	final temperature, K
T_r	reference temperature, K
T_u	temperature of unburned gas mixture, K
T_0	initial temperature, K
UFL	upper flammability limit, %
v_f	flame speed, m/s
V	enclosure volume, m^3
w	vent cover mass per unit area, kg/m^2
y_i	mole fraction of the ith component

α	parameter of Eq. (1)
α	parameter of Eq. (22)
α	venting parameter, Eq. (75)
β	parameter of Eq. (1)
β	parameter of Eq. (22)
γ	parameter of Eq. (22)
γ_a	specific heat capacity ratio C_p/C_v of air
γ_b	specific heat capacity ratio C_p/C_v of burned gas
γ_u	specific heat capacity ratio C_p/C_v of unburned gas
Γ	vent parameter, Eq. (57)
ΔA	vent area increment for an elongated enclosure, Eq. (34) or (36), m^2
ε	parameter of Eq. (3)
ε	vent duct surface roughness, m
ζ_i	flow resistance coefficient
μ	generalised discharge coefficient
ν	kinematic viscosity of air, m^2/s
ρ_0	initial density, kg/m^3
ϕ	$br_{t,\,vd}$ / br_t, Eq. (82)
Φ_d	duct inertia parameter, Eq. (58)
χ	flame stretch or turbulence factor
Ψ_d	friction loss parameter, Eq. (59)